Dissecting the genotype to phenotype relationships of Genomic Disorders

Lesley Ruth Hart

Submitted to the University of Sussex for the degree of Doctor of Philosophy (DPhil)

June 2013

Declaration

I hereby declare that this thesis has not been, and will not be, submitted in whole or in part to another University for the award of any other degree.

Signature…… Date……..

This thesis is dedicated in loving memory of my parents,

Andrew and Karen

This is for you.

"A good name is more desirable than great riches; to be esteemed is better than silver or gold"

Acknowledgements

First and foremost I offer my sincerest gratitude to my supervisor, Professor Mark O'Driscoll. Over the last four years Mark has instilled in me, by example, a strong sense of discipline and integrity and I consider it a true honour to have been able to complete my research in his lab. His continued encouragement, enthusiasm and guidance has made this thesis possible. One simply could not wish for a better or friendlier supervisor.

I would also like to thank Professor Antony Carr for his continued support throughout my studies, particularly during the second year of my research.

In my daily work, I have been blessed with the most cheerful and fun-loving lab group I could have asked for; Rita Colnaghi, Emily Outwin, Diana Alcantara, Iga Abramowicz and Gill Carpenter. I am immensely grateful for both the support and the happy memories they have given me over the past four years. Much of what I know now is thanks to them and for that, I am eternally thankful.

I acknowledge the Medical Research Council for their financial support enabling me to carry out this research. I would also like to express my utmost appreciation for being given the opportunity to carry out my research within the Genome Centre and I thank all the staff for their never-ending assistance and support.

I owe my deepest gratitude to my family, partner and friends for supporting and encouraging me to pursue my dreams. In particular my Dad, without whom University would not have been an option and who will forever continue to be my inspiration in life. To my extended family; "The Murray's" and "The Bourke's", your overwhelming support and love has helped me through several hurdles in life. Without that, I could not have gone so far. Thank you.

University of Sussex

Lesley Ruth Hart

DPhil Biochemistry

Dissecting the genotype to phenotype relationships of Genomic Disorders

SUMMARY

Over the last decade, major advances in the development and application of microarray-based comparative genomic hybridisation (aCGH) technology have significantly contributed to our understanding of Genomic Disorders. My aims here were to provide insight into the genotype to phenotype relationships of three Genomic Disorders; CUL4B-deleted X-Linked Mental Retardation (XLMR), Wolf-Hirschhorn Syndrome (WHS) and 16p11.2 Copy Number Variant Disorder. *CUL4B* encodes a structural component of the Cullin-RING-ligase 4-containing class of E3 ubiquitin ligases. *CUL4B*-deleted XLMR represents a syndromal form of mental retardation whereby patients exhibit other clinical features aside from the MR, such as seizures, growth retardation and disrupted sexual development. I used *CUL4B*-deleted patient-derived cell lines to investigate the impacts of CUL4B loss on mitochondrial function. I have shown that loss of CUL4B is associated with a distinct set of mitochondrial phenotypes, identifying *CUL4B*-deleted XLMR as a disorder associated with mitochondrial dysfunction. Furthermore, I have uncovered a reciprocal relationship between CUL4B and Cereblon, providing evidence of a potential role for the CUL4-CRBN E3 ligase complex in maintaining mitochondrial function. Deletion or duplication of the 16p11.2 region is associated with macro-/microcephaly respectively. Here, I have evaluated the cellular consequences of 16p11.2 CNV, specifically with regards KCTD13 expression, DNA replication and checkpoint activation. WHS is typically caused by a small hemizygous telomeric deletion of the 4p16.1 region. Haploinsufficiency of 4p16.1 is associated with microcephaly, growth retardation and complex developmental abnormalities. I investigated the impacts of *LETM1* copy number change in WHS patient-derived cells. Here, I have shown that copy number change of *LETM1* specifically segregates with mitochondrial dysfunction, likely underlying the seizure phenotype exhibited by the large subgroup of WHS patients whose deletions incorporate *LETM1* as well as the rarer instances of the reciprocal duplication. In this thesis I use patient-derived cell lines from three Genomic Disorders as a fundamental tool providing new pathomechanistic insight into the clinical presentation of these conditions.

Table of Contents

Abbreviations

aCGH: Microarray-based Comparative Genomic Hybridisation

ACC: Acetyl-CoA-Carboxylase

ARNSMR: Autosomal Recessive Non-Syndromal Mental Retardation

AICAR: 5-amino-1β-D-ribofuranosyl-1H-imidazole-4-carboxamide

ATP: Adenosine TriPhosphate

BFB: Break Fusion Bridge

Ca^{2+}: Calcium

CCCP: Carbonyl cyanide m-chlorophenyl hydrazone

CCR: Complex Chromosomal Rearrangement

CNS: Central Nervous System

CRBN: Cereblon

CNV: Copy Number Variation

CPT: Camptothesin

CRL4: Cullin RING ligase 4

CUL4A/B: Cullin 4 A/B

DCAF: DDB1 Cullin Associated Factor

DDR: DNA Damage Response

DSB: Double Strand Break

ETC: Electron Transport Chain

FACS: Fluorescent-Activated Cell Sorter

FITC: Fluorescein isothiocyanate

FoSTeS: Fork Stalling Template Switching

GR: Growth Retardation

HECT: Homologous to E6-associated protein

HR: Homologous Recombination

HU: Hydroxyurea

KHE: Potassium Hydrogen Exchange Activity

LCR: Low Copy Repeat

LBL: Lymphoblastoid cell line

MMBIR: Microhomology-mediated Break-Induced Repair

mPTP: Mitochondrial Permeability Transition Pore

MR: Mental Retardation

mtDNA: mitochondrial DNA

MTG: Mitotracker Green

mTOR: mammalian Target of Rapamycin

MTR: Mitotracker Red

NAHR: Non-Allelic Homologous Recombination

nDNA: nuclear DNA

NER: Nucleotide Excision Repair

NHEJ: Non-Homologous End Joining

PE-A: Phycoerithrin

RING: Really Interesting New Gene

ROS: Reactive Oxygen Species

SNP: Single Nucleotide Polymorphism

SOD: Superoxide Dismutase

SSB: Single Strand Break

UPS: Ubiquitin Proteasome Pathway

UV: Ultraviolet

WHS: Wolf Hirschhorn Syndrome

WT: Wild Type

XLMR: X-Linked Mental Retardation

List of Tables

List of Figures

Chapter One

Introduction: Copy Number Variation and Genomic Disease

1.1: Introduction

Genetic variation within the human genome can range from large microscopically visible chromosome anomalies (deletions, insertions, duplications and translocations) to single-nucleotide polymorphisms (SNPs). It was previously thought that any two 'normal' individuals are 99.9% similar genetically and that SNPs in DNA were the most prevalent and important source of genetic variation (Collins et al, 1997; Kwok et al, 1996). However, due to advances of the Human Genome Project and the advent of microarray based Comparative Genomic Hybridisation (aCGH), the significance of deletions, insertions, duplications and complex re-arrangements collectively termed Copy Number Variations (CNVs) was realised (Collins & Mansoura, 2001; Pinkel et al, 1998; Solinas-Toldo et al, 1997). In 2004, two separate studies revealed that CNVs are widespread and represent a significant source of genetic variation within the human genome (Iafrate et al, 2004; Sebat et al, 2004). Current evidence suggests that locus specific rates of CNV formation occur at several orders of magnitude more frequently than SNPs, with estimates of CNV locus-specific mutation rates ranging from 1.7×10^{-6} to 1.0×10^{-4} per locus per generation (Lupski, 2007; Stankiewicz & Lupski, 2010). Consequently, it is now widely appreciated that CNVs contribute to complex sporadic disease and relatively common conditions such as Autism, Schizophrenia, Idiopathic Intellectual Disability and Cancer (de Smith et al, 2007; Redon et al, 2006; Tuzun et al, 2005; Wong et al, 2007).

1.2: Copy Number Variation

CNV's are found in all humans and are defined as DNA segments that are present at variable copy number in comparison to a reference genome, wherein the usual copy number is 2. CNVs are generally >1kb in size and a significant proportion of the human genome (12%) appears to be subject to CNV (Iafrate et al, 2004; Redon et al, 2006; Sebat et al, 2004). CNVs often occur in regions containing, or flanked by, large homologous repeats termed "Low Copy Number Repeats" (LCRs) (Shaw & Lupski, 2004; Stankiewicz & Lupski, 2002). Up to 5% of the haploid reference genome is present in two or more copies and these LCRs are defined as DNA

fragments of 10 to 300 kilobase in size and of ~95-97% sequence identity (Bailey et al, 2001). LCRs may either be in direct or inverted orientation but can also be present in more complex forms consisting of multiple adjacent LCRs in tandem and reverse orientation which provide the structural basis for a variety of rearrangements (Fig.1.1).

The distribution of these CNVs within the human genome is thought to be non-random and several 'hotspots' have been identified. For example, Cooper et al report 250 regions of 1Mb DNA sequence within which >50% of bases are within variants (Cooper et al, 2007). Furthermore, CNVs tend to occur towards centromeres and telomeres which may be due to the repetitive nature of these regions (Nguyen et al, 2006). Despite extensive studies, the total number, size, position, gene content and distribution of CNVs within the human genome remains elusive. To date (June 2013), 66741 distinct benign and pathogenic CNVs have been reported and are catalogued in various databases such as DGV (*T*he *D*atabase of *G*enomic *V*ariants: http://projects.tcag.ca/variation/), DECIPHER (*D*atabas*E* of *C*hromosomal *I*mbalance and *P*henotype in *H*umans using *E*nsembl *R*esources: http://decipher.sanger.ac.uk/) and ECARUCA (*E*uropean *C*ytogeneticists *A*ssociation *R*egister of *U*nbalanced *C*hromosome *A*berrations: http://umcecaruca01.extern.umnc.nl:8080/ecaruca.jsp) (Feenstra et al, 2006; Firth et al, 2009; Swaminathan et al, 2012).

Given the frequency and range of genes incorporated within CNVs it is now appreciated that CNVs make a considerable contribution to human disease. The pathological disorders arising from such genomic rearrangements of regions containing a dosage sensitive gene/s are collectively referred to as 'Genomic Disorders' (Lupski, 1998; Lupski & Stankiewicz, 2005; Turner et al, 2008). In some cases, a change in copy number of a single gene only is thought to underlie specific developmental anomalies. This is exemplified by the duplication of *PMP22* in Charcot-Marie-Tooth Disease type 1A (CMT1A) and the deletion of *RAI1* in Smith-Magenis syndrome (SMS) (Lupski et al, 1992; Roa et al, 1991; Skre, 1974; Slager et al, 2003). In other cases, dosage changes of a contiguous set of genes is thought to contribute to the complex disorder phenotype, for example the 1.5-1.8Mb deletion

in Williams-Beuren syndrome, encompassing ~20-30 genes at chromosome 7q11.23 (Peoples et al, 2000).

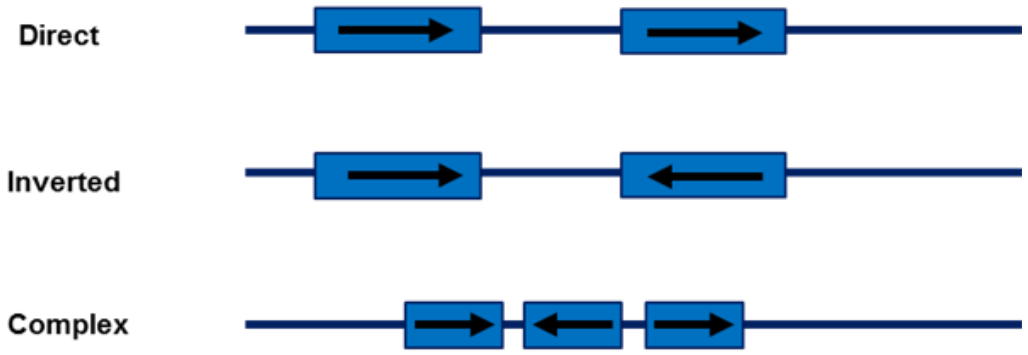

Figure 1.1 - Low copy number repeats (LCRs). Orientations of LCRs can be direct, inverted or complex. LCRs are depicted by blue boxes with black arrows indicating their orientation.

1.3: Recurrent and non-recurrent CNV formation

The mechanisms underlying CNV formation have not yet been fully elucidated but it is apparent that there are different subgroups of CNVs within the human genome. CNVs can be categorized into two principal groups; (i). recurrent, and (ii). non-recurrent. Recurrent CNVs occur in multiple individuals sharing a common breakpoint size and exhibit stable regions flanked by consistent boundaries (Fig 1.2a). In contrast, non-recurrent rearrangements, some which can be highly complex, show more variable breakpoints with a smallest region of overlap (SRO) between affected individuals (Fig 1.2b). These different variant types are thought to occur through recombination-based mechanisms such as homologous/non-homologous recombination and replicative-based mechanisms such as fork stalling and template switching.

1.3.1: Recurrent CNVs: Low Copy Repeats and Non-Allelic Homologous Recombination

Due to the high degree of sequence identity between LCRs, LCRs represent substrates of homologous recombination (HR). In addition complex LCRs, particularly those with inverted repeats, can also form structures such a cruciforms and β-quadriplexes which may trigger rearrangements. Non Allelic Homologous Recombination (NAHR) between region-specific LCRs is a frequent mechanism underlying common recurrent genomic rearrangements (Stankiewicz & Lupski, 2002; Stankiewicz & Lupski, 2010). Misalignment of chromosomes or chromatids as a result of utilising homologous sequences in different chromosomal positions can result in unequal crossing over and subsequent genomic rearrangement. Depending on the location and orientation of the LCRs, the outcome of NAHR between these repeats can vary (Fig 1.3a). Unequal crossing over between non-allelic, directly repeated, homologous sequences located on homologous chromosomes (interchromosomal) results in deletion and/or duplication of the genomic segment between them (Fig.1.3aA). Unequal crossing over between direct LCRs on sister chromatids, termed interchromatid, can also result in deletion and/or duplication (Fig.1.3aB). Intrachromatid NAHR, between

LCRs located on the same chromatid in direct orientation, can result in deletions and the formation of ring chromosomes whereas intrachromatid NAHR between LCRs in inverted orientation can lead to inversion of the intervening sequence (Fig.1.3aC and D).

Importantly, the outcome of NAHR is not limited to these alterations; changes in copy number can convey phenotypes through their impact on gene function such as gene disruption, gene fusions and revealing a recessive allele or positional effect in the context of a deletion (Fig. 1.3b and Table 1.1) (Coman & Gardner, 2007; Henrichsen et al, 2009; Kleinjan & van Heyningen, 2005). Such rearrangements, when involving a dosage-sensitive gene, can impact on activity in complex ways (Veitia & Birchler, 2010). Aside from altering gene dosage of the genes located within the CNV interval, CNVs can also profoundly affect the expression of genes located within their vicinity and this effect can extend to over half a megabase into the neighbouring regions (Henrichsen et al, 2009; Merla et al, 2006).

Interestingly, the NAHR mechanism of CNV formation predicts that for a Genomic Disorder caused by a deletion, there could also be a reciprocal duplication-associated disorder. Indeed, the first reported instance for this was that of the Charcot-Marie-Tooth Disease Type 1A locus on chromosome 17q (Lupski et al, 1991; Raeymaekers et al, 1991). Further examples include DG/VCF syndrome and Smith-Magenis syndrome (McDermid & Morrow, 2002; Potocki et al, 1999; Ricard et al, 2010). However, the frequency of deletion syndromes is higher than that of duplication disorders due to the fact that intrachromatid NAHR can only result in deletion. Table 1.2 lists some examples of deletions and their reciprocal duplication disorders.

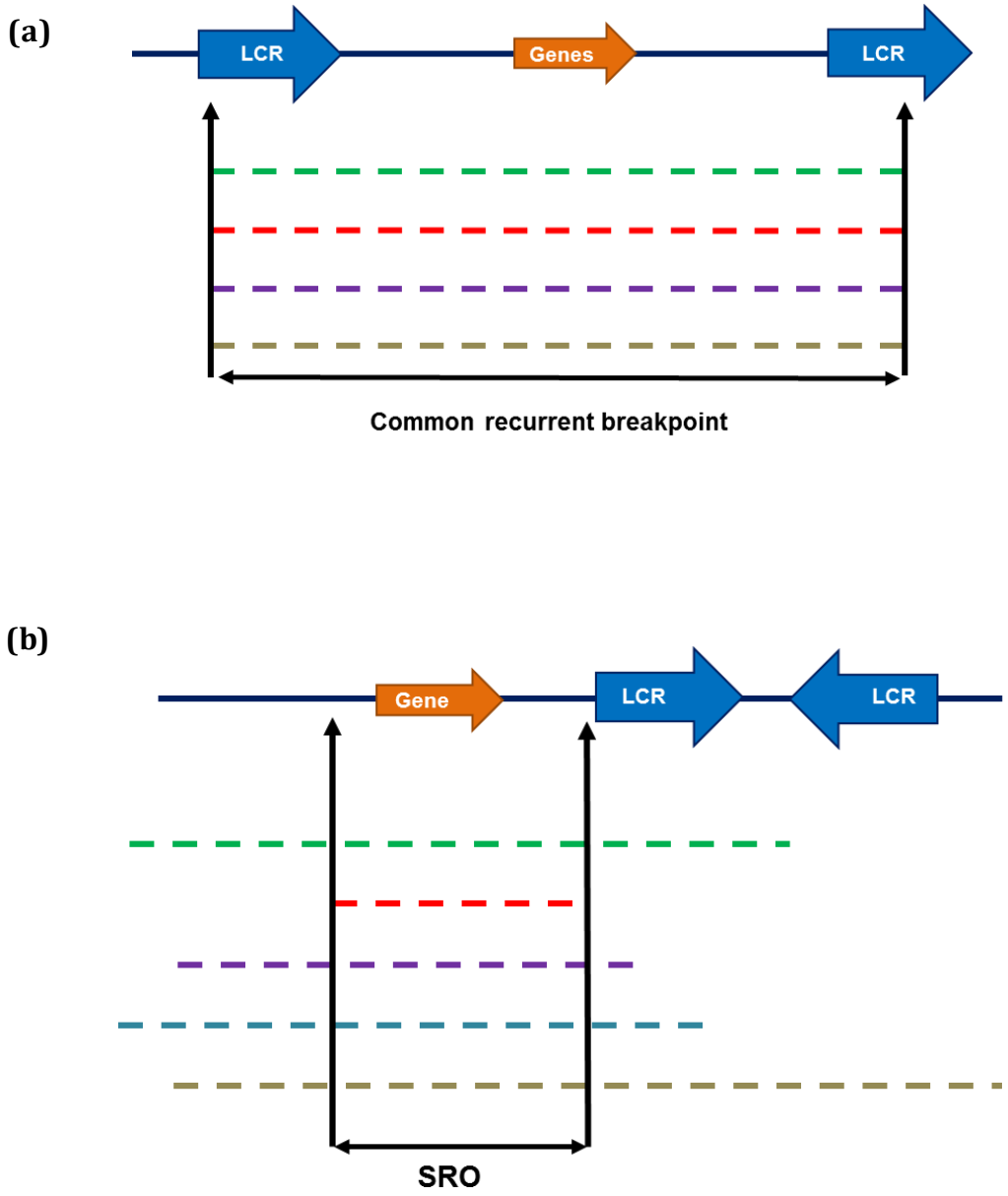

Figure 1.2 – Recurrent and Non-recurrent rearrangements. **(a)** Recurrent rearrangements have same sized deletions/duplication and share breakpoints which map within low copy number repeats (LCRs). The dashed lines represent distinct patients. **(b)** Non recurrent rearrangements have scattering of breakpoints but share a smallest region of overlap (SRO). Sometimes, LCRs are present within the vicinity of the breakpoint. Dashed lines represent distinct patients.

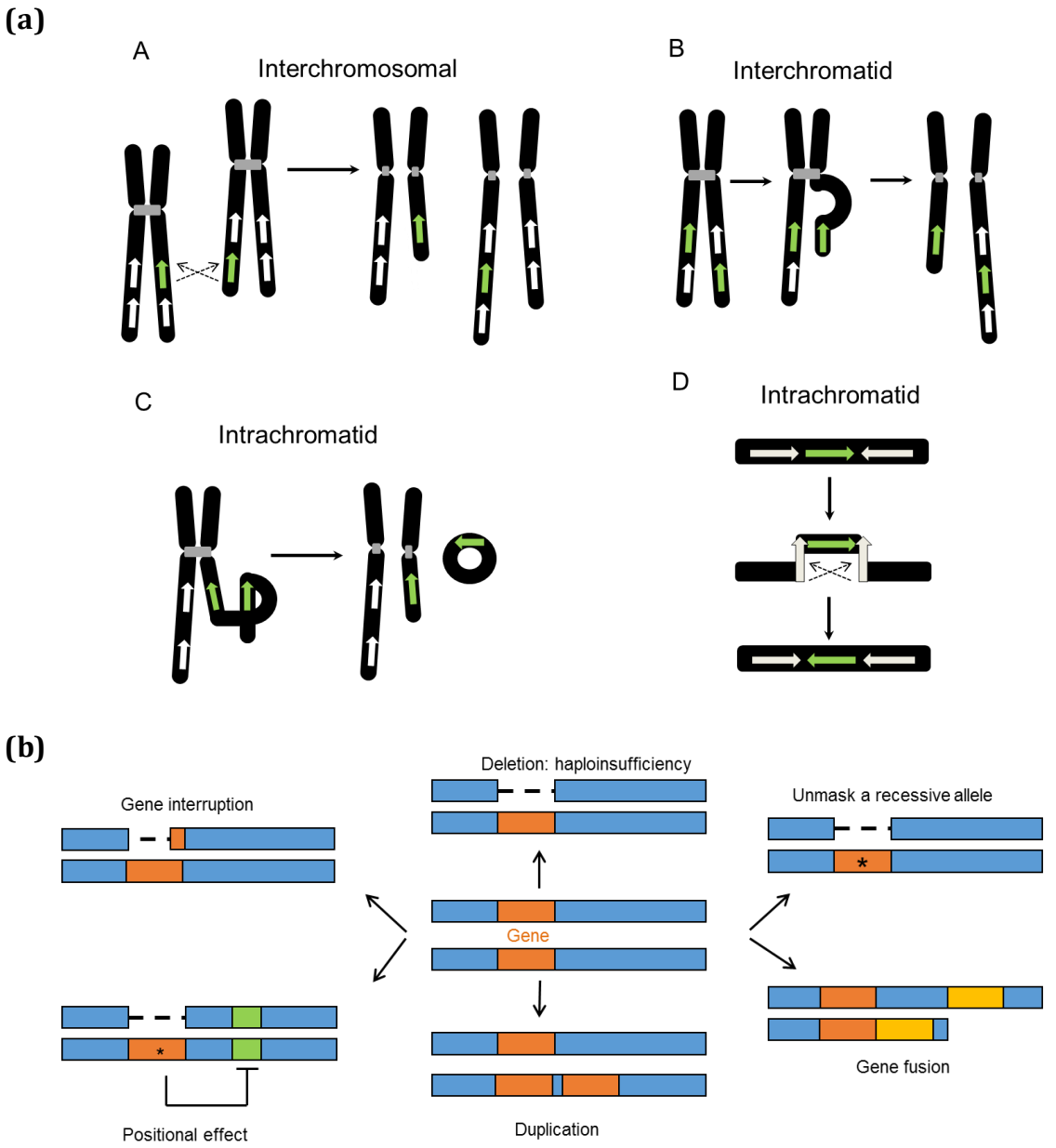

Figure 1.3 – NAHR between LCRs can result in genomic rearrangement. **(a).** Schematic representation of reciprocal duplications and deletions mediated by interchromosomal (A), interchromatid (B) and intrachromatid (C) non-allelic homologous recombination (NAHR) using pairs in direct (A- C) or inverted orientation (D). Chromosomes are shown in black with the centromere depicted by the grey box. The orientation of the LCR is indicated by the direction of the arrow head. Interchromosomal and interchromatid NAHR between directly orientated LCRs results in deletion and duplication (A, B) whereas intrachromatid results only in deletion (C, D). Intrachromatid NAHR between LCRs in opposing orientation can result in re-arrangement (D). **(b)** NAHR can have complex consequences for gene function. NAHR not only results in deletion and duplication but can also impact on gene function through gene interruption, gene fusions, unmasking a recessive allele (asterix) and/or reveal recessive alleles which result in positional effects on the functions of distal genes (green segment).

Table 1.1 - Examples of diseases arising from differing consequences of altered genomic copy number. CMT1A/HNPP; Charcot-Marie Tooth Disease Type 1A/Hereditary Neuropathy with liability to Pressure Palsies.

Mechanism	Affected gene	Disease	Reference
Gene dosage	*PMP22*	CMT1A/HNPP	(Lupski et al, 1992; Roa et al, 1991)
Gene interruption	*Red-green opsin genes*	Colour blindness	(Nathans et al, 1986)
Gene fusion	*CYP11B1/2*	Hypertension	(Lifton et al, 1992)
Position effect	*SOX9*	Campomelic dysplasia	(Velagaleti et al, 2005)
Unmasking a recessive allele	*FXII*	Sotos syndrome	(Kurotaki et al, 2005)

Table 1.2 - Specific examples of copy number variation and the phenotypes (Genomic Disorders) they convey. HNPP; Hereditary Neuropathy with liability to Pressure Palsies, CMT1A; Charcot-Marie Tooth Disease Type 1A.

Phenotype	Locus	CNV	Reference
Williams Beuren Syndrome	7q11.23	Deletion	(Peoples et al, 2000)
7q11.23 duplication syndrome	7q11.23	Duplication	(Berg et al, 2007)
Smith Magenis Syndrome	17p11.2/*RAI1*	Deletion	(Chen et al, 1997)
Potocki-Lupski syndrome	17p11.2	Duplication	(Potocki et al, 2007)
HNPP	17p12/*PMP22*	Deletion	(Chance et al, 1994; Reiter et al, 1996)
CMT1A	17p12/*PMP22*	Duplication	(Chance et al, 1994; Reiter et al, 1996)
Miller-Dieker lissencephaly syndrome	17p13.3/*LIS1*	Deletion	(Cardoso et al, 2003)
Di George Syndrome/VGF	22q11.2/*TBX1*	Deletion	(Edelmann et al, 1999)
Microduplication 22q11.2	22q11.2	Duplication	(Ensenauer et al, 2003)
Schizophrenia	1q21.2, 15q11.2, 15q13.3	Deletion	(Magri et al, 2010; Stefansson et al, 2008)
Alzhiemer Disease	*APP*	Duplication	(Rovelet-Lecrux et al, 2006)
Autism	3q24 16p11.2	Inherited homozygous deletion Deletion/duplication	(Crepel et al, 2011; Shinawi et al, 2010)

NAHR in germ line cells (meiosis) resulting in unequal crossing over can lead to genomic rearrangements that represent benign polymorphisms or manifest as genomic disorders (Lupski & Stankiewicz, 2005; Turner et al, 2008). These genomic disorders can either be inherited or sporadic depending on when the rearrangement was transmitted (Lupski, 2007). One of the best characterised inherited Genomic Disorders caused by NAHR is that of Charcot-Marie-Tooth Disease type 1A, arising from a duplication encompassing the dosage sensitive gene *PMP22,* thus conferring a phenotype (Lupski et al, 1991; Raeymaekers et al, 1991; Roa et al, 1991). Examples of sporadic genomic disorders include Potocki-Lupski syndrome/Smith Magenis Syndrome caused by the duplication/deletion on 17p11.2 respectively. NAHR can also occur in mitosis resulting in mosaicism of somatic cell populations. It is also well appreciated that many cancers are related to genomic rearrangements of somatic cells, some of which are due to NAHR (Darai-Ramqvist et al, 2008; Fridlyand et al, 2006). Genomic disorders which result from somatic rearrangements present with mosaic manifestations, one example is that of *NF1* deletions causing neurofibromatosis (Steinmann et al, 2007).

The knowledge of NAHR between LCRs as a mechanism for CNV generation plays a pivotal role in uncovering novel Genomic Disorders. The recent use of BAC array techniques has enabled the identification of a number of novel genomic disorders caused by NAHR-mediated rearrangements. In a "genome-first" approach, Sharp et al developed a BAC-based array Comparative Genomic Hybridisation (aCGH) pipeline designed to interrogate 130 potential NAHR rearrangement sites or 'hotspots' throughout the human genome (Sharp et al, 2006). Using this approach, they screened patient cohorts with a defined phenotype of Idiopathic Mental Retardation and subsequently identified five novel causative microdeletions (17q21.31, 1q21.1, 15q13, 15q25 and 17q12) (Sharp et al, 2006). Furthermore, the widespread usage of aCGH techniques has also aided the deeper characterisation of many well-known genomic disorders. (Carter, 2007; Cheung et al, 2005; Lee et al, 2007a; Shaffer et al, 2006)

1.3.2: Non-recurrent CNVs and Non-Homologous End Joining

Some genomic rearrangements can be non-recurrent and show scattered breakpoints which share a smallest region of overlap (SRO) in clinically similar patients (Fig. 1.2b) (Gu et al, 2008; Stankiewicz & Lupski, 2002). However, the size of the breakpoint is variable and most non-recurrent CNVs occur at sites of limited homology (2-15bp). The mechanistic basis underlying non-recurrent rearrangements is thought to involve the DNA double strand break (DSB) repair pathway of Non-Homologous End-Joining (NHEJ) (see Fig 1.4). The canonical role of the NHEJ pathway is in V(D)J recombination, the process by which B and T cell receptor diversity is generated in the immune system (Gellert, 2002). During V (D) J recombination, hairpin capped DSBs are created by the RAG1/2 nucleases which cleave the DNA at recombination signal sequences. These are then opened by the Artemis nuclease and joined by NHEJ. This process couples "variable", "diversity" and "joining" regions, which when assembled together create the variable region of a B-cell or T-cell receptor gene. The importance of the NHEJ pathway is highlighted by disorders arising from mutations in NHEJ genes which impart a SCID (Severe Combined Immunodeficiency) phenotype in affected patients (O'Driscoll et al, 2004; Revy et al, 2006) This is due to defective V(D)J recombination and the subsequent inability to produce functional B/T-cells. Several human syndromes are associated with dysfunctional NHEJ such as LIG4 syndrome and XLF-SCID (O'Driscoll et al, 2004; Revy et al, 2006).

Unlike NAHR, NHEJ does not require substrates with extensive homology and the break ends are directly ligated with very little or often no need for homology. NHEJ utilizes short homologous DNA sequences termed 'microhomologies' to guide the repair. These microhomologies are frequently present in the single stranded overhangs on the ends of DSBs. When these overhangs are compatible the break is repaired accurately, however imprecise repair can lead to the loss of nucleotides at the re-joining point leaving a characteristic 'molecular scar' within the breakpoint. Although LCRs are not thought to be involved in the generation of non-recurrent rearrangements, NHEJ may still be stimulated by certain genomic architectures and LCRs are often found within the vicinity of the breakpoints.

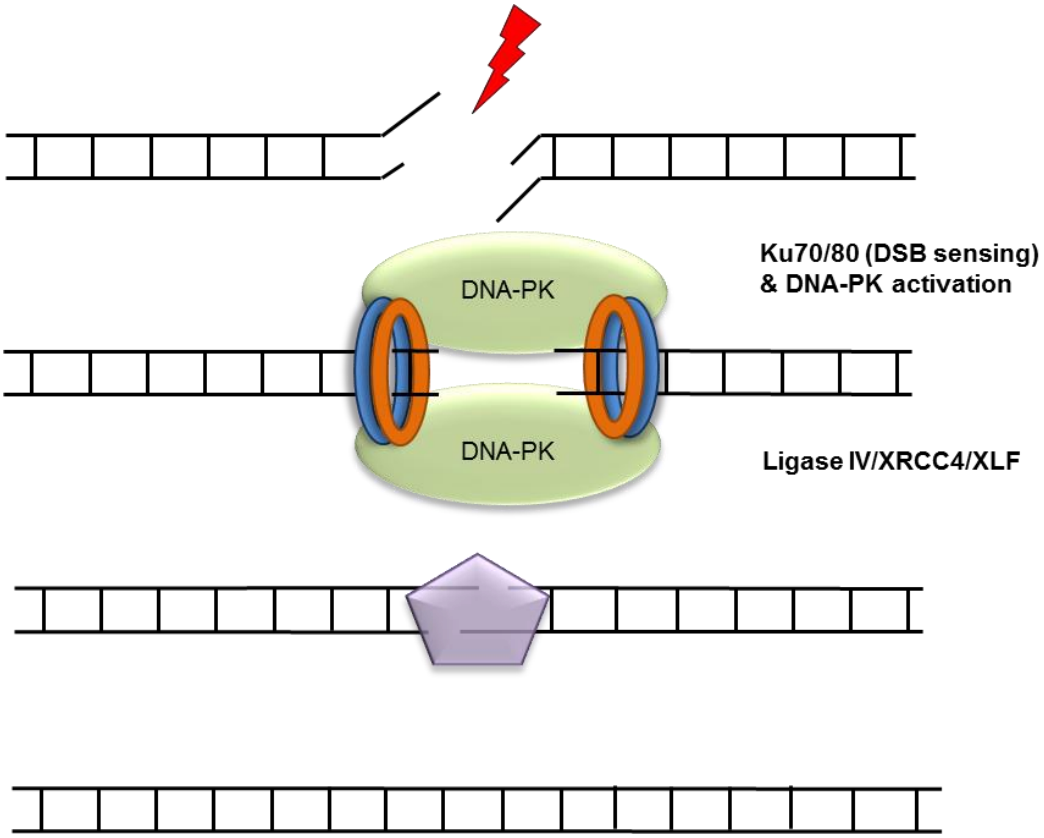

Figure 1.4 – Non-Homologous End Joining. Double stranded breaks (DSB) are sensed by a heterodimer formed Ku70 and Ku80 proteins (blue and orange rings). These Ku proteins have a ring-like structure and are able to bind and stabilize the ends of DSB, acting as sensors. Subsequently, the Ku proteins recruits the transducer kinase, DNA-PKcs (DNA dependent protein kinase catalytic subunit, shown here as a green oval shape). DNA-PK is a large Ser/Thr kinase belonging to the PIKK family (PI3-kinase like family of protein kinases). Once located to the DSB it phosphorylates and activates the NHEJ effector complex – Ligase IV/XRCC4/XLF (purple pentagram shape). The effector complex is responsible for re-joining the two DNA ends. Ligase IV provides the catalytic activity, while XRCC4 stabilizes and stimulates its activity.

1.4 Complex Chromosomal rearrangements

Some CNVs cannot be readily explained by NAHR/NHEJ mechanisms and are therefore termed Complex Chromosomal Rearrangements (CCRs). These CCRs are characterised by multiple breakpoints and exchanges interspersed within regions of normal copy number (Zhang et al, 2009b). Several mechanisms have been proposed to explain the origins of these CCRs including Fork Stalling and Template Switching (FoSTeS), Microhomology Mediated Break-Induced Repair (MMBIR) and the Break-fusion-bridge cycle (BFB) (reviewed in Hastings et al. 2009). I will now describe each in turn:

1.4.1: Fork Stalling and Template Switching

The study of stress-induced amplification of the lac genes using the E.coli system led Slack et al to propose that template switching is not confined to just single replication forks but can also occur between different forks via a process of template switching (Slack et al, 2006). In 2007, Lee et al analysed the junction sequences in patients with Pilizaeus-Merzbacher disease (PMD), an X-linked dysmyelinating disorder caused most frequently by the non-recurrent duplication of the *PLP1* gene (Lee et al, 2007b). Their analysis uncovered evidence for sequence complexity at some junctions consistent with a replication based mechanism which they termed FoSTeS (Fork Stalling and Template Switching). They propose that complex rearrangements associated with PMD, and other nonrecurrent rearrangements, could be explained the FoSTeS mechanism (Lee et al, 2007b). This model proposes that upon stalling of a replication fork the lagging strand disengages and invades another nearby replication fork that shares microhomology (4-15bp). The invading strand anneals via the 3' end and primes its own template DNA synthesis thus causing deletion, duplication, inversion or translocation depending on the position of the other replication fork (Fig 1.5) (Hastings et al, 2009b; Lee et al, 2007b; Slack et al, 2006). Template switching to a downstream fork will result in deletion whereas switching to an upstream fork is causative of duplication. This mechanism of disengaging, invading and synthesising can occur multiple times in series and thus can further add to the complexity of the

rearrangement (x1,x2, x3 etc.). In fact, reanalysis of the breakpoint sequence data of 23 deletion CNVs published by Perry et al found that at least 22% of CNV breakpoints were highly complex and consistent with two or more FoSTeS events (Perry et al, 2008; Zhang et al, 2009c). In addition to the Pilizaeus-Merzbacher disease region on chromosome Xq22, the FoSTeS mechanism has been demonstrated in other genomic regions such as the *MECP2* duplication in Xq28, deletions and duplications in 17p13.3 and deletions and duplications in 17p11.2p12 (Bi et al, 2009; Carvalho et al, 2009; Nagamani et al, 2009; Zhang et al, 2009d).

1.4.2: Microhomology-Mediated Break-Induced Repair

Recently, based on experimental observations from human, bacteria, yeast and other model organisms, the FoSTeS model has been refined into a more generalised replicative template-switch model termed the Microhomology-Mediated Break-Induced Repair (MMBIR) model of CCR formation (Hastings et al, 2009b). MMBIR is based upon the mechanism of Break Induced Repair (BIR) of single double-stranded ends (Hastings et al, 2009a) . When a replication fork encounters a nicked template, the resultant one sided DSB undergoes resection generating a single stranded DNA required to initiate the template switch to a proximal replication fork. When Rad51 function is limiting, classical BIR cannot occur; BIR relies on Rad51 as it involves the invasion of a 3' end into the dsDNA of the repair partner (Davis & Symington, 2004). MMBIR therefore postulates that when strand invasion is limited (Rad51 is down-regulated), the 3' end of the collapsed fork will anneal to any single-stranded template sharing microhomology and in physical proximity (Fig 1.6). For example, this could be the ssDNA in the lagging strand template of another replication fork. This annealing reaction does not rely on Rad51 and requires very little homology, therefore this annealing may occur with the sister molecule either in front of or behind the originating collapsed replication fork leading to deletion ore duplication respectively. Microhomology may also be found on a different chromosome leading to translocation rearrangements whereas annealing with the homologous chromosome as opposed to the sister chromatid could be a cause of extensive loss of heterozygosity (LOH)

(Hastings et al, 2009a). Repeated extension and separation from the template strand may cause several of these changes to occur ultimately forming CCRs. The FoSTeS/MMBIR mechanism represents a major mechanism underlying non-recurrent CNVs and CCRs (Hastings et al, 2009a). Furthermore, it has also been suggested as a mechanism for the formation of LCRs themselves (Hastings et al, 2009b; Zhang et al, 2009a).

1.4.3: The Break-Fusion-Bridge Cycle

The Break fusion bridge (BFB) cycle was originally described by Barbara McClintock more than 60 years ago to explain gene amplification (McClintock, 1951). Replication of a chromosome that has lost its telomeric end due to a DSB can lead to initiation of the BFB cycle (Fig 1.7). After DNA replication, the ends of sister chromatids fuse, giving rise to a dicentric chromosome (i.e. two centromeres). During anaphase the two centromeres will be pulled to the two opposite poles of the mitotic spindle. The dicentric chromosome is then broken leading to the uneven distribution of genetic material between the two products. However, both products still lack telomeres which results in re-initiation of the BFB process, ultimately establishing a cycle (Fig 1.7). The BFB cycle is thought to underlie gene amplification in mammalian cells but may also be of relevance to cancer where large inverted repeats are a common characteristic (Pipiras et al, 1998).

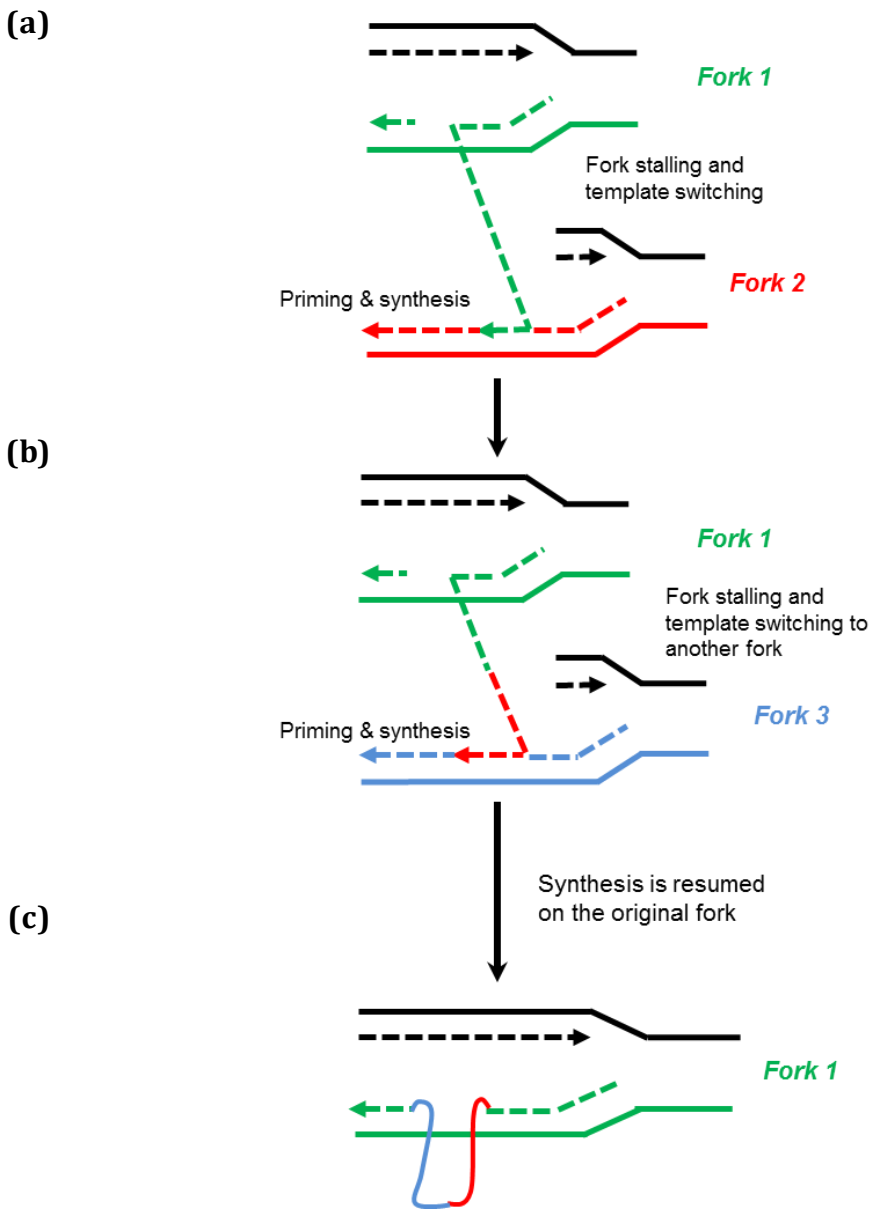

Figure 1.5 – The FoSTeS mechanism of CCR formation. **(a).** FoSTeS: The lagging strand of replication *Fork 1* stalls (green) and disengages. The exposed 3' end may then invade a proximal replication fork that shares microhomology (Fork 2, shown in red) thus causing deletion/duplication/inversion/translocation depending on the position of the other replication fork **(b).** Repeated FoSTeS events further add to the complexity of the rearrangement. If Fork 1 stalls and disengages again, the strand derived from Fork 1, which now also contains material derived from Fork 2, template switches into a distinct fork (Fork 3, shown in blue). **(c)** When synthesis resumes on Fork 1, the extra material derived from forks 1 and 2 contributes to the rearrangement. Each line represents a single DNA strand.

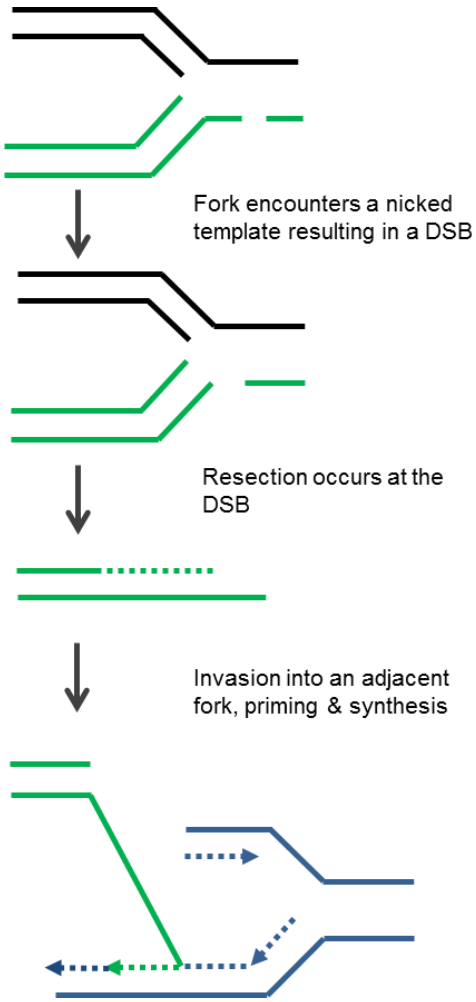

Figure 1.6 – Microhomology mediated Break-induced Repair (MMBIR) model of CCR formation. Replication fork collapse can occur when the fork encounters a nicked template resulting in the formation of a one-sided double strand break (green). This DSB is recessed from the 5' end, generating a 3' tail. This 3' tail (single stranded DNA) can then initiate template switch into a proximal replication fork (blue) sharing microhomology. Each line represents a single DNA strand.

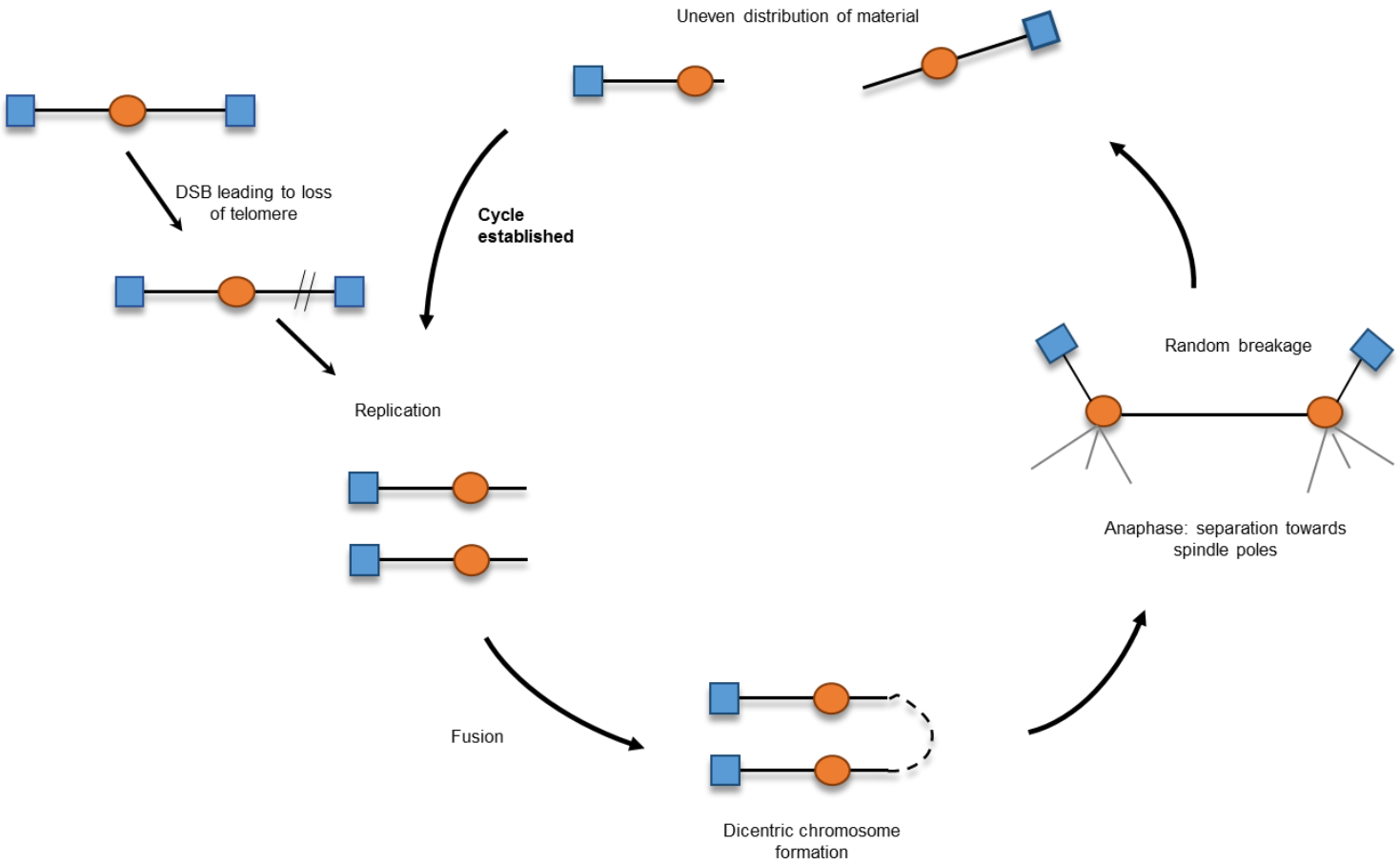

Figure 1.7 – The Break Fusion Bridge Cycle. Centromeres are depicted by orange circles, telomeres by a blue block. A DSB occurs in an unreplicated chromosome leading to loss of its telomere. Following replication, both sister chromatids, lacking telomeres undergo end-fusion forming a dicentric chromosome. During anaphase, the two centromeres of the dicentric chromosome are pulled towards the two opposite spindle poles and the chromosome is broken in a random position. The chromosome once again has an unprotected end (no telomere) and thus a cycle is established and continues until a telomere is acquired from another source.

1.5: CNVs, genome stability and cancer

Until recently, it was not fully appreciated that CNV represents a fundamental contributor to cancer origin and progression. However, over recent years the combined contributions of aCGH and next generation sequence technologies have led researchers to propose several novel pathogenic models of cancer-associated genome instability: *Chromothripsis* and *Kataegis* (Stephens et al, 2011; Taylor et al, 2013). As described in the previous sections, the mechanisms of CNV formation invariably involve DNA repair pathways such as NHEJ and HR. Therefore, if a CNV were to incorporate a gene or genes encoding a protein(s) involved in genome stability and/or the DNA damage response (DDR), this could disrupt those pathways resulting in genome-wide instability. In fact, there is increasing evidence from mouse models that haploinsufficiency of genes encoding key proteins involved in multiple DNA repair pathways are associated with cellular and organismal features (Cabelof, 2012). Furthermore, specific familial cancer predisposition syndromes highlight a pathological association between CNVs and genome stability pathways. For example, deletions incorporating *CHEK2*, an important effector of the ATM apical protein kinase of the DDR, are associated with breast and prostate cancer (Reviewed in Colnaghi et al, 2011).

In 2008, Shlein and co-workers investigated the consequences of compromised genome stability on the CNV landscape in Li Fraumeni Syndrome (LFS) (Shlien et al, 2008). LFS is an autosomal dominantly inherited cancer predisposition syndrome characterized by a strikingly increased risk to early onset of a wide array of malignancies in individuals harbouring germline *TP53* mutations (p53: "The Guardian of the Genome"). The underlying basis of the highly variable clinical phenotype between affected family members has long remained a mystery. Using high density genome-wide oligonucleotide arrays, Shlein and colleagues interrogated the CNV landscape of LFS compared to the normal population. They subsequently found that whilst the number of CNVs within a healthy control population was well conserved, CNV frequency was strikingly increased in these cancer-prone individuals. The authors suggested that this constitutional variation may act as the genetic platform on which more variants build, ultimately leading to

the development of cancer.

1.6: Summary

To conclude, CNVs appear in the human genome at higher locus-specific rates than SNPs and significantly contribute to genetic variation. Sporadic and inherited disorders, common complex traits such as autism and schizophrenia, and disease susceptibility are a result of CNVs. CNV formation can arise from both recombination-based mechanisms such as NAHR and NHEJ and replicative-based mechanisms such as FoSTeS and MMBIR. It is hoped that the widespread use and continuing development of aCGH coupled with the explosive progression in next generation sequencing technology development and application, will significantly contribute to our understanding of both the causes and consequences of genomic structural variation. Moreover, an important step in understanding the biological impact of CNV is to unravel the genotype-phenotype relationships within Genomic Disorders.

The aims of my PhD studies were to investigate the genotype to phenotype relationships of three genomic disorders; *CUL4B*-deleted/mutated X-Linked Mental Retardation (XLMR), 16p11.2 microdeletion/duplication syndrome and Wolf Hirschhorn Syndrome (WHS). In the case of CUL4B-XLMR the CNV involves deletion of the *CUL4B* gene whereas in WHS and 16p11.2 microdeletion/duplication syndrome, the CNV involves a change in 2 or more adjacent genes. All three Genomic Disorders are characterised by neurodevelopmental anomalies such as intellectual disability and developmental delay. They also present with other clinical features such as micro/macrocephaly, seizures, growth retardation and in some cases, distinctive clinical facial characteristics. Understanding the genotype-phenotype relationships in these disorders will not only further the understanding of the biological consequences of distinct CNVs and rearrangements, but may also provide insight into possible therapeutic interventions in the management of such disorders.

Chapter Two

Materials and Methods

2.1: Cell culture

LBLs were cultured in RPMI 1640 (without L-glutamine) supplemented with 2mM L-Glutamine, 500U/ml penicillin, 50µg/ml streptomycin and 15% FCS (foetal calf serum) at 37°C in humidified incubators with 5% CO_2. C2C12 myoblasts and Neuro-2A (N2A) cells were maintained in Dulbecco's Modified Eagle Medium supplemented with 2mM L-Glutamine, 500U/ml penicillin, 50µg/ml streptomycin and 10% FCS. Fibroblast cell lines were cultured in Minimum Essential Medium supplemented with 2mM L-Glutamine, 500U/ml penicillin, 50µg/ml streptomycin and 10% FCS. T98G human glioblastoma cells were cultured in Dulbecco's Modified Eagle Medium supplemented with 10% FBS, 1% Non-Essential Amino Acid (NEAA) and 1% Sodium Pyruvate (NaP), 2mM L-Glutamine, 500U/ml penicillin and 50µg/ml streptomycin. Cell cultures were kept at 37°C in a humidified atmosphere containing 5% CO_2.

For long term storage, cells were pelleted and re-suspended in culture medium containing 10% DMSO. 2ml aliquots were transferred into cryotubes and cooled slowly at -80°C before being transferred into liquid nitrogen towers.

2.2: Antibodies

Antibodies used include; anti-CUL4B (HPA011880), anti-CRBN (HPA045910), anti-α-tubulin (T5168) were obtained from Sigma Aldrich Prestige Antibodies. Anti-MCM2 (sc9839, N19), anti-LETM1 (sc271232, D5), anti-β-tubulin (sc9104, H235), anti-PCNA (sc-56), anti-Parkin (sc136989, H8), anti-AMBRA1 (sc130116, N18), anti-TAO2K (sc47447 and sc366021) and anti-KCTD13 (sc133706) were from Santa Cruz. Antibodies for anti-LC3A (4599, D5OG8), anti-p21 (12D1), anti-p27, anti-Hexokinase 1 (2024, C35C4), anti-phospho-AMPK (2603, 23A3), anti-AMPK (2535, 40H9), anti-ACC (3676, C83B10), anti-phospho-ACC (3661), anti-phospho-p44/42 MAPK (4695,137F5), anti-p44/42 MAPK (9101), anti-phospho-Chk1 (23445, S317), anti-phospho-Chk2 (2661S, T68), anti-phospho-TLK (s695) and anti-TLK (4125) were obtained from Cell Signalling Technology. Anti-FK2 (BML-PW8810-0500) antibody was purchased from Enzo Life Sciences. A second KCTD13 (POLDIP1) antibody was obtained from Abcam (ab32974).

Table 2.1: Cell Lines used in this thesis.

Cell Line	Source/Reference
Fibroblasts	
1BR.3 (WT)	GDSC cell bank
92025337 (*CUL4B*-deleted)	Sent by Bertrand Isidor, Universitare De Nantes, France (Isidor et al, 2010)
Lymphoblasts	
AG03987 (*CUL4B*-deleted)	GDSC cell bank
CV1845	Established from patient blood under contract by The European Collection of Cell Cultures (ECACC), Porton Down, Wiltshire, UK
329-01	Sent by Dr F. Lucy Raymond, CIMR, Cambridge, UK (Tarpey et al, 2007)
83273 (LBL 83)	Obtained from Joris Vermeesch, KU Leuvin, Belgium (Maas et al, 2008)
78522 (LBL 78)	"
88219 (LBL 88)	"
355618 (LBL 355)	"
WHSCR-2 (LBL CR)	Obtained from Prof. Dr. Med. Anita Rauch, University of Zurich, Switzerland (Rauch et al, 2001)
GM04368	Coriell Cell Repositories, New Jersey, USA
GM11907A	"
GM13740	"
09-22	Sent by Dr Evica Rajcan-Separovic, Children's and Women's Health Centre of BC, Vancouver, Canada
06-32	"
12-32	"
12-33	"
12-14	"
12-56	"
Other	
C2C12 (mouse myoblast)	Prof. Simon Morley, School of Life Sciences, University of Sussex, UK
T98G (human glioblastoma)	GDSC cell bank
Neuro-2A (mouse neuroblastoma)	GDSC cell bank

2.3: Reagents

5-Fluorouridine (47580), Bafilomycin A (B1793), valproate (P4543), α-tocopherol (258024), thalidomide (T144), nigericin (N7143) and Ionomycin (13909) were obtained from Sigma-Aldrich (Dorset, UK). All Mitotrackers (M7512, M7514, M36008), Cell ROX red (C10422), JC-1 (M34152) and Calcium-1 AM (C3012) probes were obtained from Life Technologies (Paisley, UK).

2.4: siRNA knockdowns

Stealth (Life Technologies) siRNAs were designed against the 3'UTR region using the BLOCK-IT™ RNAi designer (Life Technologies, Paisley, UK). Oligos (20nmol) were resuspended in 1ml of DPEC-treated water to a final concentration of 20μM. Transfections were performed with 2 x 10μL (2 x 40nM) of siRNA against *Cul4b* or 1 x 5μL (20nM) of siRNA against *LETM1*, using Metafectene Pro (Biontex). Transfections were performed in T25 flasks in the presence of 5mls of the appropriate growth medium.

Cul4b (mouse): 5'-AUAUAAGGUACGAUGGAAGGAACUG-3'

LETM1 (human): 5'- CCACAGAAUCGUGUCUGGAUCCACA-3'

SMARTpool siRNAs (a mixture of 4 distinct oligonucleotides) against *Letm1* (L-049478-01-0005, mouse) and *Crbn* (L-048249-01-0005, mouse) were obtained from Thermo Scientific. ON-TARGETplus SMARTpool siRNAs (5nmol) were resuspended in 250μL of DPEC-treated water to a concentration of 20μM. Transfections were performed in T25 flasks with 1 x 5μL (20nM) siRNA against *Letm1* or 2 x 10μL (2 x 40nM) against *Crbn* using metafectene pro (Biontex). Sense targeting sequences are:

Letm1: **(1)** AGGUAGACAACAAGGCGAA, **(2)** CCAACAACUUCCUGCGUUU,
(3) CUAAAUAGUCGGGUGACAUA, **(4)** CUGCCUAAUUCAUGAGUAA.

Crbn: **(1)** GAAAAGUGUAAGUACGUAA, **(2)** GAUCUAUGCCUAUCGAGAA,
(3) GGAUGGAAAUUUACAGCCA, **(4)** GACCAGUAUUCAUGUAAAU.

2.5: Extract preparation:

2.5.1: Urea-based whole-cell extracts

Cell pellets were washed 2X in PBS and stored immediately at -20°C or lysed in 50µL-100µL (unless otherwise stated) of urea-based lysis buffer. Whole cell extracts were obtained following lysis in urea buffer (9M urea, 50mM Tris-HCl at pH 7.5 and 10mM 2-β-mercaptoethanol), followed by a 12 second sonication, 30% amplitude to solubilize. Protein concentration was determined using the Bradford assay at a UV absorbance of 595nm. Samples were then stored at -20°C or immediately boiled in 2X SDS-loading buffer (5% SDS, 10% glycerol, 10% 2-β-mercaptoethanol, pH 6.8 and 0.2% bromophenol blue) and loaded onto SDS-PAGE gels.

2.5.2: Soluble extracts (for immunoprecipitation)

Soluble extracts were obtained following treatment with detergent lysis buffer. Cell pellets were incubated in IP buffer [50mM Tris-HCl, pH 7.5, 150mM NaCl, 2mM EDTA, 2mM EGTA, 25mM NaF, 25mM β-glycerolphosphate, 0.1mM Na-orthovanadate, 0.2% Triton-X-100, 0.3% IPEGAL and protease inhibitor cocktail tablets (Roche) for one hour on ice. Protein concentration was determined using the Bradford assay at a UV absorbance of 595nm (Bio-Rad). Samples were then stored at -20°C or immediately boiled in 2X SDS-loading buffer (5%SDS, 10%glycerol, 10% β-mercaptoethanol, 125mM Tris-HCl, pH 6.8 and 0.2% bromophenol blue) and loaded onto SDS-PAGE gels.

2.5.3: Mitochondrial extracts - µMACS Isolation Kit

Mitochondrial extracts were obtained using the Miltenyi Biotech Human Mitochondrial Isolation Kit (Miltenyi Biotech, UK: Cat no – 130-094-532). 10^7 cells were lysed using the buffer provided and homogenized using a glass mini-stokes homogenizer, with 10-15 strokes per sample on ice. Lysate was incubated with Anti-TOM22 MicroBeads for 1 hour at 4°C with gentle shaking (Miltenyi Biotech). An LS column was placed in the magnetic field of a QuadroMACS separation unit and the lysate was then applied to the LS column (Miltenyi Biotech). Once the lysate had run through, the column was washed 3 times with the supplied buffer before being removed from the magnetic field and placed on a collection

tube/ependorff. The magnetically labelled mitochondria were then eluted and centrifuged at 13,000g for 2 minutes to pellet them. The mitochondria pellet was resuspended in 60µL urea lysis buffer and sonicated for 15 seconds at 30% amplitude to give a pure mitochondrial extract. Samples were then stored at -20°C or immediately boiled in 2X SDS-loading buffer (5%SDS, 10%glycerol, 10% β-mercaptoethanol, 125mM Tris-HCl, pH 6.8 and 0.2% bromophenol blue) and loaded onto SDS-PAGE gels.

2.6: Immunoprecipitation

For immunoprecipitation, 400µg of soluble cell extracts was used. Following IP, reactions were incubated with 40µL Dynabeads (100-04D, Life Technologies) for 1 hours on a rotating wheel at 4°C, magnetically recovered and eluted at 95°C using 30µL SDS-PAGE sample loading buffer. Proteins were separated on a 10% SDS-PAGE gel and immunoblotted using semi-dry transfer (BioRad) onto a PVDF membrane.

2.7: 5-Fluorouridine incorporation and indirect immunofluorescence

Well-proliferating cells were pulse labelled with 2mM 5-Fluorouridine for 0-15 minutes. Cells were pelleted and resuspended in 1ml 75mM KCl and left at room temperature for 10 minutes to allow the cells to swell. Cells were pelleted by centrifugation and the supernatant removed by aspiration. Pellets were resuspended in 100µL 3.7% paraformaldehyde and incubated for 10 minutes. The supernatant was aspirated and samples were stored in 70% ethanol at 4°C until processing. ¼ of each sample was cytospun onto a Poly-Lysine coated slide at 500-700 rpm for 5-7 minutes. Cells were lysed in 100-200µL of 0.2% Triton-X100/PBS for 1 minute and then washed in PBS. Cells were blocked for 10 minutes in 100-200µL of BSA/PBS and then washed 1X PBS. 150µL of primary antibody (mouse monoclonal anti-BrdU, Sigma) was added to the slide and left for 25 minutes at room temperature following by 1X PBS wash. The secondary antibody (FITC/Cy3 labelled) was added at a 1:200 dilution and left for 25 minutes in the dark following by 1X PBS wash. DAPI was added directly to the slides at a 1:50,000 dilution of a 1mg/ml stock and left for 5 minutes in the dark. Following 3X PBS

wash, slides were mounted using Vectashield and coverslips sealed with nail polish. Slides were then stored in the dark until further analysis.

2.8: Agarose-formamide gel electrophoresis

TAE/formamide electrophoresis was performed in 1.2% agarose gels containing 1 X TAE buffer (0.04M Tris-acetate, 1mM EDTA). Before electrophoresis RNA samples were mixed with deionized formamide in the amount giving a final concentration of at least 60% (v/v) formamide, with 1/10 sample volume of 10X loading dye (50mM Tris-HCl, pH 7.6, 0.25% bromophenol blue, 60% glycerol) and 1µL ethidium bromide. Samples were denatured by heating at 65°C for 5 minutes and immediately chilled on ice for 5 minutes. Samples were loaded onto the gel and electrophoresis was performed at a voltage gradient of 5 V/cm

2.9 Semi-quantitative duplex PCR

To measure the mtDNA content in WT and *CUL4B*-deleted LBLs, total DNA was extracted. Primer sets for two mtDNA-encoded genes, ND2 and 16S RNA, were used for PCR analysis, together with a primer set for the nuclear DNA-encoded gene, 18s (Life Technologies). 500ng of template (DNA) was used and the PCR cycle consisted of; 3 minutes at 94°C, 25 x 30 seconds at 94°C, 30 seconds at 56°C, 1 minute at 72°C and a final step of 8 minutes at 72°C. PCR products were electrophoresed on a 1% (w/v) agarose gel, stained with 0.5µg ethidium bromide, and visualised with an UV transilluminator. mtDNA content was assessed by determining the ratio of ND2:18s RNA and 16s:18s RNA by scanning and comparing intensities using Image J.

Table 2.2: Primers used for PCR.

18S Forward	5'-TAGAGGGACAAGTGGCGTTC-3'
18S Reverse	5'- CGCTGAGCCAGTCAGTGT-3'
16S Forward	5'-CCAATTAAGAAAGCGTTCAAG-3'
16S Reverse	5'- CATGCCTGTGTTGGGTTGACA-3'
ND2 Forward	5'- CTAGCCCCCATCTCAATCATA-3'
ND2 Reverse	5'-GAATGCGGTAGTAGTTAGGAT-3'

2.10: Mitochondrial function; MitoTrackers

Cells in suspension i.e. LBLs were pelleted by centrifugation and resuspended in pre-warmed growth medium containing the Mitotracker Red/Green/SOX probe (250nM). Cells were incubated for 15 minutes under growth conditions. After staining, cells were washed once in PBS. Cells were then resuspended in 500µL 1X PBS and filtered into BD FACS falcon tubes for immediate flow cytometry analysis using the BD FACS Canto flow cytometer. For microscopy based analysis of Mitotracker Red/Green, cells were resuspended into 600µL PBS and ¼ of the sample was cytospun onto a poly-lysine slide for microscopy based analysis.

Attached cells (C2C12, T98G, and N2A) for microscopy-based analysis were grown on coverslips in a 6 well dish until 60% confluent. Cells were then incubated with 250nM Mitotracker probe for 15 minutes and then washed in PBS. Cells were stained with DAPI and the coverslips were then mounted onto Poly-lysine slides for visualization using the Zeiss Axiovert microscope. For flow cytometry-based analysis, attached cells were incubated with 250nM of the Mitotracker probe (Red, Green/SOX) and washed once with PBS. Cells were then trypsinised or detached using a cell scraper and filtered into a BD FACS falcon tube for flow cytometry analysis using the BD FACS Canto flow cytometer.

2.11: Mitochondrial membrane potential; JC-1

For each sample, 1 x 10^6 cells were suspended in 1ml of warm 1X PBS and stained with 2µM JC-1 (5,5' -6,6'-tetraethylbenzimidazol-carbocyanineiodide)(Molecular Probes) and incubated under growth conditions for 30 minutes. To confirm that the JC-1 probe was responding to changes in mitochondrial transmembrane

potential, cells were incubated with 50µM CCCP (supplied with the kit) simultaneously with JC-1. Cells were then pelleted by centrifugation and resuspended in 500µL 1X PBS and immediately analyzed using a BD FACS Canto flow cytometer.

2.12: Complex I activity

Extracts were made according to the manufacturers protocol (Abcam, cat #: ab109720) and varying amounts of protein were then loaded into the wells of a 96-well plate. Once the dipstick had been incubated with the various buffers supplied in the kit, as per the protocol, 300µL of deionized water was added to stop the reaction. The dipsticks were then dried and the intensity of the Complex I capture mAb band (~7mm from the bottom) was scanned using a flat-bed scanner and the signal intensity measured in Image J.

2.13: MitoProbe Transition Pore Assay

For *CUL4B*-LBLs; LBLs were resuspended in pre-warmed HBSS/Ca^{2+} at a final concentration of 1 x 10^6 cells/ml. 6 x 1ml aliquots were prepared per cell line (Tubes 1-6). 10nM calcein AM was added to all 6 tubes, $CoCl_2$ was added to tubes 2-5, 500nM ionomycin was added to tube 3 only, 50nM ionomycin was added to tube 4, 5nM ionomycin was added to tube 5 and 0.5nM ionomycin was added to tube 6. Samples were incubated for 15 mins at 37°C, protected from light. Cells were pelleted by centrifugation, resuspended in 500µL 1X PBS and filtered into BD FACS Falcon tubes for flow cytometry analysis. Samples were analysed using 488nm excitation and emission filters appropriate for fluorescein. A sample containing no added reagents was used for instrument set up.

For WHS-LBLs; LBLs were resuspended in pre-warmed HBSS/Ca (Hanks balanced Salt Solution with Ca^{2+}) at a final concentration of 1 x 10^6 cells/ml. 3 x 1ml aliquots were prepared per cell line (Tubes 1-3). 10nM calcein AM was added to each tube, 400µM $CoCl_2$ was added to tubes 2 and 3 and 500nM ionomycin was added to tube 3. Samples were incubated for 15 mins at 37°C, protected from light. Cells were pelleted by centrifugation, resuspended in 500µL 1X PBS and filtered into BD FACS

Falcon tubes for flow cytometry analysis. Samples were analysed using 488nm excitation and emission filters appropriate for fluorescein. A sample containing no added reagents was used for instrument set up.

2.14: Calcium measurements

Cells were incubated with 10μM Calcium-1 AM probe (C-3012, Life Technologies) for 20 minutes under normal growth conditions. Cells were then washed with 1X PBS, resuspended in 500μL PBS and filtered into BD FACS Falcon tubes. Flow cytometry analysis was performed using 506/531nm excitation/emission filters.

2.15: *LETM1* overexpression

T98G human glioblastoma cells were transfected with 2μg of a plasmid encoding *LETM1* (pCMV6-XL4), purchased from OriGene, in the presence of 5μL Metafectene Pro (Biontex) under normal growth conditions. Cells were harvested 24 hours post transfection for flow cytometry, microscopy or Western blot-based analysis.

2.16: *LETM1* complementation

T98G cells were transfected with 30nM *si*RNA against *LETM1* in the presence of 5μL Metafectene Pro (Biontex) ± 2μg plasmid encoding *LETM1* under normal growth conditions. T98G controls were either treated with Metafectene Pro only, *si*RNA only, or the cDNA construct only. 24 hours post transfection, cells were incubated with 250nM MitoSOX and analysed by flow cytometry using the BD FACS Canto. To determine the efficiency of the *si*RNA-mediated knockdown and cDNA construct addback, cell were pelleted and washed twice in PBS and then resuspended in urea-based lysis buffer. Protein concentration was determined using the Bradford assay and 50μg of whole cell extract in 2X SDS loading buffer were boiled for 5 minutes. Samples were electrophoresed on an 8% SDS-PAGE gel followed by standard Western blot analysis.

2.17: S-phase progression

Logarithmically growing LBLs were pulse labeled for 30 minutes with 20μM BrdU. Colcemid (100μg/ml) was added to stop cells from cycling and BrdU incorporation

was monitored every two hours for up to 6 hours. Cells were then fixed with ice-cold ethanol (100%) and left overnight at -20°C. Samples were then spun at 2500g for 10 minutes at 10°C and the pellet was resuspended in 1ml of 2M HCl/PBS/Triton X-100 drop-wise. Samples were then incubated at room temperature for 30 minutes. Samples were spun at 2500g for 10 minutes at 10°C and the pellet resuspended in 1ml of 0.1M $Na_2B_4O_7x10H_2O$ pH 8.5 (Borax) to neutralise the acid. Samples were spun again at 2500g for 10 minutes at 10°C and the pellet was resuspended in 500µL 1% BSA/0.05%Tween20/PBS. 10µL of anti-BrdU-FITC was added to each sample and incubated for 30 minutes in the dark at room temperature. Samples were washed once with 1%BSA/0.05%Tween20/PBS and once with 600µL PBS/0.05%Tween20 + 5µg propidium iodide (PI) + 30µL RNase. Samples were stored at 4°C until FACS analysis.

2.18: Recovery after HU treatment

LBLs were treated with 250µM HU for up to 6 hours. S-phase efficiency was measured every two hours by incubating with 20µM BrdU for 30 minutes prior to the end of the time point. Cells were fixed in ice cold ethanol (100%) and left overnight at 20°C. Samples were prepared as above and stored at 4°C until FACS analysis.

Chapter Three

X-Linked Mental Retardation and CUL4B; a pathomechanistic dissection of the impact of *CUL4B* deletion in human patient-derived cells

3.1: Introduction

Mental Retardation (MR) or as it is now more frequently termed; Intellectual Disability (ID) (Schalock et al, 2007), is a lifelong disability which places heavy demands on society and the health service. From here on, in accordance with the referenced literature, I will use the originally designated term 'MR' rather than ID. There are three criteria that must be met when defining MR;

1. There must be significant sub-average general intellectual functioning, defined by the intelligence quotient, IQ.
    a. IQ of 50-70; Mild MR
    b. IQ of 35-49; Moderate MR
    c. IQ of 20-34: Severe MR
    d. IQ of <20; Profound MR
2. This must be accompanied by limitations in adaptive functioning in at least two areas such as self-care, health, social skills, communication; this refers to how well an individual copes with the common demands of life.
3. The onset must occur before the age of 18.

MR affects approximately 1-3% of the population, with it being ~3 fold more common in males due to many mutations being found on the X chromosome (Leonard & Wen, 2002). Approximately 16% of mutations are X-Linked leading to X-Linked Mental Retardation (XLMR) which can be classified as either syndromic or non-syndromic, whereby patients may or may not exhibit other clinical features aside from MR such as ataxia, short stature and distinct facial features (Chiurazzi et al, 2008). Figure 3.1 summarises the genes found on the X chromosome reported to cause XLMR, some of which are known to encode proteins that function in the ubiquitin proteasome pathway of protein degradation (Fig 3.1 - circled in red).

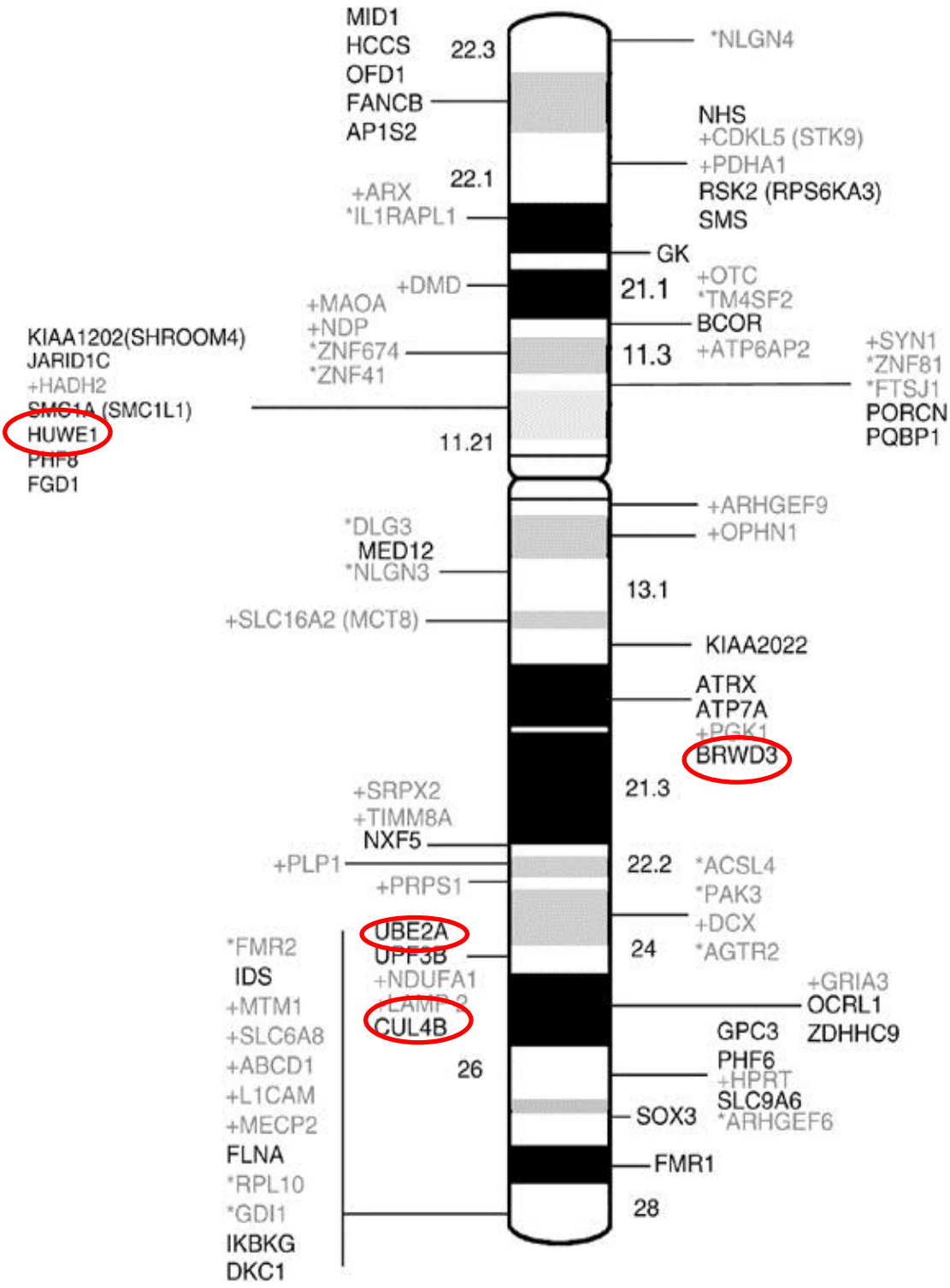

Figure 3.1 - An ideogram of the X chromosome with the position of 82 known XLMR genes. Adapted from Chiurazzi et al, 2008. Those genes in black cause syndromes characterized by multiple congenital abnormalities and defects, those in grey with a + cause neuromuscular conditions but no malformations and those in grey with * cause nonspecific (MRX) conditions where MR is the only consistent clinical manifestation among individuals. Those genes highlighted by red circles encode proteins known to be involved in the ubiquitin pathway.

3.1.1: The ubiquitin-proteasome pathway of protein degradation

Many neurodevelopmental disorders such as Angelman's Syndrome (UBE3A deficient) Alzheimer's and Parkinson's disease (various mutations) are associated with disruption to the ubiquitin-proteasome pathway (UPS) resulting in the altered degradation of target proteins. The UPS is a fundamental cellular mechanism for regulating protein activity and is therefore important in a variety of cellular processes. These include the regulation of cell cycle and division, involvement in the cellular response to stress, modulation of cell surface receptors and DNA repair (discussed further in section 3.1.1.1) and the regulation of neuronal morphogenesis. The UPS serves both proteolytic and non-proteolytic functions and the distinction between the two pathways is achieved through either mono (usually regulatory) or poly-ubiquitination (usually degradative) of target substrates on specific lysine residues. The conjugation of ubiquitin, a highly conserved 76-amino acid residue polypeptide, to a protein substrate proceeds through a cascade mechanism (Fig 3.2);

1. Activation of ubiquitin through a two-step reaction involving an E1-ubiquitin activating enzyme. The E1 enzyme activates the C-terminal glycine residue of ubiquitin which facilitates the transfer of ubiquitin to the active site of the E1 enzyme. This results in a thioester linkage between the C terminal of ubiquitin and the cysteine sulphydryl group of the E1.

2. One of several E2-ubiquitin conjugating enzymes then transfers the active ubiquitin to the substrate which is bound by a member of the E3 ubiquitin ligase family. In this step, the transfer of ubiquitin can either be directly to the E3-bound substrate or via an additional E3-ubiquitin high-energy thiol ester intermediate. It is the specific combination of E2 and E3 enzymes that creates a plethora of enzymatic capability in this pathway.

3. The final step creates an isopeptide bond between a lysine side chain of the target protein and the C-terminal glycine of ubiquitin in an E3 ligase-dependent manner. Polyubiquitin chains typically serve as a recognition

marker for degradation pathways whereas a monoubiquitin chain usually serves regulatory roles on the substrate.

4. Following conjugation, free and reusable ubiquitin is released by the action of deubiquitinating isopeptidases which liberate ubiquitin from its substrate.

The organisational structure of the UPS appears hierarchical, where a single E1 activates the ubiquitin required for all modifications and can subsequently transfer the ubiquitin to several E2 enzymes. E2 enzymes then act in concert with E3 ligases where E2's can transfer the ubiquitin to one or several E3 proteins. The human genome contains four E1 enzymes, 21 E2 enzymes and numerous E3's which can take many forms; HECT (*Homologous to E6-associated protein C-Terminus*), U-box or RING domain (*Really Interesting New Gene*). Figure 3.3 illustrates the various E1, E2 and E3 enzymes identified to date by the Kyoto Encyclopaedia of Genes and Genomes (KEGG) pathway database (www.kegg.jp/kegg/pathway.html).

3.1.1.1: The role of ubiquitin in the DNA Damage Response

The ubiquitination of proteins has emerged as an important regulatory mechanism impacting on the DNA damage response (DDR). Many DDR repair and checkpoint pathways utilise the ubiquitin system in their response to genotoxic lesions highlighting the importance of functional cooperation between E3 ligases in genome maintenance and stability (Jackson & Durocher, 2013; Stone & Morris, 2013). The ubiquitin system has key roles in the assembly of repair and signalling proteins at sites of double-strand DNA breaks (DSBs). Specifically, DSB's are detected by the Mre11-Rad50-NBS1 (MRN) complex (de Jager et al, 2001; Panier & Durocher, 2009). The MRN complex initiates the DNA damage signalling response through a direct interaction with ATM resulting in its autophosphorylation and activation. Active ATM then functions to phosphorylate a wide set of proteins including the histone H2A variant H2AX on Ser139, forming γH2AX (Fernandez-Capetillo et al, 2004). This phosphorylated form of H2AX is recognised by MDC1

(mediator of DNA damage checkpoint), which through a direct interaction with ATM and NBS1 forms a positive feedback loop amplifying the γH2AX signal (Lou et al, 2006; Stewart et al, 2003; Stucki et al, 2005). In addition, MDC1 itself is phosphorylated in an ATM-dependent manner leading to the recruitment of RING finger protein 8 (RNF8) to the double strand break (DSB) site (Kolas et al, 2007; Mailand et al, 2007). Chromatin bound RNF8 cooperates with UBC13 (ubiquitin conjugating enzyme) to mediate the ubiquitination of histone H2A and H2AX (Mailand et al, 2007; Wu et al, 2009). RNF8 also interacts with the giant HECT type E3 ligase HERC2 through its FHA domain (N-terminal forkhead-associated) which acts to stabilise the RNF8/UBC13 interaction (Bekker-Jensen et al, 2010). Ubiquitinated histones are recognised by a second E3; RNF168 which functions to amplify the local concentration of lysine 63-linked ubiquitin (UbK63) conjugates at DNA lesions. It does so by promoting the formation of UbK63 conjugates and the recruitment of additional repair proteins (Doil et al, 2009). RNF8-RNF168 mediated ubiquitination is critical for the recruitment of downstream checkpoint and repair proteins such as BRCA1 and 53BP1 (Doil et al, 2009; Stewart, 2009; Wang & Elledge, 2007). BRCA1 does not contain any ubiquitin binding motifs itself but interacts with Abraxas and RAP80 to accumulate at DSB sites (Wang et al, 2007). BRCA1 also associates with the RING domain protein BARD1, to form an active E3 ligase complex crucial for DNA repair (Morris & Solomon, 2004).

The importance of the RNF8-RNF168 pathway is demonstrated by biallelic mutations in the *RNF168* gene which cause a complex disorder originally termed RIDDLE (radiosensitivity, immunodeficiency, dysmorphic features and learning difficulties) (Stewart et al, 2009; Stewart et al, 2007). However, a more recent report identified an individual with a homozygous truncating mutation of *RNF168* (Devgan et al, 2011). Interestingly, this patient did not present with the previously characterised RIDDLE syndrome but displayed ataxia, ocular and bronchial telangiectasia in addition to microcephaly, short stature and low IgA (Devgan et al, 2011). The authors proposed that the difference between this case and the previous case reported by Stewart and colleagues was due to the absence of both MIU (*M*otif *I*nteracting with *U*biquitin) domains in this second patient. In this same year, an *Rnf168*-/- mouse model was generated where *Rnf168*-deficient mice

exhibited immunodeficiency, increased radiosensitivity and defective spermatogenesis (in male mice) (Bohgaki et al, 2011). This mouse model has thus provided evidence for a role of RNF168 in V(D)J and class switch recombination, the processes responsible for B and T cell receptor diversity within the immune system (Bohgaki et al, 2011).

DNA damage checkpoints function to arrest or slow down cell cycle progression in response to DNA damage allowing time for repair of the damaged DNA or controlled engagement of programmed apoptosis pathways. Two classes of ubiquitin ligases; the SCF (SKP2/Cul1/F-box) and the APC/C (Anaphase-promoting complex) complexes, regulate cell cycle progression and are therefore linked to checkpoint control (Cardozo & Pagano, 2004). One example of an SCF complex is the SCF $^{\beta TrCP}$ complex which is important for the DNA damage-induced degradation of CDC25A, resulting in CDK inhibition and cell cycle arrest (Mailand et al, 2000). The APC functions to regulate exit from the mitotic phase of the cell cycle and controls entry into S-phase (Sullivan & Morgan, 2007). All of the above examples provide insight into the fundamental roles of the ubiquitin-mediated cascade pathway in regulating DNA damage repair.

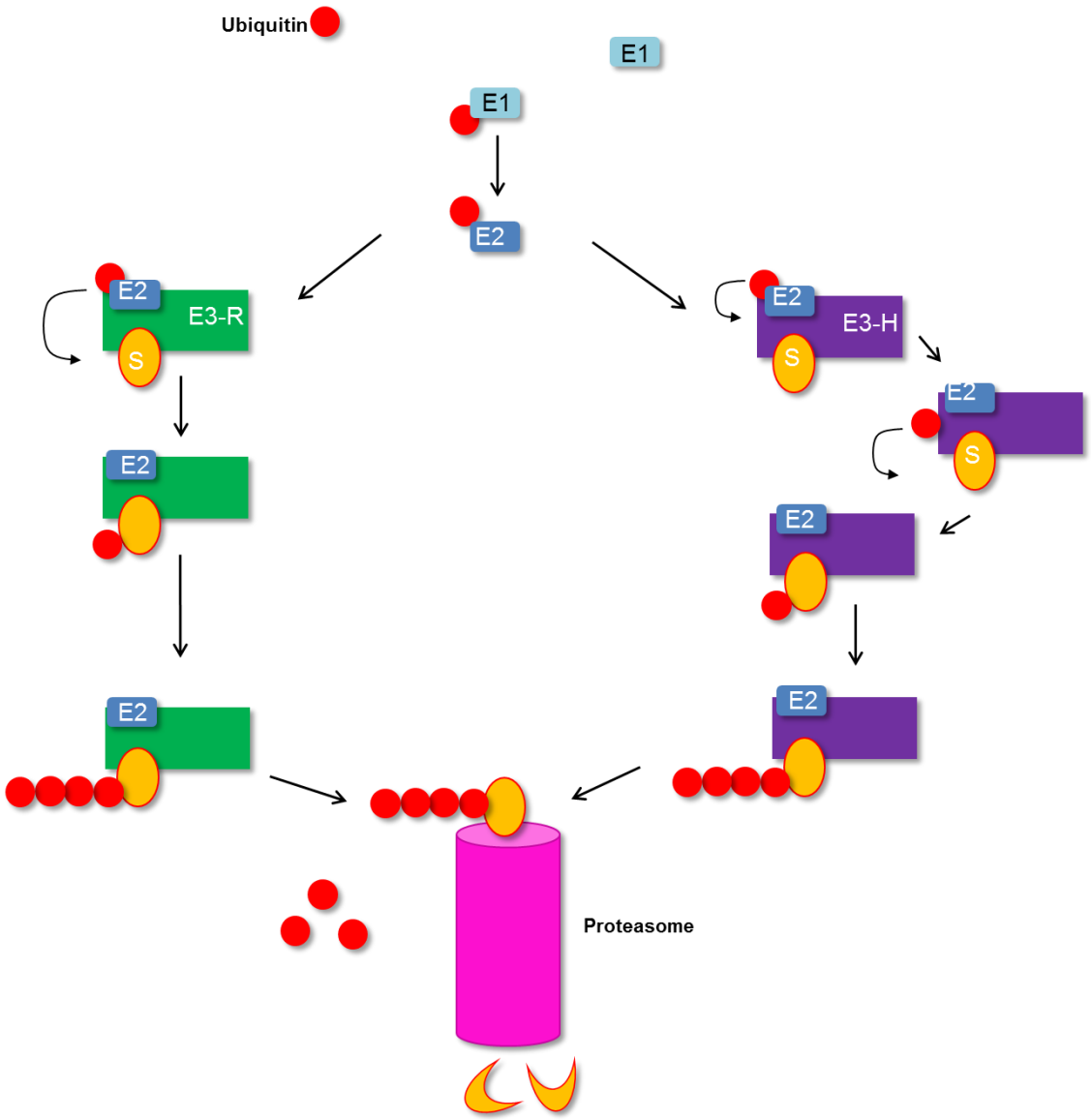

Figure 3.2 - Schematic illustration of the ubiquitin-proteasome pathway of protein degradation. Activation of ubiquitin is achieved by an E1 enzyme, an E2 then transfers the ubiquitin to the substrate (S) bound by an E3. RING E3's (E3R) directly transfer the ubiquitin to the substrate whereas HECT E3's (E3H) act as an adaptor molecule by bringing the target and the E2 into close proximity to allow ubiquitination of the target substrate. Multiple ubiquitin molecules are attached forming a polyubiquitin chain and the substrate is subsequently directed the 26S proteasome for degradation.

Figure 3.3 - Members of the E1, E2 and E3 families of enzymes. To date, four E1 ubiquitin-activating enzymes and 21 E2 ubiquitin conjugating enzymes have been identified. Numerous E3 ubiquitin ligases have been reported which can possess HECT, U-box or RING finger domains and these have specificity to their substrates. The RING finger type E3s can be further categorised into two groups; simple or multisubunit. The multisubunit RING-type E3s are exemplified by cullin-RBX E3s and APC/C. RING-type E3s consist of a RING-finger-containing subunit RBX1 or RBX2 that functions to bind E2s, a scaffold-like cullin backbone, adaptor proteins and a substrate binding receptor. The CUL4-containing E3 ligase complex family is highlighted in green.

3.1.2: The Cullin family of E3 ligases

E3 ubiquitin ligases are a diverse group of proteins characterised by defining motifs. The HECT (*Homologous to E6-associated protein C-terminus*) domain E3 ligases form a catalytic intermediate with ubiquitin and then directly transfer ubiquitin to the substrate, whereas RING and U-Box domain E3 ligases facilitate ubiquitination by acting as an adaptor molecule. They do so by bringing the E2 enzyme and the target substrate into close proximity to promote ubiquitination of the target (See Fig 3.2; E3H vs. E3R). The Cullin family of proteins encode the subunits for several RING domain E3 ligases involved in a series of ubiquitin-protein ligase complexes regulating the programmed degradation of various cellular proteins including p21 and CDT1 (Abbas et al, 2008; Nishitani et al, 2006).

Although cullins do not contain a RING domain themselves, they can bind to small RING proteins; ROC1 and ROC2 (*ROC; Ring of Cullin*) which then form the basis of a Cullin-Ring E3 Ligase (CRL) (Deshaies, 1999). Cullins also rely on substrate receptors, attached to the cullin backbone by a 'linker' protein, as they cannot bind their substrates directly (Fig 3.4). There are seven CUL isoforms (CUL-1, -2,-3, -4A, -4B, -5 and -7) and the very wide functional diversity of this class of enzyme is based on their interactions with various adaptor proteins and substrate specific receptors (Petroski & Deshaies, 2005b) and Fig 3.4). Cullin ligases are regulated by the CAND1-NEDD8 cycle in which CAND1, a 120kDa protein, negatively regulates cullins by preventing the binding of the adaptor protein and therefore preventing subsequent binding of substrates. Cullins are covalently modified by the addition of Nedd8 which dissociates CAND1. Once the polyubiquitinated substrate is degraded by the 26S proteasome, the COP9 signalosome is involved in the removal of Nedd8, allowing CAND1 to re-associate with the cullin and thus inhibition is resumed (Liu et al, 2002; Pan et al, 2004; Zheng et al, 2002a).

In humans, CUL4 exists as two closely related paralogues: CUL4A and CUL4B. They are over 80% identical however CUL4B possesses a unique amino acid terminal extension whose function is still largely unknown. CUL4 differs from other cullins in that it interacts with the WD40-like repeat containing protein, DDB1, at its N terminal which acts as an adaptor protein (Angers et al, 2006; He et al, 2006;

McCall et al, 2005). DDB1 was originally identified as DNA damage binding protein due to its interactions with DDB2 to recognise UV-induced DNA lesions and employ the NER pathway to remove and repair the DNA damage (Chu & Chang, 1988). CRL4's have been shown to play important roles in NER via the ubiquitination of histones, CSB, XPC and DDB2, where DDB1 can act either as a direct substrate receptor or an adaptor protein to bind specific substrate receptors (Dai & Wang, 2006; Hannah & Zhou, 2009). The substrate receptors conferring the specificity of CRL4-containing E3 ligase complexes are still being identified however the identification of over 60 novel DCAFS (DDB1 and CUL4 associated factors) as putative substrate receptors implicates the CUL4-DDB1 complex in a wide and expanding variety of fundamental processes, ranging from DNA repair to transcription and translation (Lee & Zhou, 2007).

Recently, Cereblon (CRBN) was identified as a component of a CRL4 complex involving CUL4 and DDB1 (Ito et al, 2010). *CRBN* encodes a protein containing a domain with 50% similarity to the ATP-dependent Lon protease family involved in the regulation of mitochondrial replication and transcription. Mutations in *CRBN* have been associated with a form of non-syndromal X-Linked Mental Retardation (Higgins et al, 2004b), the relevance of which will be discussed in further detail in Chapter 4. At present, approximately 20 CUL4 ligase substrates have been reported but it is likely that there are numerous unidentified substrates (Table 3.1). Many of the known substrates to date are involved in the cell cycle and the DNA damage repair pathway (NER) but newly identified substrates play a role in non- DNA repair pathways such as sex-hormone signalling and the mTOR pathway (Ghosh et al, 2008; Hu et al, 2008b; Ohtake et al, 2007) (discussed later in Section 3.1.4)

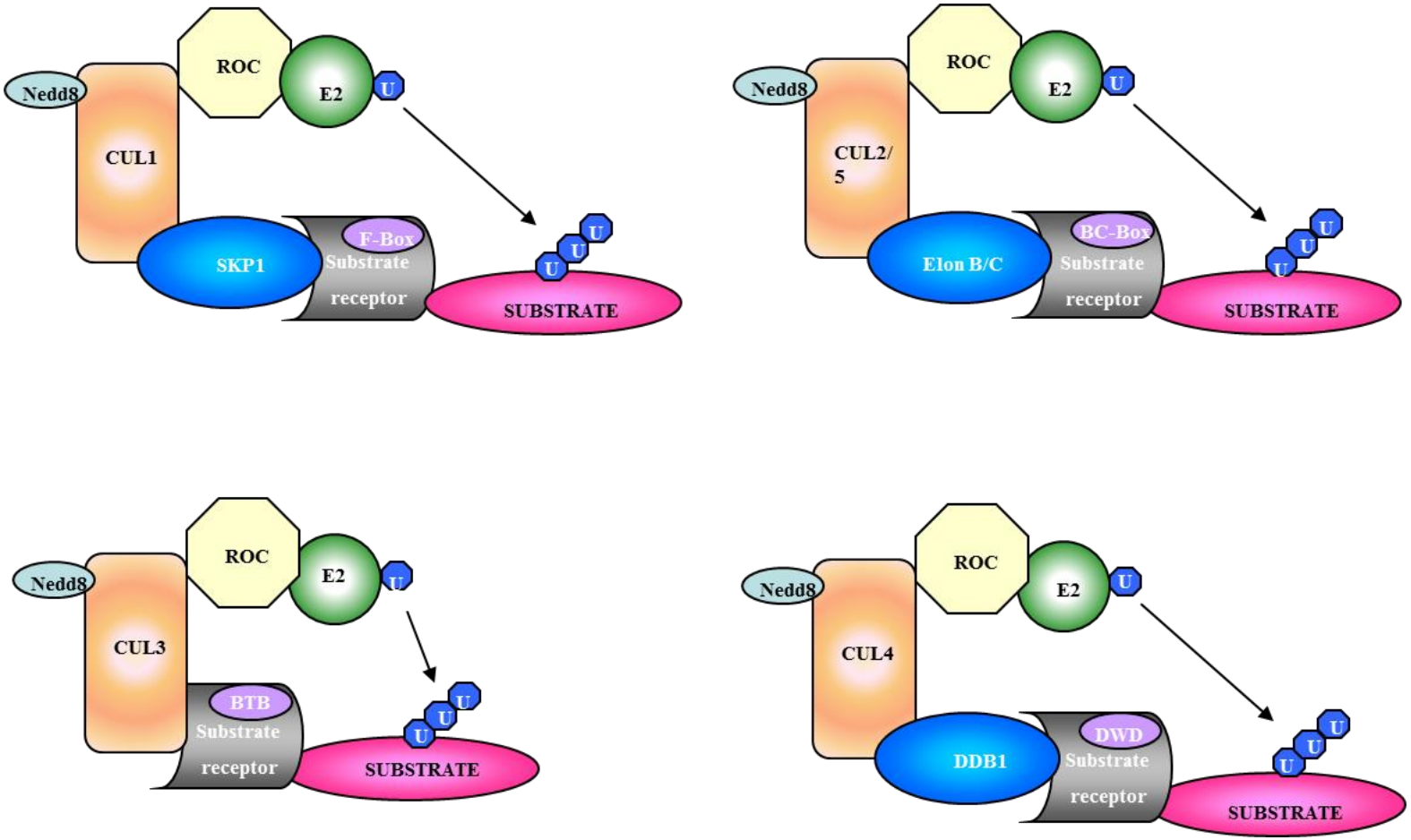

Figure 3.4 - Modular assembly of the cullin-RING ligase 4 containing E3 ubiquitin ligase (CRL4). The N-terminal interacts with DDB1 and the terminal domain binds with a small RING protein (RBX1 or ROC) which recruits an E2 enzyme to transfer ubiquitin to the substrate. DDB-1-Cullin-associated factors (DCAFs) associate with DDB1 to confer substrate specificity and further specificity is determined by substrate receptors. Over 60 novel DCAFs have been identified implicating CRL4's in a variety of fundamental processes. CUL4 is regulated by neddylation (NEDD8) (Kerzendorfer et al, 2011). U; Ubiquitin, Elong B/C: Elongin B/C, ROC: Ring of Cullin, DDB1: DNA Damage Binding protein 1, SKP1: S-phase Kinase-associated protein 1.

Table 3.1 – Some of the known CRL4 substrates identified to date (*Homo sapiens)*; those which are CUL4B specific are indicated by purple text.

Substrate	Function	Reference
CDT1	DNA replication	(Higa et al, 2003; Nishitani et al, 2006; Zhong et al, 2003)
p21	CDK inhibitor	(Abbas et al, 2008; Kim et al, 2008b; Nishitani et al, 2008)
p27	CDK inhibitor	(Higa et al, 2006; Li et al, 2006)
Merlin	Tumour suppressor	(Huang & Chen, 2008)
UNG2	Uracil DNA glycosylase	(Schrofelbauer et al, 2005)
SMUG	Uracil DNA glycosylase	(Schrofelbauer et al, 2005)
Histone H2A, H3, H4	Chromatin formation	(Kapetanaki et al, 2006) (Wang, Zhai et al. 2006)
XPC	Nucleotide Excision Repair	(El-Mahdy et al, 2006)
DDB2	Nucleotide Excision Repair	(El-Mahdy et al, 2006)
TSC2	mTOR pathway	(Hu et al, 2008a)
STAT 1,2, 3	Transcription factor	(Ulane & Horvath, 2002)
ER-alpha	Oestrogen receptor	(Ohtake et al, 2007)
c-Jun	Proto-oncogenic TF	(Wertz et al, 2004)
HOXA9	Development	(Zhang et al, 2003)
CHK1	Cell cycle checkpoint	(Leung-Pineda et al, 2009)
GRK5	Serine/threonine kinase	(Wu et al, 2012)
Beta-catenin	Development; Wnt signalling	(Tripathi et al, 2007)
WDR5	Histone modification	(Nakagawa & Xiong, 2011)
Peroxiredoxin III	Mitochondrion-ROS scavenger	(Li et al, 2011)
CSN5	COP9 signalosome complex	(He et al, 2013)

3.1.2.1: Mouse models of CRL4 deficiency

CUL4A

Previously, a *Cul4a* knock out mouse deleted for exon 1 was reported to be embryonically lethal leading to the suggestion that CUL4A and CUL4B are non-redundantly functionally distinct (Li et al, 2002). However, this has recently been challenged by Liu et al who reported a viable *Cul4a* knockout mouse created by targeting exons 17-19 (Liu et al, 2009). It was suggested that the previous report of embryonic lethality could be explained by the additional, unanticipated and mistargeted disruption of the adjacent gene *Pcid2*, a gene essential for the proteasome. Unexpectedly, these *Cul4a* $^{-/-}$ mice displayed no gross phenotypic abnormalities however they exhibited dramatic *resistance* against UV-induced skin tumourigenesis (Liu et al, 2009). It was argued that *Cul4b* may in part compensate for the loss of *Cul4a* in mice due to the observation of rapid loss of viability resulting from silencing of *Cul4b* in *Cul4a*$^{-/-}$ mice. Independently of the above studies, Kopanja et al also generated a different *Cul4a*$^{-/-}$ mouse model by deleting exons 4-8 (Kopanja et al, 2009). Embryonic fibroblasts (MEFs) showed severe deficiency in cell proliferation after deletion of *Cul4a* and this therefore indicates that *Cul4a* is required for efficient cell proliferation, control of centrosome amplification and thus genome stability. Furthermore those cells also exhibit *sensitivity* to UV irradiation however the reasons underlying the differences observed between the various reported *Cul4a*$^{-/-}$ mouse models are unclear. More recent work has identified an essential role for *Cul4a* in spermatogenesis and male fertility (Kopanja et al, 2011).

CUL4B

Although many reports have suggested that CUL4A and CUL4B are functionally redundant and can compensate for each other's loss; the one caveat to this is that there are clinically affected *CUL4B*-mutated and *CUL4B*-deleted XLMR patients (Kopanja et al, 2011; Sarikas et al, 2011; Tarpey et al, 2007a; Zhou). The existence of this essential clinically severe condition indicates that CUL4A cannot

redundantly compensate for CUL4B loss in humans supporting a distinct role for CUL4B in cognitive and physical development. Whilst human CUL4B XLMR patients live to adulthood, *Cul4b* knockout mice die as early as E7.5. Liu et al generated mice with targeted disruption of *Cul4b* (*Cul4b*$^{-/Y}$) and observed embryonic lethality consistent with the lethality observed upon inactivation of the *Cul4b* by gene trapping (Cox et al, 2010; Liu et al, 2012). They reported a differential expression of *Cul4a/b* in extra-embryonic tissue and suggested that the embryonic lethality during early post-implantation development is due to defects in extra-embryonic tissues which express low levels of *Cul4a (Liu et al, 2012)*. In contrast the epiblast expresses both *Cul4a* and *Cul4b* which allows *Cul4a* to compensate for the loss of *Cul4b* and maintain viability of the embryo proper. Liu et al further showed that epiblast-specific deletion of *Cul4b*, achieved by crossing *Cul4b*$^{f/y}$ or *Cul4b* $^{f/f}$ mice with Sox2-Cre, prevented embryonic lethality giving rise to viable *Cul4b* null mice (Liu et al, 2012). Interestingly, these mice displayed no overt developmental abnormalities although behavioural and neurological analyses were not reported for this particular model. However, these results do suggest an important role for *Cul4b* during the early developmental stage.

In the same year, Chen et al also generated a viable *Cul4b* mouse model using the exact same strategy previously employed by Liu et al (Chen et al, 2012). However in addition, they provided the first detailed behavioural, neurochemical and morphological features of adult *Cul4b*$^{-/-}$ mice *(Cul4b*$^{\Delta/Y}$). *Cul4b*$^{\Delta/Y}$ mice appeared phenotypically normal but displayed specific impairments in spatial learning and memory as well as increased seizure susceptibility (Chen et al, 2012). *Cul4b*$^{\Delta/Y}$ mice also displayed a decrease in parvalbumin- (PV) positive GABAergic interneurons in the hippocampus implying a PV-neuron-mediated decline of inhibitory regulation in the dentate gyrus which may permit disorganised neuronal firing. In addition, Chen et al further reported altered morphometric features in hippocampal neurons of *Cul4b*$^{\Delta/Y}$ mice such as reduced dendritic complexity and spine density. They suggest that these alterations may disrupt conduction of neural signals along dendrites and affect transmission and integration of synaptic inputs in *Cul4b*$^{\Delta/Y}$ mice. These alterations may account for the hippocampus-dependent learning deficits and increased epileptic susceptibility

seen in this mouse model. This report of a viable *Cul4b* null mouse, which models the core syndrome of *CUL4B*-patients, is a major advance that could potentially improve our understanding of the pathological and physiological functions of CUL4B which may underlie the aetiology of this disorder.

3.1.3: CUL4B X-Linked Mental Retardation

Interestingly, no disorder associated with *CUL4A* mutations has been reported to date, however mutations in *CUL4B* have been identified as causative of X-Linked Mental Retardation (XLMR). It is conceivable, considering the CRL4 substrates described, that a human disorder arising from a *CUL4* mutation may display some clinical overlap with NER-defective conditions such as Xeroderma Pigmentosa and Cockayne Syndrome. However, as mentioned no such syndrome in humans has been described.

As discussed previously in Section 3.1, many mutations associated with MR are found on the X chromosome. Identification of the causal genes for X-Linked Mental Retardation (XLMR) is challenging. However, a large project aiming to identify the genes associated with XLMR found mutations in *CUL4B* by sequencing the entire X chromosome in 250 families with XLMR (Tarpey et al, 2007b). *CUL4B,* as described previously, encodes an E3 ubiquitin ligase whose function has previously been linked to Nucleotide Excision Repair (NER) (Guerrero-Santoro et al, 2008). Mutations were found in 8 of the 250 families screened, one of which was originally identified by Cabezas *et al* (Cabezas et al, 2000); representing the most common identified genetic cause of syndromal XLMR to date (Fig 3.5). Simultaneously a nonsense mutation in *CUL4B* was reported by Zou *et al* in an XLMR family in the same year (Zou et al, 2007). Patients with *CUL4B* mutations exhibit a syndromal form of mental retardation thereby exhibiting other clinical features aside from MR including; growth retardation, sexual development problems, motor neuron impairment and muscle wasting (Table 3.2 and Fig 3.5). Recently the first report of a patient with a genomic deletion incorporating *CUL4B* was published, suggesting total loss of CUL4B is compatible with life (Isidor et al, 2010) (Fig. 3.6a, 3.6b). Nevertheless, the male patient reported showed similar

signs to those possessing a mutation in the gene: syndromic MR, hypogonadism and ataxia. More recently, Ravn et al reported a 29kb deletion involving *CUL4B* in a Danish monozygotic (MZ) twin pair (Fig 3.6c and Table 3.2) (Ravn et al, 2012). This is the smallest deletion to date involving *CUL4B;* providing further evidence that complete loss of CUL4B function is compatible with viability, with severe and pleiotropic features (Ravn et al). Table 3.2 compares the clinical features of the various patients discussed above.

The genotype-phenotype relationships in this condition are unexplored and are largely unclear, based on the previously described role of CUL4-containing E3 ligases in Nucleotide Excision Repair. *CUL4B*-mutated/deleted patients exhibit overlapping clinical features with other diseases such as Spinocerebellar Ataxia with Axonal Neuropathy (SCAN-1), Mitochondrial Depletion syndrome (MD) and androgen- related disorders such as Kennedy Disease and Androgen Insensitivity Syndrome (AIS). Overlapping clinical features include ataxia, seizures, sexual development problems and evidence of peripheral neuropathy. Growing evidence reporting interactions of CUL4B with components of various crucial pathways such as the mTOR signalling pathway, support a role for CUL4B in development and provide clues as to the underlying aetiology of specific features of this disorder (Ghosh et al, 2008; Ohtake et al, 2007; Zhao et al, 2012)

3.1.4: CUL4A and CUL4B are functionally distinct; identification of CUL4B-specific substrates

Much of the literature to date does not functionally distinguish between CUL4A and CUL4B, however recently a number of CUL4B-specific substrates have been identified. CUL4B-containing E3 ligases have been implicated in various cellular pathways including the regulation of dioxin-dependent aryl-hydrocarbon receptor (AhR) signalling, regulation of the mTOR signalling pathway, degradation of Peroxiredoxin III and also in the regulation of neuronal gene expression through ubiquitination of WDR5 (See Table 3.1 purple text). It is conceivable that the mis-regulation of these substrates could begin to explain the patient phenotypes seen

in this disorder. In the subsequent sections I will speculate upon some of these potential associations.

(a)

(b)

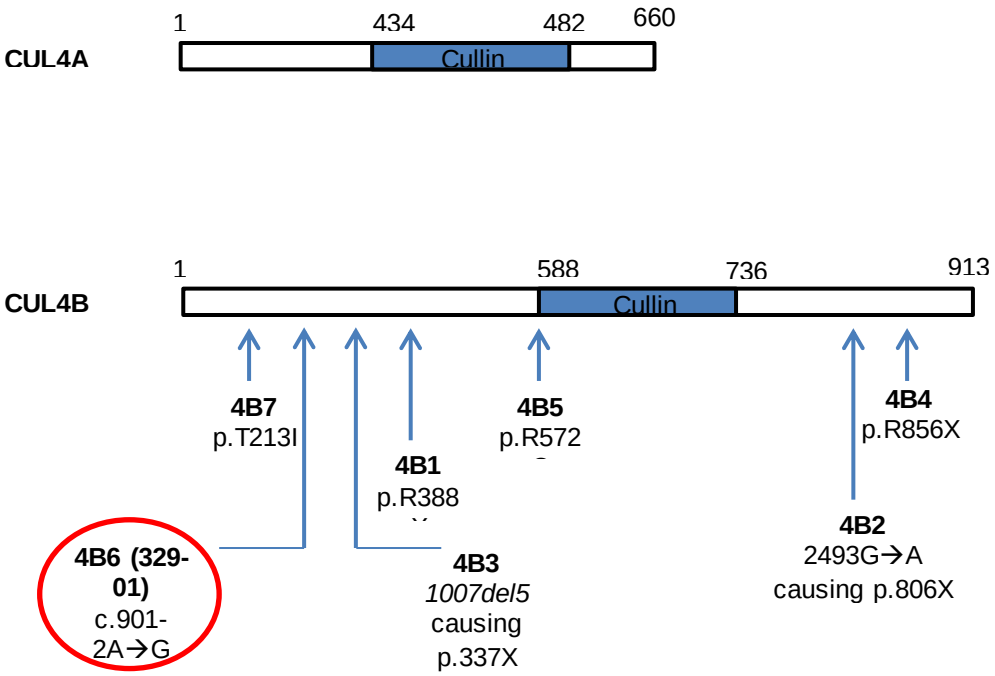

Figure 3.5 – *CUL4B*-mutated XLMR patients: (a) Patients identified by Tarpey et al, 2007 showing abnormalities of the feet, obesity, kyphosis, micropenis and gynaecomastia, (b) A summary of the various pathogenic mutations in CUL4B identified by Tarpey et al, 2007. The p.R388X alteration has also been reported in a second patient by Zou et al, 2007. The mutation highlighted by the red circle indicates the patient cell line used to interrogate aspects of transcription and translation in the context of CUL4B-deficiency in the results section 3.2.1.

(a)

(b)

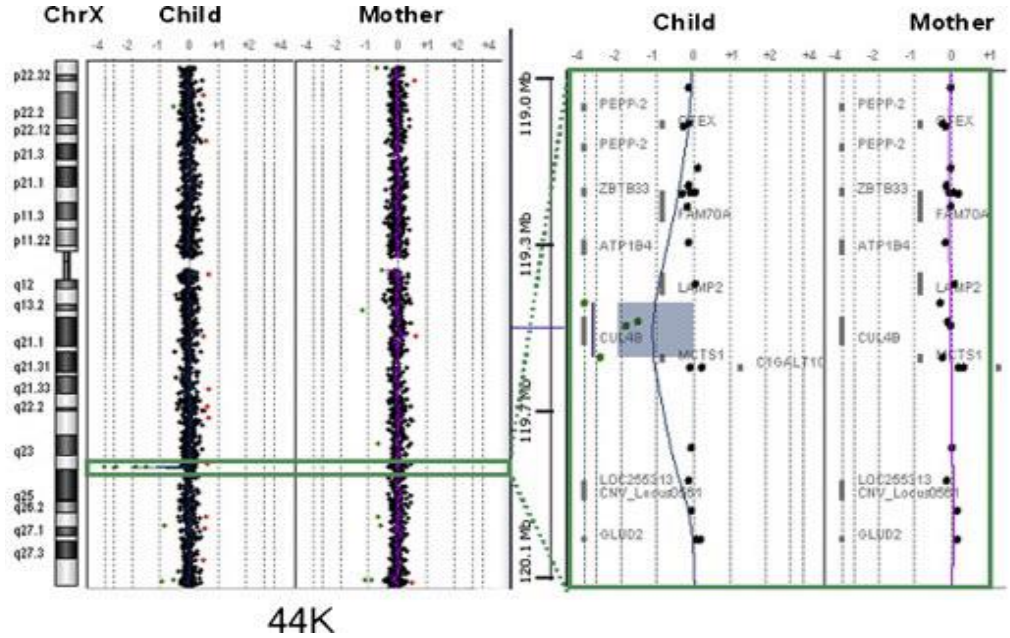

(c)

Figure 3.6 – *CUL4B*-deleted XLMR patients (a) Facial appearance of a *CUL4B*-deleted patient reported by Isidor et al 2010 (b) Agilent 44K array-derived profile of chromosome X from this deleted patient. A detailed view of the region of interest is shown, the abnormal genomic region is shaded in blue (taken from Isidor et al, 2010) (c) MZ twin pair at age 14 showing short stature, central obesity and characteristic facial dysmorphism as reported by Ravn et al 2012.

Table 3.2 – Comparative summary of the clinical features between various CUL4B XLMR patients described in the literature, to date. NR; not reported.

Clinical Feature	8 families (Tarpey et al, 2007b)	1 patient (Isidor et al, 2010)	MZ twins (Ravn et al, 2012)
Motor delay	5/5	+	+
Speech delay	18/18	+	+
Seizures before 2 years of age	8/11	-	+
Height in adulthood <10th percentile	7/11	+	+
Head circumference >97th percentile	8/11	-	+
MR	22/22	+	+
Impaired speech/non verbal	11/15	+	+
Aggressive outburst	12/15	+	+
Tremor	11/13	+	+
Truncal obesity	15/19	-	+
Abnormal toes	11/13	+	NR
Small feet	7/14	NR	NR
Pes Cavus	7/8	+	+
Muscle wasting in lower legs	7/12	NR	NR
Small testes	10/15	+	-
Gynaecomastia	7/10	NR	NR
Prominent lower lip	6/17	+	+
Gait ataxia	6/12	+	+
Kyphosis	3/18	+	NR

3.1.4.1: CUL4B and steroid sex hormone signalling

Ohtake et al reported a CRL4-E3 involving the arylhydrocarbon receptor (AhR) specifically implicating CUL4B and not CUL4A, in the regulated turnover of steroid sex hormone receptors; the oestrogen and androgen receptors (ER and AR) (Ohtake et al, 2007). The AR is a tightly regulated transcription factor encoded on the X-chromosome whose degradation and rapid re-synthesis is an important regulatory mechanism (Lee & Chang, 2003; Li & Al-Azzawi, 2009). Mutations in the *AR* gene can result in Androgen Insensitivity Syndrome (androgen resistance; AIS). As the name suggests, this occurs when a genetically male individual is either completely or partially resistant to the male hormone, androgen and thus presents with external sex characteristics of a female. AIS is divided into two categories; complete AIS and incomplete AIS. Major abnormalities associated with AIS range in severity from mild to severe but include; hypospadias (abnormally place urinary meatus or male external urethral orifice), microphallus (micropenis), cryptorchidism (the absence of one or both testes from the scrotum), azoospermia (complete absence of sperm in the ejaculate) and a degree of gynaecomastia (enlargement of the male breast tissue) at puberty (Amrhein et al, 1977; Wisniewski et al, 2000). Specifically, patients with incomplete AIS show partial sensitivity to the effects of androgens and can clinically present with the Reifenstein phenotype. Patients with the Reifenstein phenotype present with a phallus smaller than a typical penis yet larger than a normal clitoris (Amrhein et al, 1977). In addition, the labioscrotal folds are partially fused producing a small perineal pouch termed a 'pseudovagina' and the testes often remain in the abdomen. Due to the considerable degree of ambiguity in these patients, they are not simply assumed to be normal female infants like those with complete AIS. Interestingly, CUL4B patients exhibit overlapping clinical features with AIS such as hypogonadism and gynaecomastia which may be a result of a skewed sex hormone axis.

The androgen receptor (AR) is thought to be required for myogenesis (Wannenes et al, 2008) and studies in mice have shown that overexpression of wild-type AR results in atrophy and severe muscle weakness suggesting that excessive AR may be toxic to muscles (Monks et al, 2007). Furthermore, Kennedy Disease (also

termed spinal bulbar muscular atrophy) is caused by a polyglutamine tract expansion in the *AR* gene and patients present with muscle weakness, atrophy, denervation and gynaecomastia. CUL4B patients also present with muscle wasting, therefore mis-regulation of the AR in the context of CUL4B loss may contribute to the muscle wasting exhibited here. If confirmed, this could in theory also provide a route for possible therapeutic intervention. However, it is important to note that other E3 ubiquitin ligases have been implicated in the regulation of the AR such as MDM2 and RNF6. Importantly however, the relative contributions of each are largely unknown. Nevertheless, it is tempting to speculate that mis-regulation of the AR as a consequence of CUL4B loss potentially contribute to both the muscle wasting and sexual development abnormalities experienced by these patients. The androgen receptor has also been implicated in regulating synaptic plasticity and function (Hajszan et al, 2008). Therefore, loss of CUL4B and subsequent mis-regulation of the AR may contribute to the neurological deficits of CUL4B-patients such as seizures and MR.

3.1.4.2: CUL4B and WDR5

Among the estimated 100 human DCAFs (DDB1, Cullin- Associated Factors) is WDR5, a core subunit of histone H3 lysine 4 (H3K4) methyltransferase complexes. Studies looking to identify a substrate of the WDR5-CRL4 complex led to the unexpected finding that WDR5 itself is a substrate (Nakagawa & Xiong, 2011). Nakagawa et al reported that the ubiquitination and degradation of WDR5 was blocked by the knockdown of *CUL4B* but not *CUL4A* and furthermore, overexpression of *CUL4B* led to increased ubiquitination of WDR5 (Nakagawa & Xiong, 2011). In addition, they reported that the N terminal sequence of CUL4B is essential for the ubiquitination of WDR5 and when engineered into CUL4A, this conferred CUL4A the ability to ubiquitinate and degrade WDR5. This provides an explanation for the functional distinction between the two CUL4 genes, at least in this specific instance. Finally, they demonstrate that the ubiquitination of WDR5 by CUL4B is important for neural gene expression, neuronal differentiation and axonal arborisation of PC12 cells (Nakagawa & Xiong, 2011). Their findings have pointed to a molecular defect of abnormal activation of neural gene expression as a

result of altered histone modification. WDR5 is also present in many other chromatin-modifying complexes such as the NIF-1 histone methyltransferase complex, RING1b histone ubiquitin ligase complex and the ATAC histone acetyltransferase complex (Garapaty et al, 2009; Sánchez et al, 2007; Wang et al, 2008). As WDR5 has such a broad range of functions, CUL4B therefore may play more extensive roles in chromatin control. More recently, WDR5 was identified in a genome-wide association study as one of the candidate genes affecting cognitive ability. This suggests that CUL4B-mediated ubiquitination of WDR5 may potentially be involved in learning and memory (Davis et al, 2010).

3.1.4.3: CUL4B and Peroxiredoxin III

The peroxiredoxins (Prx's) are a family of thiol-specific antioxidant proteins. Human Prx's include six isoforms (PrxI-PrxVI) and Prx III has recently been identified as a novel substrate of a CUL4B-containing CRL4 ubiquitin ligase (Li et al, 2011). In addition, it was shown that the integrity of the DDB1-CUL4B-ROC1 complex is essential for promoting CUL4B-mediated Prx III degradation. Silencing of *CUL4B* led to a striking decrease in ROS production and resulted in resistance to apoptosis after hypoxia and H_2O_2 treatments in HEK293 cells (Li et al, 2011). Recent evidence suggests that high ROS levels can promote proliferation and self-renewal of certain stem cells (Le Belle et al, 2011). Furthermore, a decrease in normal cellular ROS levels has a negative effect on the self-renewal and differentiation potential that is required for normal neural stem cell functions (Le Belle et al, 2011). Li et al suggest that the reduction in ROS levels, as a consequence of accumulated PrxIII, may not be high enough to sustain normal neural stem cell proliferation and therefore may impair neurogenesis in *CUL4B*-mutated patients. These findings may have significant implications for the pathogenesis of many clinical features observed in *CUL4B*-patients. However, there may be numerous CUL4B specific substrates involved in brain development and neural functioning therefore further investigation is needed within this area.

3.1.4.4: A role for CRL4's in the mTOR signalling pathway

The PI3-kinase-mTOR (*mammalian target of rapamycin*) signalling pathway plays a central role in controlling cell growth through the regulation of protein translation. In addition to regulating cell growth, mTORC1 also regulates autophagy; the process by which cells break down organelles and cytosolic compartments in order to ensure there are sufficient metabolites when nutrients are running low. The process of autophagy will be discussed further in the results section of this chapter. The mTOR pathway is activated by insulin, growth factors (EGF, FGF) and amino acids amongst other stimuli. Once activated, mTORC1 (consisting of mTOR, Raptor and mLST8) phosphorylates PP2A, S6K1 (p70α) and eIF4E-BP. The phosphorylation of eIF4E-BP releases eIF4E to initiate protein synthesis and ribosome biogenesis. mTOR receives both inhibitory and activating signals from the tuberous sclerosis complex (TSC1-TSC2) and AKT respectively in order for the cell to co-ordinate it translational response to conditions such as energy sensing (AMP:ATP ratio), hypoxia and membrane receptor signalling (Fig 3.7).

It has recently been reported that the effects of CUL4B loss on the mTOR pathway mimic those of Raptor loss. Furthermore, the authors reported that siRNA-mediated knockdown of *CUL4B* significantly reduced phosphorylation of S6K1, a process mediated by mTOR (Ghosh et al, 2008). These results suggest that the CUL4B-DDB1 E3 ligase activity plays an important role in the regulation of the mTOR pathway, although the authors did not reveal a precise molecular mechanism (i.e. a substrate) defining how this effect occurs (Ghosh et al, 2008). CRL4's have been implicated in mediating the degradation of TSC2 and REDD1, both negative regulators of mTOR. With regards to TSC2, a CRL4 ubiquitin ligase complex containing DDB-ROC1-FBW5 has been shown to mediate the degradation of TSC2 however the relative contributions of CUL4A and CUL4B were not investigated (Hu et al, 2008b). Furthermore, reports implicating the CUL4A-DDB1-ROC1-βTRCP ligase complex in the degradation of REDD1 do not specifically exclude CUL4B as a component of the complex (Katiyar et al, 2009). However this year, Wang and colleagues reported that XLMR *CUL4B*-mutants are defective in promoting TSC2 degradation and augmenting mTOR signalling in neocortical

neurons of the frontal lobe (Wang et al, 2013). This suggests that CUL4B specifically plays fundamental roles in the regulation of the mTOR pathway.

Correct mTOR signalling is crucial for many processes such as autophagy, protein translation and neuronal development, to name but a few. Therefore, loss of CUL4B could potentially have disastrous effects for its regulation impacting on multiple cellular processes. In neurons, increased mTORC1 activity is a result of several stimuli including growth factors such as brain derived neurotrophic factor (BDNF), leptin, influxes of calcium and neurotransmitters through the activation of receptors. The PI3-Kinase-mTOR pathway regulates the differentiation, maturation and survival of neurons and has also been implicated in long term potentiation, learning and memory through its regulation of ribosome biogenesis and protein synthesis (Crino, 2011; Garelick & Kennedy, 2011; Martin, 2004; Tang et al, 2002; Wang et al, 2010). Therefore, mis-regulation of the mTOR signalling pathway could potentially impart some effect on cognition and is believed to be one of the molecular mechanisms underlying intellectual disability or MR (Troca-Marin et al, 2012). In fact, reduced neuronal mTOR function has been implicated in Huntington's disease highlighting an important association between optimal mTOR pathway signalling and neuronal function (Ravikumar et al, 2004). However, whether disrupted mTOR signalling plays a role in the origin of MR associated with *CUL4B* mutation/deletion is unclear.

Defects in negative regulators of mTOR are associated with several human disorders such as Tuberous Sclerosis (*TSC1/TSC2*) and Cowden Disease (*PTEN*) (Inoki et al, 2005). Although the severity of TSC is variable, many patients suffer from epilepsy and mental retardation, two key clinical features of CUL4B patients (Kwiatkowski, 2003; Tarpey et al, 2007b). Furthermore, a recent study identified that CUL4B mRNA and protein are highly expressed in the cerebral cortex, cerebellum and hippocampal regions of the mouse brain (Chen et al, 2012). In light of recent data presented by Wang et al in neocortical neurons (described above), it is likely that CUL4B regulates mTOR signalling activity in the cerebral cortex where it plays an essential role in mediating synaptic plasticity, memory and learning (Hoeffer & Klann, 2010; Swiech et al, 2008; Wang et al, 2013). This is

achieved via promoting the removal of TSC2 and positively regulating the mTOR signalling cascade. Loss of CUL4B here would impair TSC2 ubiquitination and degradation resulting in downregulation of mTOR signalling which may lead to malfunction of the frontal cortex and mental retardation. Consistent with this, *Cul4b* knockout mice display reduced dendritic arborisation and impaired spatial memory function (Chen et al, 2012). Defective mTOR signalling has also been linked to growth retardation in disorders such as Donohue and 3M syndromes (Huber et al, 2005; Kadowaki et al, 1988; Sarikas et al, 2008; Xu et al, 2008). As CUL4B patients exhibit short-stature, albeit modest in comparison to that of 3M and Donohue syndromes, it is possible that defective mTOR signalling could in part underlie this feature and is an area worthy of further investigation.

3.1.5: CUL4B-dependent Topoisomerase I degradation

In 2010, Kerzendorfer et al reported that the degradation of Topoisomerase I (Topo I) following camptothecin (CPT) treatment was a CRL4-dependent process (Kerzendorfer et al, 2010). Topo I is an essential enzyme that introduces nicks into the DNA backbone to relieve torsional tension generated by DNA supercoiling. This occurs as a normal feature of replication and transcription (Fig 3.8a) To allow the repair of these nicks, Topo I is partially degraded and then cleaved and released by TDP1 (Marin, 2009). Kerzendorfer at al reported delayed Topo I degradation and ubiquitination in response to CPT treatment in *CUL4B*-mutated LBLs (Kerzendorfer et al, 2010). CPT functions to stabilize Topo I complexes on the DNA. When these complexes collide with replication or transcription forks this leads to fork collapse and the generation of overt DNA double strand breaks. Hence in the absence of CUL4B, Topo I ubiquitination and degradation is impaired, allowing it to remain attached to the DNA, increasing the number of DNA breaks present (Fig 3.8b).

Impaired processing of Topo I has also been implicated in the peripheral neuropathy associated with SCAN1, a monogenic condition caused by a defect in the Topo I cleaving enzyme TDP1. The SCAN1-associated mutation in *TDP1* results in a qualitative change in the enzymatic activity of the encoded protein allowing it

to become covalently attached on the DNA. In contrast, as modelled by the *tdp1* knock out mouse model; complete ablation of the protein has no effect therefore indicating that SCAN1 arises from a neomorphic TDP1 defect (Hirano et al, 2007; Takashima et al, 2002) and Fig 3.8. CUL4B patients exhibit overlapping clinical features (albeit more severe) to SCAN1 patients (Table 3.3). This highlights a potentially overlapping pathogenic mechanism between these disorders, involving prolonged Topo I cleavage complexes (CC's), elevated levels of DNA breakage and subsequent neuronal death and/or dysfunction.

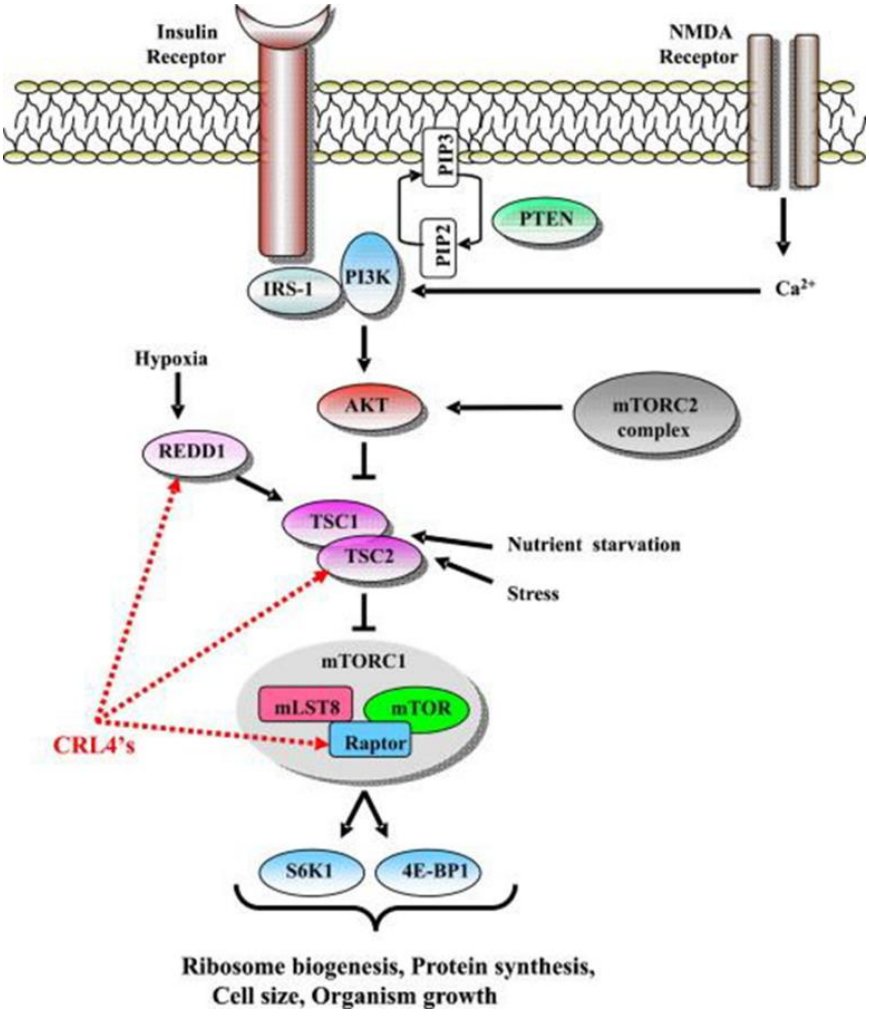

Figure 3.7 - A highly simplified summary of the mTOR-PI3K-signal transduction pathway. The mTOR pathway centres upon the activation of the mTORC1 complex, a kinase involved in regulating ribosome biogenesis and protein translation. An important negative regulator of mTORC is the TSC1-TSC2 complex. The mTOR pathway is activated by membrane-bound receptors such as the insulin receptor but also via voltage-gated neurotransmitter receptors such as the NMDA receptor. The sites of action of distinct CRL4's are shown as indicated by the red dashed line. (CRL4=Cullin RING ligase 4 containing E3 ligase) (Kerzendorfer et al, 2011).

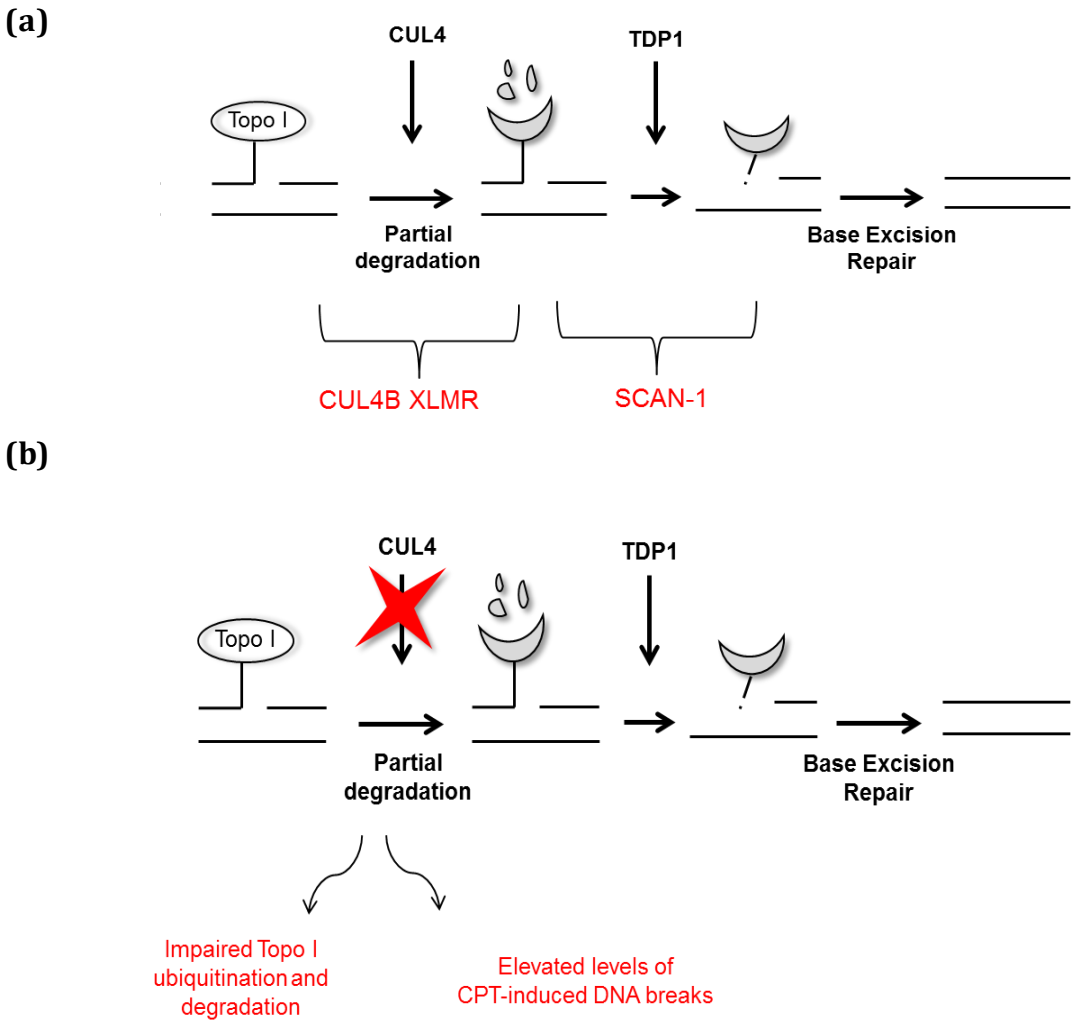

Figure 3.8 - A schematic illustration of the repair of Topo-I induced DNA nicks. **(a)** Removal of Topo I from DNA involves the partial degradation to facilitate optimal TDP1-induced Topo I cleavage and resealing of the Topo I-induced nicks by Base Excision Repair. **(b)** Loss of CUL4B impair ubiquitination and degradation of Topo I and allows Topo I complexes to remain attached to the DNA. This increases the likelihood of collision with DNA replication or transcription machinery (DNA/RNA Pol respectively) and thus can potentially turn Topo I –induced single strand nicks into DNA double strand breaks. CUL4B LBL's exhibit elevated levels of CPT-induced DNA breaks.

Table 3.3 - Overlapping clinical features of CUL4B-XLMR and SCAN1 patients.

	CUL4B	**SCAN1**
Gene	*CUL4B*	*TDP1*
Gait	*Ataxia, tremor, muscle wasting*	*Muscle weakness and mild ataxia*
Speech	*Non-verbal communication*	*Dysarthria*
Topo I	*Impaired degradation and ubiquitination following CPT*	*Impaired removal of DNA bound Topo I complexes*

3.1.6: Mitochondria are dynamic organelles

CUL4B-XLMR patients exhibit clinical overlap with many mitochondrial disorders. Overlapping features include ataxia, neuropathy and seizures (Tarpey et al, 2007b, Isidor et al, 2010). Mitochondria, considered as the "biochemical powerhouse" of the cell, are double-membrane subcellular organelles functioning to produce most, but not all, of the cellular energy (ATP) via oxidative phosphorylation. They also play an important role in other pathways such as urea production, steroid biogenesis, calcium regulation and apoptosis-programmed cell death. The two membranes give rise to different regions; the inner and outer membranes themselves (IMM and OMM), the cytosolic side of the OMM, the intermembranal space and the matrix (Fig 3.9). The IMM harbours the electron transport chain (or respiratory chain complexes), the OMM is protein-rich and small molecules can pass freely from the cytoplasm and the IMS due to the presence of a number of pores within the OMM. The IMM however, is completely impermeable to even small molecules. This enables the complexes of the respiratory chain to build up a proton gradient across the IMM; the details and relevance of which will be discussed further in results section 3.2.2.3.

Mitochondria are dynamic organelles. Not only is their size and shape highly variable but they can also be actively transported to various subcellular regions. This is particularly evident in neurons where mitochondria are transported along cytoskeletal filaments by energy-dependent motors to areas with high demands for ATP and calcium buffering such as synapses and axon terminals (Cai & Sheng, 2009; Fang et al, 2012; Hollenbeck & Saxton, 2005). Removing mitochondria from axon terminals results in aberrant synaptic transmission and many neurodegenerative diseases involve defects in the transport of mitochondria. This highlights the importance of mitochondrial transport for various neuronal processes (Ma et al, 2009; Stokin & Goldstein, 2006; Verstreken et al, 2005). The size and shape of the mitochondria is determined by two fundamentally regulated events known as fission (splitting) and fusion (merging). These processes enable them to respond to the energy demands of the cell and maintain their mtDNA copy number (Berman et al, 2008). At a steady state, these two events are balanced to maintain the population. Fission involves the splitting of one mitochondrion into

two daughter mitochondrion, both containing multiple copies of mtDNA. Mitochondrial fission relies on the large dynamin related GTPase DRP1 (Dynamin-related 1) which is recruited from the cytosol and also FIS1 (Fission-1), an outer mitochondrial membrane protein. DRP1 is further regulated by MARCH5, a mitochondrial E3 ubiquitin ligase functioning to promote the ubiquitination of DRP1. Parone et al reported that prevention of mitochondrial fission by down regulating the expression of DRP1 in HeLa cells lead to the loss of mtDNA and subsequent mitochondrial dysfunction (Parone et al, 2008). In contrast, mitochondrial fusion involves the merging of two mitochondria into one. This event frequently occurs when a mitochondrion becomes dysfunctional; fusion provides a means of allowing the exchange of intramitochondrial content therefore maintaining the health of the mitochondrial population. Fusion is essential for the maintenance of the mtDNA and relies on a set of components, mainly Mitofusins 1 and 2 (MFN1/2) and Optic Atrophy-1 (OPA-1). Furthermore, inhibiting fusion has been shown to reduce the activity of the electron transport chain (ETC) (Chen et al, 2005).

Perturbations in mitochondrial dynamics result in specific developmental defects and several human diseases arising from mutations in the proteins carrying out the fission/fusion processes highlight their importance for cellular homeostasis. Examples include; Charcot Marie Tooth Disease 2A (mutations in *MFN2*) and Autosomal Dominant Optic Atrophy (mutations in *OPA1*) where neuropathy is a well noted clinical feature (Chance et al, 1994; Zheng et al, 2002b). In addition, evidence suggests that impairing the fission/fusion balance results in abnormally long or short mitochondria which can lead to neurodegeneration (Knott & Bossy-Wetzel, 2008)

3.1.6.1: Mitochondrial disorders; disorders associated with disrupted mtDNA replication

The mitochondrion differs from most other organelles as it has its own small, 16.6kb, circular double-stranded genome which replicates independently of the cell (mtDNA) (Fig 3.10). Each organelle contains multiple mtDNA copies

(polyploidy) which encode a critical subset of genes necessary for the respiratory chain complex and subsequent ATP production (Chen & Butow, 2005). Mitochondria are inherited maternally and the tightly preserved mtDNA codes for 37 genes; 13 polypeptides; 7 subunits of Complex I, 1 of Complex III, 3 of Complex IV and 2 of Complex 5V, 22 transfer RNA's (tRNA) specific for mitochondrial protein synthesis and 2 mitochondrial specific ribosomal RNA's (12S and 16S). The remaining mitochondrial proteins (>98%) are encoded by the nDNA and imported via specialised import systems (Anderson et al, 1981).

Since the first association of a human disease with a mitochondrial defect in 1989 by Holt (Holt et al, 1988), numerous mutations have been identified as causative of various 'Mitochondrial Diseases' such as MERRF (myoclonic epilepsy with ragged-red fibres), MELAS (Mitochondrial encephalomyopathy, lactic acidosis, and stroke - like episodes, Leigh Syndrome and KSS (Kearns Seyre Syndrome). Mutations in both the nuclear DNA (nDNA) and mitochondrial DNA (mtDNA) can affect a number of genes essential for mitochondrial functioning such as those coding for a). mt-tRNA, b). subunits of the respiratory complexes, c). assembly factors or chaperones required for complex formation, d). transport of fission and fusion proteins and e). the mtDNA replication machinery. With respect to mtDNA mutations, due to the large mtDNA copy number per cell (1000-10,000 per cell), for an mtDNA mutation to have a detrimental effect on function it must reach a minimum critical level of frequency before disruption to the electron transport chain occurs. Obviously, this threshold is lower in those tissues and organs with a high dependency on oxidative phosphorylation. mtDNA mutations frequently result in conditions where ataxia is a prominent and consistent feature in affected patients. Some of the most frequent and well characterised mtDNA-related syndromes associated with an ataxic phenotype are: Kearns Seyre Syndrome, Myoclonic Epilepsy with Ragged Red Fibres (MERRF) and Neurogenic weakness, Ataxia, and Retinitis Pigmentosa (NARP) (Zeviani et al, 2012) (Table 3.4).

The mitochondrial genome has no capacity for independent replication and therefore relies on the nuclear-encoded polymerase gamma (POLG), amongst other proteins such as the Twinkle helicase, in order to replicate (Petroski & Deshaies, 2005a). Mitochondrial diseases associated with defects of mtDNA

replication include; PEO (Progressive External Opthalmoplegia), Alpers Syndrome, MDS (Mitochondria Depletion Syndrome), MIRAS (Mitochondrial Recessive Ataxia Syndrome) and SANDO (Sensory Ataxia, Neuropathy, Dysarthria, Opthalmoplegia). Mitochondrial Disorders are among the most frequently inherited disorders and, in addition to ataxia, also commonly present with peripheral neuropathies, seizures and in some cases, mild cognitive impairment as frequent clinical features (McKenzie et al, 2004) (Table 3.4). Many of these are key overlapping phenotypes of *CUL4B* patients suggestive of an overlapping pathomechanism.

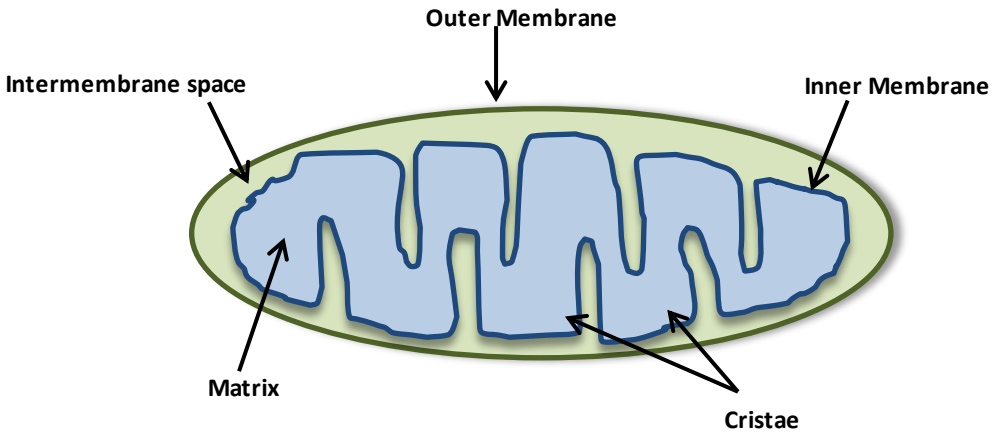

Figure 3.9 - The Mitochondrion: An Illustration of the mitochondria, indicating the various organelle compartments and membranes.

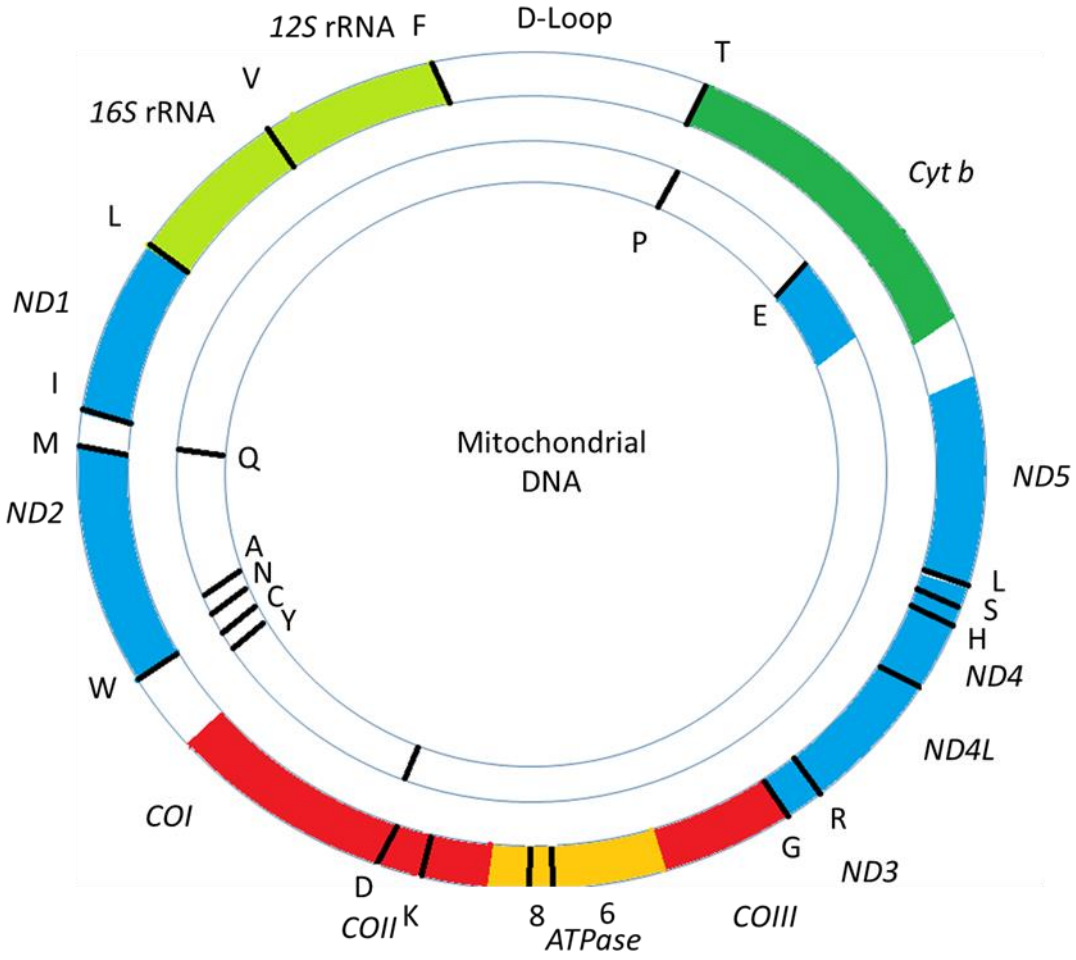

Figure 3.10 - The Mitochondrial genome: A map of the mitochondrial genome. Genes encoding subunits of Complex I are shown in blue; cytochrome c oxidase in red; cytochrome b of complex III in dark green subunits of the ATP synthase in yellow. The two ribosomal RNA are shown in purple and the 22tRNAs are indicated by black lines and their single letter code. The displacement loop (D-Loop) contains sequences crucial for the initiation of replication and transcription.

Table 3.4 - Mitochondrial disorders; MDs can result from mutations in both mitochondrial DNA (mtDNA) and nuclear DNA (nDNA) with a variety of clinical manifestations.

Disorder	Features	MtDNA or nDNA mutation?
Leigh Syndrome	Severe failure of oxidative metabolism, dystonia	Both
Kearns Seyre Syndrome (KSS)	Retinitis pigmentosa Progressive external Opthalmoplegia Ataxia	mtDNA
Mitochondrial encephalopathy, lactic acidosis and stroke-like episodes (MELAS)	Muscle weakness, seizures, stroke-like episodes, lactic acidosis, ataxia	mtDNA
Myoclonic Epilepsy with Ragged Red Fibres (MERRF)	Myoclonus, Proximal muscle wasting, generalised epilepsy, cerebellar ataxia	mtDNA
Mitochondrial Neuro-Gastro-Intestinal leuko-Encephalopathy (MNGIE)	Intestinal malabsorption, cachexia, peripheral neuropathy, hearing loss	nDNA
Dominant Optic Atrophy	Loss of visual acuity and legal blindness	nDNA
Charcot Marie Tooth Disease 2A (CMT2A)	Peripheral neuropathy, scoliosis tremor, intestinal problems,	nDNA

3.1.6.2: Mitochondrial Topoisomerase; Top1mt

As previously discussed in section 3.1.5, Topoisomerase I degradation has recently been found to be CRL4-dependent (Kerzendorfer et al, 2010). Interestingly, Zhang et al reported that mitochondria possess their own dedicated topoisomerase-I, Top1mt, encoded by a gene distinct to that of nuclear Topo I on chromosome 8q24.3 (Zhang et al, 2001). Other reports suggest two other topoisomerases are also present in the mitochondria; Top3α and Top3β; however Top1mt is the only one encoded by a nuclear gene specific for mitochondria and present in all vertebrates. Top1mt functions to relieve the torsional tension generated during replication and transcription of the mtDNA (Zhang et al, 2001). Recently, it was shown that Top1mt-deficiency is associated with the activation of mitophagy, DNA damage response pathways and increases in ROS levels and glycolysis; highlighting its importance for the maintenance of cellular homeostasis (Douarre et al, 2012). As nuclear Topo I has been identified as a CUL4B-dependent substrate, it is tempting to speculate that Top1mt could also be a CUL4B-dependent substrate. If so, loss of CUL4B could result in aberrant mtDNA replication and transcription resulting in a plethora of disastrous effects on mitochondrial dynamics and subsequent cellular homeostasis.

3.1.7: Summary

In light of the functional defects and various associations presented above, I sought to investigate whether *CUL4B* patients harbour mitochondrial defects which may in part underlie the ataxic and muscle wasting features they exhibit. Furthermore, since neurons rely heavily on mitochondria and their transportation along axons to sites of high energy demands is essential for neuronal function, any mitochondrial deficit could have a significant effect on neuronal development, function, maturation and maintenance and thus may play a contributing role in the pathogenesis of the MR and/or seizure phenotypes of *CUL4B* XLMR. In addition, the role of CUL4B in the mTOR signalling pathway, an important pathway in the brain, may contribute to the MR phenotype in these patients. *CUL4B* patients also exhibit clinical features indicative of skewed sex hormone signalling. Interestingly,

a CUL4B containing E3 complex has been implicated in the turnover of steroid sex hormone receptors suggesting that CUL4B may play important roles in sexual development. Figure 3.11 summarises the clinical features associated with *CUL4B*-XLMR and the possible CUL4B-interacting factors that may potentially underlie or contribute to specific phenotypes. With these associations in mind, I set out to provide supportive experimental evidence for these in an attempt to understand genotype to phenotype relationships in the context of CUL4B loss. Specifically a key aim here was to uncover the cellular and biochemical consequences of defective CUL4B-function and how this relates to genomic instability and cell homeostasis.

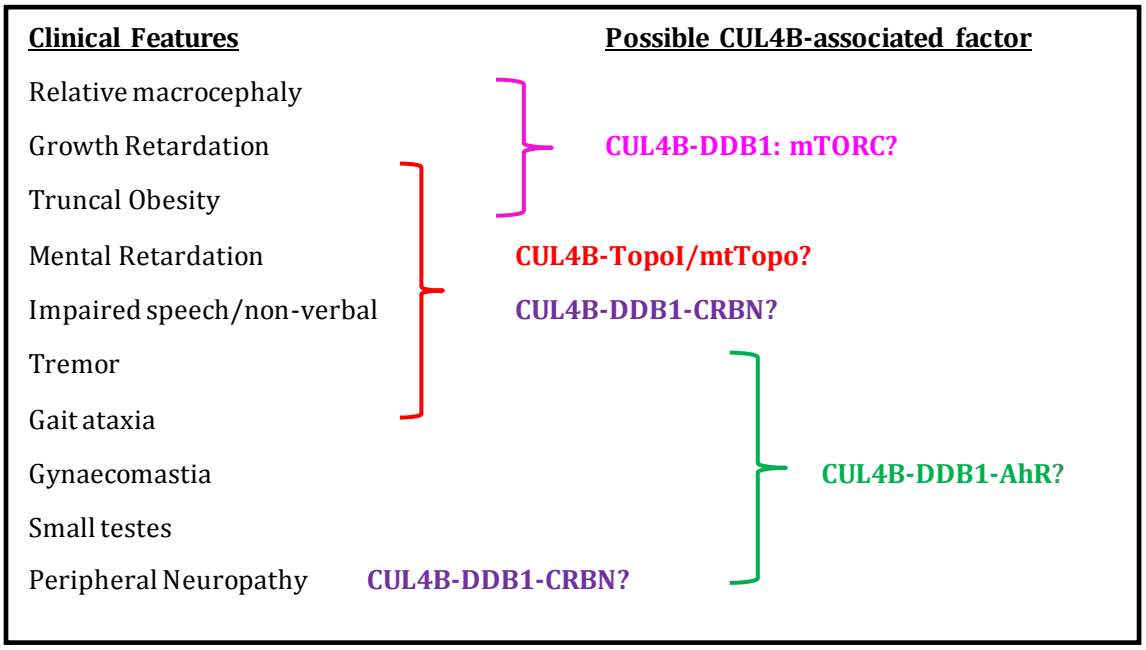

Figure 3.11 - Clinical features associated with CUL4B XLMR and the possible CRL4 complexes implicated in each. CRBN – Cereblon; AhR - Arylhydrocarbon receptor; mTORC - mammalian target of rapamycin 1; mtTopo – mitochondrial topoisomerase.

3.2: Results

3.2.1: Characterisation of defective CUL4B function in lymphoblastoid cells from an individual carrying a novel X-chromosome deletion

Recently the first report of a *CUL4B*-deleted patient was published suggesting that total loss of CUL4B is compatible with life (Isidor et al, 2010). The authors identified a 60kb, Xq24 deletion encompassing the 3' portion of the *CUL4B* gene. They also reported that the *MCTS1* gene was deleted in this child (Fig 3.6). I obtained EBV-transformed lymphoblastoid cells (LBLs) and primary fibroblasts from this patient. These are a novel tool and provide excellent models to study complete CUL4B ablation as the issue of residual CUL4B function is unlikely to be relevant due to the complete deletion of the *CUL4B* gene (Fig 3.6).

Initially, I sought to characterize the line for CUL4B protein expression levels and as expected, I found that extracts from LBLs derived from this particular *CUL4B*-deleted patient show no expression of CUL4B (Fig 3.12a) Consistent with previous findings from three *CUL4B*-mutated lines (Kerzendorfer et al, 2010), I found that extracts from LBLs derived from this *CUL4B*-deleted patient exhibit spontaneous overexpression of two well-known CRL4 substrates; p21 and p27 (Fig 3.12b). These findings are consistent with a known role for CRL4-containing E3 ubiquitin ligases in the ubiquitination and degradation of both these CDK inhibitors (Abbas et al, 2008; Higa et al, 2006; Kim et al, 2008b; Li et al, 2006; Nishitani et al, 2008). These findings confirm a molecular defect in this deletion case to substantiate defective CRL4 function. This unique human patient-derived cellular model of complete *CUL4B* ablation was employed as my primary research tool in the subsequent analyses described here.

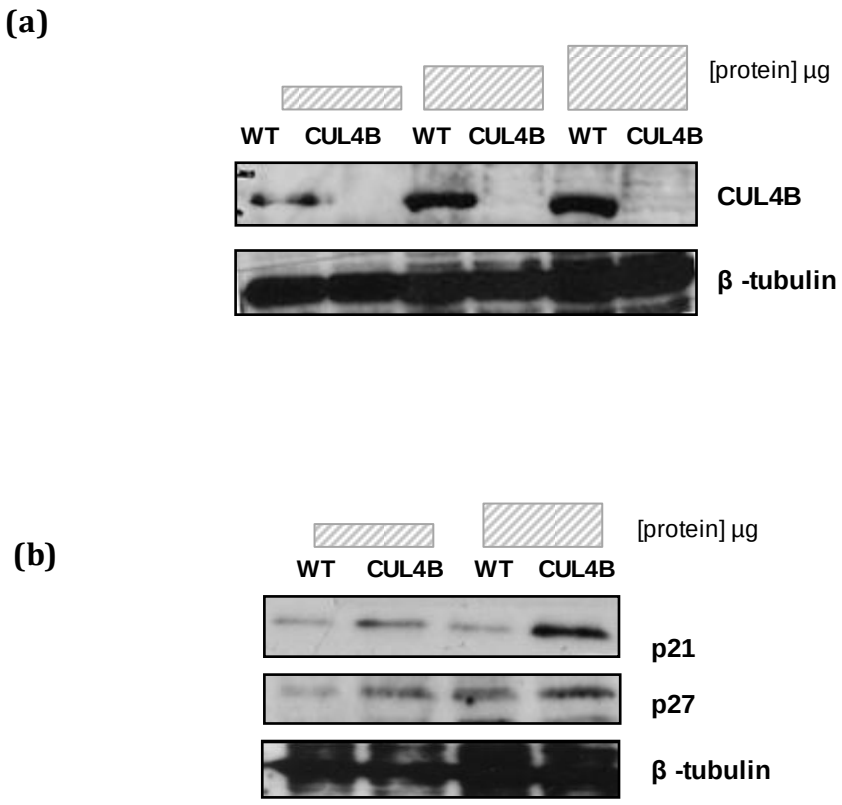

Figure 3.12 - Characterisation of *CUL4B*-deleted patient line (CV1845) by western blotting. Cell lysates were prepared using urea extraction buffer and increasing concentrations loaded. **(a)** Expression of CUL4B in Wild-type (AG093875 or WT) vs. *CUL4B*-deleted (CUL4B). CUL4B expression is absent in *CUL4B* deleted-patient line. The blot was reprobed for β-tubulin as a loading control. **(b)** Expression of p21 (upper panel) and p27 (lower panel) in Wild-type (WT) vs. *CUL4B*-deleted patient derived LBLs (CUL4B); expression of both p21 and p27 are increased in the patient line. The blot was probed for p21 then reprobed for p27. β-tubulin was used as a loading control. Grey hatched boxes represent increasing protein concentration loads; (a) 25, 50,100 µg and (b) 50-75 µg.

3.2.2: Understanding the impacts of CUL4B deficiency on mitochondrial function

3.2.2.1: Mitochondrial topoisomerase; Top1mt

CUL4B-XLMR patients exhibit many overlapping clinical features with various 'Mitochondrial Disorders' such as ataxia, epilepsy, muscle wasting and peripheral neuropathy suggesting that mitochondrial dysfunction may play a role here (discussed in section 3.1.6) (Folbergrova & Kunz, 2012; Vital & Vital, 2012; Zeviani et al, 2012). Furthermore, mental retardation has been reported in some mitochondrial disorders including MEHMO (Mental Retardation, Epileptic Seizures, Hypogenitalism, Microcephaly, Obesity), MTS (Mohr-Tranebjaerg syndrome) and in disorders involving mutations in subunit 6 of the ATPase gene and the F1F0-ATPase gene (Bauer et al, 1999; de Coo I. F, 1996; Leshinsky-Silver et al, 2002; Puddu et al, 1993).

As mitochondria possess their own genome and dedicated Topoisomerase (discussed in Section 3.1.6), one explanation for a possible mitochondrial defect is that overall mtDNA content in *CUL4B*-deleted mitochondria may differ as a result of defective Top1mt degradation impacting upon mtDNA replication. Using semi-quantitative duplex PCR as previously shown by Ambrose et al (Ambrose et al, 2007), genomic and mtDNA content was measured by PCR amplification using primers designed to target two mitochondrial encoded genes; NADH dehydrogenase 2 (ND2) and 16S RNA (16S) and one nuclear encoded gene; 18S RNA genome (18S). The results are interpreted by analysing the ratio of mtDNA: genomic DNA, i.e. ND2:18S and 16S:18S. The results shown in Figure 3.13a indicate that mitochondrial content did not grossly differ between Wild-type (lanes 1 and 3) and *CUL4B*-deleted LBLs (lanes 2 and 4) therefore inconsistent with a major defect in mtDNA replication and propagation.

Although mtDNA content does not differ, this does not rule out differences in mitochondrial mass (number of mitochondria present). To investigate aspects of mitochondrial functioning and physiology, various cell-permeant mitochondrion

specific probes known as “Mitotrackers” were used to analyse distinct aspects of mitochondrial membrane potential and functionality, localisation and abundance within *CUL4B*-deleted LBLs (Probes for Mitochondria-section 12.2, Molecular Probes, www.invitrogen.com). I also obtained LBLs from patients with 3 well-known mitochondrial disorders to enable me to compare and contrast their Mitotracker profiles to those of *CUL4B*-deleted LBLs.

- Leigh Syndrome (GM13740) – defect in MTATP6 (ATPase 6): p.L156R (mtDNA base pair 8993 T>G) (Coriell Cell Repositories NI, USA).
- Myoclonic Epilepsy with Ragged Red Fibres (GM11907A, MERRF) – mutant tRNA; Lys A>G transition at mtDNA base pair 8344/WT (Coriell Cell Repositories NI, USA).
- Kearns-Seyre Syndrome (GM04368, KSS) – a defect in MTND4; p.R340H (1178 G>A) (Coriell Cell Repositories NI, USA).

3.2.2.2: Mitotracker Green FM as an indicator of mitochondrial mass

Mitotracker Green FM accumulates in the lipid environment of the mitochondria regardless of membrane potential (discussed later in section 3.2.2.3) and exhibits a bright green, fluorescein-like fluorescence (FITC). Measurement of fluorescence intensity therefore allows determination of the mitochondrial mass or absolute mitochondrial content of a cell and/or population. As mtDNA content was not significantly different, I investigated whether the number of mitochondria present differed which may in turn indicate disrupted mitochondrial biogenesis. LBLs were incubated with 250nM Mitotracker Green for 15 minutes at 37°C and washed in PBS. Samples were then analysed for FITC fluorescence using the FACS Canto Flow Cytometer and BD FACS Diva analysis software. The FITC profiles for Mitotracker Green staining show a wider, right-shifted peak in the *CUL4B*-deleted patient LBLs compared to WT control LBLs with a proportion of events falling at very high FITC intensities. This is indicative of a slightly increased mitochondrial mass (Fig 3.13b). This same distribution is seen in the mitochondrial disorder Leigh Syndrome but the physiological significance is unclear. Looking further into this phenotype it becomes apparent that although there may be a subtle increase in mitochondrial

mass, this may be due to an excess of non-functional mitochondria. Some examples of processes which, when disrupted, could lead to the accumulation of non-functional mitochondria are mitophagy, the mitochondrial membrane potential maintenance and/or the mitochondrial fission-fusion processes.

Mitotracker Green can also be analysed by microscopy, giving an indication of the distribution of the mitochondria within a single cell. I obtained primary fibroblasts from the same *CUL4B*-deleted patient, again a novel tool and an excellent model for visualising fluorescent-labelling of mitochondria in attached cells. The mitochondrial distribution within wild-type control fibroblasts (1-BR) appeared to surround the nucleus of the cell with lesser staining being observed in the peripheries (Fig 3.14 left panels). However, the mitochondrial distribution in the *CUL4B*-deleted fibroblasts appeared more dispersed throughout the cell, many mitochondria surrounded the nucleus as in a WT however many mitochondria were distributed throughout the cytoplasm of the cell (Fig 3.14 right panels). The relevance of this difference in mitochondrial distribution for mitochondrial functioning in these cells is unclear. Nevertheless, abnormal mitochondrial distribution is a feature of certain mitochondrial disorders and so may be consistent with abnormal aspects of mitochondrial function in the context of *CUL4B*-deletion (Dias et al, 2002; Groisman et al, 2003; Kamura et al, 2004; Mahrour et al, 2008; Pick et al, 2007).

It would be interesting to investigate mitochondrial distribution in a *CUL4B*-deleted neuronal cell model. The local need for ATP and calcium handling is especially important at synapses and axon terminals and thus mitochondria are appropriately distributed to serve the different spatial and temporal demands of neurons. Altered mitochondrial distribution within neuronal cells in the context of *CUL4B* loss may have implications for neuronal excitability and synaptic transmission and thus may begin to explain the MR and seizures exhibited by *CUL4B*-patients.

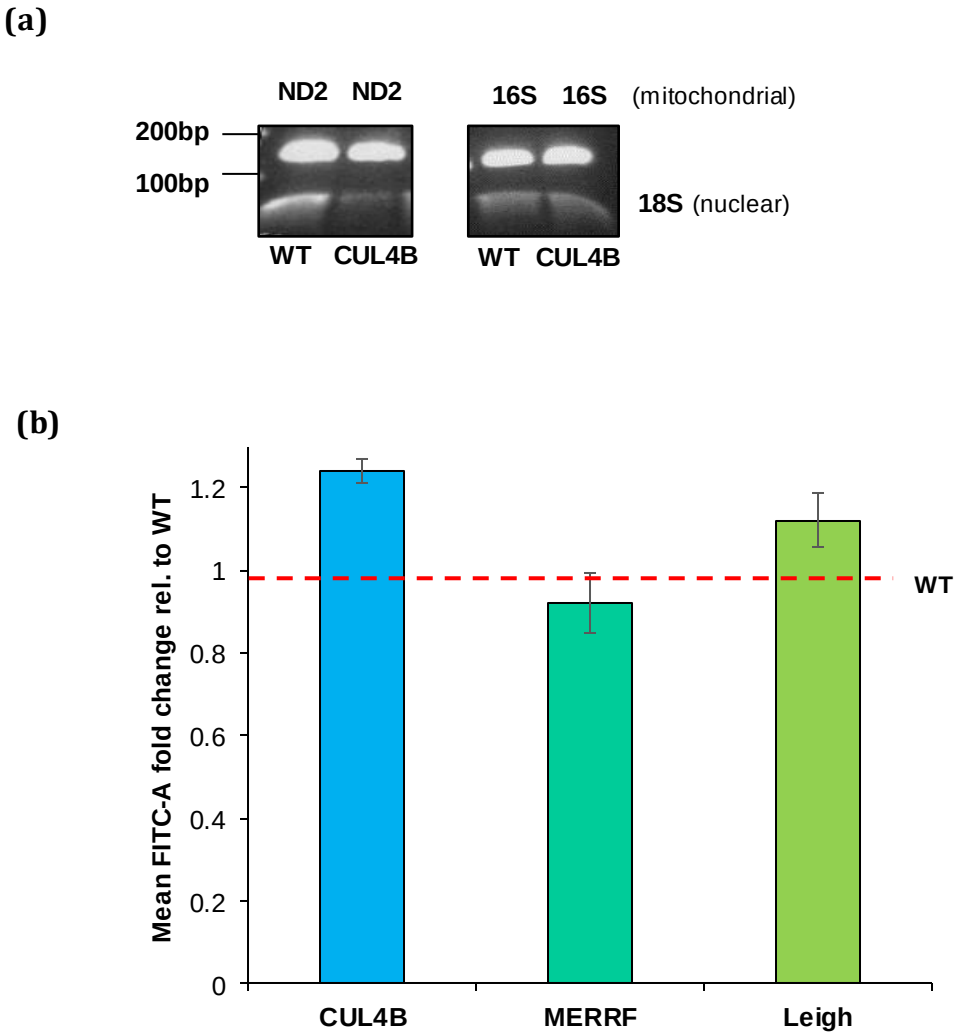

Figure 3.13 – *CUL4B*-deleted LBLs show similar mitochondrial content to wild type control. **(a)** Semi quantitative PCR; total DNA was extracted and primers for two mitochondrial-DNA encoded genes; *ND2* and *16S* and one nuclear DNA encoded gene; *18S* were used for analysis. The PCR program consisted of a 3 minute step at 94°C, 30 cycles of 30 seconds at 94°C, 1 minute at 72°C and a final step at 72°C for 8 minutes. PCR products were electrophoresed on a 1.5% agarose gel. Lanes 1 and 2; top band-ND2, bottom band-18S. Lanes 3 and 4; top band -16S, bottom band -18S. WT; Wild-type, CUL4B- *CUL4B*-deleted. **(b)** Wild type LBLs, *CUL4B*-deleted LBLs and LBLs from two patients with well-known mitochondrial disorders; MERRF and Leigh Syndrome were incubated with 250nM Mitotracker Green for 20 minutes and analysed for FITC fluorescence on the FACS Canto flow cytometer. The histogram represents the mean fold change in FITC mean fluorescence intensity (MFI) relative to wild-type controls (red dashed line). MERRF; Myoclonic Epilepsy with Ragged Red Fibres, Leigh; Leigh Syndrome.

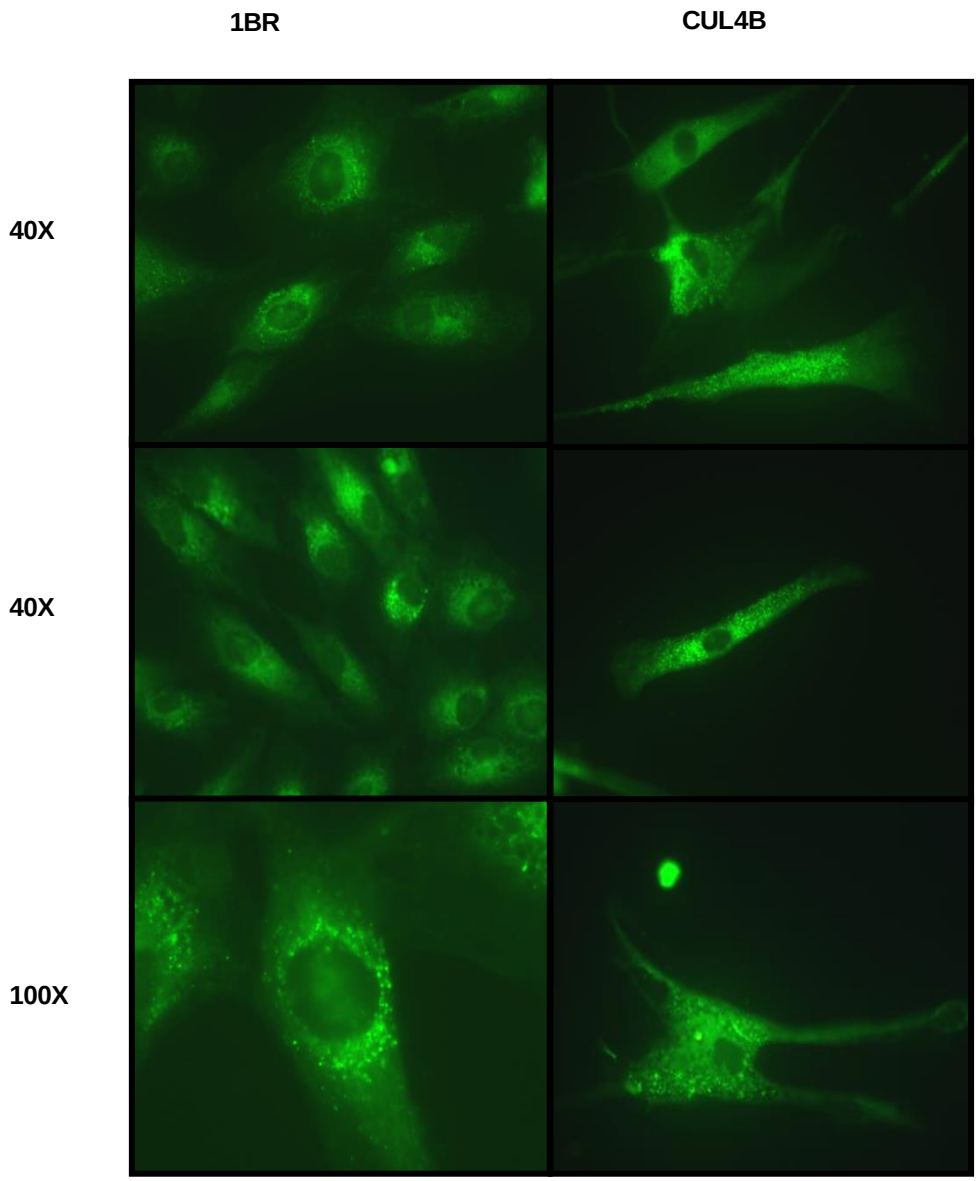

Figure 3.14 - *CUL4B*-deleted hTERT fibroblasts exhibit altered mitochondrial distribution**.** Cells were grown on Poly-lysine coated coverslips and once semi-confluent cells were incubated with 250nM Mitotracker Green for 20 minutes and analysed by microscopy using the Zeiss Axiovert microscope. Images were captured using the *same* exposure times. 1BR; wild type control fibroblasts, CUL4B; *CUL4B*-deleted hTERT fibroblasts (92025337) obtained from the *CUL4B*-deleted patient described by Isidor et al, 2010. Cells were obtained from Bertrand Isidor, Universitare De Nantes.

3.2.2.3: CUL4B-deleted LBLs exhibit disruption of the mitochondrial membrane potential, Ψ^m

Mitochondria utilize oxidisable substrates to produce what is known as a membrane potential (Ψ^m) across the inner mitochondrial membrane (IMM). This highly negative (~180mV) proton gradient is a key indicator of cellular viability and it is this electrochemical gradient that acts as the driving force behind ATP production. As mentioned briefly in the previous section, Mitotracker Green accumulates independently of the mitochondrial membrane potential and thus gives no indication of mitochondrial functionality in this population. The mitochondria, through their essential roles in ATP synthesis, are thought of as the biological 'powerhouse' of the cell. However, although the Ψ^m is the basis of coupling oxidative phosphorylation and ATP production, it is also crucial for the handling of ions with signaling functions, most notable of which is calcium. Similarly, calcium is an overall positive regulator of Ψ^m and oxidative phosphorylation and thus a physiological stimulus for ATP synthesis.

The generation of a Ψ^m is achieved and maintained through the actions of the Electron Transport Chain (ETC). The ETC resides in the IMM and is composed of 5 complexes that function as a series of electron donors and acceptors; Complexes I - IV and ATP synthase (Complex V). Electrons from NADH and succinate, generated via the citric acid cycle, are passed through the ETC to oxygen which is then reduced to water, a process known as oxidative phosphorylation (OXPHOS) (Fig 3.15). The energy released by electrons flowing through this ETC is used to transport protons across the IMM generating an electrical potential or Ψ^m. This Ψ^m is essential for ATP generation as ATP Synthase (Complex V) uses this proton potential to transport one proton back down the gradient, using the energy to complete the phosphorylation of ADP to ATP. Preservation of this membrane potential is also essential for intracellular calcium regulation and the generation of reactive oxygen species. This will be discussed in greater detail in section 3.2.2.5. The Ψ^m is a key indicator of mitochondrial functioning as it reflects the metabolic activity and integrity of the mitochondrial population. Many mitochondrial disorders are a consequence of ETC alterations and therefore highlight the

importance of Ψ^m maintenance for overall cellular homeostasis. Figure 3.15 summarizes the events that take place during the ETC.

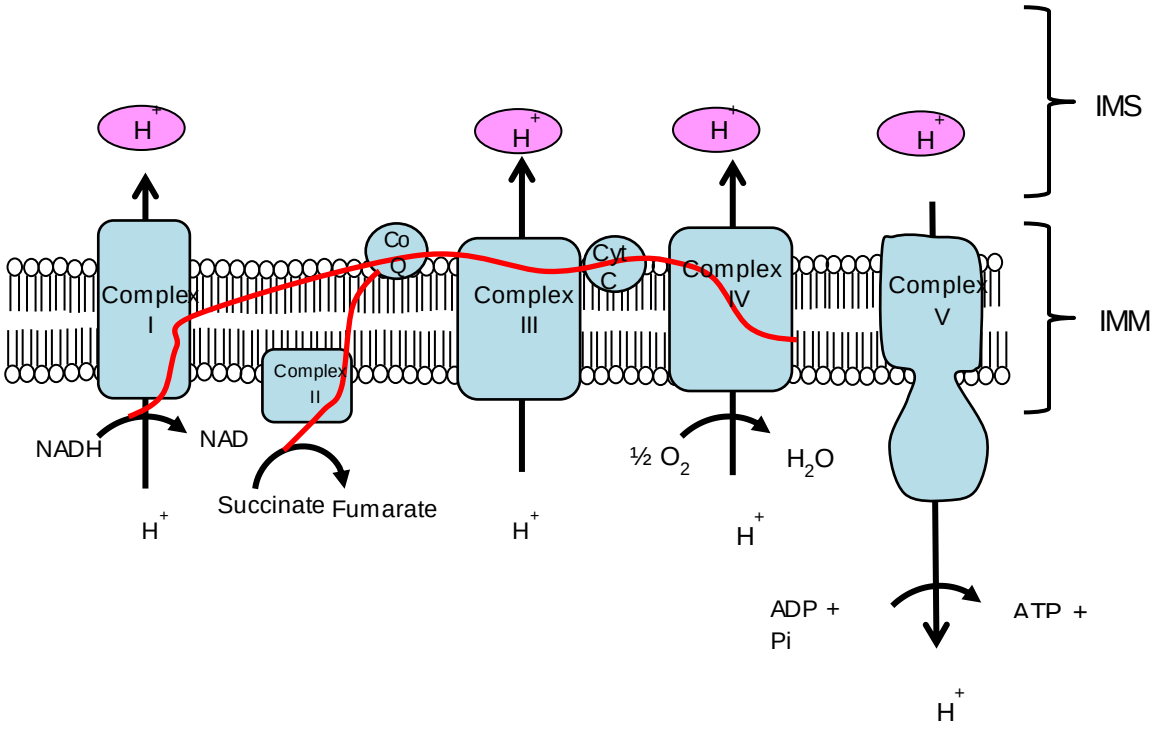

Figure 3.15 – The Electron Transport Chain (ETC). The ETC is composed of 5 complexes (I-V), each containing several different electron carriers. Complex I accepts electrons from NADH and serves as a link between glycolysis, the citric acid cycle, fatty acid oxidation and the electron transport chain. Ultimately, two electrons are transferred from this complex to Coenzyme Q (CoQ) resulting in the net transport of 4 protons (H^+) from the matrix side to the intermembranal space where the H^+ ions accumulate generating a proton motive force. Complex II, also known as succinate dehydrogenase, binds succinate and generates fumarate. This complex then transfers 2 electrons to coenzyme Q to produce $CoQH_2$. $CoQH_2$ is then passed to Complex III where it passes electrons from $CoQH_2$ to cytochrome c via the Q-cycle. The net result of the Q cycle is 2 electrons are passed to cytochrome c and 4 protons are released into the intermembranal space. Cytochrome c is a mobile electron carrier that diffuses through the intermembranal space shuttling electrons from complex III to complex IV. Complex IV, also known as cytochrome c oxidase accepts electrons from cytochrome c and directs them towards the four electron reduction of molecular oxygen to form 2 molecules of water. The reduction of oxygen to water involves the transfer of four electrons and two protons are released into the intermembranal space. This forms the basis of the mitochondrial membrane potential and this is used to transport one proton back down the gradient to complete the phosphorylation of ADP to ATP. IMS; intermembranal space, IMM; inner mitochondrial membrane.

3.2.2.3.1: JC-1 and Ψm

To investigate mitochondrial Ψ^m, I employed the cationic carbocyanine dye, JC-1 (5', 6 6'-tetrachloro-1, 1', 3, 3'-tetraethylbenzimidazolylcarbocyanine iodide) as an indicator of membrane potential. The JC-1 dye accumulates within the mitochondria in a membrane potential-dependent manner. This is indicated by a shift in fluorescence emission from green to red. JC-1 exists as a monomer and at low concentrations/low membrane potential it yields a green fluorescence (529nm). In well-preserved mitochondria, JC-1 forms aggregates known as 'J-aggregates' which yield red fluorescence (~590nm) due to the preservation of a higher membrane potential. This potential-sensitive fluorescence shift is a marker for membrane potential and depolarisation of the membrane (loss of membrane potential) is indicated by a reduction in red: green fluorescence intensity. Carbonyl cyanide-3 chlorophenylhydrazone (CCCP), a mitochondrial depolarising agent, can be used in conjunction with JC-1 to provide a positive green control indicative of complete membrane depolarisation. CCCP functions to inhibit respiration by blocking cytochrome oxidase (complex IV). CCCP-treated cells were used as a positive control for each cell line here and user-defined flow cytometry (FACS) gating was applied before analysing the test samples.

As expected, Wild-type (WT) LBLs showed aggregation of JC-1 confirmed by a shift from green to red fluorescence in the absence of CCCP, indicative of a preserved membrane potential (Fig 3.16 top two panels; 43.6% aggregates). CUL4B LBLs also exhibited a shift from green to red fluorescence in the absence of CCCP, although the magnitude of this shift was reduced compared to WT controls (Fig 3.16 middle two panels; 34.1% aggregates). This suggests that the membrane potential is relatively depolarized compared to wild type controls, thus exhibiting a more negative membrane potential. LBLs from a patient with Leigh syndrome were analyzed as a positive 'mitochondrial disorder' control and were found to exhibit a striking reduction in the red: green ratio with only 7.2% of events exhibiting a red fluorescence (representing JC-1 aggregates) in the absence of CCCP, indicative of membrane potential depolarization (Fig 3.16 bottom two panels). The data presented here is suggestive of a potential disruption to the mitochondrial membrane potential in the context of CUL4B loss. These observations were the

basis for employing a more sensitive and sophisticated mitochondrial probe such as Mitotracker Red.

3.2.2.3.2: Mitotracker Red and Ψ^m

JC-1 staining revealed subtle differences in the membrane potential of *CUL4B*-deleted LBLs. To investigate this further, I used Mitotracker Red CMXRos (MTR) to gain information regarding the membrane potential at a single-cell level. MTR only accumulates in actively respiring mitochondria where it emits a red fluorescence (PE) indicative of an intact and active membrane potential. A decrease in fluorescence represents a reduced membrane potential. LBLs were incubated with 250nM MTR for 15 minutes and analysed by flow cytometry. Wild-type LBLs showed a defined PE peak at approx. 10^4 indicative of a well-preserved membrane potential. CUL4B LBLs however, exhibit a leftward- shift in the PE peak corresponding to a reduced membrane potential – consistent with JC-1 data (profiles not shown). This finding is similar to that of two well-known mitochondrial disorders; Leigh Syndrome and MERRF which also exhibit a reduced membrane potential (See figure 3.17 for mean of 3 independent repeats). These results indicate that CUL4B LBLs exhibit overlapping mitochondrial features with those of well-known mitochondrial disorders.

As mentioned previously, CCCP is a mitochondrial depolarising agent. When cells are incubated with MTR in the presence of CCCP, this gives an indication as to the fluorescence intensity values associated with complete disruption of the membrane potential. Addition of CCCP uncouples the membrane resulting in a dramatic leftward-shift in the PE FACS profiles, corresponding to low intensity values. To investigate the percentage of the overall population that exhibited a reduced membrane potential, 50μM CCCP was added to cells to induce complete depolarisation of the mitochondrial membrane. As expected, the FACS profiles of CCCP-treated cells exhibited a leftward shift (indicated by the red-dashed line in Fig 3.18). These profiles were then overlaid onto the profiles of untreated cells and the percentage of overlap was calculated. Wild-type LBLs overlapped with the CCCP profile by 15% whereas CUL4B LBLs showed a higher overlap, with 37% of

the total events falling within the CCCP-depolarised range (Fig 3.18). This confirms that a high proportion of *CUL4B*-deleted mitochondria exhibit mitochondrial depolarisation.

Mitotracker Red (MTR) can also be analysed by fluorescence microscopy, giving a better indication of the polarisation and distribution at a single-cell level. LBLs were incubated with 250nM MTR for 15 minutes and fixed in 2% formalin. Wild-Type LBLs displayed an even distribution of MTR fluorescence with mitochondria lining the periphery of the cell. This indicated well preserved and actively-respiring mitochondria. In striking contrast, *CUL4B*-deleted LBLs displayed significantly reduced fluorescence intensity with a vast number of cells displaying very low or no mitotracker staining whatsoever. Staining also appeared to accumulate at one side of the cell as shown in the bottom right panel of Figure 3.19a. Interestingly, a proportion of CUL4B LBLs exhibit an extremely high fluorescence in comparison to the majority of the population. Figure 3.19b represents the DAPI stained CUL4B LBLs s in the first panel and the Mitotracker Red labelling of the same CUL4B LBLs in the second panel. The majority of the population had a reduced membrane potential as indicated by those stained with DAPI but with very low MTR staining. However, there were a number of cells exhibiting extremely bright MTR staining in comparison to the overall population (Fig 3.19b). By reducing the exposure time, visualisation of these bright cells was possible and in fact highlighted the extent of depolarisation in the majority of cells. It became apparent that although much of the *CUL4B*-deleted population exhibited depolarisation, a significant minority of cells were 'hyperpolarised'. Whether these hyperpolarised cells were of similar fluorescence levels to 'normal' WT cells and therefore fully functional is unclear. Nevertheless this data has still uncovered a novel and extreme mitochondrial phenotype associated with CUL4B loss.

Consistent with the findings observed in *CUL4B*-deleted LBLs, both mitochondrial membrane potential depolarisation and hyperpolarisation was also observed in *CUL4B*-deleted fibroblasts from the same *CUL4B*-deleted patient (Fig 3.20). Many *CUL4B*-deleted fibroblasts exhibited depolarisation of the mitochondrial membrane potential compared to wild type controls (Fig 3.20a-b). However, consistent with the phenotypes observed in *CUL4B*-deleted LBLs a substantial

proportion of *CUL4B*-deleted fibroblasts exhibited striking hyperpolarisation of the mitochondrial membrane (Fig 3.20c). The extent of this mitochondrial phenotype, consisting of both depolarisation and hyperpolarisation, was only manifest upon direct immunofluorescence-based microscopic analysis of single cells rather than the more conventional flow cytometry-based (FACS) analysis of whole populations. Examining whole-cell populations by FACS analysis masks this striking phenotype whereby those few hyperpolarised cells emit a substantial fluorescence which then skews the data. FACS analysis revealed significant depolarisation in *CUL4B*-deleted LBLs, however microscopy based analysis not only confirmed this depolarisation but also uncovered a much more novel and striking phenotype indicative of widespread mitochondrial membrane potential disruption. These results provide the first evidence of a mitochondrial respiratory chain dysfunction in CUL4B-deficiency which may have many implications for cellular homeostasis ranging from disrupted ATP production and the generation of reactive oxygen species to defects in signalling pathways and ion regulation, specifically that of calcium which relies heavily on the presence of an intact mitochondrial membrane potential.

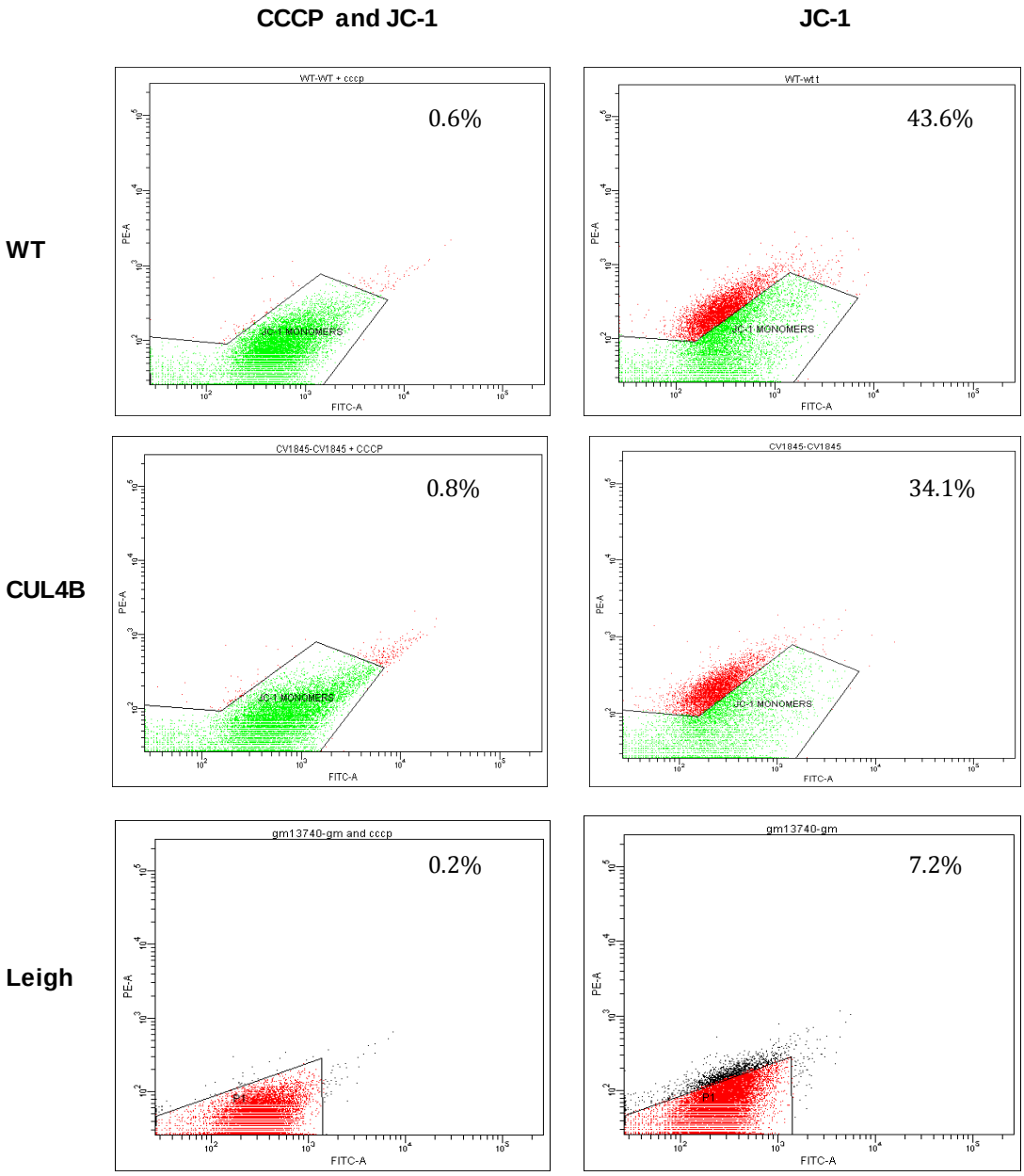

Figure 3.16: JC-1 aggregation as an indicator of mitochondrial membrane potential preservation. Cells were resuspended in 1ml warm RPMI -/+ 50µM CCCP and incubated at 37' for 5 minutes. 2µM JC-1 reagent was then added and cells were incubated for 15 minutes. Cells were washed in PBS, resuspended in 500µL PBS and filtered into BD FACS Falcon tubes. Cells were analysed on the FACS Canto Flow Cytometer with 488nm excitation and 530/30nm and 585/42nm band pass emission filters. Events falling within the user-defined 'P1' gate (gating is specific to each cell line) correspond to JC-1 monomers and those falling outside of this area correspond to JC-1 aggregates (indicative of an intact membrane potential). % of events falling outside the P1 gate are shown on each profile. Top two panels; WT, middle panels; CUL4B, bottom two panels; Leigh Syndrome. Left hand panels + CCCP, right panels JC-1 only. X axis: PE, Y axis; FITC.

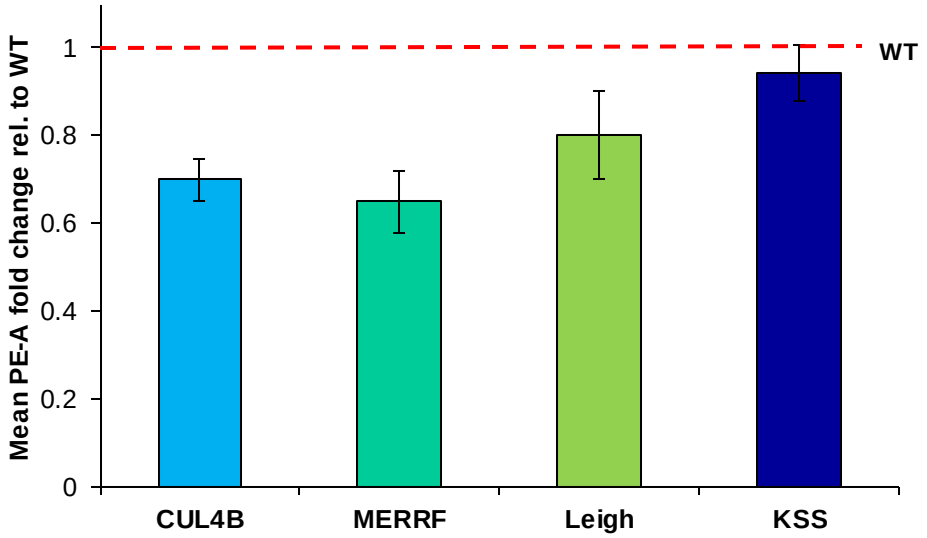

Figure 3.17 - *CUL4B*-deleted LBL's exhibit depolarisation of the mitochondrial membrane similar to that of LBLs from a patient with MERRF (*p<0.05 Student t-test*). Histograms showing mean PE-A fluorescence intensity (FACS measurement) normalized fold change relative to WT (red dashed line) for CUL4B LBL's and control LBLs from three mitochondrial disorders; Leigh Syndrome (Leigh), Myoclonic Epilepsy with Ragged Red Fibres (MERRF) and Kearns Seyre Syndrome (KSS). Data represents the mean ± SD of 5 independent determinations. CUL4B; *CUL4B*-deleted.

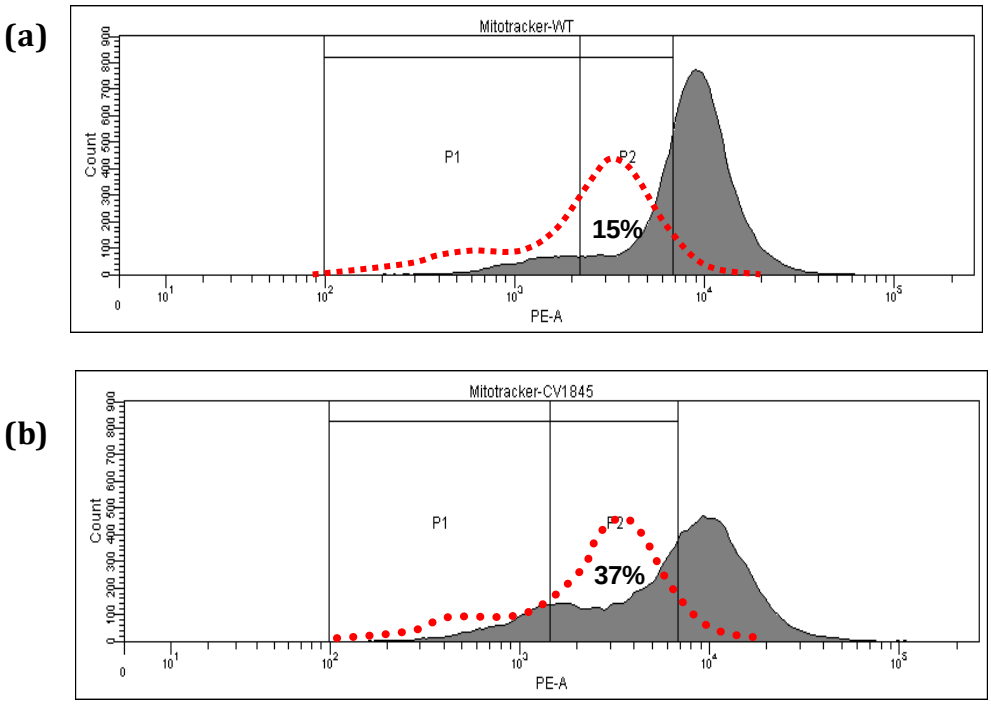

Figure 3.18 –Mitotracker Red Flow Cytometry profiles (FACS). FACS PE-A profiles of **(a)** WT and **(b)** *CUL4B*-deleted LBL's following Mitotracker Red CMXRos (250nM) incubation for 15 minutes. The red dashed line indicates the profile of CCCP (50μM) treated cells. The numbers (15/37) represent the percentage overlap between the two profiles. This overlap is indicative of depolarised cells within the whole population.

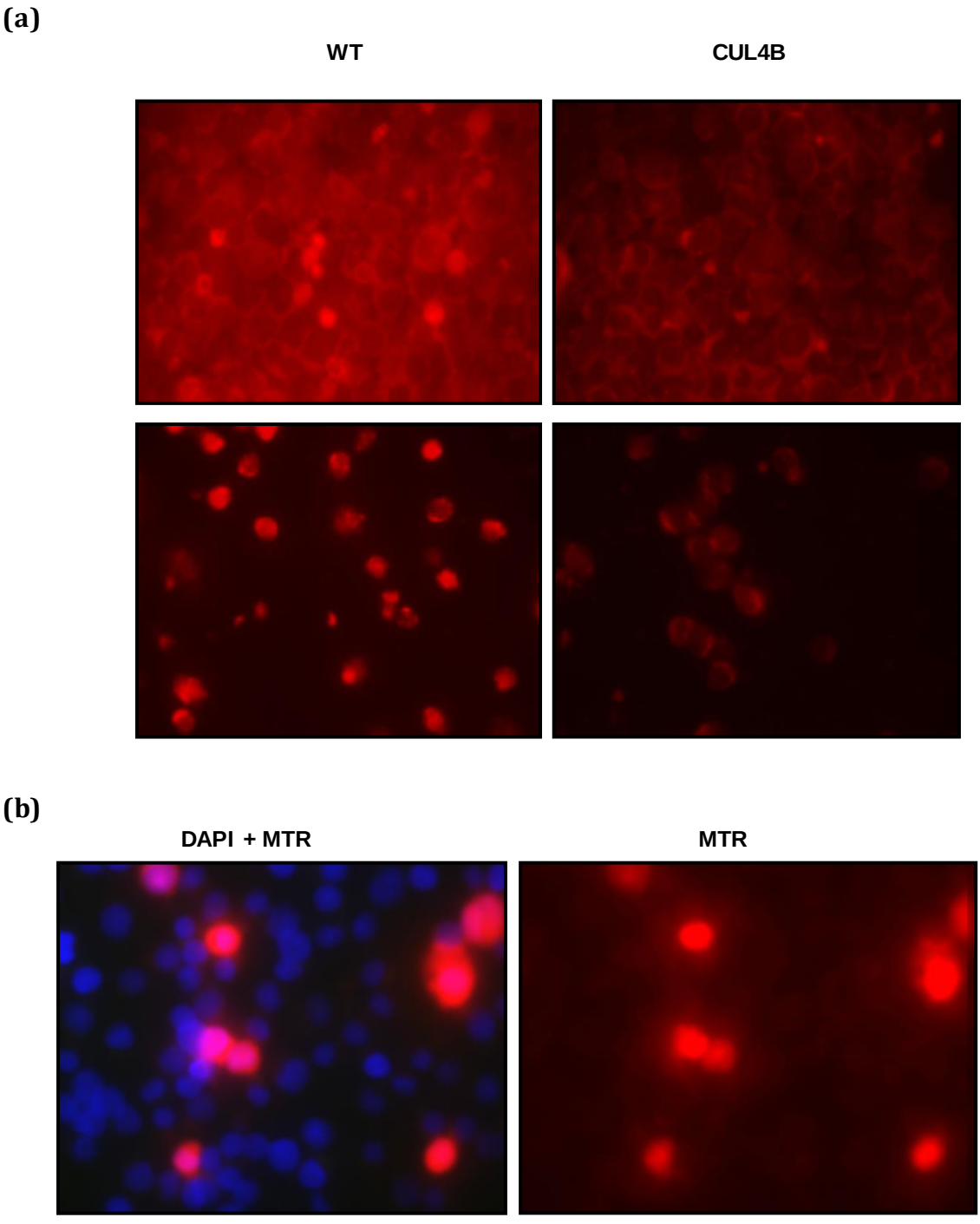

Figure 3.19 - Microscopy-based analysis of Mitotracker Red staining of *CUL4B*-deleted LBLs. **(a)** Top two panels – Wild-type (left) and *CUL4B*-deleted (right) LBL's stained with 250nM Mitotracker Red CMXRos and visualised at 40X. Bottom panels – WT (left) and CUL4B (right), less confluent area of slides visualised at 40X. All images captured with the same exposure timings. **(b)** Left panel: DAPI with MTR overlay. Right panel – MTR only, a significant number of CUL4B LBL's appear to be 'hyperpolarised' but the majority of the population exhibit very low fluorescence as indicated by DAPI stain but no MTR.

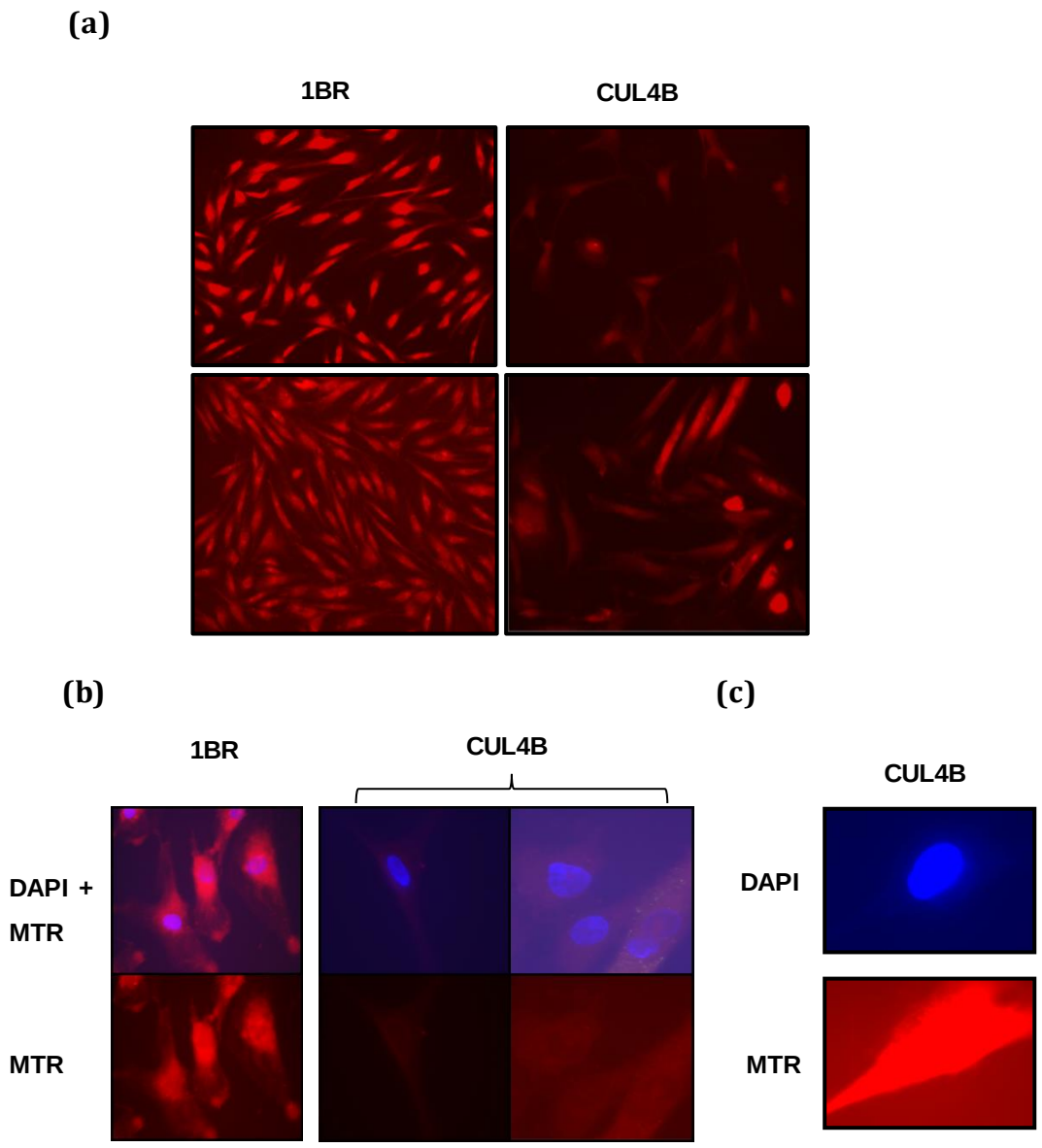

Figure 3.20 – Microscopy-based analysis of Mitotracker Red staining of *CUL4B*-deleted hTERT fibroblasts. **(a)** Left panels; 1BR control, Right panels; CUL4B-deleted fibroblast (9209537) top panel shows depolarised cells, bottom panel shows a more confluent area with hyper- and depolarised cells. Cells were incubated with 250nM Mitotracker Red CMXRos and visualised at 10X. Images were captured with the *same* exposure times. *CUL4B*-deleted fibroblasts exhibit depolarisation of the membrane potential as indicated by reduced Mitotracker Red fluorescence. **(b)** 40X magnification of a subset of cells from the cell populations in panel A. Top three panels; Mitotracker Red (red) with a DAPI (blue) overlay for 1BR control fibroblasts (1BR, right) and *CUL4B*-deleted fibroblasts (CUL4B, left). Bottom three panels: Mitotracker Red fluorescence only. Images were captured with the same exposure times of 0.1 seconds. **(c)** 40X magnification of a single *CUL4B*-deleted fibroblast from a different section of the same slide exhibiting hyperpolarization. This image was taken at the same exposure time as the images in panel B. MTR; Mitotracker Red.

3.2.2.4 CUL4B-deleted LBLs exhibit reduced ATP levels consistent with ETC dysfunction

The respiratory chain and subsequent generation of a mitochondrial membrane potential is essential for the synthesis of ATP by Complex V of the ETC. This ubiquitous molecule is the main energy source for most cellular functions including the synthesis of DNA, RNA and proteins, extra and intracellular signalling pathways and also plays key roles in the maintenance of ion gradients. In addition, the mitochondria are crucial regulators of both intracellular calcium signalling and the generation of reactive oxygen species. Furthermore, a reciprocal relationship between all three has been suggested where each factor can influence the others and therefore, disruption to one will have knock on effects on the others (Brookes et al, 2004). The correct regulation of all three factors relies on an intact membrane potential and is fundamental for various neuronal and muscle-related processes, both of which are disrupted in CUL4B patients. It is therefore likely that one or more of these factors are disrupted in the context of CUL4B loss and identification of these alterations may provide clues into the underlying pathomechanistic aetiology and progression of this disorder.

The data reported so far indicated that loss of CUL4B imparts detrimental effects on respiratory chain functioning suggesting that ATP production may be sub-optimal. Intracellular ATP concentrations were assayed using a colorimetric ATP assay kit (ab8335; Abcam). Wild type and *CUL4B*-deleted LBLs (1 x 10^7 cells) were lysed according to the manufacturer's protocol and loaded into a 96-well plate. Samples were incubated with a reaction mix for one hour and the absorbance was then read at 570nm using the Nanodrop spectrophotometer. The data presented in Figure 3.21 indicated that *CUL4B*-deleted LBLs exhibited reduced ATP concentrations compared with wild type controls. *CUL4B*-deleted LBLs displayed 50% reduction in ATP levels relative to wild type controls. The membrane potential is the driving force behind ATP production therefore, this data is consistent with my previous finding of a reduced mitochondrial membrane potential in *CUL4B*-deleted LBLs.

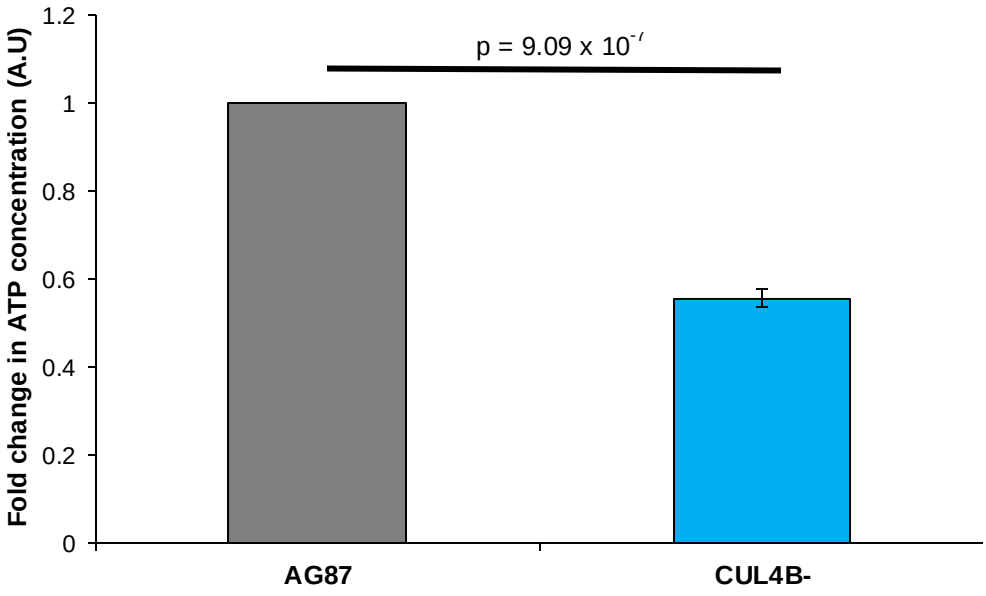

Figure 3.21 – ATP concentration is reduced in *CUL4B*-deleted LBLs. 1 x 10^7 cells were lysed in 50µL provided assay buffer and loaded into a 96-well plate. The reaction mix was made according to the manufacturer's protocol and 50µL was added to each sample well. After a 1 hour incubation the absorbance was read at 570nm using the Nanodrop spectrophotometer. All measurements represent the mean of three independent experiments ±SD. This histogram shows the fold change in ATP concentrations of *CUL4B*-deleted LBLs (0.5 fold) relative to wild-type (AG87) control LBLs (1 fold). CUL4B-deleted LBLs display a 50% reduction in ATP levels compared to WT control LBLs (*p< 0.05, Student t-test*). A.U; Arbitrary Units, CUL4B-; *CUL4B*-deleted.

3.2.2.5: Reactive Oxygen Species; the good and the bad

The generation of reactive oxygen species (ROS) is inevitable for aerobic organisms and normally occurs at a controlled rate. It is noteworthy that although ROS have long been thought of as damaging to the cell, cumulating evidence suggests that ROS are not only detrimental by-products of cellular metabolism but also play a key role in regulating several pathways. The potential for ROS to mediate cell signalling has gained significant attention in recent years and ROS is thought to play key roles in important pathways such as autophagy, the regulation of immunity, gene expression and the activation of cell signalling cascades (Bulua et al, 2011; Chandel et al, 1998; Fleury et al, 2002; Hancock et al, 2001; Lee & Wei, 2000; Rhee, 1999; Tal & Iwasaki, 2009). It appears that a threshold exists for ROS levels and when this threshold is exceeded, ROS become detrimental to the cell leading to oxidative stress. There are several pathways associated with the production of reactive species under normal physiological conditions. These include but are not limited to; membrane-bound NADPH oxidases, Xanthine oxidase, uncoupled NO synthases and mitochondrial respiration (Bedard & Krause, 2007; Satoh et al, 2005).

3.2.2.5.1: Mitochondria-derived ROS

The first report identifying the respiratory chain as a generator of ROS came in 1966 followed closely by the work of Chance and co-workers in the 1970's, who showed that mitochondria produce hydrogen peroxide (H_2O_2) (Jensen, 1966; Loschen et al, 1974; Loschen et al, 1971). Later, it was confirmed that this H_2O_2 arose from the dismutation of superoxide generated in the mitochondria (Loschen et al, 1974). In agreement with these studies the discovery of a mitochondrial manganese superoxide dismutase, MnSOD, confirmed the significance of mitochondrial ROS production.

The mitochondria produce significant amounts of superoxide (O_2^-) as a normal by-product of oxidative phosphorylation (Murphy et al, 2011). In the electron transport chain, electrons are passed through the respiratory complexes via a series of oxidation-reduction reactions (discussed previously in section 3.2.2.3 and

illustrated in Fig 3.15). The resulting oxygen molecule is reduced to produce water however approximately 1-3% of oxygen is incompletely reduced, giving rise to the superoxide radical (O_2^-). O_2^- is formed via the transfer of a free electron to oxygen and is thought to be produced mainly from Complexes I and III of the ETC (Muller et al, 2004) (Bleier & Drose, 2013; Dröse & Brandt, 2012) and Fig 3.22. The location of O_2^- within the mitochondria is important as it is unable to diffuse across membranes. Recent studies suggest that Complex I releases O_2^- into the matrix whereas Complex III can release O_2^- into the matrix and the IMS (Muller et al, 2004). O_2^- is moderately reactive and thought of as the 'primary ROS' which itself can be toxic, especially through inactivation of proteins that contain iron-sulphur centres such as aconitase and succinate dehydrogenase. Ferrous iron released during the inactivation of these proteins is an important reactant for the Fenton Reaction. This reaction involves the oxidation of ferrous iron by hydrogen peroxide to produce ferric iron, a hydroxyl radical and a hydroxyl anion (equation 1 below). Ferric iron is reduced back to ferrous iron, a peroxide radical and a proton by hydrogen peroxide (equation 2 below).

Equation 1 - $Fe^{2+} + H_2O_2 \rightarrow Fe^{3+} + OH\cdot + OH^-$

Equation 2 - $Fe^{3+} + H_2O_2 \rightarrow Fe^{2+} + OOH\cdot + H^+$

Hydrogen peroxide (H_2O_2) is formed through the dismutation of O_2^- by superoxide dismutase's (SODs) but can also occur spontaneously (Equation 1 below and Fig 3.19). Three SOD's exist in mammalians: a cytosolic CuZn SOD (SOD1), an intramitochondrial manganese SOD (SOD2) and an extracellular CuZn SOD (SOD3). H_2O_2 generated by these SOD1 and SOD2 is membrane permeable and can diffuse out of the mitochondria however H_2O_2 can, in turn, produce the highly reactive hydroxyl species ($OH\cdot$) (Equation 2). This species has an estimated physiological half-life of 10^{-9} seconds (Pryor, 1986) and causes peroxidative damage to proteins, lipids and DNA. In addition O_2^- can react with nitric oxide (NO^-), formed by the mitochondrial nitric oxide synthase (NOS), to generate peroxynitrate, another highly reactive species (Equation 3-5).

Equation 3 - $2\ O_2^- + 2H^+ \rightarrow H_2O_2 + O_2$

Equation 4 - $H_2O_2 + Fe^{2+} \rightarrow Fe^{3+} + OH\cdot + OH^-$

Equation 5 - $O_2 + NO^- \rightarrow ONOO^-$

The deleterious effects of ROS are to a large extent prevented by antioxidant systems within the cell. Antioxidant enzymes such as the superoxide dismutase, thioredoxins and peroxiredoxins play important roles in combating oxidative stress. H_2O_2, formed from the reduction of O_2^- by SOD's, can be readily converted to water by mitochondrial glutathione peroxidase (GPX), oxidising reduced glutathione (GSH) to oxidised glutathione (GSSG) (Cadenas & Davies, 2000; Esworthy et al, 1997; Fridovich, 1995; Han et al, 2003) and Fig 3.22. The significance of MnSOD in particular is clearly demonstrated in models of MnSOD-knockout mice, where superoxide produced in the mitochondria is not removed by the normal mechanisms. Mice develop lactic acidemia, cardiomyopathy, degradation of basal ganglia and neuronal axonopathy mimicking many of the symptoms seen in children with genetic defects of the respiratory chain (Lebovitz et al, 1996; Li et al, 1995; Melov et al, 1998). In addition to GSH, peroxiredoxins are also effective in scavenging H_2O_2 by using thioredoxin (Trx) to detoxify H_2O_2 in the following reactions;

Equation 6 - Prx (reduced) + H_2O_2 → Prx (oxidized) +2 H_2O

Equation 7 - Prx (oxidized) + Trx (reduced) → Prx (reduced) + Trx (oxidised)

Interestingly Peroxiredoxin III encoded by the *PDRX3* gene, is localized in the mitochondria and has recently been identified as a CUL4B substrate (Li et al, 2011). Several other low-molecular weight antioxidants including α-tocopherol and ubiquinol are also present and are particularly effective in scavenging lipid peroxyl radicals.

The scavenging actions of antioxidants are not absolute and the reactive species that evades them can damage proteins, lipids and DNA. An important point to remember here is that this includes the mtDNA which lacks histones and is

therefore though to be less protected from ROS-induced damage compared to nuclear DNA (Duchen, 2004). Furthermore, the products of protein and lipid oxidation can cause secondary damage to proteins which may result in a loss of catalytic function and subsequent selective degradation. Mitochondrial proteins are an important target of oxidative damage and protein oxidation and nitration results in disruption to functioning of components of the ETC. One such example is the adenine nucleotide translocator (ANT), a target of nitric oxide and peroxynitrate. Oxidative damage impairs the influx of ADP into the mitochondrial matrix resulting in disrupted ATP synthesis (Vieira et al, 2001). Respiratory chain dysfunction, as a consequence of elevated ROS levels, can lead to further increases in reactive species generation with following oxidative stress and cellular damage thereby creating a 'vicious circle' (Rottenberg et al, 2009).

Elevated ROS production has been associated with many pathophysiological settings including the aging process, epilepsy and neurodegenerative disorders (Cadenas & Davies, 2000; Lin & Beal, 2006; Navarro & Boveris, 2007; Seo et al, 2010; Trojanowski, 2003; Winklhofer & Haass, 2010). Ataxia-Telangiectasia is a progressive neurodegenerative condition caused by mutations in the *ATM* gene (McKinnon, 2012). ATM plays an important role in DNA DSB signalling but cells from A-T patients exhibit elevated oxidative stress associated with mitochondrial dysfunction. A-T cells exhibit a decreased membrane potential and elevated production of ROS (Pallardó et al, 2010). As the name suggests, one of the main clinical features of this disorder is ataxia and for over 30 years researchers have assumed that this is due to impaired DNA repair (reviewed in (McKinnon, 2012). However, some suggest that an increase in ROS generation and disruption of respiratory chain function could also be relevant (reviewed in (Ditch & Paull, 2012). In section 3.2.2.3, I have shown that CUL4B LBLs display disruption of the mitochondrial membrane potential which could have profound impacts on the generation of ROS from the ETC. Interestingly, CUL4B patients also present with an ataxic phenotype and this suggests that mitochondrial dysfunction may play a role here. Furthermore, another invariant clinical feature of CUL4B patients is epileptic seizures (Tarpey et al, 2007a). Epilepsy has long been associated with mitochondrial dysfunction and ROS production. In fact, many patients with

mitochondrial disorders present with seizures from an early age (Cock & Schapira, 1999; Folbergrová & Kunz, 2012; Kudin et al, 2009; Waldbaum & Patel, 2010). It is conceivable that the seizures experienced by CUL4B patients may also, in part, be a consequence of mitochondrial dysfunction (Folbergrová & Kunz, 2012; Waldbaum & Patel, 2010; Wu et al, 2010; Zsurka et al, 2010).

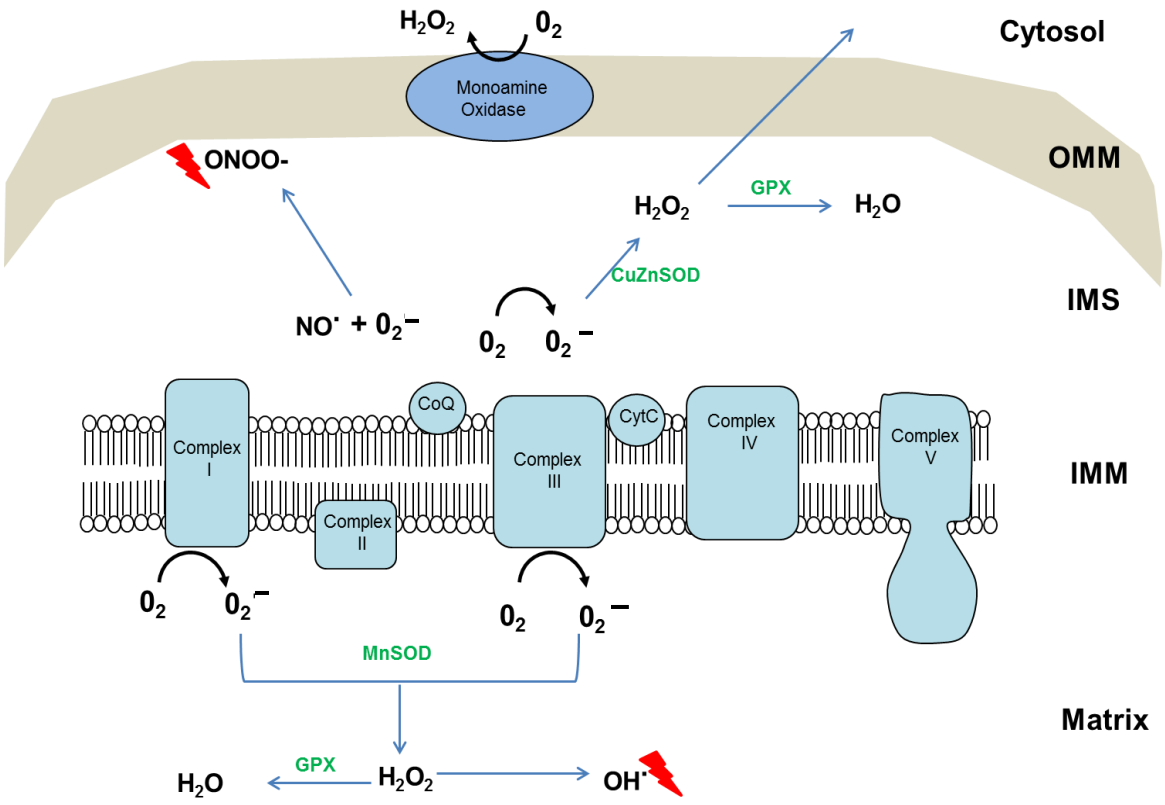

Figure 3.22: Sources of mitochondrially-derived reactive oxygen species. Mitochondrially derived superoxide is generated mainly from complexes I and III of the electron transport chain. Superoxide is scavenged by the superoxide dismutases; MnSOD and CuZnSOD to form hydrogen peroxide (H_2O_2). Glutathione peroxidase (GPX) then converts this to water. H_2O_2 can also form the highly reactive hydroxyl species (OH^-). Nitric Oxide (NO^-) formed by mtNOS can react with superoxide to form peroxynitrate ($ONOO^-$), another highly reactive species. OMM; Outer mitochondrial membrane, IMS; intermembranal space, IMM; inner mitochondrial membrane. Red lightning bolt indicates harmful hydroxyl species.

3.2.2.5.2: MitoSOX; CUL4B LBLs show increased levels of mito-specific ROS

To investigate the levels of ROS within CUL4B-mitochondria, I employed the fluoro-probe, MitoSOX. This probe allows the selective detection of the mitochondrial-specific superoxide. This novel probe enters the mitochondria where it subsequently emits a bright red fluorescence once oxidised specifically by superoxide. In addition to the CUL4B-XLMR patient-derived LBLs, I obtained LBLs from a patient with MERRF syndrome, an established mitochondrial disorder, for use as a positive control when using this probe. LBLs were incubated with 250nM MitoSOX for 15 minutes and then analysed on the FACS Canto Flow Cytometer. Wild-type LBLs exhibited low fluorescence indicative of low levels of mitochondrial-superoxide (Black line Fig 3.23a). MERRF LBLs, as expected, exhibited a right-shifted peak with high fluorescence where 48% of the total events fell within a ROS positive range (Red line Fig 3.23a). This result is consistent with reports of increased levels of mtROS associated with this disease (Wu et al, 2010). Interestingly, *CUL4B*-deleted LBLs exhibited a similar profile to that of MERRF LBLs; a wide peak spanning across high fluorescent intensity values with 40.4% of the total events falling within a ROS positive range (Green line Fig 3.23a and Fig 3.23b). To confirm that the ROS production was specifically mitochondrially-derived, I employed another cell-permeant dye; Cell ROX Red to determine total cellular ROS levels. Data is shown in Figure 3.23c-d and indicates that total cellular ROS levels in *CUL4B*-deleted LBLs appear similar to those of a WT control.

The data presented here provides evidence that the elevated generation of ROS in *CUL4B*-deleted LBLs is mitochondria-specific, indicative of a potential mitochondrial dysfunction. ROS production is heavily influenced by the coupling state of the mitochondria therefore these results are consistent with a disruption of the membrane potential as previously indicated by Mitotracker Red (section 3.2.2.3.2). Whether elevated ROS generation is a cause or consequence of altered OXPHOS (and subsequent disruption to ATP production) is still under debate within the literature. However, these two processes are intimately linked and disruption of one will lead to disruption of the other thus creating a continually damaging cycle. The association of a highly polarised membrane potential and

increased generation of ROS is widespread in the literature and is thought to be due to slowed electron transport (Madamanchi & Runge, 2007; Ohashi et al, 2006). In support of this are the observations that mitochondrial membrane depolarisation, either by chemical uncouplers or overexpression of mitochondrial uncoupling proteins, results in decreased ROS production (Brennan et al, 2006; Toime & Brand, 2010). With this in mind, the results presented here would be inconsistent with the depolarisation indicated by reduced Mitotracker Red fluorescence. However, there is evidence to suggest that depolarisation of the mitochondrial membrane potential is associated with increased ROS generation (Lebiedzinska et al, 2010). It has been proposed that physiological ROS signalling occurs within an optimised membrane potential, however oxidative stress occurs either at extreme hyperpolarization or depolarization (Aon et al, 2010). Furthermore, excessive ROS generation can promote opening of the mitochondrial permeability transition pore which, once opened, leads to loss of the mitochondrial membrane potential and further mitochondrial dysfunction (Brenner & Moulin, 2012). Therefore, the depolarisation seen in *CUL4B*-deleted mitochondria may be a consequence of chronic ROS generation and subsequent mPTP induction. This will be further discussed in section 3.2.2.8.

3.2.2.6: ETC Complex I activity is unaltered in CUL4B-deleted LBLs

As briefly mentioned in section 3.2.2.5.1, mitochondrial ROS is mainly generated from Complexes I and III of the ETC (Bleier & Drose, 2013). Complex I (NADH: ubiquinone oxidoreductase), located in the inner mitochondrial membrane, is the largest enzyme in the respiratory chain and provides the entry point for electrons into the ETC. Complex I deficiency is the most frequent mitochondrial disorder presenting in childhood and is characterised by marked clinical and genetic heterogeneity, The most common clinical presentations include; Leigh Syndrome, cardiomyopathy, MELAS and early-onset neurodegenerative disorders (Fassone et al, 2011; Liolitsa et al, 2003; Rahman et al, 1996). Altered complex I activity has also been implicated in the pathogenesis of Parkinson's disease and Bipolar Disorder (Andreazza Ac, 2010; Esteves et al, 2010). As mentioned in section 3.2.2.5.1, Complex I is one of the main sites of electron leakage and subsequent

generation of superoxide within the mitochondria (Han et al, 2003; Talbot et al, 2004). As CUL4B LBLs display marked increases in mtROS generation with disruption of the mitochondrial membrane potential, I looked to investigate whether this was a result of altered complex I activity.

I employed the Complex I Enzyme Activity Dipstick Assay Kit to determine the relative specific activity of immunocaptured Complex I. A dipstick with immunocaptured Complex I is immersed in a buffer solution containing NADH and nitrotetrazolium blue (NBT). Complex I oxidises NADH which in turn reduces NBT to form a blue precipitate at the antibody line on the dipstick (~7mm from the bottom). The signal intensity, corresponding to the relative activity of immunocaptured Complex I, can then be read using standard imaging software (Image J) (Abcam: http://www.abcam.com/Complex-I-Enzyme-Activity-Dipstick-Assay-Kit-ab109720.html). The data shown in Figure 3.24 indicates that the relative Complex I activity in CUL4B LBLs was similar to that of WT-LBLs indicating that Complex I activity is not altered by the loss of CUL4B. As discussed in 3.2.2.5, ROS are mainly generated from complexes I and III of the ETC. There is also evidence that ROS can be produced from Complex II (Ganesh et al, 2013; Rustin & Rotig, 2002). Although the data presented here is not suggestive of increased levels of Complex I-generated ROS, the excessive ROS could be produced from one or more of the other ETC complexes such as Complex II and/or III. Specific analysis of the activity of other ETC complexes may allow the identification of the site of excessive ROS generation in this setting.

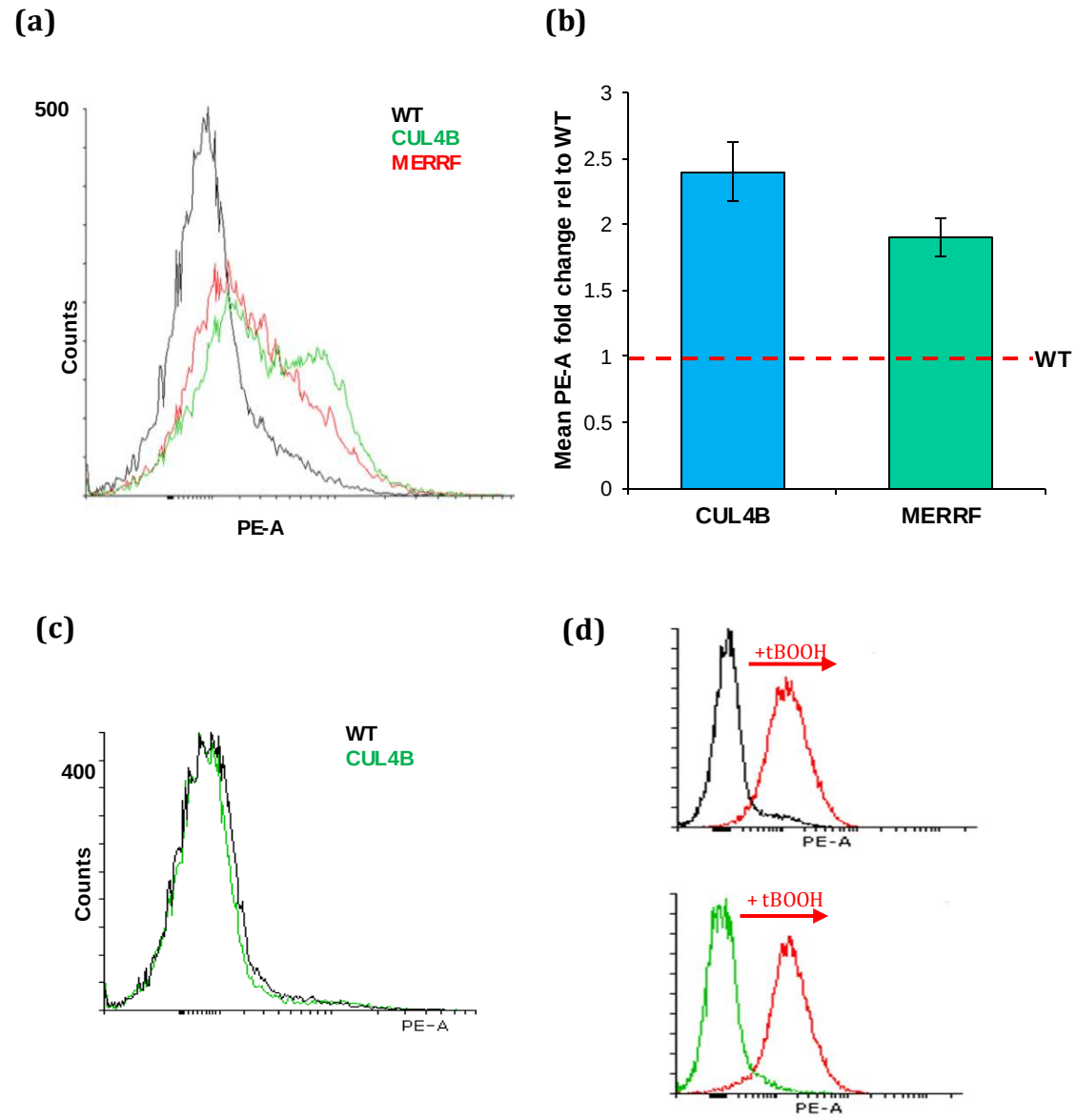

Figure 3.23 - CUL4B LBL's show elevated levels of mitochondria-specific ROS. **(a)** Overlaid MitoSOX FACS profiles showing PE-A intensity of 20,000 events. Cells were incubated with 250nM MitoSox for 15 mins (Black; Wild-type LBLs, Red; MERRF LBLs, Green; CUL4B LBLs). **(b)** Histogram showing overall PE-A (measured by FACS) mean fluorescence intensity fold change of *CUL4B*-deleted LBLs and MERRF LBLs relative to WT controls (red dashed line). MERRF and CUL4B-deleted LBLs exhibit increased production of O_2^- (*$p<0.05$ Student t-test).* Data represents the mean ±SD of 5 independent experiments. **(c)** Total cellular ROS levels in *CUL4B*-deleted LBLs are similar to wild type controls as determined by Cell ROX Red fluorescence. Cell ROX Red FACS profiles showing PE-A intensity of 20,000 events. Black; Wild type, Green; *CUL4B*-deleted. **(d)** As a positive control for total cellular ROS, WT (top panel) and *CUL4B*-deleted (bottom panel) LBLs were treated with 100μM tertiary-butyl peroxide (t-BOOH) for one hour prior to Cell ROX Red incubation. The rightward shift in the FACS PE-A profile of LBLs treated with t-BOOH (indicated in red) compared to untreated LBLs (black for WT, green for CUL4B) is indicative of increased cellular ROS.

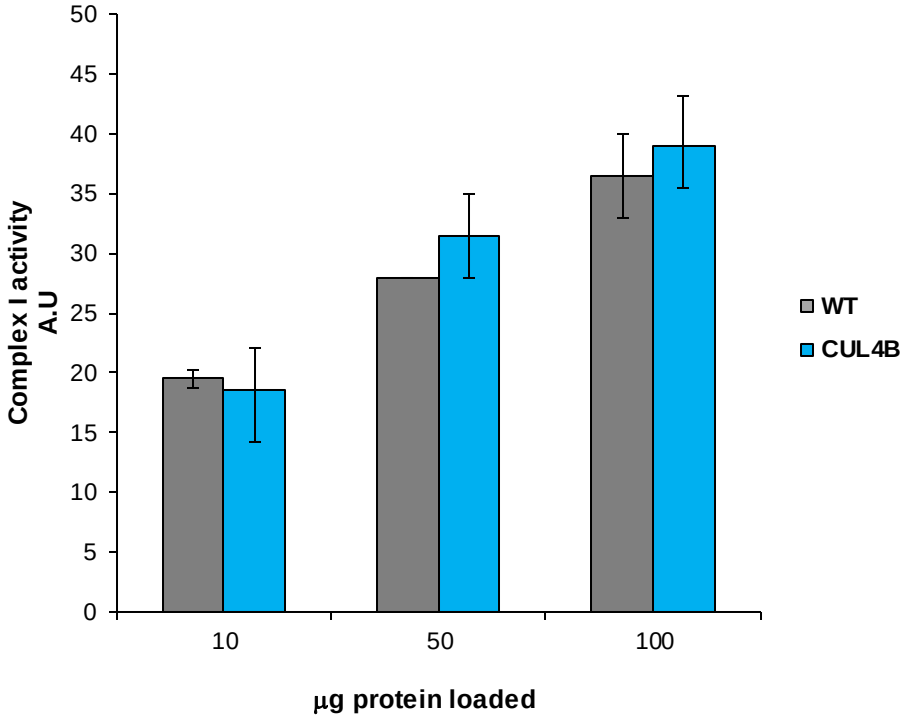

Figure 3.24 – Complex I enzyme activity appears unaltered in the context of CUL4B loss. Increasing amounts of extract (10-100µg) were analysed for Complex I activity using a dipstick assay method. Immunocaptured Complex I oxidises NADH, reducing NBT to form a blue precipitate at the antibody level ~7mm from the bottom of the dipstick. Signal intensity of this blue precipitate was scanned and measured using Image J software. A.U; arbitrary units from Image J analysis. Data represents the mean ± SD of 3 independent experiments.

3.2.2.7: Intracellular calcium levels are increased in CUL4B-deleted LBLs

Mitochondria play a substantial role in calcium (Ca^{2+}) homeostasis. The mitochondria are the main repository for Ca^{2+} in the cell through their action as spatial Ca^{2+} buffers regulating local Ca^{2+} concentrations and so regulating the activity of calcium dependent processes (Duchen, 2000; Wong et al, 2012). Ca^{2+} transport across the IMM is achieved by the action of various transporters through a complex system consisting of two modes of influx and two of efflux. The most intensely studied Ca^{2+} influx mechanism is that of the uniporter (UP), which functions to transport calcium without coupling it to the transport of any other ion or molecule (Patron et al, 2013). The transport of Ca^{2+} via this route is dependent on the electrochemical gradient for Ca^{2+} which is developed and maintained by the mitochondrial membrane potential. The primary role of this Ca^{2+} transport system is to relay changes in cytosolic Ca^{2+} into the mitochondrial matrix to increase the H+ extrusion important for both the maintenance of the driving force behind Ca^{2+} uptake and for ATP production (Gunter et al, 2000; McCormack & Denton, 1993). Under normal physiological conditions, Ca^{2+} is an overall positive regulator of mitochondrial function, however perturbations in Ca^{2+} homeostasis have negative effects and can be a stimulus for excessive mitochondrial-ROS generation, cytochrome c release, opening of the mitochondrial permeability transition pore and apoptosis. Conversely, increases in ROS generation can both inhibit and stimulate calcium signalling (Baumgartner et al, 2009; Brookes et al, 2004; Duchen, 2000; Gordeeva et al, 2003).

The results presented so far indicated that in the context of *CUL4B* deletion in patient-derived cells, both OXPHOS and the generation of ROS are disrupted. Therefore, in light of the striking mitochondrial phenotypes identified so far, I set out to investigate intracellular calcium levels in the context of CUL4B loss. I employed the long-wave calcium indicator, Calcium Green -1 AM. This probe is prepared in its cell-permeant acetoxymethyl (AM) ester form and upon binding to calcium, exhibits an increase in fluorescence emission intensity with little shift in wavelength, as measured by flow cytometry. FACS analysis revealed that CUL4B LBLs exhibit increased calcium 1-AM fluorescence indicative of increased intracellular calcium levels (Fig 3.25). The phenotype revealed here is consistent

with my previous findings of disruption to the membrane potential and elevated ROS levels which contribute to mitochondrial dysfunction in the context of CUL4B loss. Furthermore, optimal calcium regulation is essential for many neuronal processes including neurotransmitter release, integration and propagation of postsynaptic signals and neurite outgrowth. In particular, both increased and decreased intracellular calcium have been reported to be cytotoxic to neurons (Arundine & Tymianski, 2003; Choi, 1988). Therefore, the increased levels of calcium observed here may have important implications for neuronal development, maturation and function thus potentially contributing to some of the neurological deficits associated with CUL4B-deficiency.

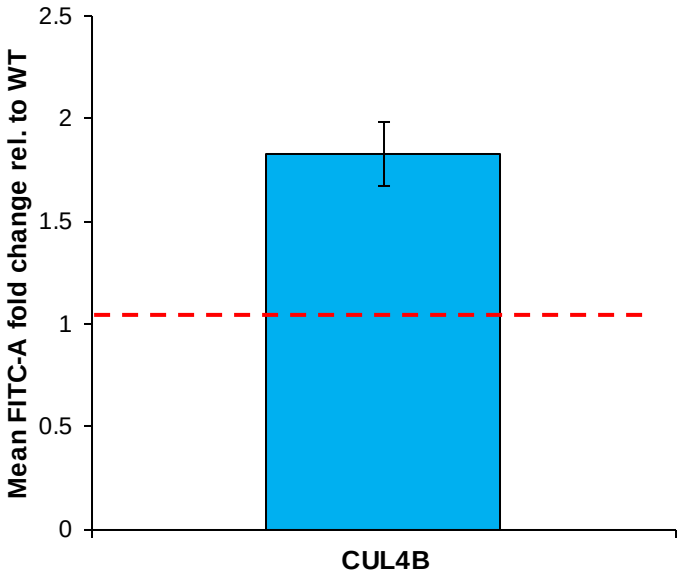

Figure 3.25 – Intracellular calcium levels are increased in *CUL4B*-deleted LBLs. Wild-type and *CUL4B*-deleted LBLs were incubated with 10μM Calcium 1-AM for 20 minutes at 37 °C. Cells were then washed in PBS and analysed by flow cytometry for FITC fluorescence. Excitation/emission filters; 506/531. This data represents the mean of 3 independent experiments ± standard deviation, relative to wild-type controls (red dashed line).

3.2.2.8: CUL4B-deleted LBLs exhibit hypersensitivity of the mitochondrial transition pore

Calcium uptake by the mitochondria evokes a rise in mitochondrial matrix calcium concentrations which, in turn, exerts control over several steps of energy metabolism and ATP production. In a healthy cell, as calcium is taken up and released by mitochondria, a low conductance permeability transition pore, the mitochondrial Permeability Transition Pore (mPTP), appears to flicker between open and closed states (Brenner & Moulin, 2012). The mPTP is a non-selective voltage-dependent mitochondrial channel whose precise molecular constitution is still largely unknown (Siemen & Ziemer, 2013). With regards to its location, the PTP component forming the channel is proposed to reside in the IMM. Although the exact composition of the mPTP is ill-defined, several reports have suggested ANT, VDAC, CypD and Hexokinase as promising constituents (Cesura et al, 2003; Giorgio et al, 2013; Leung et al, 2008; Shimizu et al, 2001; Siemen & Ziemer, 2013; Zhivotovsky et al, 2009).

Opening of the transition pore leads to the onset of mitochondrial permeability transition (MPT). MPT is defined as a sudden increase in the unselective permeability to ions and metabolites >1.5kDa across the mitochondrial inner membrane. In response to various stimuli such as ROS, increased cytoplasmic Ca^{2+} concentrations and misfolded mitochondrial proteins, sustained and irreversible opening of the mPTP ensues allowing solutes to accumulate within the matrix. Furthermore, rising mitochondrial Ca^{2+} concentrations can stimulate the generation of ROS which, in turn, contribute to mPTP activation (Peng & Jou, 2010). One major consequence of sustained mPTP opening is the dissipation of the membrane potential leading to the uncoupling of OXPHOS which prevents ATP production. A second consequence of mPTP opening is the expansion of the matrix space with subsequent rupturing of the OMM. This leads to the release of the intermembranal space contents, including the release of accumulated Ca^{2+}, release of cytochrome c, ultimately resulting in cell death via apoptosis or necrosis.

PTP function is central to many key mitochondrial functions and can play a considerable role in many pathophysiological conditions. Recent studies have

shown that the threshold for mPTP opening is significantly reduced by pathological conditions such as heart failure and diabetes in addition to several well-known neurodegenerative disorders such as Parkinson's Disease (Abou-Sleiman et al, 2006; Gautier et al, 2012). A common mechanism underlying this increased sensitivity is the excessive generation of ROS. Here, I have shown that CUL4B LBLs exhibit elevated levels of ROS suggesting that mPTP opening may also be altered by CUL4B loss. Furthermore, *CUL4B*-deleted LBLs display considerably increased levels of intracellular calcium in addition to depolarisation of the mitochondrial membrane, both activatory stimuli for mPTP opening. I set out to determine whether these imbalances had a knock-on effect on the opening of the permeability pore in response to treatment with ionomycin. Ionomycin is an ionophore which increases the permeability of the membrane to calcium ions. It is possible that the mPTP of *CUL4B*-deleted cells has adapted to the local environment of high calcium and ROS levels and therefore does not respond to further elevations in calcium. Similarly, it is also possible that this environment could render the mPTP hypersensitive to even very small increases in mitochondrial calcium, induced by low concentrations of ionomycin.

The MitoProbe Transition Pore Assay Kit employs calcein AM, a colourless and non-fluorescent esterase substrate, and cobalt chloride ($CoCl_2$), a quencher of calcein fluorescence, to provide a direct method to selectively label mitochondria (Life Technologies™, http://products.invitrogen.com/ivgn/product/M34153) (Fig 3.26). This assay involves 4 key steps;

1. Cells are loaded with the acetoxymethyl ester form of calcein dye, calcein AM (Ca-AM). This passively diffuses across into the cell accumulating in the cytosolic compartments (including the mitochondria) (Fig 3.26a A).
2. Once inside the cell, intracellular esterases function to cleave the acetoxymethyl ester, liberating the very polar fluorescent dye, calcein. This form is unable to cross the mitochondrial or plasma membranes and exhibits high fluorescence (Fig 3.26aB and Fig 3.26b grey line)
3. Addition of $CoCl_2$ quenches the fluorescence from cytosolic calcein only therefore maintaining the mitochondrial-specific calcein fluorescence (Fig 3.26aC and Fig 3.26b green line).

4. Cells can then be treated with the ionophore, ionomycin, to allow the entry of excess calcium into the mitochondria triggering activation and opening of the mPTP. This allows the mitochondrial calcein fluorescence to be quenched by the $CoCl_2$ resulting in a loss of fluorescence indicative of continuous pore activation (Fig 3.26b).

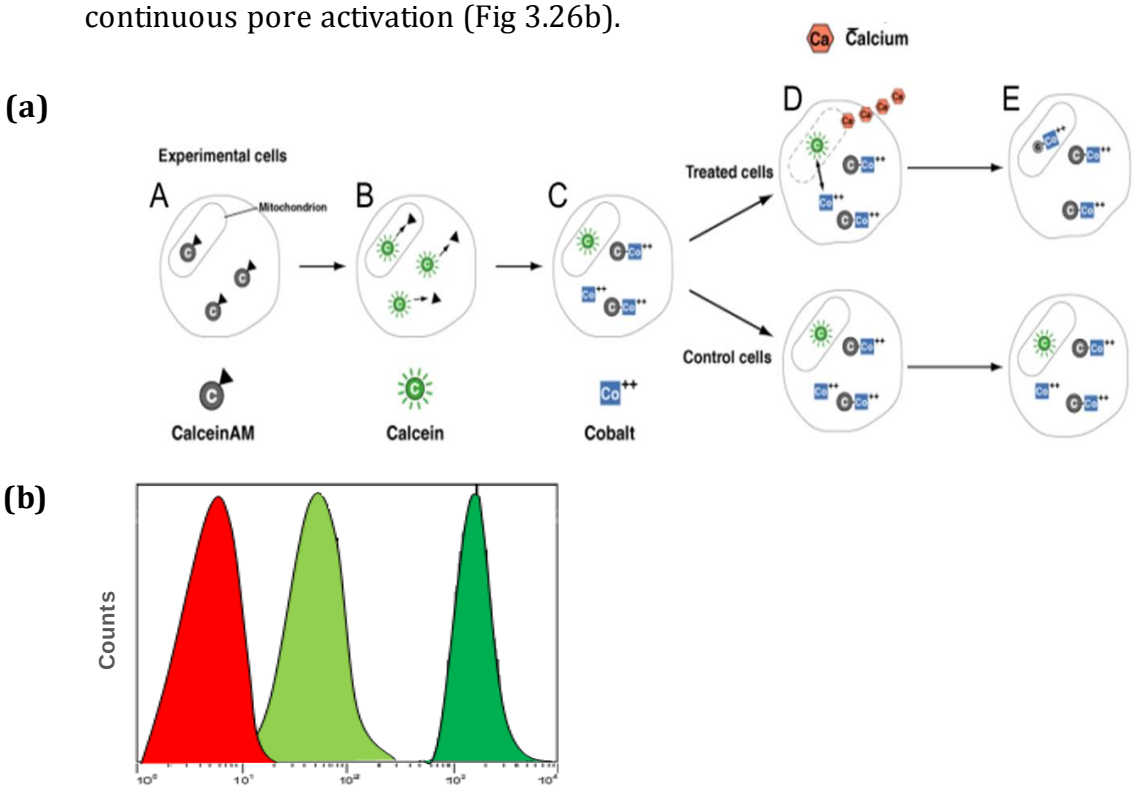

Figure 3.26 - The Mitoprobe ™ Transition Pore Assay Kit (Molecular Probes M34153). **(a)** Schematic illustration of the assay mechanisms. (A) The Calcein dye is prepared in its acetoxymethyl ester form and added to cells, (B) Once inside the cells it is then cleaved by esterases and emits a bright green fluorescence. This fluorescent calcein is present in both the cytosol and the mitochondria, (C) In the presence of $CoCl_2$, calcein in the mitochondria emits a signal, but the cytosolic calcein fluorescence is quenched resulting in reduced overall fluorescence compared to the addition of calcein alone, D) When $CoCl_2$ and ionomycin are added to cells at the same time as calcein AM, the fluorescence signals from both the cytosol and the mitochondria are largely abolished resulting in a dramatic reduction in fluorescence. The change in fluorescence from C → D indicates the continuous activation or the mitochondrial permeability transition pores. **(b)** Illustration of the FACS profiles at each step of the pathway illustrated in (a). The dark green profile represents calcein fluorescence of cells treated with calcein only - whole cell fluorescence. The light green profile represents the shift in calcein fluorescence intensity following the addition of $CoCl_2$ - mitochondrial calcein fluorescence only. The red profile represents the calcein fluorescence intensity upon addition of CaAM, $CoCl_2$ and ionomycin. The shift in fluorescence from the light green profile to the red profile indicates the opening of the transition pores. CaAM; calcein AM, $CoCl_2$; cobalt chloride.

Addition of $CoCl_2$ to WT and *CUL4B-/-* LBLs resulted in a fluorescence shift corresponding to the mitochondrial-specific calcein fluorescence. Initially, it appeared that the addition of ionomycin (500nM as per the manufacturers' protocol) to both WT and CUL4B LBLs resulted in a dramatic reduction (~50-80%) in FITC fluorescence intensity (Fig 3.27; Unt vs. 500nM). This reduction was indicative of mPTP opening and appeared to be comparable between WT and CUL4B-/- LBLs. This data suggested that CUL4B loss did not affect the functioning of the mPTP. However, upon titration of the ionomycin concentration to a much lower level (0.5nM-500nM), it became apparent that *CUL4B*-deleted LBLs responded differently to WT LBLs in this assay. Opening of the mPTP and the subsequent loss of calcein fluorescence in *CUL4B*-/- LBLs was evident upon addition of very low concentrations of ionomycin (0.5nM, 5nM), concentrations of which did not result in opening of the pore in WT LBLs. In particular, the addition of 5nM ionomycin to WT LBLs led to a 7% reduction in fluorescence intensity suggesting that the mPTP was not activated at this concentration (Fig 3.27; WT white bar). However, addition of 5nM ionomycin to CUL4B LBLs led to a dramatic 80% reduction in fluorescence intensity indicating that the mPTP was activated and opened (Fig 3.27; CUL4B white bar).

The results presented here suggest that *CUL4B*-deleted LBLs appear to show hypersensitivity to overloads of intracellular calcium induced by the addition of ionomycin. I have previously shown that *CUL4B*-deleted LBLs exhibit elevated levels of intracellular calcium and ROS, both of which are known to activate the mPTP. Therefore, in this setting, an imbalance acting in favour of pore opening already exists and thus it appears that the mPTP is rendered hypersensitive to any further perturbations. This hypersensitivity could have detrimental effects on cellular homeostasis as continuous activation of this pore results in membrane depolarization and cell death. Consistent with this, I have already shown in section 3.2.2.3.2 that the majority of *CUL4B*-deleted cells appear depolarized with a minority exhibiting a dramatic hyperpolarization.

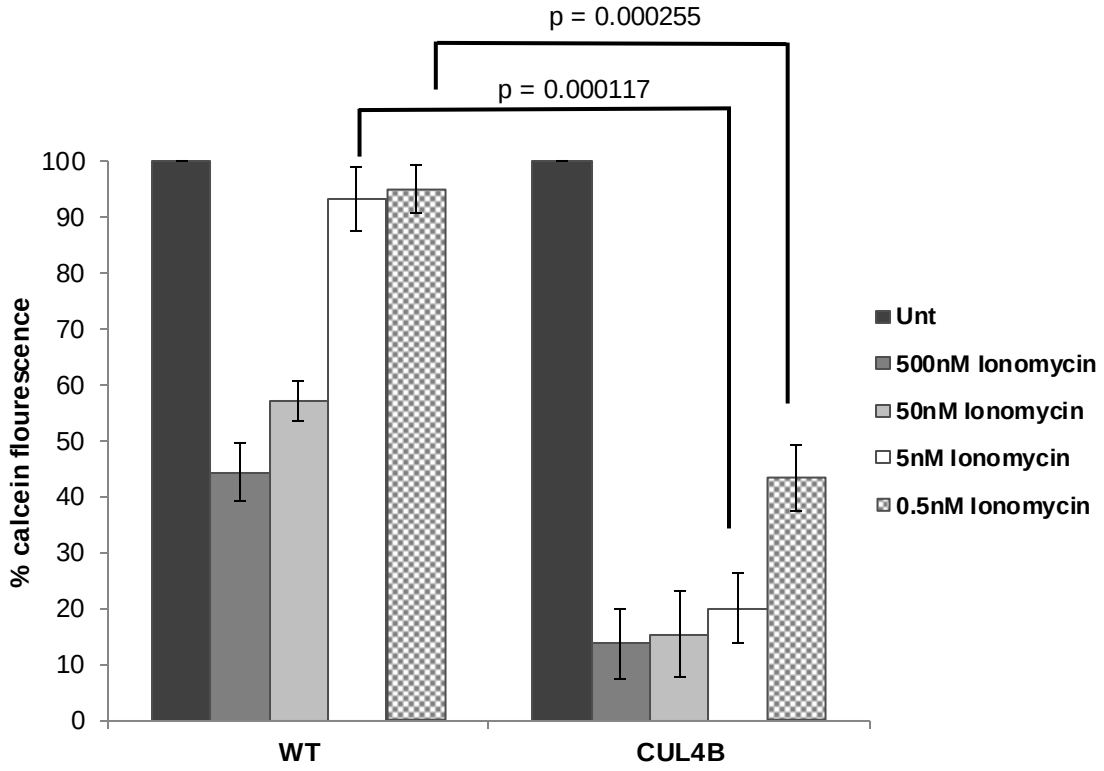

Figure 3.27 –*CUL4B*-deleted mitochondria exhibit mPTP hypersensitivity. Wild-type (WT) and *CUL4B*-deleted (CUL4B) LBLs were suspended in Hanks Balanced Salt Solution with Calcium (HBSS/Ca^{2+}) at final concentration of 1 x 10^6 cells/ml. 5 tubes were prepared containing one ml of cells per cell line; tube 1 (Unt): calcein AM and $CoCl_2$ only, tube 2 (500nM): Calcein AM, $CoCl_2$ and 500nM ionomycin, tube 3 (50nM) Calcein AM, $CoCl_2$ and 50nM ionomycin, tube 4 (5nM): Calcein AM, $CoCl_2$ and 5nM ionomycin, tube 5 (0.5nM): Calcein AM, $CoCl_2$ and 0.5nM ionomycin. Cells were incubated at 37°C for 15 minutes and then washed with 3.5ml HBSS/Ca^{2+}. Cells were resuspended in PBS for FACS analysis. Cells were analysed using the FACS Canto Flow cytometer with 488nm excitation and emission filters appropriate for fluorescein. A change in fluorescence between untreated (no ionomycin) and treated (+ ionomycin) samples indicate the continuous activation of mitochondrial permeability transition pores. Wild-type cells showed activation of the pores upon addition of 500nM and 50nM ionomycin but not at lower concentrations of 0.5-5nM. *CUL4B*-deleted cells also exhibited activation of the pores upon the addition of 50-500nM ionomycin but activation of the pores also occurred in response to much lower (0.5 and 5nM) ionomycin concentrations. The reduction in % calcein fluorescence indicates the opening of mitochondrial transition pores; this is observed at all concentrations in *CUL4B*-deleted cells but only at higher concentrations in WT cells (*WT versus CUL4B: 5nM/0.5nM, p<0.05 Student t-test, as indicated*).

3.2.3: CUL4B is present within isolated mitochondrial extracts

The *CUL4B* gene harbours a nuclear localization signal and therefore the CUL4B protein is thought to be predominantly localized in the nucleus. Due to the severe mitochondrial dysfunction associated with its loss, I speculated that CUL4B may have unknown roles within the mitochondria specifically and thus may be present in or on the mitochondria. To investigate the presence of CUL4B in isolated mitochondrial extracts, I employed the µMACS Mitochondrial Isolation Kit to isolate mitochondria using an affinity purification method. Using this kit, cells are lysed on ice using a stokes homogenizer and then magnetically labeled with Anti-TOM22 (OMM translocase) MicroBeads. The monoclonal Anti-TOM22 antibody then binds to the TOM22 of human mitochondria. This lysate is subsequently loaded into a MACS column which is then placed inside the magentic field of a MACS separator. The magnetically labeled mitochondria are retained in the column whilst the unlabelled cell components are run through. Once the column is removed from the magnetic field, the retained mitochondria can be eluted (See Figure 3.28).

Mitochondria were isolated using the technique described above and resuspended in 60µL of urea buffer. Increasing amounts of mitochondrial extract were immunoblotted for CUL4B protein expression levels. Interesingly, CUL4B expression was detected in isolated mitochondrial extracts from Wild-type controls. However, consistent with *CUL4B* deletion, CUL4B protein expression was absent in mitochodnria derived from *CUL4B*-deleted patient derived LBLs (Fig 3.29). This is the first report identifying CUL4B as a mitochondrially-localized protein and this novel data suggests that CUL4B loss may impart negative effects on mitochondrial function, such as those reported here. However, the precise roles for CUL4B within the mitochondria or more likely, associated with the mitochondrial membrane are unknown. The Miltenyi affinity mitochondrial isolation kit isolates intact, live mitochondria. It is possible that the CUL4B detected here is interacting with the outer mitochondrial membrane.

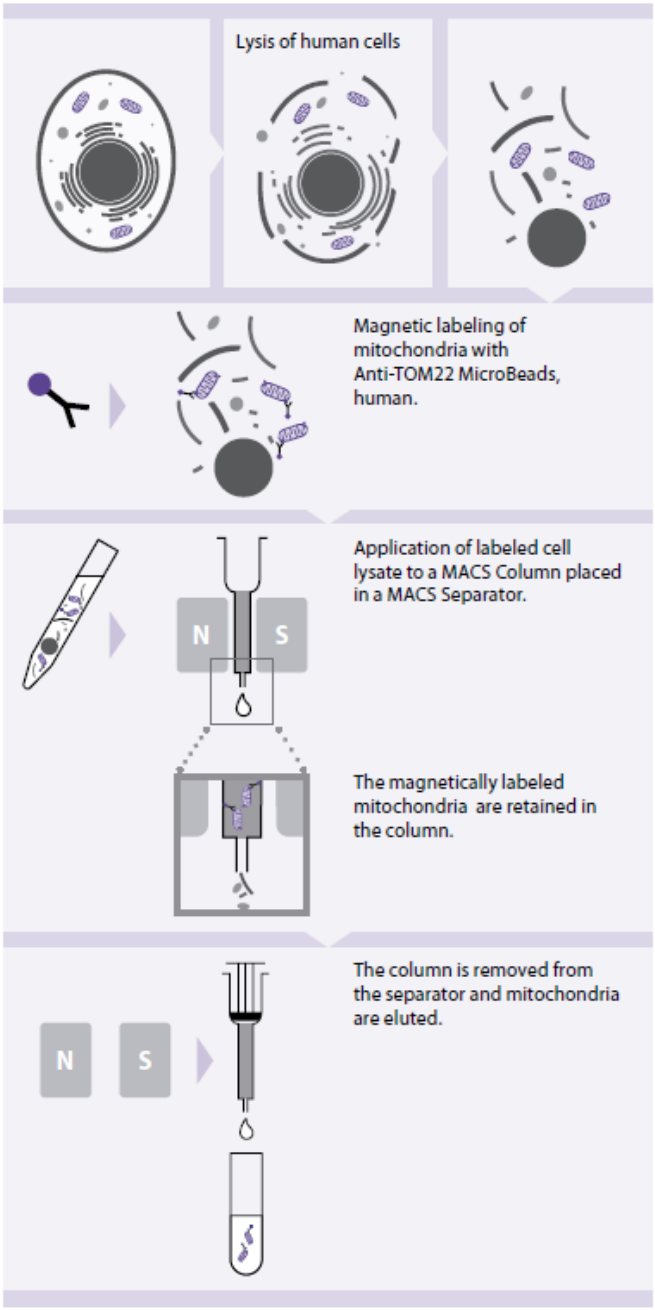

Figure 3.28 – A schematic representation of the Miltenyi Biotech Human Mitochondrial Isolation Kit (Miltenyi Biotech, Surrey, UK: Cat no – 130-094-532). **(a)** Cells are lysed using a stokes homogenizer, **(b)** lysates are then incubated with Anti-TOM22 Microbeads for 2 hours. **(c)** This labelled lysate is then loaded into a MACS separation column, placed into the magnetic field of the Miltenyi Quadro MACS separator and then washed several times with the supplied buffer. **(d)** The column is removed from the magnetic field and the mitochondria are eluted into an ependorff tube. Mitochondria are then either centrifuged a 13,000g and resuspended in storage buffer (supplied with the kit) or resuspended in urea-based extraction buffer for extract preparation.

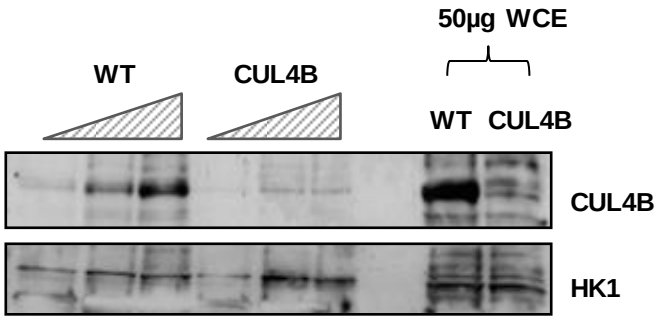

Figure 3.29 – CUL4B is present in mitochondrial extracts from WT LBLs. Mitochondria were isolated from 1 x 10^7 LBLs per cell line using the Miltenyi QuadroMACS Mitochondria Isolation Kit. Isolated mitochondria were then resuspended in 60µL urea buffer and sonicated for 15 seconds to create a mitochondrial protein extract. 5-15µL of mitochondrial extract was loaded onto a gel, 50µg whole cell extracts (WCE) were also loaded as input controls. CUL4B protein expression was visible in WT mitochondria extracts but absent in *CUL4B*-deleted mitochondria extracts. The blot was reprobed for the mitochondrial protein Hexokinase 1 (HK1) which serves as a loading control. WT; wild-type, CUL4B; *CUL4B*-deleted.

3.2.4: siRNA-mediated knockdown of *Cul4b* confirms the mitochondrial phenotypes observed in patient cells

Here, I have uncovered novel phenotypes associated with *CUL4B* deletion using unique patient-derived cell lines; LBLs and fibroblasts. Employing two independent mouse cell lines, one of neuronal providence: Neuro-2A (N2A) and the other a myoblast cell line: C2C12, I investigated mitochondrial function following siRNA-mediated knockdown of *Cul4b*. The cell line C2C12 is an immortal line of mouse skeletal myoblasts which, under appropriate culture conditions, can differentiate into myoblasts/myocytes. The N2A cell line is a mouse neural crest-derived cell line frequently used to study neuronal differentiation, axonal growth and signalling pathways. These cell lines were chosen based on the clinical deficits in these tissue systems in account of CUL4B loss in humans

Sequential (double) transfection of both C2C12 and N2A cells with siRNAs directed against the 3'UTR of *Cul4b* efficiently reduced expression of the *Cul4b* protein (C2C12; ~94%, N2A; ~60%) (Fig 3.30a-c). Consistent with observations in *CUL4B*-deleted patient-derived cells, siRNA mediated knockdown of *Cul4b* in both N2A and C2C12 cell lines was associated with mitochondrial dysfunction. Immunofluorescence-based microscopic analysis of Mitotracker Red staining revealed that siRNA-mediated knockdown of *Cul4b* in C2C12 myoblasts resulted in depolarisation of the mitochondrial membrane potential (Fig 3.31). Furthermore, some cells exhibited striking hyperpolarisation following silencing of *Cul4b* compared to non-transfected controls, consistent with data from a *CUL4B*-deleted patient line (Fig 3.31). siRNA-transfected N2A and C2C12 cells were also analysed for ROS generation. Flow cytometry analysis of MitoSOX fluorescence revealed a ~1.6 fold increase in mitochondrial-specific ROS following knockdown of *Cul4b* in both cell lines (Fig 3.32a-c). Collectively, these data are consistent with the phenotypes observed in patient-derived cells and suggest that loss of CUL4B has important implications for mitochondrial function and homeostasis.

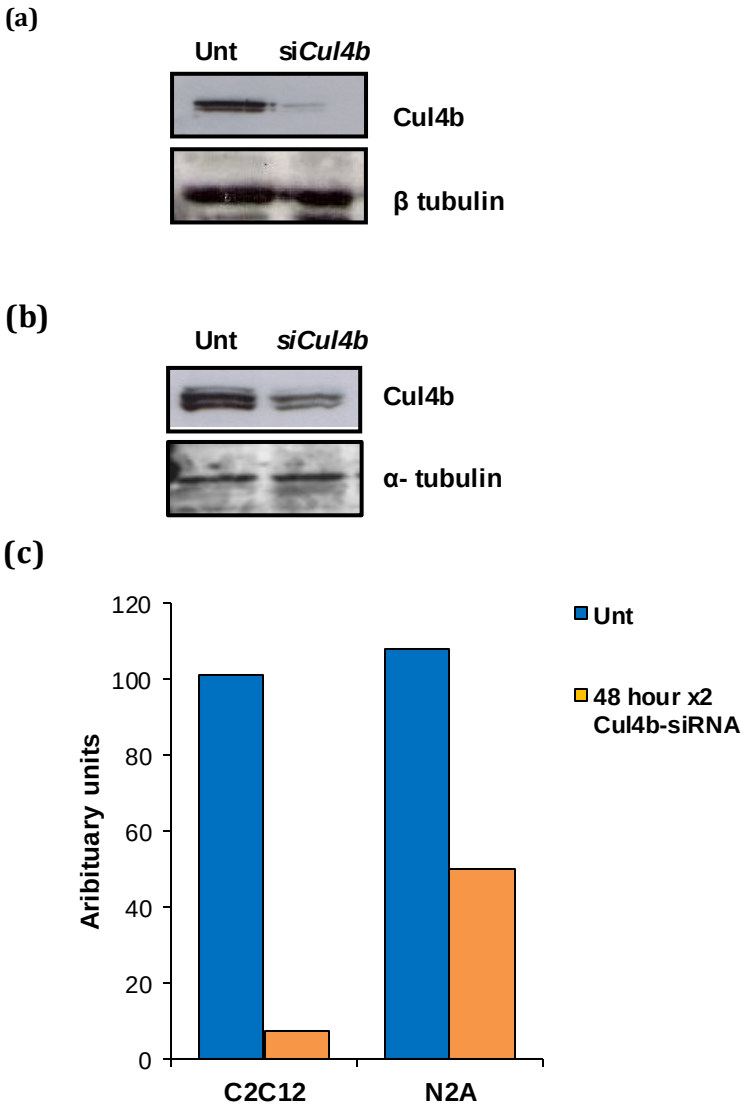

Figure 3.30- siRNA mediated knockdown of *Cul4b* results in alterations to mitochondrial membrane potential. **(a)** Whole cell extracts were examined for expression levels of cul4b 48 hours post-transfection (double transfection) into mouse myoblast line C2C12. The blot was reprobed for β-tubulin as a loading control. Unt; Untransfected + 10μL metafectene pro, si*Cul4b; Cul4b*-specific siRNA. **(b)** Whole cell extracts were examined for expression levels of cul4b 48 hours post-transfection (double transfection) into mouse neuroblastoma line N2A. The blot was reprobed for α-tubulin as a loading control. Unt; Untransfected + 10μL metafectene pro, si*Cul4b; Cul4b*-specific siRNA. **(c)** Representative histogram of CUL4B protein expression levels in C2C12 and N2A untransfected cells (blue bar) vs. *Cul4b* siRNA-transfected C2C12 and N2A cells (shown in orange) as measure by Image J.

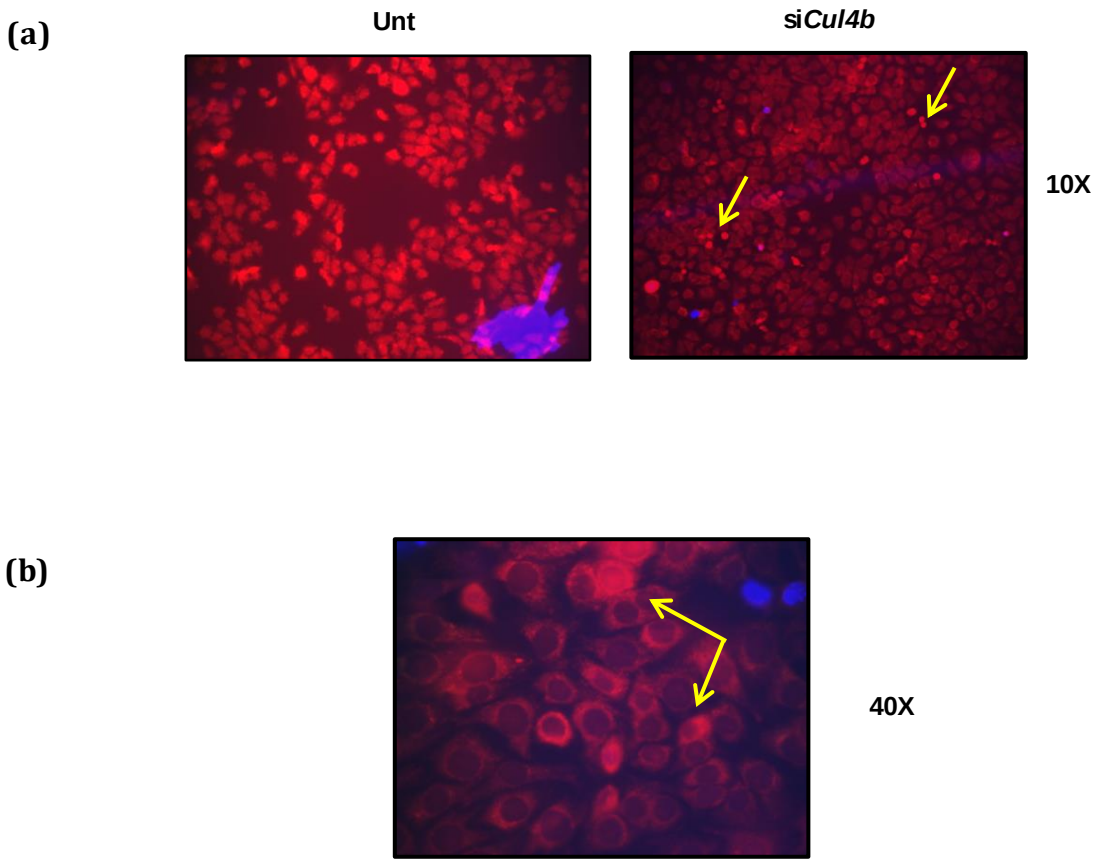

Figure 3.31 – Microscopy based analysis of Mitotracker Red fluorescence of *Cul4b* siRNA transfected myoblasts. siRNA-transfected C2C12 myoblasts exhibit depolarisation and hyperpolarisation following *Cul4b* knockdown. **(a)** Unt; untreated, untransfected + 10µL Metafectene pro (Biotec). siCul4b; *Cul4b*-specific siRNA + 10µL metafectene pro. Following a 48 hour sequential (2x) transfection, C2C12 myoblasts were incubated with 250nM Mitotracker Red for 15 minutes, cytospun onto Poly-lysine slides and visualised at 10X. All images were captured at the same exposure time of 0.01 seconds. **(b)** Higher magnification of a subset of cells captured in (a), *Cul4b* siRNA-transfected C2C12 myoblasts visualised at 40X 48 hours post transfection. Yellow arrows indicate those cells exhibiting hyperpolarisation.

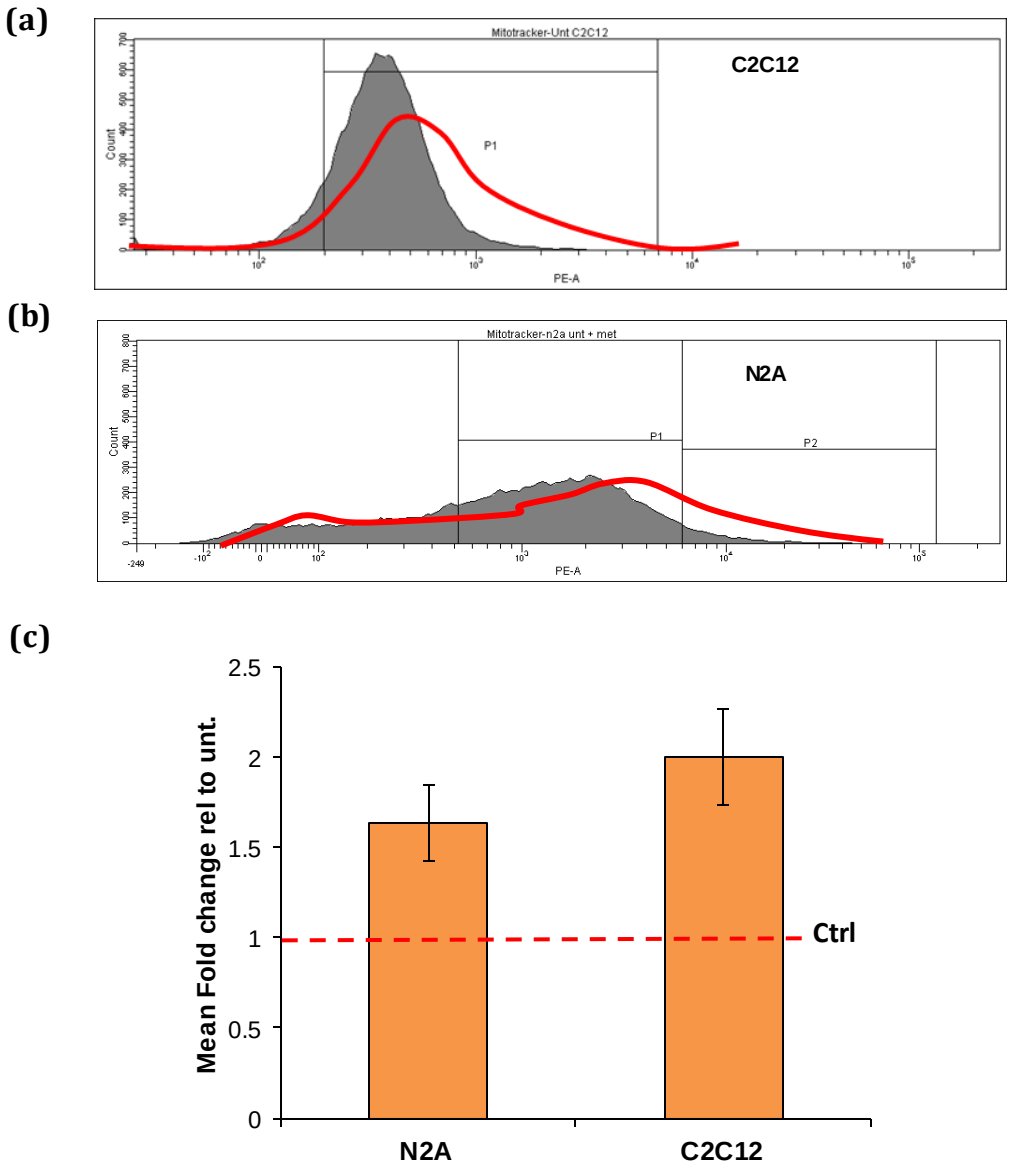

Figure 3.32 – siRNA-mediated knockdown of *Cul4b* in C2C12 and N2A cell model systems leads to elevations in ROS generation. **(a)** C2C12 myoblasts; Overlaid MitoSox FACS profiles showing the PE-A intensity of 20,000 events. 48 hours post double transfection, C2C12 myoblasts were incubated with 250nM MitoSOX for 15 minutes and analysed by flow cytometry for PE-A fluorescence. Grey profile; untreated, untransfected, Red line; *Cul4b* siRNA profile overlay. **(b)** N2A neuroblastoma cells; Overlaid MitoSox FACS profiles showing the PE-A intensity of 20,000 events. 48 hours post double transfection, N2A cells were incubated with 250nM MitoSOX for 15 minutes and analysed by flow cytometry for PE-A fluorescence. Grey profile; untreated, untransfected, Red line; *Cul4b* siRNA profile overlay. **(c)** Representative histogram showing the mean fold change in mean MitoSOX fluorescence intensity (PE-A) of *Cul4b* siRNA-transfected Neuro-2A cells (*p<0.05 Student t-test*) and C2C12 myoblasts (*p<0.05 Student t-test*) relative to untransfected controls (red dashed line; control untransfected cells). The data represents the mean ±SD of three independent experiments.

3.2.5: Autophagy

Autophagy is a homeostatic process occurring in all eukaryotic cells involving the degradation of cellular components via the lysosomal pathway. When a pro-autophagy stimulus is received such as nutrient deprivation or energy imbalance, a membrane called the phagophore is formed. Initial phagophore formation requires the assembly of the beclin-1 interacting complex consisting of Beclin-1 and the vacuolar sorting proteins 15 and 34 (Beclin1-VPS34 Class III PI3K complex). Phagophore elongation is mediated by two systems; the ATG5-ATG12-ATG16 conjugation system and the ATG8/LC3 conjugation system functioning in the conversion of the cytosolic truncated form of LC3 (LC3-I) to its phagophore membrane- associated phosphatidylethanolamine conjugated form (LC3-II) (Kabeya et al, 2004; Mizushima et al, 1999). The resultant double-membraned structure, known as an autophagosome, then fuses with a lysosome for breakdown by resident hydrolases (Mizushima et al, 2008). Although autophagy plays a prominent role during nutrient deprivation, it also plays crucial housekeeping roles to maintain quality control through the regulated turnover of specific organelles and protein aggregates (Hanna et al, 2012; Quinsay et al, 2010).

Key regulators of autophagy include the BCL-2 family of proteins (BCL-1, BCK-XL, BNIP3 and NIX), AMP-activated protein kinase, mTOR pathway, Reactive Oxygen Species and p53 (Brady et al, 2007; Budanov & Karin, 2008; Feng et al, 2011; Feng et al, 2007; Høyer-Hansen et al, 2007; Pattingre et al, 2005; Quinsay et al, 2010; Sandoval et al, 2008; Schweers et al, 2007). Furthermore, the autophagy process is regulated by intracellular calcium levels. Evidence suggests that elevations in cytosolic free calcium can act as inhibitory or activating autophagic stimuli (Reviewed in (Cárdenas & Foskett, 2012). However, the majority of data suggests that Ca^{2+} can induce autophagy by a signal transduction pathway involving Ca^{2+} activation of CaMKKβ, its phosphorylation of AMPK (AMPK-activated protein kinase) and AMPK-mediated inhibition of mTOR (discussed further in Chapter 4 section 4.1.2.4).

3.2.5.1: Mitochondria-specific autophagy; mitophagy

There are two types of autophagy; selective and non-selective. Non-selective occurs in response to starvation and nutrient deprivation to provide cells with essential nutrients for survival. Selective autophagy occurs specifically to remove damaged or excessive organelles and several organelle-specific autophagy processes have been reported including pexophagy (removal of peroxisomes), ribophagy (ribosomes) and mitophagy (mitochondria) (Kraft et al, 2008; MacIntosh & Bassham, 2011).

The mitochondria are able to defend themselves against the harmful effects of aberrant mitochondria by selective sequestration and degradation of dysfunctional mitochondria through the process of mitochondrial specific autophagy; mitophagy. The mechanisms behind the regulation of mitophagy are not fully understood however multiple pathways have been proposed to regulate mitochondrial homeostasis such as mitochondrial fragmentation, the Hsp90-cdc37 and ATG-ULK1 complexes and the PINK1/Parkin pathway (Barsoum et al, 2006; Egan et al, 2011; Gomes & Scorrano, 2008; Joo et al, 2011; Kundu et al, 2008; Narendra et al, 2008; Narendra et al, 2010b). Furthermore, Ding et al (2012) recently proposed a two-step mitophagy model involving the induction of canonical ATG-dependent macroautophagy followed by subsequent mitochondrial priming, occurring through multiple Parkin-dependent or independent mechanisms (Fig 3.33) (Ding & Yin, 2012).

The PINK1/Parkin pathway is a central regulator of mitophagy and loss of function mutations in the *PARK2* gene are associated with early onset Parkinson's Disease. PINK1 (PTEN-induced putative kinase) is a serine/threonine kinase with a mitochondrial targeting sequence. PINK1 is present at very low levels within mitochondria harbouring an intact membrane potential due to its cleavage by PARL1 at the IMM (Jin et al, 2010; Narendra et al, 2010b). However, collapse of the membrane potential allows PINK1 to accumulate on the mitochondrial membrane, form a complex with the translocase of the OMM and recruit Parkin (Narendra et al, 2010b). Parkin, an E3 ubiquitin ligase that is mutated in familial forms of Parkinson's Disease (PD), is primarily located in the cytosol. Parkin is also known

to catalyse its own ubiquitination and proteosomal-mediated degradation, thus regulating its own cellular levels (Choi et al, 2000; Zhang et al, 2000).

Upon dissipation of the mitochondrial membrane, Parkin rapidly translocates to the mitochondria where it functions to ubiquitinate a subset of mitochondrial proteins such as VDAC, MFN1/2 and MIRO (Gegg et al, 2010; Geisler et al, 2010; Wang et al, 2011). These ubiquitinated proteins then serve as markers for autophagy adaptor proteins such as p62/SQSTM1 and NBR1 which function to tether the mitochondria to the LC3 positive autophagosomes (Ding et al, 2010; Lee et al, 2010a; Pankiv et al, 2007). However, the importance of this mechanism requires clarification as studies using *p62* null cells find that p62 is crucial for perinuclear aggregation of damaged mitochondria but not for mitophagy (Narendra et al, 2010a; Okatsu et al, 2010). In addition, following mitochondrial membrane depolarization both proteasomes and p97 (an AAA+ ATPase) are recruited to mitochondria in a Parkin-dependent manner (Chan et al, 2011; Tanaka et al, 2010; Yoshii et al, 2011). Although the role of parkin in mitophagy is not disputed, the molecular mechanisms occurring between parkin-mediated ubiquitination of mitochondrial proteins and the subsequent degradation of the mitochondria by the autophagy process remain unresolved.

Parkin is also able to interact with AMBRA1, a protein which promotes general autophagy by activating the class III phosphatidylinositol 3-kinase complex (PI3K). Specifically, this interaction is enhanced during prolonged mitochondrial depolarisation (Fimia et al, 2007; Van Humbeeck et al, 2011). Although there is no evidence for *ubiquitination* of AMBRA1 by Parkin, AMBRA1 is recruited to perinuclear clusters of depolarized mitochondria in a Parkin-dependent manner where it contributes to their clearance (Van Humbeeck et al, 2011). Interestingly, AMBRA1 is also termed DCAF3. As discussed in section 3.1, DCAFs forms the substrate receptor of cullin 4 based E3 ligases. However, whether this CUL4-AMBRA1 E3 ligase complex directly functions in the mitophagy process is not known. Due to the central roles of both AMBRA1 and the ubiquitin pathway in mitophagy, it is tempting to speculate that the loss of CUL4B here may impart effects on mitophagy through the non-formation of a CUL4-based E3 ligase complex.

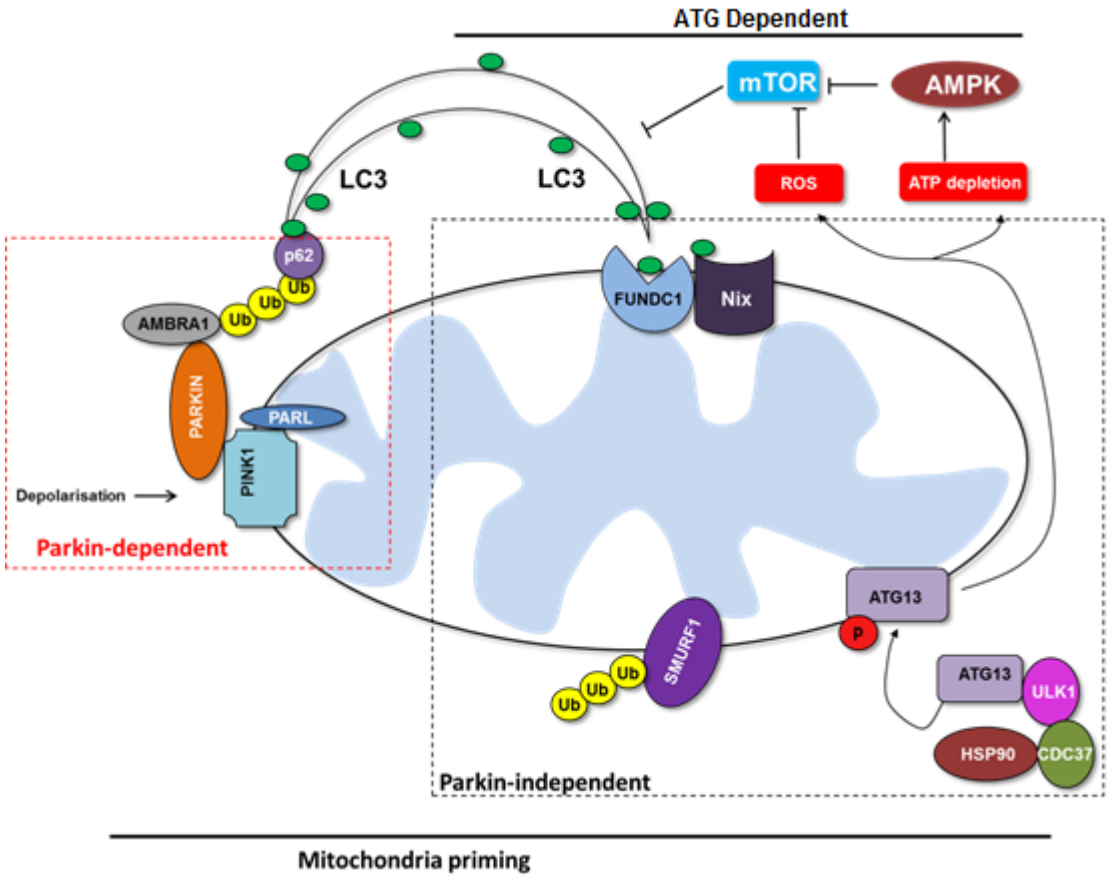

Figure 3.33 – Two-step mitophagy model in mammalian cells proposed by Ding et al (2012)-the induction of canonical ATG-dependent macroautophagy and mitochondrial priming. The induction of macroautophagy requires ATG proteins and involves mTOR suppression mediated by mitochondrial damage-generated ROS production and ATP-depletion mediated AMPK activation. Priming of the mitochondria is mediated by multiple parkin-dependent or independent mechanisms. In the presence of Parkin, one common mechanism is that mitochondrial depolarisation results in impaired PARL-mediated PINK1 cleavage leading to PINK1 stabilisation and recruitment of Parkin to the mitochondria. Mitochondria-localized Parkin promotes the ubiquitination of mitochondrial proteins such as VDAC and the Mitofusins. These ubiquitinated proteins may be degraded by the proteasome or serve as markers for p62. P62 can then act as an adaptor molecule through interaction with LC34 which recruits autophagosomes. Parkin can also interact with AMBRA1, activating the Class III PI3K complex around mitochondria to facilitate mitophagy. Parkin-independent mechanisms include; 1) the increased expression of FUNDC1 and Nix which the recruit autophagosomes to the mitochondria, 2) SMURF1 which targets mitochondria and promotes mitophagy, most likely through the ubiquitination of mitochondrial proteins and 3) the activation of ULK1 by the Hsp90-cdc37 complex which functions to phosphorylate ATG13. This phosphorylated form of ATG13 is then recruited to damaged mitochondria to promote mitophagy. Ub; Ubiquitin. p; phosphate.

3.2.5.2 CUL4B-deleted LBLs exhibit disrupted autophagic flux

Loss of CUL4B imparts negative effects on the regulation of the mTOR pathway, a central player in the regulation of autophagy (Ghosh et al, 2008; Wang et al, 2013) (discussed in section 3.1.4.4). Furthermore, *CUL4B*-deleted LBLs display characteristics consistent with a significant level of mitochondrial dysfunction; altered membrane potential, increased levels of ROS and disrupted calcium homeostasis. The presence of such a high proportion of non-functioning mitochondria suggests that the process of autophagy may be disrupted in the context of CUL4B loss which could result in the accumulation of dysfunctional mitochondria. Conversely, this striking level of mitochondrial dysfunction may up-regulate autophagy in an attempt to destroy those dysfunctional mitochondria. However, loss of CUL4B and the mitochondrial dysfunction associated with it may in turn affect mitochondrial biogenesis whereby newly synthesised mitochondria also quickly become dysfunctional, creating a continuous pool of sub-optimal mitochondrial function.

One of the most striking mitochondrial phenotypes observed in *CUL4B*-deleted LBLs is that of excessive ROS production. As discussed in section 3.2.2.5, the mitochondria are both the source and target of reactive oxygen species and have developed sophisticated antioxidant systems to protect themselves from ROS under normal conditions (Turrens, 2003). However, dysfunctional mitochondria frequently produce excessive amounts of ROS which can overwhelm these antioxidant mechanisms. ROS can cause damage to mitochondrial proteins, lipids and mtDNA which can subsequently result in mitochondrial dysfunction and mitophagy. In fact, superoxide has been shown to be the major ROS regulating autophagy and treatment with ROS scavengers or overexpression of *SOD2* has been shown to decrease rotenone-induced autophagy in HeLa cells (Chen et al, 2009; Chen et al, 2007). ROS have also been shown to directly regulate the formation of autophagosomes by targeting a conserved cysteine (82) on ATG4 and inhibiting its protease activity (Scherz-Shouval et al, 2007). Furthermore, recent evidence suggests that hydrogen peroxide activates PARP-1, which stimulates the LKB1-AMPK pathway leading to activation of autophagy (Huang et al, 2009). As CUL4B LBLs show excessive production of ROS, it is likely that disruption of

mitophagy will result. Furthermore, *CUL4B*-deleted LBLs display elevated levels of intracellular calcium. Calcium is a key player in the regulation of autophagy and thus this suggests that altered calcium levels in the context of CUL4B deficiency may contribute to disruption of the autophagy process.

LC3 (Microtubule-associated protein light chain 3) is a key constituent of the autophagosome. During autophagy, the cytoplasmic form of LC3; LC3-I, is recruited to the autophagosome where it is then conjugated with phosphatidylethanolamine to form LC3-II, present on the autophagosome membrane. The most widely used method to test cells for autophagic activity is LC3 immunoblotting where tracking the conversion of LC3-I to LC3-II is indicative of autophagic activity. The amount of LC3-II correlates with the number of autophagosomes present and is therefore a good indicator of autophagosome formation. However, LC3-II itself is degraded by autophagy therefore it is important to measure the amount of LC3-II by comparing LC3-II levels in the presence of either a lysosomal protease inhibitor such as pepstatin A or an autophagosome-lysosome fusion inhibitor such as Bafilomycin A. Autophagic flux is represented by differences in the total amount of LC3-II between samples in the presence or absence of one of these inhibitors (Mizushima & Yoshimori, 2007).

To investigate mitophagy in the context of CUL4B-XLMR, *CUL4B*-deleted patient derived LBLs and WT controls were first treated with 10nM Bafilomycin A for 2 hours. Whole cell extracts were then immunoblotted for LC3-I and LC3-II expression. Following treatment with 10nM Bafilomycin A, wild type LBLs showed a 1.4 fold increase in LC3-II expression levels, indicative of autophagic flux (Fig 3.34). This was in striking contrast to *CUL4B*-deleted LBLs where very little increase in LC3-II levels was observed following Bafilomycin A treatment (Fig 3.34). This indicates that autophagy is disrupted in the context of CUL4B loss whereby accumulation of autophagosomes is already apparent even without the addition of an autophagy flux inhibitor. This suggests that *CUL4B*-deleted LBLs exhibit disruption of the autophagy process at the autophagosome-lysosome fusion step. Furthermore, *CUL4B*-deleted LBLs exhibit this phenotype without the addition of an autophagy stimulus suggesting that the basal levels of autophagy in CUL4B LBLs are increased compared to WT. Disruption to the autophagy process

could lead to the accumulation of defective (depolarized) organelles and protein aggregates. In addition, it could begin to explain the presence of a substantial number of depolarised mitochondria in the context of CUL4B loss, whereby the cell is unable to degrade defective mitochondria and thus they accumulate and contribute to the mitochondrial dysfunction identified here.

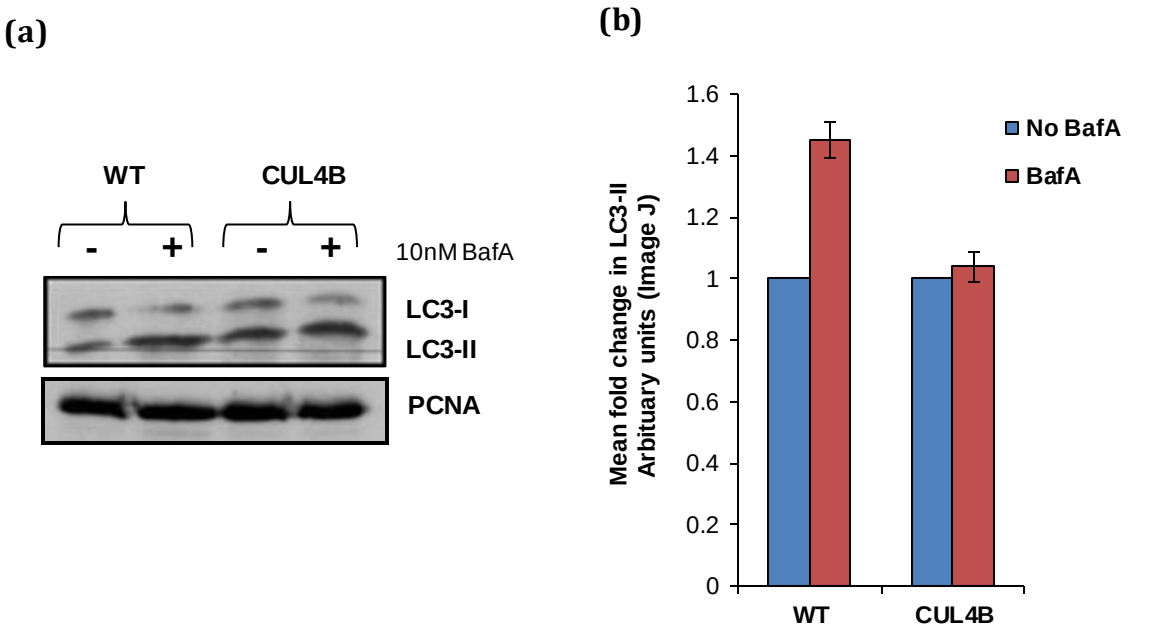

Figure 3.34 – *CUL4B*-deleted LBLs exhibit disrupted autophagic flux. **(a)** Wild-type and *CUL4B*-deleted LBLs were treated with 10nM Bafilomycin A for 2 hours and immunoblotted for LC3 protein expression. Addition of Bafilomycin A to WT LBLs resulted in the increased expression of LC3-II (lanes 1 and 2 of panels 1 and 3). Bafilomycin treatment in *CUL4B*-deleted *LBLs* however did not increase LC3-II protein expression to the same extent as WT LBLs (lanes 3 and 4 of panels 1 and 3). Western blots from 2 separate experiments are shown here. Each blot was reprobed for PCNA as a loading control (panels 2 and 4). **(b)** A representative histogram showing the mean fold change in LC3-II expression ± BafA. This data represents the mean of 3 independent experiments ± SD. Blots were scanned and the band intensity was determined by Image J.

3.2.5.3: Parkin ubiquitination is altered in the context of CUL4B loss

The data reported so far indicates that CUL4B loss imparts effects on autophagic flux without the addition of an autophagy inducing stimuli. As described in section 3.2.5.1, the PINK1/Parkin pathway is a key regulator of mitophagy; mitochondria-selective autophagy. Parkin is recruited to mitochondria following collapse of the mitochondrial membrane potential. To investigate whether CUL4B loss imparts deleterious effects on mitophagy specifically, I looked at the protein levels of endogenous Parkin in response to complete dissipation of the mitochondrial membrane potential. Wild-type and *CUL4B*-deleted LBLs were treated with 10μM CCCP for 0-24 hours and analysed by western blotting for Parkin expression. I detected comparable levels of Parkin in WT and *CUL4B*-deleted whole cell extracts. Parkin protein expression was increased at 2 and 4 hours and subsequently reduced following a 24 hour CCCP treatment (Fig 3.35). This protein expression pattern was similar between WT and *CUL4B*-deleted whole cell extracts. However, additional bands of high molecular weight were observed possibly corresponding to ubiquitinated Parkin (indicated in Fig 3.35). The expression of these bands appeared to differ between control and *CUL4B*-deleted samples; following 1-4 hours CCCP treatment these high molecular weight bands were visible in WT whole cell extracts (WCE) but were not visible in treated *CUL4B*-deleted WCE. If these higher bands correspond to ubiquitinated Parkin (and their size would be consistent with this), this suggests that Parkin ubiquitination may be altered in the context of CUL4B loss. I also analysed the protein expression levels of AMBRA1 following treatment with 10μM CCCP. AMBRA1 is known to interact with Parkin following mitochondrial depolarisation to promote mitophagy; however no difference in the protein expression levels of AMBRA1 was observed between WT and *CUL4B*-deleted LBLs following CCCP-induced mitochondrial depolarisation (Fig 3.36).

To demonstrate whether the observed Parkin antibody immunoreactive bands of higher molecular weight were due to ubiquitination of Parkin, I performed immunoprecipitation experiments to identify both mono- and poly-ubiquitinated species. Indeed, western blot analysis of Parkin immunoprecipitates from WT cells revealed the presence of highly ubiquitinated species following a 3 hour CCCP

treatment detected using an Anti-FK2 antibody which specifically detects conjugate ubiquitin and not free ubiquitin (K29, K48 and K63 linkages) (Fig 3.37 lanes 1-2). Interestingly, *CUL4B*-deleted immunoprecipitates exhibited a distinct lack of ubiquitinated species following CCCP treatment suggesting that Parkin ubiquitination or parkin-mediated autoubiquitination may be impaired in the context of CUL4B loss (Fig 3.37 lanes 3-4). Moreover, this reduced ubiquitination could either represent a very high turnover of the parkin protein or conversely it could represent impaired enzymatic activity in response to prolonged mitochondrial depolarisation in the context of CUL4B loss. This data is consistent with the data presented in section 3.2.5.2 and collectively suggests that the autophagy/mitophagy process is disrupted by loss of CUL4B.

3.2.6: Summary

Here, I have investigated how loss of CUL4B impacts upon mitochondrial function in patient-derived lymphoblastoid cells and fibroblasts. I have uncovered novel mitochondrial phenotypes in this context consistent with substantial mitochondrial dysfunction. I have provided the first evidence to show that CUL4B is present within isolated mitochondria extracts suggesting that CUL4B may play an essential role in maintaining mitochondrial function and homeostasis. Furthermore, using a variety of approaches and flow cytometry analyses I have revealed that although the enzymatic activity of Complex I appears unchanged, there is considerable disruption to the mitochondrial transmembrane potential. Consistent with this, *CUL4B*-deleted LBLs display reduced ATP production and increased generation of mitochondria-specific ROS. Calcium homeostasis and signalling is altered in the context of CUL4B-deficiency whereby intracellular calcium levels are increased in conjunction with hypersensitivity of the mPTP to a calcium ionophore. Finally, I have presented evidence suggestive of altered mitophagy in the context of CUL4B loss. Collectively, these data indicate that loss of CUL4B leads to severe mitochondrial dysfunction which may in part begin to explain the clinical phenotypes of CUL4B-XLMR patients such as MR, epilepsy and peripheral neuropathy.

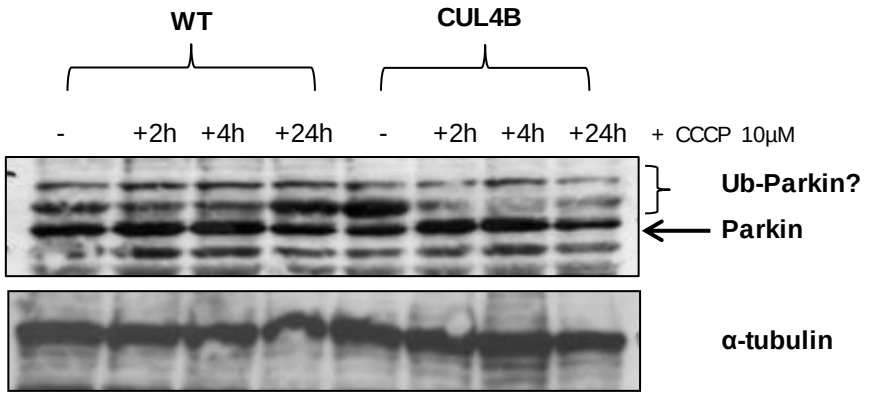

Figure 3.35 – Expression levels of Parkin and AMBRA1 are unchanged following CCCP treatment. Cells were treated with 10μM CCCP for up to 24 hours and immunoblotted for Parkin protein expression. Levels of Parkin were comparable between WT and *CUL4B*-deleted LBLs, however higher molecular weight bands, possibly representing ubiquitin, were visible in CCCP-treated WT extracts but not in CCCP-treated *CUL4B*-deleted extracts.

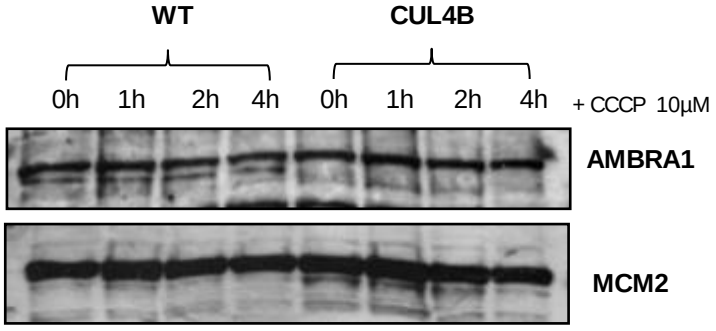

Figure 3.36 – AMBRA expression is similar in wild type and *CUL4B*-deleted LBLs following 10uM CCCP treatment. LBLs were treated with 10μM CCCP for 0-4 hours, cells were harvested and urea-based protein extracts were subjected to SDS-PAGE and immunoblotted for AMBRA1 expression levels. MCM2 protein expression was used as a loading control.

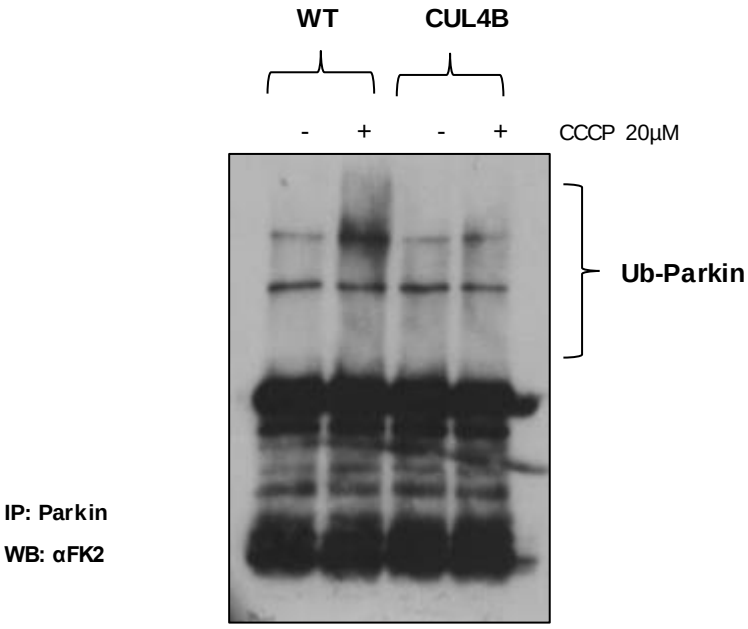

Figure 3.37 - Parkin ubiquitination is altered in the context of CUL4B loss. Wild type (WT) and *CUL4B*-deleted (CUL4B) LBLs were treated with 20μM CCCP for 3 hours. Soluble extracts prepared from each cell line (400μg) were subjected to IP using an anti-Parkin antibody and probed for FK2 expression following SDS-PAGE and immunoblotting. CCCP-treated *CUL4B*-deleted LBLs exhibited decreased levels of Parkin ubiquitination compared with WT controls.

3.3: Discussion

The CUL4B protein forms the core backbone of many CRL4-containing E3 ubiquitin ligase complexes which catalyse the polyubiquitination of a diverse range substrates within the cell. Due to the ever-increasing number of CUL4B-specific substrates being identified, CUL4B is implicated in a wide range of cellular processes ranging from DNA transcription and repair to signal transduction networks such as the mTOR pathway. *CUL4B*-mutated and/or deleted patients exhibit a syndromal form of MR whereby the exhibit many other clinical features aside from the MR (Tarpey et al, 2007a). Interestingly, a number of these features overlap with those of mitochondrial disorders suggesting a potential overlapping pathomechanism.

Here, I have provided the first evidence of novel mitochondrial consequences of *CUL4B*-deficiency in human patient-derived cell lines. Despite harbouring a functional NLS, I have shown that a fraction of CUL4B is localised within mitochondrial extracts consistent with a to date, unappreciated role for CUL4B in the maintenance of mitochondrial function. Furthermore, I have uncovered a distinct set of mitochondrial phenotypes associated specifically with *CUL4B* loss including transmembrane potential disruption, reduced ATP synthesis, increased superoxide generation and impaired calcium handling. These mitochondrial features may potentially underlie some of the clinical phenotypes associated with CUL4B deficiency in humans and provide a basis for future investigations with respect to understanding their aetiology. For example, *CUL4B*-mutated and/or deleted patients exhibit ataxia, seizures and evidence of peripheral neuropathy, and it is tempting to speculate that perturbed mitochondrial function may underlie these clinical features.

The organs with the highest demand for aerobic energy are the brain, heart and skeletal muscle and thus it is these organs that are the most commonly affected by mitochondrial dysfunction. Post mitotic cells such as neurons and muscle cells are unable to filter out energy-deficient cells through mitotic division and it is this feature that makes them most at risk from energy failure. Given the brains high

dependency on oxidative metabolism, it is hardly surprising that most, if not all, primary mitochondrial disorders present with neurological and cognitive deficits. Some of the most common features of mitochondrial disorders include seizures, ataxia, myopathy and peripheral neuropathies with ataxia being the most invariant clinical feature. In particular, patients with Leigh syndrome harbouring mutations in the ATPase 6 gene highlight the importance of neuronal ATP for development (Schon et al, 2001). Additionally, impaired calcium handling is a predominant feature of cytoplasmic hybrid (cybrid) cells harbouring the MERRF mutation (cells which are depleted of their endogenous mtDNA and replaced with the mtDNA of interest) indicating that mis-regulated Ca^{2+} signalling has major implications for seizure generation (Brini et al, 1999). Furthermore, mitochondrial disorders are often associated with peripheral neuropathy. The roles of neuronal and axonal mitochondria in peripheral nerve disease are well appreciated but more recent work has implicated mitochondrial deficits in Schwann cells specifically in the pathogenesis of peripheral neuropathies (Viader et al, 2011).

CUL4B-deleted mitochondria exhibit marked increases in the generation of ROS despite the vast majority of CUL4B-deficient mitochondria displaying striking depolarisation of the Ψ^{m}. Although it is widely stated in the literature that ROS production is decreased by membrane depolarisation, it is now thought that excessive ROS generation and subsequent oxidative stress can occur as a result of either high or low membrane potential (Aon et al, 2010). Furthermore, excessive ROS generation has also been shown to stimulate mitochondrial uncoupling resulting in membrane depolarisation (Echtay et al, 2002). Therefore, it is likely that the mitochondrial depolarization observed here may in fact be secondary to increased ROS generation. Moreover, it is well documented that ROS production can be modulated by Ca^{2+}, irrespective of the membrane potential (Brookes et al, 2004; Camello-Almaraz et al, 2006). *CUL4B*-deleted mitochondria appear to display cellular alterations consistent with impaired calcium handling and this may be one mechanism underlying the excessive ROS generation observed. Additionally, increased levels of ROS are known to reciprocally stimulate Ca^{2+} and thus a viscous cycle is established. Interestingly, the observations of increased ROS generation are in contrast to a recent study reporting a significant decrease in

cellular ROS production in *CUL4B*-silenced cells (Li et al, 2011). The reasons behind this discrepancy are not clear but may be due to a transient effect of CUL4B loss on ROS generation; ROS may accumulate over time and thus excessive levels of ROS are not observed after an acute *CUL4B* knockdown. The significance and more so the mechanisms underlying the striking hyperpolarisation of some *CUL4B*-deleted mitochondria also remain unclear but point towards a potential fission/fusion defect. Therefore, it may be interesting to investigate the impacts of *DRP1*/*FIS1* knockdown on mitochondrial function in *CUL4B*-deleted cells.

CUL4B-deleted LBLs also exhibit increased opening of the mPTP in response to low levels of ionomycin. Transient opening of the mPTP is associated with dissipation of the Ψ^m; therefore it is reasonable to suggest that the culmination of increased ROS and impaired calcium homeostasis may lead to mPTP hypersensitivity. This, in turn, may induce membrane uncoupling that eventually results in reduced ATP production. In fact, this has recently been observed in a *Pink1*-/- mouse model of Parkinson's Disease suggesting that increased opening of the mPTP may play important roles in the pathogenesis of a wide array of neurological deficits (Gautier et al, 2012). Future work to fully understand the consequences of mPTP hyperactivity could involve investigating whether treatment with an mPTP inhibitor such as Cyclosporin A (which locks the mPTP closed) is sufficient to rescue the Ψ^m in *CUL4B*-deleted cells.

Under normal physiological conditions, the culmination of excessive ROS generation and increased intracellular calcium levels would result in activation of mitophagy in a bid to rid the cell of defective mitochondria. However, in the context of CUL4B loss, it appears that the autophagy process is halted at the autophagosome-lysosome fusion step. Moreover, the absence of Parkin ubiquitination in *CUL4B*-deleted LBLs is consistent with disrupted mitophagy. Therefore, in the context of CUL4B loss, defective mitochondria are not degraded which can only further exacerbate the situation. It would be interesting to see if a CUL4B-specific E3 ligase complex plays a role in the regulation of specific mitophagy-related proteins. Interestingly, it was recently reported that inhibition of autophagy induces atrophy and myopathy in adult skeletal muscles and thus it is

possible that inhibited autophagy in the context of *CUL4B* loss, could have similar implications for myofiber maintenance (Masiero and Sandri, 2010).

Collectively, the observations reported here represent the first evidence identifying *CUL4B*-mutated/deleted XLMR as a disorder associated with mitochondrial dysfunction. It is likely that the mitochondrial features identified here could potentially underlie some of the neurological clinical features associated with *CUL4B* mutations/deletion in humans. It would be interesting to investigate the impacts of CUL4B loss on both mitochondrial morphology and transport in a *CUL4B*-deleted neuronal model. Recently, mitochondrial dysfunction has been observed in cells from patients with Kennedy's Disease, a condition caused by mutations in the *AR* gene (See section 3.1.4.1). Mis-regulation of the AR has major implications for muscle and sexual development as well as neuronal processes such as synaptic plasticity. Interestingly, a CRL4-containing E3 has been implicated in the regulated turnover of the AR suggesting that mis-regulation of the AR in the context of CUL4B loss may contribute to the mitochondrial dysfunction observed here (Ohtake et al, 2007). Furthermore, CUL4B has been implicated in regulating components of the mTOR pathway, a key pathway regulating autophagy which indicates that CUL4B loss may impact on mitochondrial function through multiple pathways (Papia Ghosh, 2008). Although no substrate has been identified here, these data strongly indicate that CUL4B may have mitochondria-specific substrates whose identification represents an important future challenge. Crucially, this data provides fundamental insight into the cellular consequences of CUL4B deficiency which may aid in the development of efficient therapeutic interventions to combat some of the most debilitating features of this disorder.

Chapter Four

Characterizing the reciprocal relationship between CUL4B and Cereblon

4.1: Introduction

As described in Chapter 3, mental retardation affects approximately 1-3% of the general population (Leonard & Wen, 2002). Generally, it is believed autosomal recessive inheritance accounts for approximately 25% of all individuals with non-syndromic MR (ARNSMR) (Afroze & Chaudhry, 2013; Bartley & Hall, 1978; Priest et al, 1961; Wright et al, 1959). It is noteworthy that this form of MR is in contrast to the *syndromic* form described in Chapter 3, whereby ARNSMR patients exhibit intelligent quotients of 50-70 without any congenital anomalies or other neurological features. Whilst many X-linked genes have been identified as causative of non-syndromic forms of mental retardation, there is a distinct lack of data regarding the genetic basis of ARNSMR (Afroze & Chaudhry, 2013a). Identification of causative genes for ARNSMR through genetic linkage analysis is hindered by the lack of large family pedigrees with multiple affected and non-affected members. In fact only ten genes have been implicated in ARNSMR, to date (See table 4.1). The subsequent sections will focus on one gene in particular, *CRBN* which encodes Cereblon, its association with ARNSMR and its putative roles within the cell.

4.1.1: A gene for non-syndromal MR maps to chromosome 3p25-pter

In an attempt to identify a mental retardation disease locus, Higgins et al performed linkage analysis in five nuclear families from a single pedigree with 10 affected individuals with non-syndromic MR (Higgins et al, 2000). They identified a genetic locus for ARNSMR on chromosome 3 which they termed 'MRT2A'. Further analysis refined this region to an interval flanked by loci D3S3525 and D3S1560 and provided evidence that a gene located in the telomeric region of chromosome 3 is associated with ARNSMR. In fact, evidence already exists to suggest that this region harbours an MR-related gene due to breakpoint deletion mapping studies of 3p deletion syndrome; a syndrome arising from terminal 3p deletions resulting in

a loss of material from 3p25 to 3pter, manifesting with MR as a key clinical feature (Belichenko et al, 1994; Chen et al, 2012; Fu et al, 2012; Sarikas et al, 2011). It is important to realize that the 3p syndrome phenotype is distinct to ARNSMR. Terminal 3p deletions encompass many genes and therefore patients exhibit a wide range of physical anomalies aside from the MR such as growth failure, microcephaly, deafness and craniofacial and skeletal abnormalities. (Chen et al, 2012).

By comparing their data to previous breakpoint deletion studies in 3p deletion syndrome, Higgins et al revealed that a single susceptibility gene for MR resides within the MRT2A candidate region (Higgins et al, 2000). They further suggested *CALL*, *ITPR* and *AD7c-NTP* as possible candidates for the nonsyndromic MR phenotype due to their known roles in brain development and neuronal signalling. In 2004, homozygosity mapping focused the previously identified 'MRT2A' region to a 4.2Mb interval between loci D3S3630 and D3S1304 on chromosome 3p25-pter (Higgins et al, 2004a). This region contains nine genes (*IL5RA*, *TRNT1*, *LRRN1*, *SETMAR*, *SUMF1*, *ITPR1*, *BHLHB2*, *EDEM* and *MRPS36P1)* however Higgins et al reported that a mutation did not exist in any of these genes and suggested that an unknown transcript in this region contributed to cognitive deficits in ARNSMR. Subsequently that same year, Higgins et al further reported that the MRT2A region contains five uncharacterised transcripts; LOC51185, LOC375321, LOC132049, LOC377019, and FLJ10702 (Higgins et al, 2004b). SSCP (Single-Strand Conformation Polymorphism) analysis of these transcripts identified a variation in LOC51185 that segregated with the ARNSMR phenotype and this transcript was subsequently assigned the gene name *Cereblon* (*CRBN*). Further DNA sequencing revealed that a homozygous C→T nonsense mutation causing a premature stop codon in exon 11 of the *CRBN* gene resulting in p.R419X was causative of ARNSMR (Higgins et al, 2004b).

The human *CRBN* gene is located on chromosome 3 (3p26.2) coding for approximately 442 amino acids with a molecular weight of ~51kDa (Higgins et al, 2004b). The nomenclature of the *CRBN* gene was based upon the presence of a large highly conserved ATP-dependent Lon protease domain and the putative role of CRBN in cerebral development. Human CRBN contains the N-terminal portion of

the ATP-dependent Lon protease domain (237 amino acids) which was shown to function in protein-protein interactions but does not have any protease or ATPase activity (Lee et al, 2004). Aside from this domain, CRBN also contains 11 casein kinase II phosphorylation sites, 4 protein kinase C phosphorylation sites, 1 N-linked glycosylation site and 2 myristolyation sites (Higgins et al, 2004b). CRBN is located in the cytoplasm, nucleus and peripheral membrane and is widely expressed in the testis, prostate, lung, kidney, spleen, pancreas, placenta, skeletal muscle, ovary, small intestine, colon, brain, retina and peripheral blood leukocyte (Aizawa et al, 2011; Hohberger & Enz, 2009; Mathias et al, 1996; Xin et al, 2008). In rodents, the Crbn protein is highly expressed in the hippocampus (HPC) and neocortex and localised to the cytosol and plasma membrane (Aizawa et al, 2011; Mathias et al, 1996).

Identification of the p.R419X mutation and its association with ARNSMR indicates that CRBN may play an important role in memory and learning. In fact, CRBN is highly expressed in the brain which further supports this conclusion (Aizawa et al, 2011; Higgins et al, 2004b). The p.R419X mutation interrupts an N-myristoylation site and eliminates a casein kinase II phosphorylation site at the C-terminus. Casein kinase II, highly expressed in the hippocampus (HPC), is activated during the induction of long-term potentiation therefore this mutation may disrupt its subcellular targeting and alter long term potentiation in the HPC (Charriaut-Marlangue et al, 1991; Fukunaga et al, 1996). Furthermore, Lon proteases are localized in the mitochondria where they function to degrade short-lived polypoptides and thus it is possible that this mutation may perturb mitochondrial homeostasis resulting in altered memory and learning. Nevertheless, the exact mechanisms of how this mutation and the subsequent truncation of CRBN lead to ANSMR are not understood, nor indeed are the precise physiological functions of this protein.

Table 4.1 - Genes identified to date as causative of ARNSMR. MIM #; *Online Mendelian Inheritance in Man* number (www.ncbi.nlm.nih.gov/omim).

Gene	MIM #	Protein functions	References
PRSS12	606709	Neurotrypsin; neuronal serine protease	(Molinari et al, 2002)
CRBN	609262	Cereblon; putative roles in cerebral development	(Higgins et al, 2004b)
CC2D1A	610055	Coiled-coil and C2 domain containing protein 1A; transcriptional repressor	(Basel-Vanagaite et al, 2006)
GRIK2	138244	Ionotropic kianate glutamate receptor 2; neurotransmitter receptor in the brain	(Motazacker et al, 2007)
TUSC2	601385	Tumour suppressor candidate 2	(Garshasbi et al, 2008; Khan et al, 2011; Molinari et al, 2008)
TRAPPC9	311966	Trafficking protein particle complex 9; roles in NFkB signalling, neuronal cell differentiation	(Mir et al, 2009; Mochida et al, 2009; Najmabadi et al, 2007)
TECR	610057	Trans-2,3-enoyl-CoA reductase; fatty acid elongation	(Caliskan et al, 2011; Nolan et al, 2008)
ST3GAL3	606494	Beta-galactosidase alpha 2,3 sialyitransferase II; catalyzes the transfer of sialic acid to galactose containing substrates	(Hu et al, 2011)
MED23	605042	Mediator complex subunit 23; involved in transcriptional activation	(Hashimoto et al, 2011)
MAN1B1	604346	Mannosidase alpha class 1B member 1; roles in N-glycan biosythesis	(Rafiq et al, 2011)

4.1.2: Potential roles for CRBN

4.1.2.1: CRBN and CNS development; a putative role in memory and learning

Following on from studies identifying a potential role for CRBN in memory and learning, rat Crbn was identified as a large Ca^{2+} activated potassium channel (BK_{Ca}) α subunit (Slo) binding protein in the rat brain (Jo et al, 2005) . In rodents, Crbn is abundant in the cerebellum and its intracytoplasmic distribution in neurons is similar to the reported immunostaining pattern of the BK_{Ca} channel (Grunnet & Kaufmann, 2004; Higgins et al, 2010; Jo et al, 2005; Misonou et al, 2006). Crbn regulates BK_{Ca} channel surface expression and ionic currents by directly binding to the cytosolic C-terminal of BK_{Ca} in brain regions involved in learning and memory. Consistent with a role for CRBN in regulating BK_{Ca} channel expression, human lymphoblastoid cell lines expressing the p.R419X change in CRBN exhibit persistent expression of an immature BK_{Ca} channel splice variant, *KCNMA1 SIT 2 INSERT* (Higgins et al, 2008). The authors suggest that the continued expression of this variant will alter Ca^{2+}-mediated signal transduction. Specifically, this transduction is crucial for processes of learning such as synaptic maturation and connectivity (MacDonald et al, 2006).

Interestingly, a functional defect of BK_{Ca} channels has previously been associated with autism and mental retardation (Laumonnier et al, 2006). This suggests that the altered expression of BK_{Ca} channels in developing neurons of patients with *CRBN* mutations may contribute to the MR phenotype. However, it is noteworthy that CNS functioning also requires the action of neurotransmitter transporters and receptors therefore BK_{Ca} channels are only one of many channels regulating CNS function. In fact, the Lon domain of CRBN has been shown to interact with the C-terminal of a voltage-gated chloride channel-2 (CIC-2) which functions to regulate cellular excitability and cell volume homeostasis (Hohberger & Enz, 2009). Collectively, these data provide support of a role for CRBN in memory and learning.

CRBN has also been shown to bind the UL14 protein of the Herpes Simplex Virus 1 (HSV1) (Wu et al, 2011). The abundant expression of CRBN in HPC neurons

correlates with the selective regional damage to the HPC induced by HSV1 suggesting that CRBN may be a target for HSV1-mediated hippocampal injury (Ando et al, 2008). In particular, it may play a key role in the pathogenesis of memory deficits in patients surviving HSV1 encephalitis (Ando et al, 2008; Kapur et al, 1994).

4.1.2.2: CRBN, a novel thalidomide binding protein

Thalidomide was prescribed in the 1950-1960s to pregnant women to alleviate the symptoms of morning sickness. However, this drug had unanticipated side effects which resulted in a tragedy from 1957-1962. More than 10,000 children worldwide were born with severe birth defects as a consequence of thalidomide exposure in the first trimester of pregnancy. Malformations of the limbs were the most commonly reported defect. Limb anomalies ranged from mild to severe with two forms of limb deformities; phocomelia (limbs consist of a truncated or absent zeugopod) and Amelia (complete absence of one of more limbs) being the most severe (Fraser, 1988; Taussig, 1962). Approximately 2,000 UK babies were affected, with around 50% dying within a few months of birth. Thalidomide was subsequently withdrawn as a morning sickness treatment. Since its withdrawal, thalidomide has been the subject of significant research aiming to uncover the mechanisms of thalidomide-induced teratogenicity (Franks et al, 2004; Hansen et al, 2002; Hansen & Harris, 2004; Ito et al, 2011; Knobloch & Ruther, 2008; Therapontos et al, 2009).

Many hypotheses have been proposed (~30) including anti-angiogenesis and oxidative stress models as causative of thalidomide's teratogenic effects (D'Amato et al, 1994; Hansen et al, 2002; Hansen & Harris, 2004; Knobloch & Ruther, 2008; Parman et al, 1999; Therapontos et al, 2009). However, the fundamental question as to the direct targets of thalidomide remained unanswered until recently. In an attempt to identify targets of thalidomide, Ito et al developed ferriteglycidyl methacrylate-bound thalidomide-affinity beads to enable the separation and purification of thalidomide-binding molecules (Ito et al, 2010; Sakamoto et al, 2009). Using this approach they identified CRBN as a thalidomide binding protein

and subsequently found it to be the primary target of thalidomide (Ito et al, 2010). In addition they reported that CRBN forms an E3 ligase complex with DDB1, CUL4 and ROC1. This CUL4-CRBN complex was shown to have autoubiquitination activity (*in vitro* and *in vivo*) and CRBN was therefore suggested to be a novel substrate receptor. Interestingly, Ito and co-workers reported that the expression of this E3 ligase complex was important for the expression of fibroblast growth factor 8; an essential regulator of limb development in zebrafish and chicks. They also reported that the autoubiquitination of CRBN was inhibited by thalidomide *in vitro* and furthermore, expression of a drug binding deficient mutant of Crbn in zebrafish and chicks suppressed thalidomide-induced effects (Ito et al, 2011; Ito et al, 2010). Collectively, their data suggests that thalidomide binds to cereblon and inhibits the function of the CRBN-CUL4 E3 ligase complex. Moreover, it suggests that inhibition of its ubiquitin ligase activity may be a mechanism by which thalidomide induces its teratogenic effects. Although this data clearly provides evidence of a role for CRBN in thalidomide-induced teratogenicity, several questions remain to be addressed in order to fully understand the mechanisms underlying the teratogenic effects of thalidomide.

In spite of its teratogenic effects, thalidomide is now widely recognised as an effective drug in the treatment of leprosy and myeloma (Singhal et al, 1999; van Rhee et al, 2008). Novel thalidomide derivatives such as lenalinomide and pomalinomide have been developed and possess very strong anti-cancer properties with fewer adverse side effects. Interestingly, CRBN expression is required for the anti-myeloma effects exerted by these IMiDs (Immunomodulatory Drugs) suggesting an important role for CRBN not only in mediating the teratogenic effects of thalidomide but also in mediated its anti-cancer properties (Zhu et al, 2011). Furthermore, this suggests that these pathways may overlap through CRBN.

4.1.2.3: A putative role in the cellular antioxidant response system

Recently, Lee et al reported that CRBN expression (mRNA and protein) was increased following exposure of mouse neuroblastoma N2A cells to

hypoxia/reoxygenation (Lee et al, 2010b). In addition, they reported that a hydrogen peroxide insult lead to similar increases in CRBN expression. These results suggested that *CRBN* gene expression may be controlled by ROS-dependent signalling. To further investigate this, Lee et al functionally characterised the promoter region of mouse *Crbn* and identified a single Nrf2/ARE – binding site (Lee et al, 2010b). They reported that overexpression of Nrf2 or treatment with an Nrf2-activating compound induced the expression of the endogenous *Crbn* gene. Nrf2 is a basic region leucine-zipper transcription factor which, by binding to the antioxidant response element (ARE), regulates the expression of more than 200 genes involved in antioxidant defence (Kang et al, 2005). These include the phase 2 detoxification enzyme NAD (P) H quinone oxyreductase, extracellular superoxide dismutase and glutathione S-transferase A1 and A2 (Shih et al, 2005; van Muiswinkel & Kuiperij, 2005; Zhang et al, 2006). Nrf2 has also been shown to regulate the expression of mitochondrial transcription factors and thus mitochondrial biogenesis (Shih et al, 2005). In light of this data, it is tempting to speculate that CRBN may play a key role in the cellular antioxidant defence system.

4.1.2.4: CRBN and the AMPK signalling pathway

AMP-activated protein kinase (AMPK) is a serine/threonine protein kinase with key functions in the regulation of cellular energy homeostasis. Once activated by falling energy status and/or environmental stress; AMPK inhibits ATP-consuming pathways and promotes catabolic pathways to increased ATP production and maintain energy balance (Hardie et al, 2012). Mammalian AMPK is a trimeric enzyme consisting of a catalytic α subunit and the non-catalytic β and γ subunits, interacting through the C-terminal half of the α subunit. There are 12 different isoforms of AMPK due to multiple genes encoding the various subunits (Hardie, 2007). The α2 isoform is predominantly found in skeletal and cardiac muscle whereas the α1 isoform is found pancreatic β-islet cells and white adipose tissue

AMPK is regulated in response to stresses that deplete ATP such as hypoxia, ischemia, low glucose and heat shock (See Fig 4.1). An increase in the AMP:ATP ratio, even if very small, allosterically activates the complex. ADP or AMP can bind

the γ subunit and protect the activating phosphorylation of AMPK. In addition, phosphorylation of AMPK on Thr172 of the α-subunit is also required for its activation. This occurs by at least 3 different upstream AMPK kinases (AMPKK) such as LKB1 (Woods et al, 2003). LKB1 appears to be responsible for mediating the majority of AMPK activation in most tissues. However, AMPK can also be activated by CaMKK2 (Calcium/calmodulin-dependent protein kinase kinase 2) in response to calcium flux (Hurley et al, 2005). The release of intracellular stores of calcium creates a demand for ATP and thus activation of AMPK in this setting provides a mechanism for cells to anticipate this increased demand for ATP. In particular, CaMKK2 appears to be particularly involved in the activation of AMPK in T cells and neurons (Racioppi & Means, 2012; Takemoto-Kimura et al, 2010; Wayman et al, 2008).

AMPK activation by low levels of ATP positively regulates pathways such as fatty acid oxidation (via phosphorylation of Acetyl CoA Carboxylase) and autophagy (via mTOR) in a bid to replenish the ATP supply (Egan et al, 2011; Gwinn et al, 2008). Activation of AMPK negatively regulates ATP consuming pathways such as protein synthesis. One of the most well-known mechanisms by which AMPK regulates cell growth is via suppression of the mTORC1 pathway; a pathway central to the regulation of cell growth, mitochondrial homeostasis and the control of autophagy (discussed in detail in Chapter 3). In 2003, Tokunaga et al reported a possible interplay between the mTOR signalling pathway and AMPK by showing that treatment of epithelial cells with an AMPK activator lead to the inhibition of p70 S6 kinase (p70α), a key component of the mTOR signalling pathway. Furthermore, AKT was shown to be a negative regulator of AMPK and it has been suggested that AKT-mediated inhibition of AMPK is needed for the activation of mTOR signalling in the cell. More recently, it was shown that AMPK-mediated mTOR suppression is achieved through direct phosphorylation of key enzymes involved in this pathway, TSC2 and Raptor, which block the ability of the mTORC1 kinase complex to phosphorylate its substrates (Gwinn et al, 2008).

In addition to suppressing the mTOR signalling pathway, AMPK can also trigger autophagy by directly activating ULK1, a core component of the autophagy pathway (Egan et al, 2011). Activation of AMPK and the subsequent stimulation of

ULK1 triggers the destruction of defective mitochondria through mitophagy. In addition to stimulating mitophagy, AMPK activation stimulates *de novo* mitochondrial biogenesis through PGC-1α dependent transcription (Jager et al, 2007). Therefore, this interplay between AMPK and mTOR plays a central role in regulating mitochondrial homeostasis through the process of degrading defective mitochondria and replacing them with fuel-efficient ATP generators. AMPK activation also exerts control over metabolism through direct effects on metabolic enzymes such as Acetyl-CoA carboxylase (ACC1 and ACC2) and HMG-CoA reductase, which function in fatty-acid and sterol synthesis (Carling et al, 1987; Watt et al, 2006). In addition, AMPK has been reported to regulate a number of transcription factors, coactivators such as p300, corepressors such as CtBP1 and even histones, for example histone H2B (Bungard et al, 2010; Kim et al, 2013; Zhang et al, 2011). Therefore, AMPK plays a key role in a variety of growth, metabolism, and autophagy processes in order to maintain cellular energy homeostasis (See Fig 4.1).

Recently, using a yeast two hybrid system to screen rat brain cDNA Lee et al identified that rat CRBN directly interacts with the α subunit of AMPK preventing the formation of a holoenzyme with the regulatory subunits β and γ (Lee et al, 2011). Non-formation of this complex resulted in decreased activation of AMPK. Furthermore, over-expression of rat, mouse or human CRBN in HEK293FT cells significantly reduced the activation of endogenous AMPK whereas knockdown of endogenous CRBN up-regulated the activity of AMPK. This indicates that CRBN is a negative regulator of AMPK (Lee et al, 2011). As discussed above, AMPK is a master sensor of energy balance, therefore binding of CRBN with the α1 subunit of AMPK may play a role in regulating AMPK function. In addition, long term storage of explicit memory uses a core signalling pathway involving cAMP-dependent protein kinase (PKA), mitogen-activated protein kinase (MAPK) and cAMP response element binding protein-1 (CREB-1). As CRBN has been shown to bind and inhibit AMPK, which in turn modulates CREB signalling, some have suggested that this may be a potential molecular mechanism by which CRBN affects HPC-mediated memory in mice (Rajadhyaksha et al, 2012).

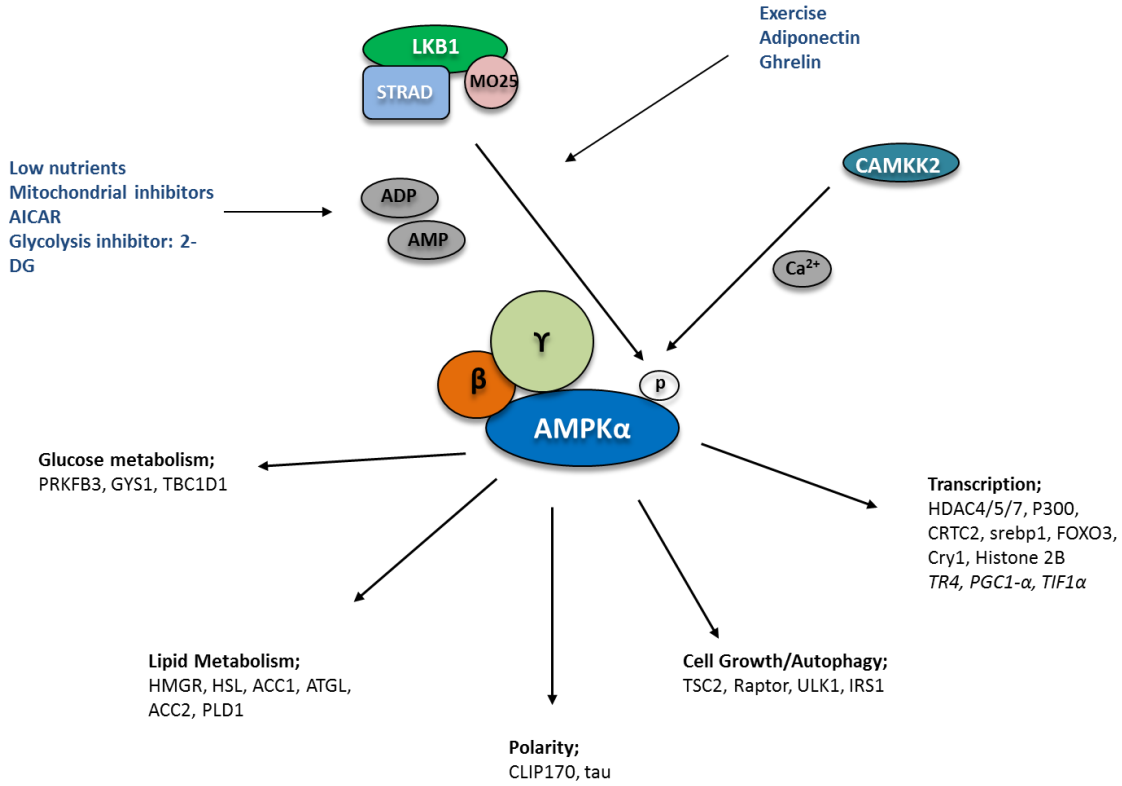

Figure 4.1 – The AMPK signalling pathway. AMPK is activated when AMP and ADP levels in the cell rise. This can be due to a variety of physiological stresses such as low nutrient and exercise and also in response to pharmacological inducers such as AICAR. LKB1, an upstream kinase, activates AMPK in response to AMP increase. AMPK can also be activated by CAMKK2 in response to rises in calcium levels. Activated AMPK directly phosphorylates a number of substrates invilved in cellular growth metabolism and autophagic processes. In addition, AMPK phosphorylates a number of transcriptional regulators that mediate long term metabolic reprogramming. Those substrates which need further *in vivo* investigation are italicized.

4.1.3: CRBN mouse models

Recently, Rajadhyaksha *et al* generated a conditional *Crbn* knockout mouse model by inactivating *Crbn* in forebrain neurons, mimicking the human condition associated with *CRBN* mutations (Rajadhyaksha et al, 2012). Exons 3 and 4 were deleted by Cre recombinase under the direction of a Ca^{2+}/calmodulin-dependent protein kinase II promoter ($CamIIK^{cre/+,}$ $cbrn^{-/-}$). Contextual fear conditioning showed a significant decrease in the percentage of freezing time in these mice and thus the results of this study demonstrate that specific deletion of *Crbn* in forebrain neurons of postnatal mice affects hippocampal (HPC)-dependent memory without any impairment of motor function, anxiety-related behaviours or social interaction (Rajadhyaksha et al, 2012). The generation of this *Crbn* knockout mouse model provides a promising model for studying the mechanisms by which Cereblon may lead to alterations in neuronal pathways.

Previously, Lee et al reported that CRBN negatively regulates the function of AMPK *in vitro* by binding directly to the α_1 subunit of the AMPK complex (Lee et al, 2013). However, the *in vivo* role of CRBN was not studied. Recently, in an attempt to elucidate the physiological roles of CRBN, Lee et al generated a *Crbn* knockout mouse model by targeting exon 1 of the *Crbn* gene. The *Crbn* KO mice displayed no apparent defects in gross morphology or basic behaviour (Lee et al, 2013). However, Lee et al reported that under normal conditions, endogenous AMPK was constitutionally hyperactivated in the liver of *Crbn* KO mice. They further reported that mice lacking *Crbn* appeared to have greater protection from body fat accumulation and obesity caused by high fat intake and are resistant to diet-induced fatty liver (See Fig 4.2). Moreover, Crbn expression in the liver was upregulated whereas that of pAMPK was downregulated in the long term by a high fat intake in wild type mice. The authors suggest that this may imply that Crbn is induced by a high fat diet and that Crbn regulates AMPK activity via a negative-feedback loop *in vivo*. In conclusion, CRBN may be considered as a novel regulator of body metabolism and energy homeostasis (Lee et al, 2013).

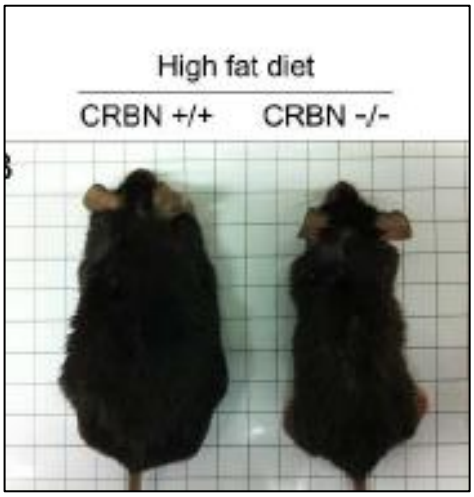

Figure 4.2 – Cereblon deficiency in mice prevents HFD-induced (high fat diet) obesity. Representative images of wild type (*Crbn*+/+) and *Crbn* KO mice (*Crbn*-/-) mice after a 14-week experimental period of being fed a HFD. Image obtained from Lee et al, 2013.

4.1.4: Summary

Mutations in *CRBN* have been identified as causative of a non syndromal form of mental retardation. Although the cellular functions of CRBN remain to be elucidated, they are thought to involve aspects of memory and learning and the regulation of key signalling pathways. Recently, CRBN was identified as the substrate-receptor component of a novel CRL4-containing complex which is inhibited by thalidomide *in vitro*. Thalidomide -induced inhibition of the E3 ligase activity of this complex is suggested to underlie the teratogenic effects of thalidomide treatment such as severe limb malformations. However, thalidomide is now used today, albeit restricted use, in the treatment of multiple myeloma patients. Interestingly, one of the main side effects of thalidomide treatment in multiple myeloma patients is that of peripheral neuropathy. This is also a key feature of the CUL4B patients described in Chapter 3 and suggests that these clinical features may arise through disrupted assembly of the CUL4-CRBN complex.

The CRBN protein has been shown to directly interact with the α-subunit of AMPK, inhibiting its actions. This provides a potential link for CUL4 in regulating AMPK via interaction with CRBN and thus supports a role for CUL4 in maintaining cellular homeostasis. In fact, loss of CUL4 has been associated with disrupted mTOR signalling, a pathway intimately linked to AMPK. Therefore, it is possible that loss of CUL4 could lead to disrupted levels of CRBN and impart a double-hit effect on both the mTOR and AMPK signalling pathways. Ultimately this may impart detrimental effects on mitochondrial homeostasis which may begin to explain some of the mitochondrial phenotypes identified in *CUL4B*-deleted LBLs. Furthermore, as discussed in section 3.1.4.4, the mTOR signalling pathway plays an essential role in mediating long term potentiation and misregulation of the mTOR signalling cascade is thought to be one of the molecular mechanisms underlying mental retardation. Mental retardation is a key feature of both *CUL4B*- and *CRBN*-mutated/deleted patients suggesting that the CUL4-CRBN complex may play a fundamental role in neuronal development and maintenance.

I sought to investigate whether loss of CRBN by siRNA-mediated knockdown phenocopies that of CUL4B loss. More specifically, I investigated whether loss of CRBN mimicked the mitochondrial phenotypes associated with CUL4B loss such as increased ROS generation. Furthermore, I sought to determine whether thalidomide treatment in a wild-type setting, and thus inhibition of the CUL4-CRBN E3 ligase activity, was able to mimic the mitochondrial phenotypes of CUL4B loss. Identification of a reciprocal relationship here may provide novel insight into some of the mechanisms underlying the MR associated with both *CUL4B* and *CRBN* mutations/deletions. Moreover, it may provide fundamental insight into the functional roles of this novel E3 ligase complex.

4.2 Results

4.2.1: Loss of CUL4B alters the expression of CRBN

CRBN was recently identified as a novel substrate receptor of a CRL4-containing E3 ligase complex involving CUL4A and DDB1 (Ito et al, 2010). Although CUL4A was identified as the Cullin backbone of this complex, CUL4B was not specifically ruled out. CUL4A and CUL4B are 80% identical and this it is tempting to suggest that CUL4B may also form an E3 ligase complex with CRBN. In the same study, CRBN was shown to have autoubiquitination activity and this activity was inhibited by thalidomide *in vitro.* Here, thalidomide functions to inhibit the activity of the CUL4-CRBN E3 ligase, rendering it non-functional. This suggests that CRBN autoubiquitination and thus regulation is only possible when this complex is formed and functionally active. Although the physiologically relevant substrates of the CUL4-CRBN E3 ligase complex are unknown, both CUL4 and CRBN have been implicated in a number of fundamental processes such as the mTOR and AMPK signalling pathways. Therefore, it is likely that this E3 ligase complex may play crucial roles in maintaining cellular homeostasis. Furthermore, mutations in both *CUL4B* and *CRBN* have been associated with mental retardation in patients suggesting that this E3 ligase complex plays a fundamental role in neuronal development processes such as synaptic plasticity and connectivity.

Initially I set out to investigate the impact of CUL4B loss, the core backbone of this E3 ligase complex, on the levels of CRBN protein expression. Cells from the CUL4B patients described in Chapter 3 provide a unique model for investigating the impacts of CUL4B loss on CRBN expression levels. Loss of CUL4B, and thus loss of the core component of this E3 ligase, would lead to non-formation of the complex and loss of E3 activity which may potentially impact on CRBN expression. As expected, Western blot analysis of whole cell extracts for CRBN protein expression levels revealed that *CUL4B*-deleted LBLs potentially display a subtle increase expression of CRBN protein compared to wild-type controls (Fig 4.3). This is consistent with previous reports of CRBN as a novel CUL4 substrate.

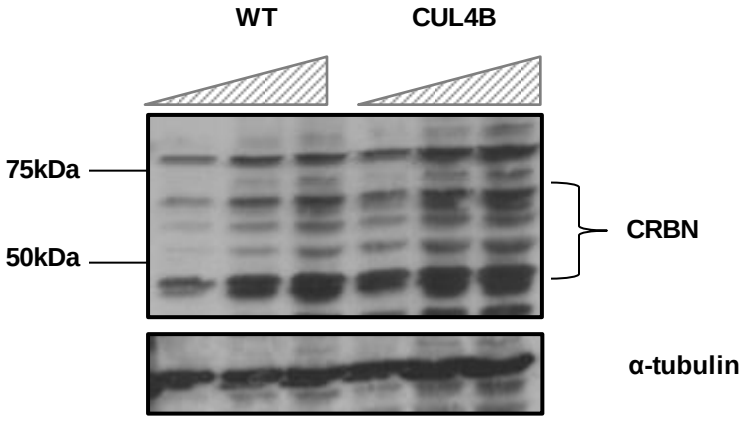

Figure 4.3 – CRBN protein expression levels are increased in *CUL4B*-deleted patient-derived LBLs. Increasing amounts of protein extract (25-100μg) were subjected to SDS-PAGE and immunoblotted for CRBN protein expression. α-tubulin was used as a loading control. WT; wild type control, CUL4B; *CUL4B*-deleted.

4.2.2: CRBN protein expression is reduced in *CUL4B*-deleted mitochondrial extracts

ATP-dependent proteases are key enzymes responsible for intracellular selective proteolysis and are thus important for maintaining cellular homeostasis. These enzymes function to eliminate mutant and/or abnormal proteins in addition to playing important roles in the turnover of short-lived regulatory proteins. There are a number of ATP-dependent protease families, one of which is Lon proteases which function in the mitochondria. There are two Lon families; LonA and LonB. LonA family members consist of an N-terminal domain, an ATPase (AAA+) domain and an N-terminal proteolytic domain. In contrast, members of the LonB family lack the N-terminal domain. Human mitochondrial Lon protease (*h*Lon) is a member of the LonA family and has been shown to degrade oxidised proteins such as aconitase. *h*Lon has also been reported to play important roles in mtDNA maintenance where it is thought to be involved in mtDNA replication, translation and/or repair.

Interestingly, human CRBN contains the N-terminal portion of the ATP-dependent Lon protease. However, it is reported to possess no protease or ATPase activity. Nevertheless, Lon proteases are found within the mitochondria suggesting that CRBN may be mitochondrially-localized. Interestingly, CUL4B was unexpectedly found to be present in isolated mitochondrial extracts (section 3.2.3). As CUL4B and CRBN have been identified as components of a novel CRL4-containing complex, the presence of CUL4B in/on the mitochondria further suggests that CRBN may also be present. If so, similar to whole cell extracts, loss of CUL4B may in turn affect the expression of CRBN within mitochondrial extracts.

Wild type and *CUL4B*-deleted mitochondria were isolated using the affinity purification technique described in Chapter 3, section 3.2.3. Increasing amounts of mitochondrial extract (5-15µL) were subjected to SDS-PAGE and immunoblotted for CRBN protein expression levels. Substantial CRBN protein expression was detected in wild-type mitochondrial extracts (Fig 4.4 lanes 1-2). However, *CUL4B*-deleted LBLs exhibited reduced CRBN protein expression levels compared with

WT controls (Fig 4.4 lanes 3-4). This data not only provides novel insight into the subcellular localisation of the CRBN protein but also suggests that loss of CUL4B imparts effects on the expression of CRBN. The protein expression levels of CRBN in whole cell extracts were increased in *CUL4B*-deleted LBLs yet they are found to be reduced in mitochondrial extracts from the same cells. This could potentially suggest that loss of CUL4B may disrupt the normal subcellular localisation of CRBN. In fact, CUL4B was also found to be present in mitochondrial extracts suggesting that the CUL4-CRBN complex may have as yet unidentified roles within or upon the mitochondria. Moreover, the reduced expression of CRBN in *CUL4B*-deleted mitochondria could be suggestive of co-stabilization limiting CRBN function in the context of CUL4B-deficiency.

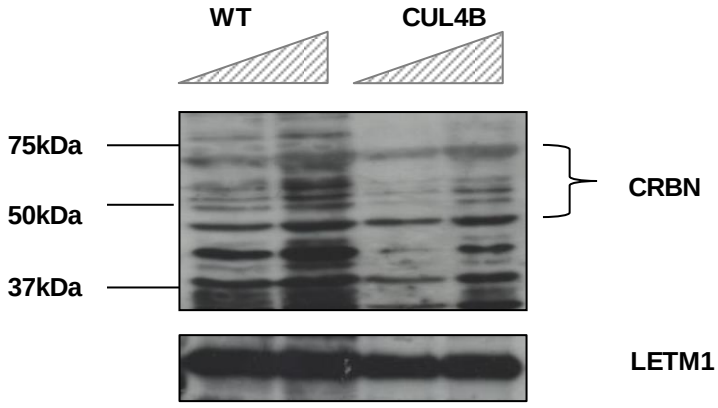

Figure 4.4 – CRBN protein expression levels are reduced in *CUL4B*-deleted mitochondrial extracts. Mitochondria were isolated from 1x 10^7 LBLs per cell line using the Miltenyi QuadroMACS Mitochondria Isolation Kit. Isolated mitochondria were resuspended in 60µL urea-based extraction buffer and sonicated for 15 seconds to create a mitochondrial protein extract. 5-10µL of extract was subjected to SDS-PAGE and immunoblotted for CRBN protein expression. CRBN expression was visible in both WT (lanes 1-2) and *CUL4B*-deleted (lanes 3-4) mitochondrial extracts but expression was reduced in *CUL4B*-deleted extracts compared to WT controls. The blot was reprobed for LETM1 expression to ensure equal loading of each sample. WT; wild-type, CUL4B; *CUL4B*-deleted.

4.2.3: AMPK phosphorylation in response to AICAR treatment is increased in *CUL4B*-deleted LBLs

Previous studies have shown that CRBN inhibits the activation of AMPK *in vitro* by directly binding to the α_1 subunit of AMPK. *CUL4B*-deleted LBLs display altered CRBN protein expression levels in both whole cell extracts and isolated mitochondria. Interestingly, CUL4B has previously been implicated in regulating the mTOR signalling pathway at multiple levels, a pathway intimately linked to AMPK activation. *CUL4B*-deleted LBLs display altered protein expression levels of CRBN which suggests that the regulation of AMPK may be altered in this context. CUL4B LBLs also exhibit elevated levels of intracellular calcium (see Chapter 3 section 3.2.2.7) which may feed into the AMPK signalling pathway and activate AMPK through CaMKKβ.

I investigated the impact of CUL4B loss on AMPK activation in response to the AMPK agonist, AICAR (5-Aminoimidazole-4-carboxamide ribonucleotide). Wild type LBLs displayed increased expression of pAMPK representing AMPK activation following a 5 minute AICAR treatment (Fig 4.5 lanes 1-4). CUL4B LBLs also exhibited AMPK activation following a 5 minute AICAR treatment but the protein expression levels of pAMPK were substantially increased compared to wild type controls (Fig 4.5 lanes 5-8). Moreover, CUL4B LBLs displayed a further increase in pAMPK expression at 15 minutes compared to wild type controls who exhibited a reduction in pAMPK at this time point. The data presented in figure 4.6 suggests that AMPK is hyperactivated in response to AICAR in CUL4B LBLs compared to wild type controls. This provides a potential link by which CUL4B may regulate AMPK via its interaction with CRBN and a possible role for CUL4-CRBN in mediating some aspects of mitochondrial homeostasis. However, cause and effect here are unclear.

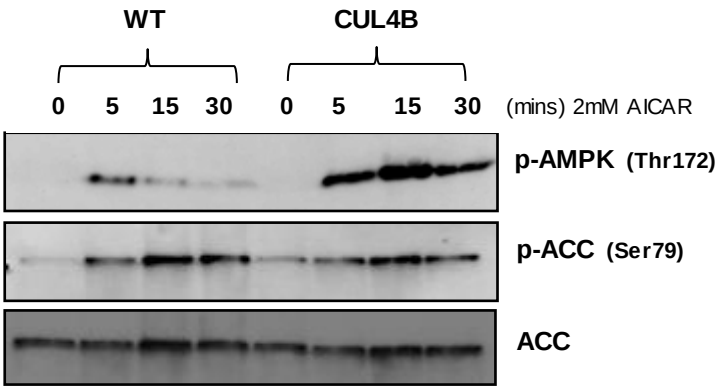

Figure 4.5 – AMPK is hyper-phosphorylated in response to AICAR in *CUL4B*-deleted LBLs. Wild type (WT) and *CUL4B*-deleted LBLs were treated with 2mM AICAR for 0-30 minutes. Urea-based whole cell extracts were then subjected to SDS-PAGE and immunoblotted for p-AMPK (top panel), p-ACC (middle panel) and native ACC protein expression levels. ACC; Acetyl-CoA Carboxylase, p-ACC; phospho-Acetyl-CoA Carboxylase, WT; Wild-type, CUL4B; *CUL4B*-deleted.

4.2.4: Thalidomide treatment mimics the cellular phenotypes of CUL4B loss

Recently, CRBN was identified as a novel thalidomide-binding protein and subsequently reported as the primary target of thalidomide. CRBN forms an E3 ligase complex with CUL4 and DDB1 and it is thought that thalidomide induces its teratogenic effects by inhibiting the E3 ligase activity of this complex. Thalidomide is widely used today in the treatment of multiple myeloma patients; however, one of the main side effects of its treatment is that of peripheral neuropathy. Peripheral neuropathy is a consistent feature of *CUL4B*-mutated and/or deleted patients so it is tempting to speculate that loss of CUL4B could underlie some aspect of both peripheral neuropathy observed in CUL4B patients through disrupted assembly of this E3 ligase complex. Moreover, MR is an overlapping clinical feature between *CUL4B*-deleted and/or mutated and *CRBN*-mutated patients suggesting that impaired activity of this E3 ligase complex may contribute to the MR observed in both disorders.

I set out to investigate the effects of thalidomide and the subsequent inhibition of this CUL4-CRBN E3 ligase complex on mitochondrial homeostasis in a wild-type setting. More specifically, I aimed to investigate the impact of thalidomide on the generation of reactive oxygen species. If thalidomide treatment here is capable of phenocopying CUL4B loss, this may suggest a putative role for the CUL4-CRBN complex in maintaining mitochondrial homeostasis. Wild-type LBLs were treated with 250μM thalidomide for 2 hours followed by 15 minute incubation with 250nM MitoSOX. Cells were then analysed for MitoSOX (red) fluorescence using the FACS Canto flow cytometer. Interestingly, thalidomide treated cells exhibited a ~2.5 fold increase in MitoSOX fluorescence compared to untreated controls (Fig 4.6). This data mimics that of *CUL4B*-deleted LBLs (see section 3.2.2.5) and suggests that the CUL4-CRBN E3 ligase complex potentially plays a key role in maintaining mitochondrial homeostasis. Consistent with this, CRBN has previously been shown to regulate the antioxidant defence system of the cell further indicating a role for this E3 complex in mitochondrial function.

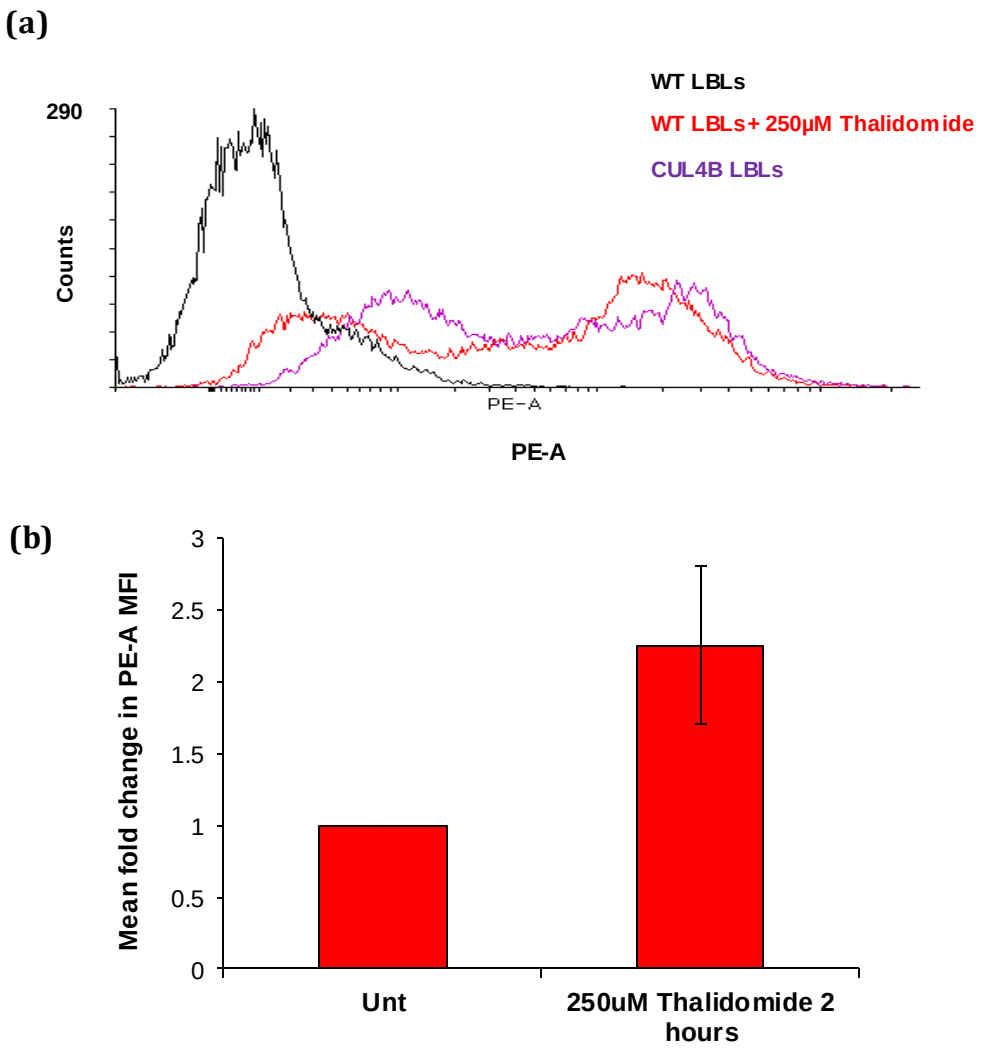

Figure 4.6 – Inhibition of the CUL4-CRBN complex by thalidomide treatment induces a ROS phenotype similar to that associated with CUL4B loss. **(a)** Wild type LBLs were treated with 250μM thalidomide for 2 hours followed by 15 minute incubation with 250nM MitoSOX. Cells (20,000 events) were then analysed for MitoSOX fluorescence by flow cytometry (red). *CUL4B*-deleted LBLs, as described in Chapter 3, were also analysed for MitoSOX fluorescence without the addition of thalidomide (pink). **(b)** Histogram showing the fold change in MitoSOX fluorescence following a 2 hour thalidomide treatment (250μM) compared to untreated (Unt) WT controls. MFI; mean fluorescence intensity of 20,000 events, Unt; untreated WT controls.

4.2.5: *Crbn* knockdown phenocopies the mitochondrial phenotypes associated with CUL4B loss

The precise physiologically relevant functions of the CUL4-CRBN E3 ligase complex or indeed its substrates remain elusive. However, the data presented here suggests that this complex may play an important role in mitochondrial homeostasis. Inhibition of the CUL4-CRBN complex by thalidomide results in a striking increase in superoxide generation. Similarly loss of CUL4B, potentially a core backbone of the CUL4-CRBN complex, is associated with a ~2 fold increase in superoxide generation (as described in Chapter 3 section 3.2.2.5). Furthermore, CRBN has been identified as a negative regulator of AMPK. I have shown that phosphorylation of AMPK in response to an activating compound is increased in *CUL4B*-deleted LBLs. This provides a potentially novel link by which CUL4B regulates AMPK and mTOR signalling through interaction with CRBN. Both the AMPK and mTOR signalling pathways are central regulators of mitochondrial biogenesis and autophagy. This suggests that non-formation of a functional CUL4-CRBN complex may impact on mitochondrial homeostasis at multiple levels. I have previously shown that loss of CUL4B or inhibition of the CUL4-CRBN complex by thalidomide results in a striking increase in ROS production. Therefore, I aimed to investigate whether loss of CRBN, the substrate receptor of this complex, results in similar mitochondrial phenotypes thereby suggesting of a novel role for the CUL4-CRBN complex within the mitochondria.

I investigated the impact of *Crbn* knockdown in a mouse C2C12 myoblast cell model. If indeed the CUL4-CRBN complex plays a key role in mitochondrial function, it would be expected that loss of *Crbn* may partially mimic the phenotypes of both *Cul4b* loss and thalidomide treatment. C2C12 myoblasts were sequentially (double) transfected with a siRNA smartpool of oligos directed against *Crbn* and *Crbn* knockdown was confirmed by Western blotting (Fig 4.7a). Flow cytometry analysis 48 hours post-transfection revealed a ~1.6 fold increase in MitoSOX fluorescence, indicative of increased superoxide levels (Fig 4.7b-c). Microscopy-based analysis of Mitotracker Red fluorescence revealed that *Crbn* siRNA-transfected C2C12 cells displayed a substantial reduction in Mitotracker

Red fluorescence indicative of transmembrane depolarisation (Fig 4.8). More interestingly, some cells appeared to exhibit extreme hyperpolarisation, a phenotype *identical* to that observed in *CUL4B*-deleted cells (Figure 4.7c and see Chapter 3 Fig 3.21). These results indicate that the CUL4-CRBN complex may play fundamental roles within the mitochondria whereby loss of CUL4B or CRBN gives rise to a distinct set of mitochondrial phenotypes indicative of mitochondrial dysfunction.

4.2.6: Summary

Loss of CUL4B is associated with a distinct set of mitochondrial phenotypes including elevated ROS production and disruption to the mitochondrial membrane potential. CRBN was recently identified as a novel substrate receptor of a CUL4-containing E3 ligase complex however its functions are unknown. Here I have shown that loss of CUL4B affects the subcellular localisation of the CRBN protein whereby its expression is increased in WCE but decreased in mitochondrial fractions. Loss of *Crbn* by siRNA-mediated knockdown has revealed mitochondrial phenotypes that are identical to those of both *CUL4B*-deleted patient derived LBLs and *Cul4b* siRNA-transfected cells. Furthermore, inhibition of the CUL4-CRBN E3 complex by thalidomide induces a ROS phenotype similar to that of patient-derived *CUL4B*-deleted LBLs. Collectively; these data suggest putative roles for the CUL4-CRBN complex in mediating some aspect of mitochondrial homeostasis such as redox status. CRBN has also been identified as a potential AMPK regulator. In the context of CUL4B-deficiency, AMPK phosphorylation is increased following AICAR treatment suggestive of a putative role for this E3 ligase complex in the regulation of AMPK.

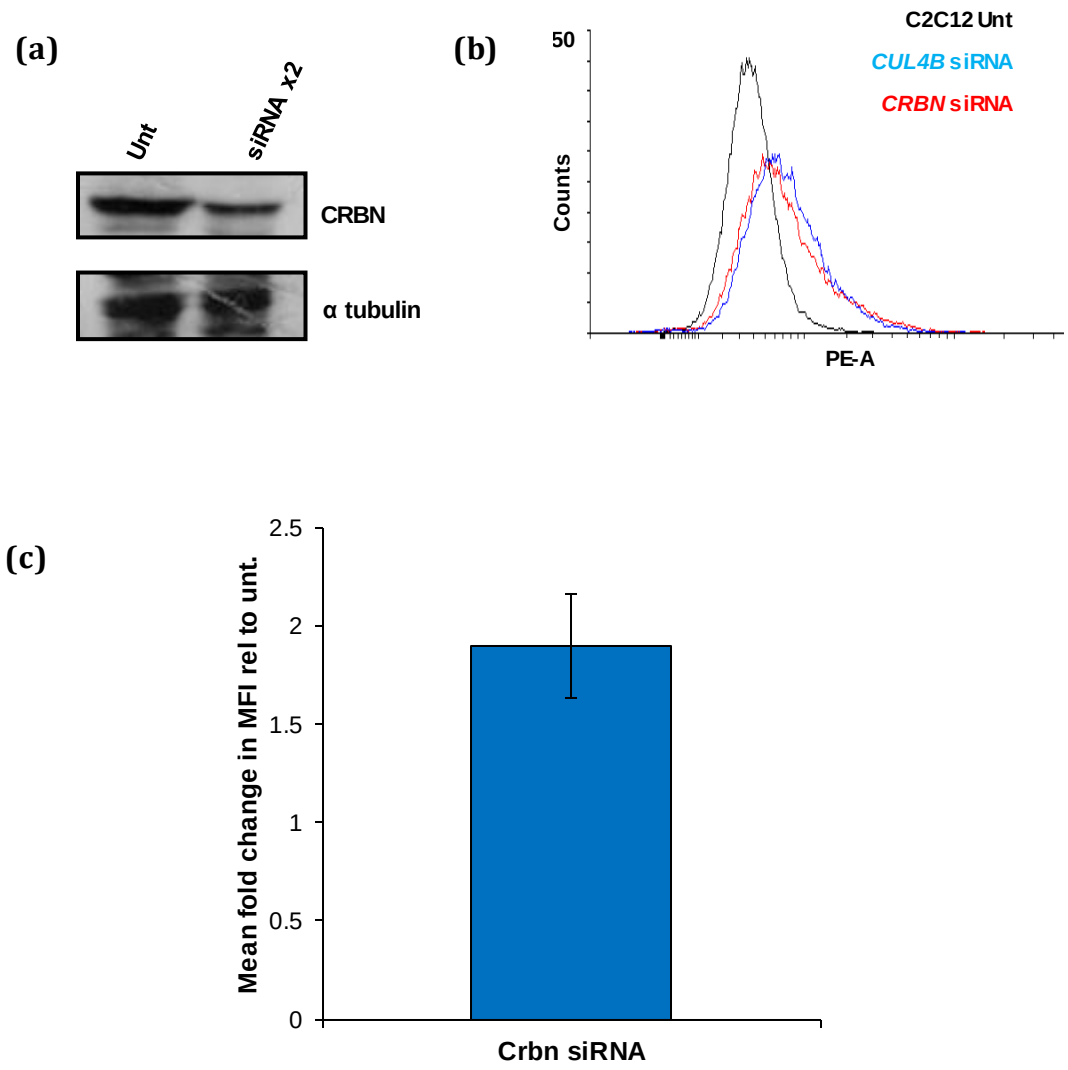

Figure 4.7 – siRNA-mediated knockdown of *Crbn* in mouse C2C12 myoblasts mimics the mitochondrial phenotypes associated with *CUL4B* loss. **(a)** C2C12 myoblasts were transfected twice (0 hours and 24 hours) with a *Crbn* oligo smartpool in the presence of metafectene pro and harvested 48 hours after the first transfection. Urea-based whole cell extracted were subjected to SDS-PAGE and immunoblotted for Crbn protein expression levels compared to untransfected (metafectene only) controls. α tubulin was used as loading control. **(b)** *Crbn* siRNA transfected C2C12s were incubated with 250nM MitoSOX 48 hours post double transfection. Cells were then analysed by flow cytometry for MitoSOX fluorescence (20,000 events). The FACS plot shown indicates the MitoSOX PE-A profiles for untransfected C2C12's (black), *Crbn* siRNA-transfected cells (red) and *Cul4b* siRNA-transfected cells (blue). **(c)** Representative histogram showing the mean fold change in MitoSOX mean fluorescence intensity (MFI) relative to untransfected C2C12 control cells (1 fold). The data represents the mean ± SD of three independent determinations.

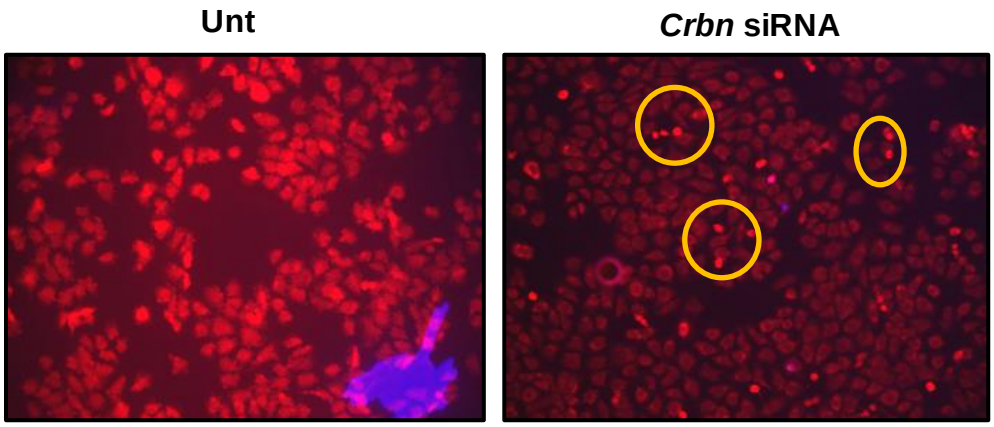

Figure 4.8 – Microscopy-based analysis of Mitotracker Red fluorescence in *Crbn* siRNA-transfected C2C12 cells. This experiment was performed at the same time as that shown in Figure 3.31, therefore the 'Unt' image shown here is duplicated. C2C12 myoblasts were grown on coverslips until 60% confluent. Cells were then incubated with 250nM Mitotracker Red for 15 minutes followed by a PBS wash. Coverslips were then mounted onto Poly-lysine slides and Mitotracker Red fluorescence was visualised using the Zeiss Axiovert microscope. Images were taken at the *same* exposure time. *Crbn* siRNA-transfected cells exhibited depolarization of the transmembrane potential, seen as an overall decrease in Mitotracker red fluorescence, but some cells displayed substantial hyperpolarisation as shown by the yellow circles. Unt; untransfected, *Crbn* siRNA; *Crbn* siRNA sequential transfection at 0 hours at 24 hours.

4.3: Discussion

Despite recent advances with regards to CRBN, its physiological functions are still not fully understood. The nonsense mutation p.R419X of CRBN has been identified in patients with Autosomal Recessive Non-Syndromal Mental Retardation (ARNSMR). CRBN has recently been identified as the substrate receptor of a CRL4-containing E3 ligase complex; however its substrates remain elusive. Interestingly, patients with *CUL4B* mutations/deletion also present with MR and thus the clinical overlap between these patients suggests that disruption of the CUL4-CRBN complex may play an important role in the pathogenesis of MR in these two conditions.

It is reported that CRBN can be ubiquitinated *in vitro* and *in vivo*, likely via CRL4-dependent auto-ubiquitination. Furthermore, this auto-ubiquitination activity can be inhibited by thalidomide suggesting that binding of thalidomide inhibits the activity of the CRBN-DDB1-CUL4-ROC1 E3 ligase complex (Ito et al, 2010). Consistent with these reports, I found that CRBN protein expression was increased in *CUL4B*-deleted patient-derived cells implicating CUL4B in this CRL4. Interestingly, although the protein expression of CRBN was increased in whole cell extracts, in contrast its expression levels were decreased in mitochondrial fractions. This could suggest that CUL4B deficiency not only results in the mis-regulation of CRBN protein levels through inhibition of autoubiquitination activity but also disrupts the subcellular localisation of CRBN. Although the functions of CRBN are not fully understood yet, its presence within mitochondrial extracts suggests that it may have important roles in mitochondrial function. In Chapter 3 I reported the presence of CUL4B in isolated mitochondrial extracts (section 3.2.3) and thus the additional presence of CRBN supports a potential role for the CUL4-CRBN complex within the mitochondria. Moreover, it indicates that this complex may have unidentified substrates residing within the mitochondria. Consistent with a role for CRBN in modulating some aspect of mitochondrial function, *Crbn* siRNA-mediated knockdown resulted in identical mitochondrial phenotypes to those seen in *CUL4B*-deleted LBLs; transmembrane depolarisation coexisting with

hyperpolarisation and marked increased in ROS production. This data further supports a role for the CUL4-CRBN complex specifically in maintaining mitochondrial homeostasis.

It has been postulated that some of the teratogenic effects of thalidomide treatment may be mediated via inhibition of the CUL4-CRBN complex. I interrogated the effects of thalidomide treatment on mitochondrial functioning in wild type cells and found that increased ROS was a clear consequence of thalidomide treatment in wild type cells. This is suggestive of a putative role for the CUL4-CRBN complex in regulating some aspect of mitochondrial redox status specifically. In fact, it has been reported that the *CRBN* promoter region harbours a Nrf2/ARE- binding site which further implicates it in cellular antioxidant defence system (Lee et al, 2010b). Interestingly, one of the side effects of thalidomide treatment in multiple myeloma patients is peripheral neuropathy; also a feature of *CUL4B*-deleted patients. Thalidomide is thought to exert its effects through inhibition of the CUL4-CRBN complex and thus the mitochondrial phenotypes observed suggest that inhibition or non-formation of the CUL4-CRBN complex, in the context of CUL4B deficiency, may play a role in the pathogenesis of neuropathy in *CUL4B*-deleted/mutated patients. It is noteworthy that *CRBN*-mutated patients do not exhibit any syndromal features like those with *CUL4B* deletion/mutations; however it is not clear whether any residual CRBN function remains in *CRBN*-mutated patients.

Whilst carrying out this work it was reported that CRBN can directly bind to the β7 subunit of the 20S core complex of the proteasome, inhibiting its enzymatic activity. The 20S proteasome plays a key role in selectively degrading oxidised proteins however; the products of *severe* oxidative stress can act as irreversible inhibitors of the 20S complex (Davies et al, 2001). *CUL4B*-deleted LBLs display both elevated levels of ROS and increased CRBN protein expression and thus the culmination of these two factors may inhibit 20S proteasome activity resulting in a vicious cycle of progressively worsening accumulation of protein oxidation products. This may be an area worthy of future investigation in order to fully elucidate the impact of CUL4B loss on CRBN function and redox status.

Furthermore, it may provide novel insight into the potential mechanisms underlying the MR in these patients.

In conclusion, it is likely that mis-regulation of the CUL4-CRBN complex may underlie some of mitochondrial phenotypes identified here and thus may potentially contribute to the overlapping MR phenotype of these patients. Importantly, this data provides a stepping stone for further investigations into potential substrates of the CRL4-CRBN E3 ligase. However, much deeper investigation is needed to provide a valuable link between impaired function of the CUL4-CRBN complex and the molecular aetiology of MR in these two disorders.

Chapter Five

16p11.2 Copy Number Variant Genomic Disorder; attempting to identify underlying and contributory genes

5.1: Introduction

Array CGH screening of large patient cohorts with defined phenotypes of Mental Retardation and/or multiple congenital anomalies (MCA) has led to the identification of multiple novel microdeletion/duplication syndromes. These include, but are not limited to, 15q24, 17q21.31 and 15q13.3 deletion syndromes (Ballif et al, 2007; Koolen et al, 2006; Sharp et al, 2006; Sharp et al, 2008). Recently, recurrent reciprocal 16p11.2 deletions and duplications have been associated with autism and DD (Kumar et al, 2008; Marshall et al, 2008; Weiss et al, 2008). Previous studies have suggested that the great majority of 16p11.2 deletions arise as *de novo* rearrangements but both inherited (autosomal dominant) and *de novo* patterns are observed in patients with 16p11.2 duplications (Shinawi et al, 2010).

Intensive phenotypic analyses of patients with 16p11.2 rearrangements has revealed strikingly opposing comorbidities; the 600kb deletion on 16p11.2 has been associated with autism, epilepsy, macrocephaly, obesity and Autism Spectrum Disorder (ASD) whereas the reciprocal duplication is associated with autism, schizophrenia, anorexia and microcephaly (Shinawi et al, 2010). These observations support the model of behavioural phenotypes in genomic sister disorders proposed by Crespi et al (Crespi et al, 2009). According to this model, diametric variation in gene copy number can generate contrasting cognitive and behavioural phenotypes associated with autistic spectrum and psychotic spectrum conditions which may represent development and evolution of the social brain. However, although 16p11.2 CNV have frequently been associated with autism, a more recent study has shown that autism is not always a presenting feature in many patients with 16p11.2 deletions (Bijlsma et al, 2009). Here, 16p11.2 deletions were associated with a much broader and variable clinical phenotype ranging from MR and/or MCI autism, and learning and speech problems to a normal phenotype. Furthermore, certain facial features are shared among patients (Shinawi et al, 2010). Those individuals with 16p11.2 deletions typically share the following features; broad forehead, micrognathia, hypertelorism and a flat midface.

The broad forehead, macrocephaly and flat midface give these patients a distinct facial gestalt. However, in the case of 16p11.2 duplications, dysmorphism appears to be more severe but has no recognisable pattern (Figure 5.1). This accumulating evidence indicates that 16p11.2 CNV is associated with a highly variable clinical spectrum.

(a)

(b)

Figure 5.1 - Facial features of individuals with 16p11.2 CNVs. **(a).** 16p11.2 deletion patients exhibit a broad forehead and flat midface. Hypertelorism and micrognathia appear to be common. (b). 16p11.2 duplication patients tend to be more grossly dysmorphic but with no recognisable pattern between affected individuals (Image taken from Shinawi et al, 2010).

5.1.1: The 16p11.2 region

As described in Chapter one, recurrent CNVs are typically flanked by LCRs which serve as substrates for NAHR. In the case of 16p11.2 CNV, analysis of the genomic structure within the rearranged region has identified two major LCR families; **(i)**. Two ~147kb LCRs in direct orientation sharing 99.6% sequence identity (147A/B) and **(ii)**. three 72kb repeats in direct orientation which share ~98.6% sequence identity (72 A/B/C) (Figure 5.2) (Shinawi et al, 2010). The 16p11.2 rearrangement interval contains ~30 annotated genes, some of which are promising candidates for the different phenotypes in patients with these syndromes such as *MAPK3, SEZ6L2, QPRT, MAZ and DOC2A* (Feldblum et al, 1988; Kumar et al, 2009; Mazzucchelli et al, 2002; Okamoto et al, 2002).

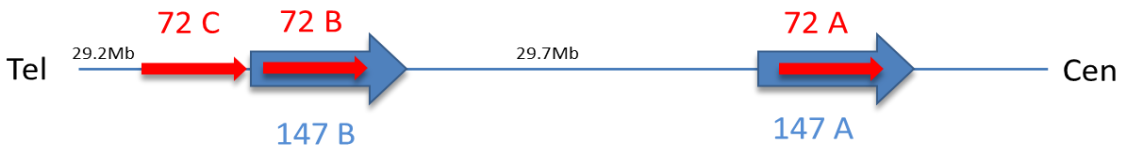

Figure 5.2 - Schematic representation of the two major LCR families in the 16p11.2 region. The blue arrows represent the two ~147kb LCRs which are in direct orientation and share 99.6% sequence identity. The red arrows, termed 72A, 72B and 72C, represent the three ~72kb LCRs. These are also in direct orientation and share ~98.6% sequence identity.

5.1.2: Mouse models of 16p11.2 CNV

Using Cre/LoxP-based chromosome engineering, Horev et al generated mice with either one copy (df/+) or three copies (dp/+) of the region corresponding to human 16p11.2 (Horev et al, 2011). Interestingly, the rate of certain behaviours appeared to be affected reciprocally by loss and gain of 16p11.2. In a novel environment, df/+ mice displayed longer distance travelled and walking time compared with WT controls. In contrast, dp/+ mice spent less time walking and travelled a shorter distance compared with WT controls. Additionally, assessment of light and dark cycling revealed that 16p11.2 dosage affected diurnal behaviours (active during the daytime and sleeping during the night). More specifically, df/+ mice had a much higher ratio of light to dark activity compared with both dp/+ and control mice (Horev et al, 2011). Further behavioural analysis revealed that 16p11.2 deletion mice displayed non-progressive, stereotypic motor behaviour. Interestingly, these behaviours were similar to the stereotypic behaviour observed in rats with lateral hypothalamic lesions and 6-hydroxydopamine-induced lesions, a well characterised model of Parkinson's Disease (Golani et al, 1979; Schallert et al, 1978).

Concordant with the macro/microcephaly observed in human subjects with 16p11.2 deletion and duplication, MRI (Magnetic Resonance Imaging) scans revealed significant changes in eight different brain regions in 16p11.2 CNV mice. Brain structures significantly altered included the basal forebrain, superior colliculus, fornix, hypothalamus, mammillothalamic tract, medial septum, midbrain and periaqueductal gray (Horev et al, 2011). Opposing volumetric changes indicated that loss and gain of 16p11.2 dosage affects these regions in a reciprocal manner. These findings are consistent with 16p11.2 CNVs as causative of brain and behavioural anomalies.

5.1.3: *KCTD13*; a gene linked to head size

Human brain development involves rapid and sustained cellular proliferation during embryogenesis and it is this feature that renders it highly sensitive to

perturbations in cell cycle dynamics. One of the most apparent clinical features of impaired neurogenesis is microcephaly. The term 'microcephaly' refers to a clinical finding; a reduction in occipitofrontal or head circumference greater than 3 standard deviations below the age-related mean. Conversely, the term 'macrocephaly' represents an enlarged head circumference greater than 2.5 standard deviations above the age-related mean.

It is hypothesized that microcephaly is a consequence of reduced neurogenesis, potentially due to increased cell death and/or reduced neuroprogenitor proliferative capacity. This ultimately leads to a reduction in the final number of cells that populate the cortex. The converse is thought to be true for macrocephalic phenotypes. There are many genetic and non-genetic causes of Primary Microcephaly (OMIM 251200). Interestingly, to date, all of the genes implicated in PM encode proteins with known/presumed roles in centrosome and/or spindle formation and maintenance (Table 5.1). Microcephaly is also a common feature of many DDR-defective disorders suggesting a fundamental role for the DDR in the developing nervous system. Microcephaly is seen in DDR-defective disorders such as ATR-Seckel syndrome, LIG4 syndrome, Fanconi Anaemia and XLF-Cernunnos-SCID (reviewed in (O'Driscoll & Jeggo, 2008) (Table 5.2). Furthermore, recent findings using patient-derived cell lines from Meier-Gorlin syndrome and Wolf-Hirschhorn syndrome have highlighted the importance of optimal DNA replication and S phase progression for normal human development (Kerzendorfer et al, 2013).

Patients with 16p11.2 CNV exhibit strong opposing clinical phenotypes, one of the most prominent being head size. Individuals harbouring 16p11.2 deletions present with *absolute* or *relative* macrocephaly, whereas patients with duplications of this region exhibit microcephaly. As shown in Figure 5.2, the 16p11.2 region harbours ~30 annotated genes, some of which are involved in regulating cellular proliferation, cell cycle progression, DNA repair or the DNA Damage Response (DDR). These include; *BOLA, TAOK2, INO80, PPP4C* and *MAPK3*. One gene that has gained significant interest in recent years is *KCTD13*, or as it is otherwise termed, *PDIP1*. *KCTD13 (potassium, channel tetramerisation domain containing 1)* encodes the polymerase delta-interacting protein 1 (PDIP1), which can also interact with

PCNA (Proliferating Cell Nuclear Antigen) (He et al, 2001). PCNA is an evolutionarily conserved protein found in all eukaryotic species and was first shown to act a processivity factor of DNA polymerase which is required for DNA synthesis during replication (Kelman, 1997). However, besides its crucial role in DNA replication, PCNA also functions in other vital cellular processes such as chromatin remodelling, Okazaki fragment processing, DNA repair and cell-cycle control. The identification of this interaction that has led researchers to propose that KCTD13/PDIP1 may play key roles in cell cycle regulation (He et al, 2001).

Consistent with a putative role for KCTD13 in neurogenesis, Golzio and co-workers reported that *KCTD13* was strongly expressed in the developing brain and deregulation of *KCTD13* levels were sufficient to establish neuroanatomical defects such as reduced or increased cell proliferation (Golzio et al, 2012). In an attempt to identify the critical loci whose dosage sensitivity could yield the microcephalic/ macrocephalic phenotypes associated with 16p11.2 duplications/deletions, Golzio *et al* investigated the effects of overexpression of each human 16p11.2 region transcript in zebrafish embryos at the two-cell stage. Systematic overexpression of 29 of the genes within this region revealed that overexpression of *KCTD13* specifically yielded the microcephalic phenotype associated with the 16p11.2 duplication, whereas reciprocal suppression of this locus using a *Kctd13* morpholino mirrored the corresponding human 16p11.2del macrocephalic phenotype (Golzio et al, 2012) (Figure 5.3). Further analysis of zebrafish embryos revealed that the microcephalic phenotype induced by *KCTD13* overexpression was accompanied by decreased proliferation of neuronal progenitors and increased cell death relative to controls. In contrast, the macrocephaly induced by *Kctd13* downregulation (~70%) arose from increased proliferation. Moreover, these shifts in cellular proliferation and death were apparent before the differences in head size developed which argues that an altered balance in cell proliferation and/or death drove the micro-/macrocephaly phenotypes.

To investigate whether downregulation of *Kctd13* in mice could recapitulate the findings of increased head size in zebrafish, Golzio et al designed short hairpin RNAs (shRNAs) against murine *Kctd13*. Consistent with a relationship between *KCTD13* expression and head size; injection of the *Kctd13* shRNA and GFP-

expressing plasmid into the ventricular space of developing brains of mouse embryos resulted in a twofold increase in BrdU/GFP labelling within the ventricular zone compared with controls (Golzio et al, 2012). This data suggests that *Kctd13* somehow impacts upon the proliferative status of cortical progenitors *in vivo*. However, it is noteworthy that an overexpression model was not reported.

Although the data presented by Golzio and colleagues supports a major contributory role for KCTD13 as a driver of the macro/microcephalic phenotypes of 16p11.2 CNV through regulation of early neurogenesis, it does not preclude a contribution from other genes towards head size in this context. Indeed, they reported that pairwise overexpression of *KCTD13* with two other 16p11.2 gene transcripts; *MAPK3* and *MVP*, enhanced the microcephalic phenotype in zebrafish. More importantly, five of transcripts within the mammalian 16p11.2 region (*SPN*, *QPRT*, *C16orf54*, *TMEM219* and *C16orf92*) are not present in the zebrafish genome and thus the relative contributions of these genes cannot be excluded or excluded. Furthermore, a second study published in the same year, also using the zebrafish model, reported that the majority of genes within the 16p11.2 are required for nervous system development (Blaker-Lee et al, 2012). In most cases an effect was only observed following a ~75% reduction in gene expression, however a 50% reduction in gene expression of two genes; *ALDOA* and *KIF22* was sufficient to cause narrowing of the forebrain and a reduction in brain volume, respectively (Blaker-Lee et al, 2012). Collectively, the data suggests there may be other genes within this region which may contribute to head size, but *KCTD13* may be *the* major driver of this mirrored phenotype.

5.1.4: A potential link between KCTD13 and autism

In 2012, a submicroscopic ~118kb deletion in 16p11.2 that segregated with ASD was discovered in a single three-generation pedigree, encompassing only five genes; *MVP*, *CDIPT1*, *SEZ6L2*, *ASPHD1* and *KCTD13*. This report was consistent with a role for haploinsufficiency of *KCTD13* as a key contributor to 16p11.2del phenotypes. Following on from their work in zebrafish, Golzio and colleagues looked to deepen their investigations by screening this restricted region in 518

individuals with autism, compared with 8328 controls (Golzio et al, 2012). The reported full segment deletions in 1.54% of ASD subjects compared with 0.06% from controls. Interestingly, they noted a *de novo* deletion of a single probe spanning exon 4 of *KCTD13* in one proband with a narrow diagnosis of autism. The deletion was restricted to the coding region of *KCTD13*; including exons 3, 4 and 5 suggesting that haploinsufficiency of *KCTD13* may contribute to the ASD phenotype associated with 16p11.2 CNV. However, when attempting to precisely localize the breakpoints by aCGH it was found that the individual harboured an additional, atypical ~300kb deletion distal to the 16p11.2 region and thus this finding obscured a potential direct link between KCTD13 and autism.

5.1.5: Summary

16p11.2 deletion and reciprocal duplications have been identified in ~1% of autistic individuals. Interestingly, deletion vs. duplication patients present with mirrored anatomical phenotypes such as macro- or microcephaly, respectively. One of the most fundamental mechanisms proposed to underlie severe microcephaly in humans is that of altered DNA replication, centrosome function and/or spindle organisation. Moreover, recent findings in patient-derived cells lines from both Meier-Gorlin syndrome and Wolf-Hirschhorn Syndrome highlight the importance of optimal replication efficiency and S-phase progression for human development, including neurogenesis. These findings indicate that impaired replication efficiency may underlie the microcephalic phenotypes of these two complex human disorders. (Kerzendorfer et al, 2012). Additionally, accumulating evidence also implicates defective DDR pathways as crucial players in the aetiology of microcephaly. The 16p11.2 region encompasses ~30 genes, some of which function in cell cycle regulation and DNA repair pathways suggesting that altered DNA replication and/or repair proficiency may underlie the micro-/macrocephalic phenotypes of 16p11.2 CNV patients. Employing a set of 16p11.2 CNV patient-derived LBLs (deletion and duplication), I chose to interrogate the expression, and by extension the functional consequences of altered copy number variation of three genes in particular; *KCTD13, TAOK2* and

MAPK3, in the context of 16p11.2 deletion/duplication. These genes were chosen based on the known or putative roles of the proteins they encode in cell cycle regulation (MAPK3), DNA replication (KCTD13) and DNA repair (TAOK2). Furthermore, I sought to investigate whether impairments in DNA replication and S-phase transit and/or elevated or reduced sensitivity to HU-induced DNA damage was a feature of these cells.

Table 5.1 - Defects in genes that encode proteins with centrosomal and/or spindle functions or localisations are associated with severe microcephaly in humans.

Gene	Disorder	Protein location	Function
MCPH1	Primary Microcephaly MCPH1 locus	Centrosome	Implicated in chromosome condensation and DDR
ASPM	Primary Microcephaly MCPH5 locus	Spindle pole	Mitotic spindle regulation
CDK5RAP2	Primary Microcephaly MCPH3 locus	Centrosome	Required for centrosome cohesion and microtubule nucleation of the γ-tubulin ring complex
CENPJ	Primary Microcephaly MCPH6 locus and Seckel Syndrome	Centrosome	Functions in centriole duplication
WDR62	Primary Microcephaly MCPH2 locus	Spindle pole	Proposed to play a role in cerebral cortical development
CEP152	Primary Microcephaly MCPH4 locus and Seckel Syndrome	Centrosome	Required for the centrosomal loading of PLK4 and CPAP
STIL	Primary Microcephaly MCPH7 locus	Spindle pole	Functions in precentriole formation and centriole duplication
CEP63	Primary Microcephaly with mild Seckel Syndrome	Centrosome	Forms a ring-like structure at the chromosome with CEP152 and controls centrosome number
CEP153	Primary Microcephaly MCPH8 locus	Centrosome	Presumed role in centriole biogenesis
PCNT	Microcephalic Osteodysplastic Primordial Dwarfism-Type II (MOPDii)	Centrosome	Microtubule nucleation
NIN	Microcephalic Primordial Dwarfism (MPD)	Centrosome	Role in coordinating asymmetric cell division

Table 5.2: A selection of DNA damage response (DDR) disorders conferring microcephaly.

Disorder	DDR-defect
NBS: Nijmegen breakage syndrome	ATM and ATR signalling and Artemis-ATM-dependent DSB repair
ATR-S: ATR-Seckel syndrome	ATR-signalling
MCPH1:Microcephalin-dependent primary microcephaly	ATR-dependent checkpoint activation
XPA & ERCC1: Xeroderma pigmentosum complementation groups	Nucleotide Excision Repair. Defective ATR-signalling in XP-A
FA (-D2): Fanconi Anaemia	Response to cross-linking agents
LIG4: DNA Ligase IV syndrome	NHEJ
XLF/Cernunnos-SCID: Xrcc4-like factor/Cernunnos-dependent severe combined immunodeficiency	NHEJ
BS: Bloom's syndrome	Unregulated HR

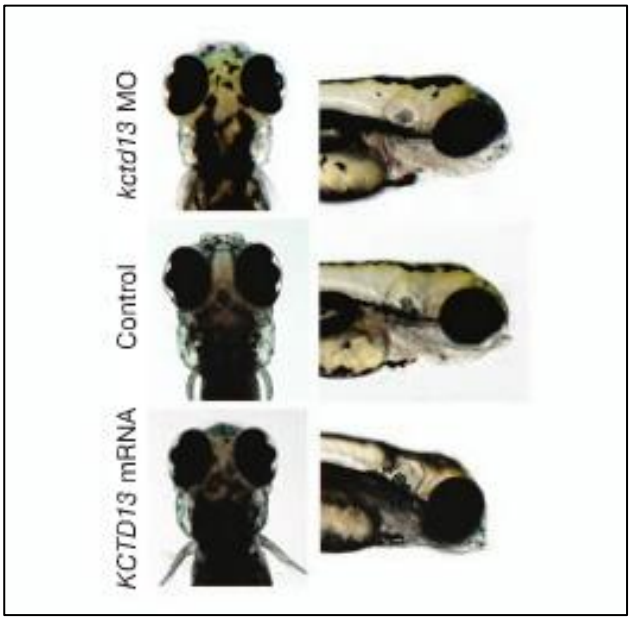

Figure 5.3: *KCTD13* dosage changes lead to changes in head size of zebrafish. Dorsal (left) and lateral (right) views of representative embryos injected with *kctd13* morpholino (MO), control or *KCTD13* mRNA (Golzio et al, 2012).

5.2: Results

5.2.1: 16p11.2 deletion and duplication LBLs exhibit corresponding protein expression of TAOK2 and MAPK3

In collaboration with Dr. Evica Rajean-Separovic at the Department of Pathology, Women's Health Centre of British Columbia and the University of British Columbia, I assembled a panel of EBV-transformed patient-derived lymphoblastoid cell lines (LBLs) from 5 patients harbouring either a hemizygous deletion of the 16p11.2 region or the reciprocal duplication (See table 5.3). To assess the cellular consequences of 16p11.2 CNVs, I chose to interrogate the protein expression levels of three proteins in particular, encoded by genes residing within the 16p11.2 region; TAOK2, MAPK3 and KCTD13. Protein expression data for 16p11.2 CNV has not previously been reported. All published data to date (June 2013) exclusively refers to mRNA levels.

TAOK2 protein expression was found to be increased/decreased consistent with deletion or duplication of the *TAOK2* gene in three different 16p11.2 CNV cell lines (Figure 5.4). LBLs derived from a male proband harbouring a paternal 16p11.2 duplication (LBL 06-32) exhibited a 1.8 fold increase in TAOK2 protein expression compared with WT controls (Fig 5.4a lanes 1-6). LBLs derived from a female proband with a *de novo* 16p11.2 deletion (LBL 12-14) and from a male proband also with a *de novo* 16p11.2 deletion (LBL 09-22) exhibited a 0.43-0.6 fold change in the protein expression levels of TAOK2 compared with WT controls, consistent with deletion of 16p11.2 (Fig 5.4a lanes 7-9, Fig 5.4b and Fig 5.4c). Also consistent with deletion/duplication of the 16p11.2 region in two patient-derived LBLs, western blot analysis of ERK1 (MAPK3) protein expression revealed increased/decreased expression respectively (Figure 5.5 panel 1). Furthermore, protein expression of the phosphorylated form of MAPK3 was also consistent with 16p11.2 copy number change (Figure 5.5 panel 3).

Table 5.3 – 16p11.2 CNV patient-derived LBL cell lines used in this thesis.

Cell Line	CNV
LBL 09-22	Male proband with a *de novo* 16p11.2 deletion
LBL 06-32	Male proband with a paternal 16p11.2 duplication
LBL 12-32	Male proband with a maternal 16[11.2 duplication
LBL 12-33	Father of 12-3; Not affected
LBL 12-56	Mother of 12-32 with a 16p11.2 duplication
LBL 12-14	Female proband with a *de novo* 16p11.2 deletion and a maternal 4q duplication

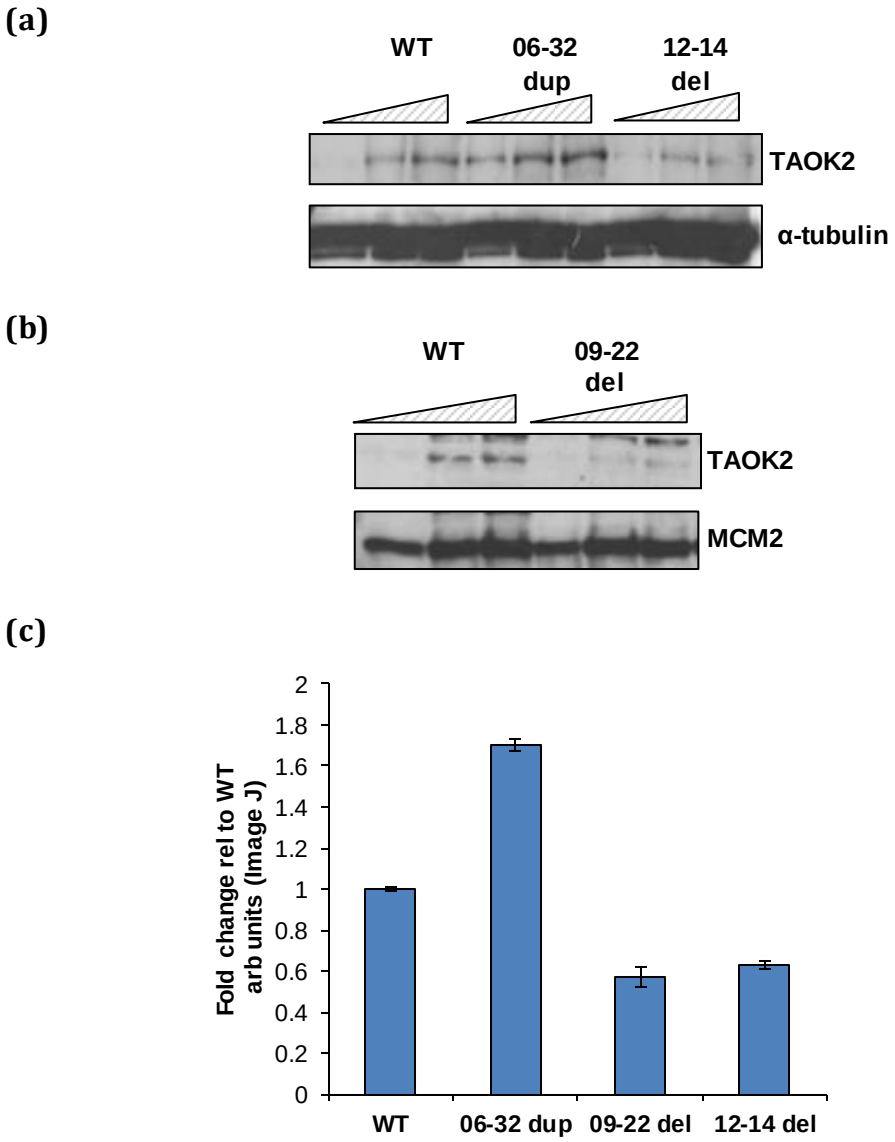

Figure 5.4 - Characterisation of 16p11.2 deleted and duplicated patient-derived cell lines by western blotting for TAOK2 protein expression, del; 16p11.2 deletion, dup; 16p11.2 duplication. **(a)** Expression of TAOK2 was increased/decreased consistent with deletion or duplication of the 16p11.2 region. 75µg of urea-based whole cell extracts for WT, 06-32 (16p11.2 duplication) and 12-14 (16p11.2 deletion) cell lines were subjected to SDS-PAGE and immunoblotted for TAOK2 protein expression. The blot was reprobed for α-tubulin expression as a loading control. **(b)** Expression of TAOK2 was decreased consistent with deletion of 16p11.2 region. 75µg of urea-based whole cell extracts for WT and 09-22 (16p11.2 deletion) cell lines were subjected to SDS-PAGE and immunoblotted for TAOK2 protein expression. The blot was reprobed for MCM2 expression as a loading control. **(c)** Representative histogram showing the fold change in TAOK2 protein expression levels in three 16p11.2 CNV patient-derived cell lines relative to WT controls as measured by Image J. Data represents the mean of 3 independent measures ± SD. Arb units; Arbitrary units, Image J.

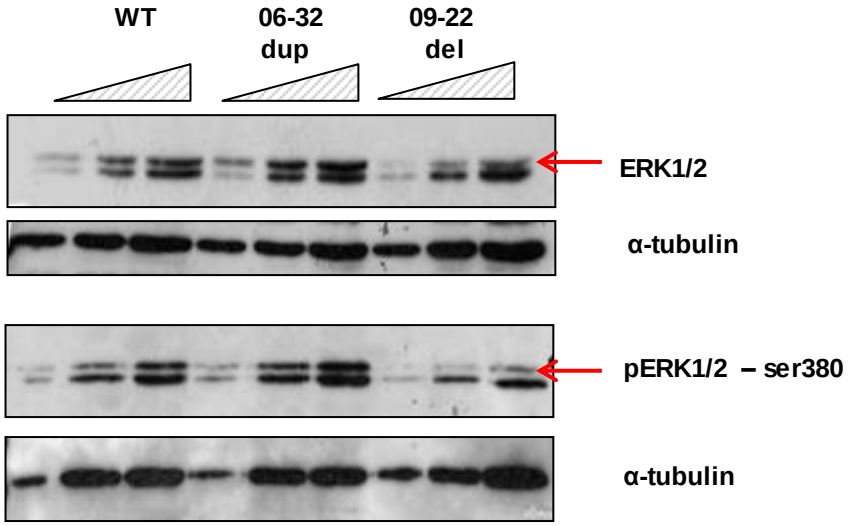

Figure 5.5 – Characterisation of 16p11.2 deleted and duplicated patient-derived cell lines by western blotting for ERK1 (MAPK3) and phospho-ERK1 (pMAPK) protein expression, del; 16p11.2 deletion, dup; 16p11.2 duplication. **(a)** Expression of ERK1 was increased/decreased consistent with deletion or duplication of the 16p11.2 region. 50µg of urea-based whole cell extracts for WT, 06-32 (16p11.2 duplication) and 09-22 (16p11.2 deletion) were subjected to SDS-PAGE and immunoblotted for ERK1/2 protein expression levels, the top band corresponds to ERK1/MAPK3. The blot was reprobed for α-tubulin expression as a loading control. **(b)** Expression of pERK1 was increased/decreased consistent with deletion or duplication of the 16p11.2 region. 50µg of urea-based whole cell extracts for WT, 06-32 (16p11.2 duplication) and 09-22 (16p11.2 deletion) were subjected to SDS-PAGE and immunoblotted for pERK1/2 protein expression levels, the top band corresponds to pERK1/pMAPK3. The blot was reprobed for α-tubulin expression as a loading control.

5.2.2: *KCTD13* copy number change does not segregate with head size in 16p11.2 patient-derived cells

KCTD13 is encoded by the *KCTD13* gene residing within the 16p11.2 region. Copy number change of this gene has recently been implicated as potentially causative of the mirroring head size phenotypes of 16p11.2 deletion/duplication patients. As discussed in section 5.1.3, *KCTD13* encodes the polymerase delta-interacting protein 1 (PDIP1) which also interacts with PCNA, a protein involved in DNA replication (He et al, 2001). This suggests that KCTD13 may play a role in DNA replication and has subsequently led researchers to speculate that that copy number change of *KCTD13* may impact upon neurogenesis (Golzio et al, 2012). Employing LBLs from patients with a 16p11.2 deletion/duplication, I set out to interrogate the impact of copy number variation of 16p11.2 on the protein expression of KCTD13.

Consistent with a decrease in copy number of the 16p11.2 region, KCTD13 protein expression levels were reduced in 16p11.2 deletion patient-derived LBLs. In contrast, increased copy number of the 16p11.2 region unexpectedly *did not* result in increased KCTD13 protein expression in patient-derived LBLs harbouring the 16p11.2 duplication (Figure 5.6). I used two different commercially available anti-KCTD13 antibodies yet failed to detect significant over-expression. Although increased copy number is generally assumed to increase protein expression, the data presented here suggests that the KCTD13 protein does not behave solely as predicted by copy number. Furthermore, this data is inconsistent with the work of Golzio and colleagues and indicates that *KCTD13* copy number change does not segregate with the micro/macrocephaly observed in 16p11.2 duplication patients (Golzio et al, 2012).

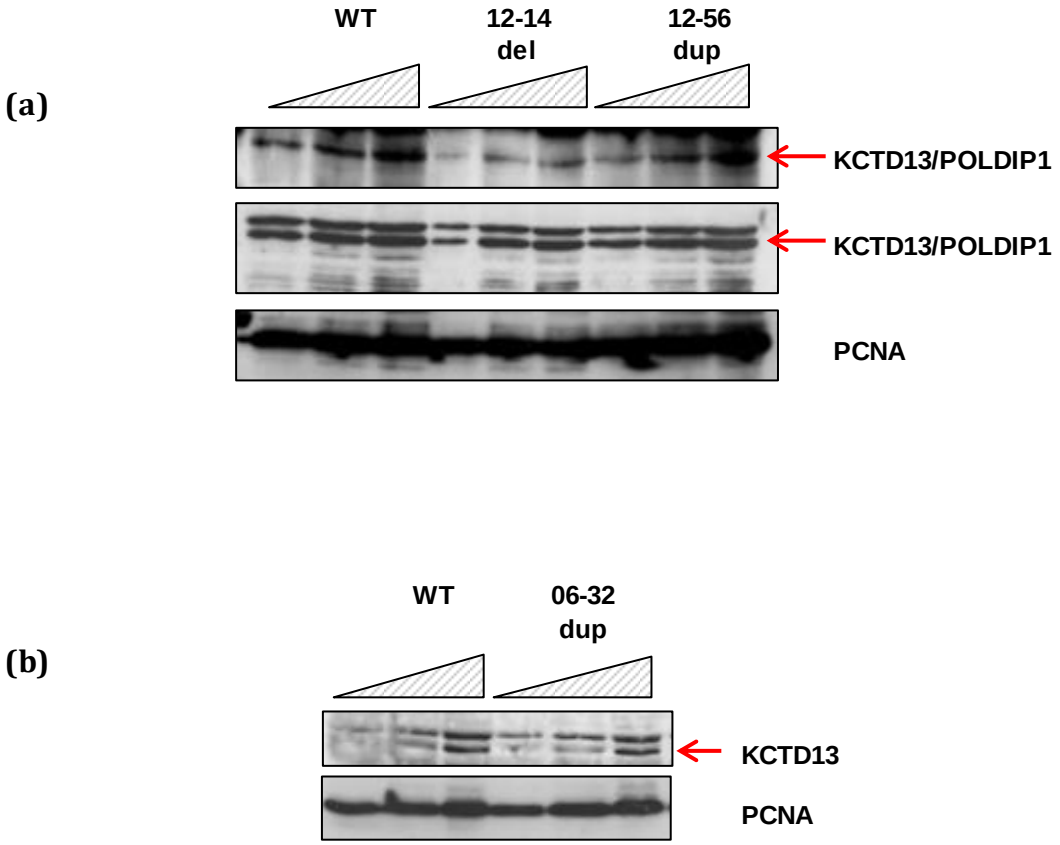

Figure 5.6 – KCTD13 protein expression is reduced consistent with 16p11.2 deletion but remains unaffected by 16p11.2 duplication in patient-derived LBLs, del; 16p11.2 deletion, dup; 16p11.2 duplication**. (a)** 50µg of urea-based whole cell extract for WT, 12-14 (16p11.2 deletion) and 12-56 (16p11.2 duplication) were subjected to SDS-PAGE and immunoblotted for KCTD13 protein expression using two different antibodies. LBLs from a patient harbouring a 16p11.2 deletion (12-14) displayed reduced KCTD13 protein expression levels consistent with the hemizygous deletion. However, LBLs from a patient harbouring 16p11.2 duplication (12-56) exhibit no increase in KCTD13 protein expression levels. **(b)** 50µg of urea-based whole cell extract for WT and 06-32 (16p11.2 duplication) were subjected to SDS-PAGE and immunoblotted for KCTD13 protein expression. LBLs from this patient exhibited no increase in KCTD13 protein expression levels, similar to the findings observed in the 12-56 duplication line displayed in (a) lanes 7-9.

5.2.3: 16p11.2 CNV LBLs display normal S-phase progression

Patients with 16p11.2 duplications present with *relative* or *absolute* microcephaly whereas those with 16p11.2 deletions present with macrocephaly. As discussed previously in section 5.1.3, impaired DNA replication has recently been postulated as a mechanism underlying the microcephalic phenotype and vice versa for macrocephaly. The 16p11.2 region contains many genes which encode proteins with known roles in DNA replication such as *BOLA2*, *KIF22*, *PPP4C*, *INO80* and *KCTD13*. This suggests that copy number change of these genes may impact upon DNA replication and potentially underlie the head size phenotypes of 16p11.2 CNV patients.

To determine whether delayed S-phase progression was a feature of unmanipulated, asynchronously growing 16p11.2 CNV patient-derived LBLs, I employed a bromodeoxyuridine (BrdU) pulse-chase approach in the presence of a colcemid trap. The colcemid trap ensures that these cells do not proceed past G2-M. BrdU is incorporated into newly synthesised DNA strands of actively proliferating cells. Following partial denaturation of the dsDNA, BrdU is detected immunochemically allowing the assessment of the population of cells, which are actively synthesising DNA. Progression through S-phase is indicated by movement of the BrdU-labelled population towards a 4N DNA content using two-dimensional flow cytometry. To monitor the speed of S-phase progression, I quantified the rate of loss of early S-phase cells (2N content, shown in red in Figure 5.7). Interestingly, both the 12-32 duplication line and 12-14 deletion line exhibited a modest delay in S-phase progression at 2 hours compared to WT; 80-90% of early S-phase cells remained compared with only 50% in WT controls (Figure 5.8). However, this difference was negligible at 6 hours indicating that all 16p11.2 CNV lines were efficient in progressing through S-phase and thus the significance of the observed 2 hour delay in two of the lines is not fully understood. Collectively, this data indicates that delayed S-phase transition is not a marked feature of 16p11.2 patient-derived LBLs.

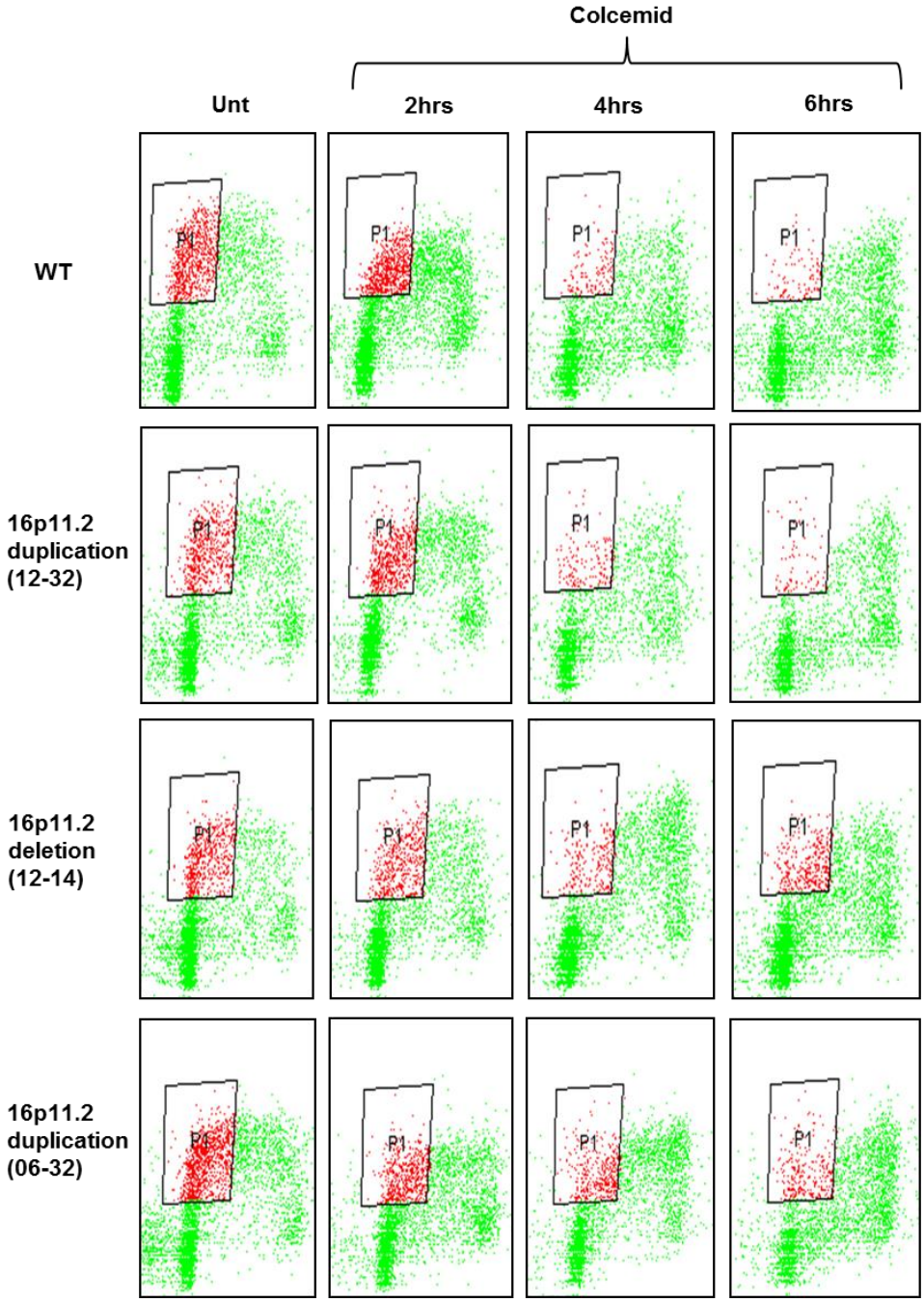

Figure 5.7 – 16p11.2 CNV cells exhibit normal S-phase progression compared to WT controls. Logarithmically growing WT and 16p11.2 CNV LBLs were pulse labelled with 20μM BrdU for 30 minutes. Colcemid was added to stop cells from cycling and BrdU incorporation was monitored every 2 hours for up to 6 hours. Cells were fixed in ice-cold ethanol and stored at -20°C overnight. Samples were prepared for FACS analysis the following day as described in the material and methods section. The p1 box indicates those cells with 2N DNA content (shown in red).

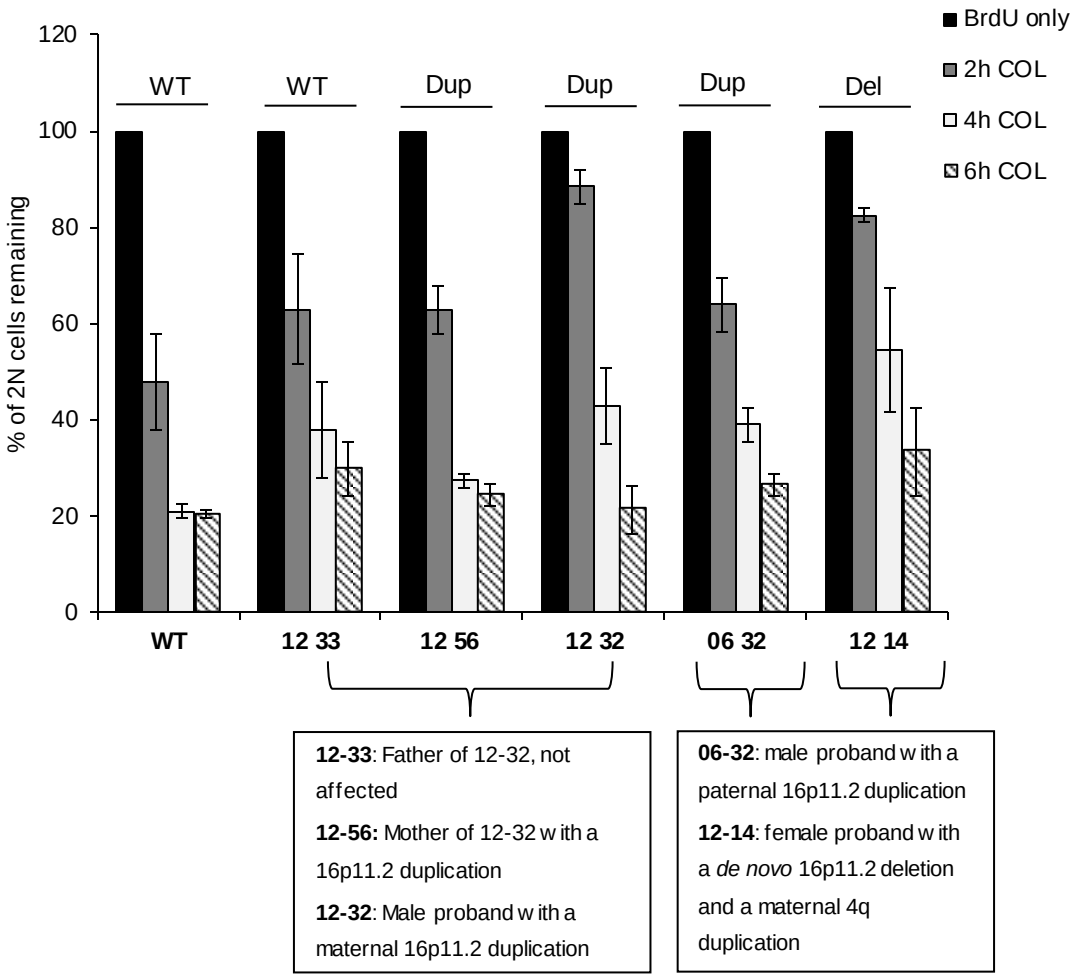

Figure 5.8 – 16p11.2 CNV (deleted and duplicated) exhibit normal S-phase progression compared to WT controls. Logarithmically growing WT and 16p11.2 CNV LBLs were pulse labelled with 20µM BrdU for 30 minutes. Colcemid was added to stop cells from cycling and BrdU incorporation was monitored every 2 hours for up to 6 hours. Cells were fixed in ice-cold ethanol and stored at -20°C overnight. Samples were prepared for FACS analysis the following day as described in the material and methods section. A representative histogram of the data shown in figure 5.6 is shown above; each bar represents the % of cells with 2N content remaining as shown in the p1 boxes depicted in figure 5.6 for each cell line. Data represents the mean of 3 independent experiments ± SD. The boxes underneath the graph indicate which cell lines represent *de novo* or inherited deletions/duplication and those lines which are derived from multiple family members. COL; Colcemid.

5.2.4: 16p11.2 CNV LBLs show altered sensitivity to replication arrest following HU treatment.

Although 16p11.2 duplicated/deleted patient-derived LBLs did not display any impairment in endogenous S-phase progression, I established whether these cells were selectively sensitive to HU-induced replication stalling in S-phase. HU is an inhibitor of ribonucleotide reductase (RR), responsible for the reduction of ribonucleotides to deoxyribonucleotides, and increasing the pools of dNTPs during the G1 and S phases of the cell cycle necessary for normal DNA replication. Upon treatment with HU, the cells limited supply of dNTP rapidly decreases, leading to stalled replication forks, often associated with some degree of DNA breaks.

WT and 16p11.2 CNV patient-derived LBLs were exposed to a low dose of HU and the replication rate was assessed by analysing the number of BrdU-incorporating cells by flow cytometry. HU treatments resulted in arrest of DNA replication in both WT and all five 16p11.2 CNV LBLs; however the rate of replication arrest exhibited subtle differences. Under these conditions, treatment with HU resulted in a less marked inhibition of DNA replication at 2 hours in two of the 16p11.2 CNV lines; 12-14 (deletion) and 06-32 (duplication) compared with wild-type controls and three other 16p11.2 CNV patient-derived cell lines (Figures 5.9 and 5.10). However, this difference was negligible at 6 hours post-treatment and resumption of the induced replication arrest appeared similar between WT and four of the 16p11.2 CNV patient-derived cell lines. Interestingly, the 12-32 16p11.2 duplicated line appeared to be extremely sensitive to replication arrest induced by HU treatment and failed to resume DNA replication efficiency following a 6 hour treatment with HU (Figures 5.9 and 5.10). The basis of this dramatic effect uncovered here is unclear, specifically since this was in contrast to the other two duplication lines; 06-32 and 12-56 suggesting that it is not a consistent feature associated with duplication of the 16p11.2 region. This may be consistent with an additional, as yet, unidentified genomic alteration contributing to this distinct cellular phenotype.

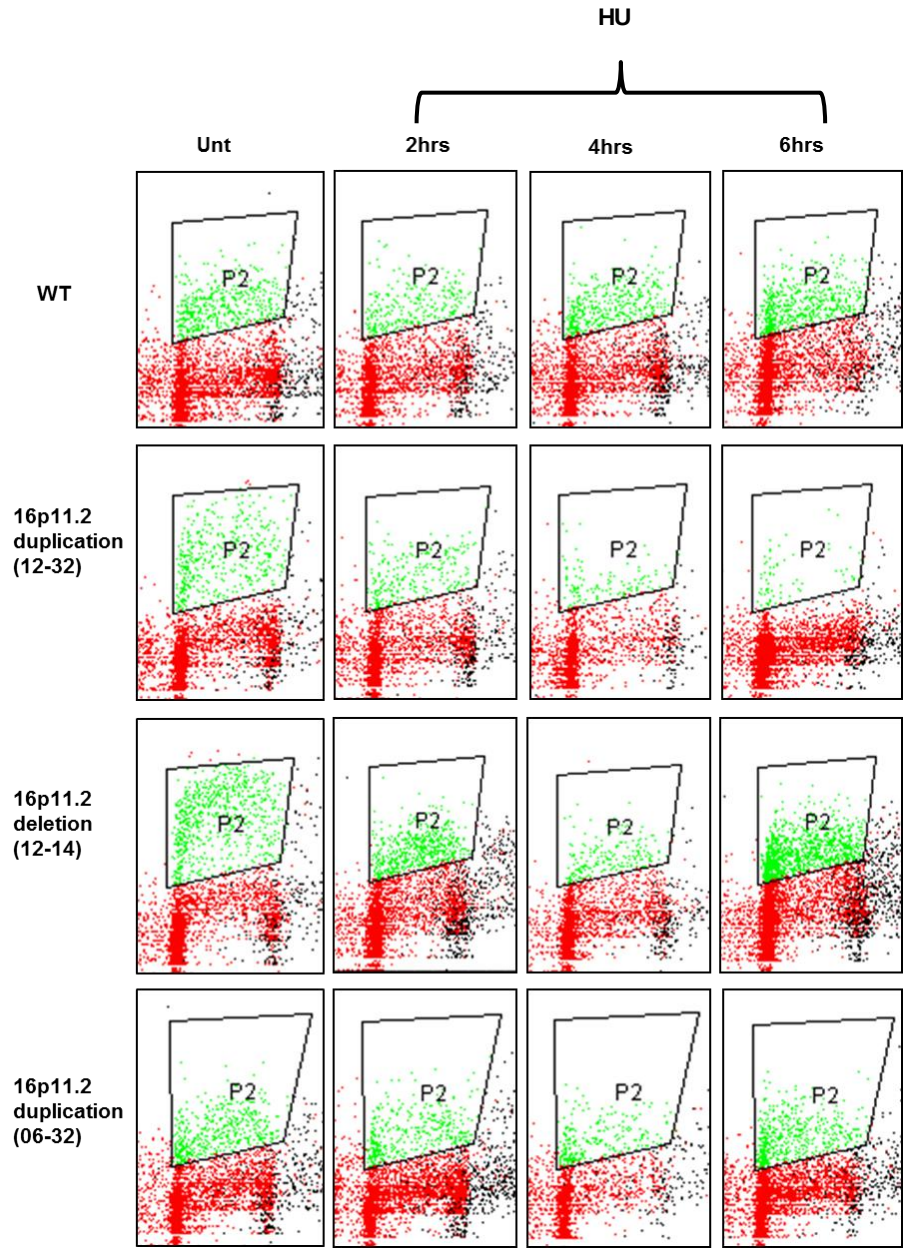

Figure 5.9 – 16p11.2 CNV syndrome patient-derived LBLs show differing sensitivities to replication arrest following treatment with a low dose of HU. LBLs from wild-type (WT) and 16p11.2 deletion/duplication syndrome were treated with 250μM HU and pulse labelled with BrdU 30 minutes prior to the end of each time point. Cells were then fixed in ice-cold ethanol and left overnight at -20°C. Cells were prepared for FACS analysis as stated in the materials and methods. Representative flow cytometry profiles are shown above with BrdU labelled cells shown in green (P2 box). Under these conditions, treatment with HU results in a greater inhibition of DNA replication at each time points in the 12-32 16p11.2 duplicated line compared to WT controls indicating the inability of this line to recover from these replication stalling condition. HU, hydroxyurea; P2 box indicates cells which are BrdU positive.

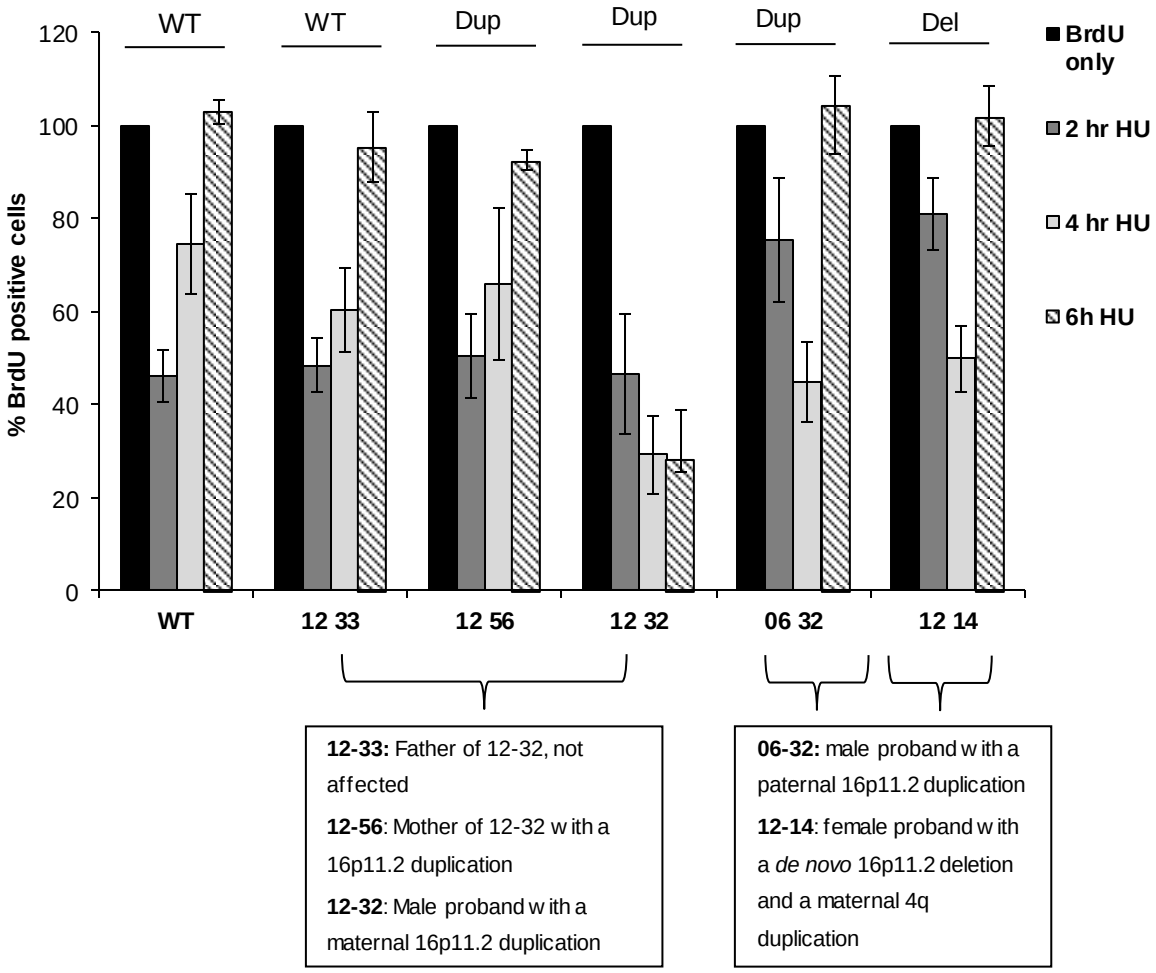

Figure 5.10 – 16p11.2 CNV syndrome patient-derived LBLs show differing sensitivities to replication arrest following treatment with a low dose of HU. Representative histogram of Figure 5.8 indicating the % of BrdU positive cells (events within the p2 gate shown in Figure 5.8) following a 0-6 hour treatment with HU. LBLs from wild-type (WT) and 16p11.2 deletion/duplication syndrome were treated with 250μM HU and pulse labelled with BrdU 30 minutes prior to the end of each time point. Samples were fixed in ice-cold ethanol, left overnight at -20°C and then prepared for FACS analysis the following day, as stated in materials and methods. A representative histogram of the data shown in figure 5.8 is shown above; each bar represents the % of BrdU positive cells as shown in the p2 boxes of figure 5.8 for each cell line. Data represents the mean of 3 independent experiments ± SD. The boxes underneath the graph indicate which cell lines represent de novo or inherited deletions/duplication and those lines which are derived from multiple family members.

5.2.5: 16p11.2 CNV LBLs exhibit normal DNA damage response activity

There are various endogenous and environmental insults which cause DNA damage including ROS, stalled replication forks, UV and ionising radiation (IR). The DNA damage response (DDR) represents a signal transduction network integrating multiple pathways including checkpoint activation, transcriptional regulation, DNA repair pathways and apoptosis to protect the cell from damage. The DDR is primarily mediated by proteins of the PIKKs family; ATM (Ataxia-Telangiectasia Mutated) and ATR (ATM and Rad3-related) (Jackson & Bartek, 2009). Although, ATM and ATR appear to phosphorylate many of the same targets, they are generally activated in response to distinct types of DNA damage; ATM is the primary mediator in the response to DSBs whereas ATR is activated following recruitment to RPA-coated ssDNA regions generated at stalled replication forks and DSBs (Shiotani & Zou, 2009).

In the canonical DDR pathway, DNA lesions are recognised by multiprotein "sensor" complexes which function to activate ATM/ATR. Once activated, ATM/ATR phosphorylates a large number of target substrate proteins in order to regulate various downstream pathways including DNA repair, checkpoint activation, and cell death. Activation of the DNA damage checkpoint is mediated by two checkpoint kinases; Chk1 and Chk2 (Smith et al, 2010). These kinases are phosphorylated and activated by ATR and ATM respectively and in turn phosphorylate important regulators such as Cdc25 and p53 to control cell cycle progression at the G1-S, intra-S and G2-M cell cycle checkpoints. The cell cycle is driven by the activities of the cyclin-dependent kinases (Cdk) which control the transitions from G1 into S phase and G2 into M phase. The phosphatase Cdc25 functions as an essential activator of Cdk's by dephosphorylating them at inhibitory sites. Therefore, phosphorylation of Cdc25 following DNA damage inactivates Cdk-cyclin complexes which acts to slow down or arrest cell-cycle progression allowing more time for DNA repair before mitosis proceeds (Mailand et al, 2000). Along with their pivotal roles in cell cycle checkpoints, Chk1 and Chk2

are also involved in other aspects of the DDR including DNA repair, induction of apoptosis and chromatin modelling.

Cellular stressors such as osmotic stress induce cell cycle arrest via activation of p38 MAP kinase (MAPK). Furthermore, p38 also regulates cell-cycle checkpoints in response to DNA damage through its ability to activate MAPKAP Kinase-2 (MK2) which functions to phosphorylate and inactivate cdc25 phosphatases, preventing cell cycle progression (Chen et al, 2003; Manke et al, 2005). Thousand and one amino acid (TAO) kinases are serine/threonine protein kinases known to regulate p38 via their ability to phosphorylate and activate the MAPK kinases, MEK3 and 6 (Chen et al, 2003). Moreover, TAO kinases have also been shown to act as important regulators of the response to genotoxic stress. Raman and co-workers reported that TAO kinases are activated acutely by ionizing radiation, ultraviolet radiation and hydroxyurea (Raman et al, 2007). Furthermore, their findings revealed that TAOs are a primary component linking the DNA damage response induced by genotoxic insults through ATM/ATR to p38. Damage-induced p38 activation was blocked by catalytically deficient TAOs or TAO siRNA (Raman et al, 2007). Furthermore, siRNA-mediated knockdown of TAOs impaired the DNA damage activated G2-M cell cycle checkpoint indicating that TAO kinases are required for activation of p38 and the G2-M checkpoint upon DNA damage. Figure 5.11 depicts the model proposed by Raman *et al* to explain the function of TAO kinases in the DDR.

As previously mentioned, microcephaly is a common feature of many DDR-defective disorders suggesting a fundamental role for the DDR in neuronal development (Table 5.2). Interestingly, one of the genes residing within the affected 16p11.2 region encodes the TAO kinase 2 (TAOK2) protein. Therefore, in light of the strong evidence presented by Raman *et al* indicating a fundamental role for TAO kinases in the response to DNA damage, I sought to investigate the impact of 16p11.2 deletion/duplication on the DDR. I have already described in section 5.2.1 that CNV of 16p11.2 does impact upon TAOK2 expression (Fig 5.4) To determine whether CNV of the 16p11.2 region impacted upon the ATR/ATM-dependent DDR, I examined UV- and IR-induced G2-M checkpoint arrest in patient-derived LBLs. The response to UV is specifically dependent on ATR whereas the

response to DSBs induced by IR is dependent on ATM. 16p11.2 deletion and duplication LBLs (LBL 09-22 and LBL 06-32) arrested as efficiently as control cells, evident by a decreased mitotic index under both conditions (Fig 5.12a). ATR-Seckel LBLs were used as a control for this experiment and, as expected, exhibited defective UV-induced G2/M checkpoint arrest (Fig 5.12a). This data indicates that copy number variation of the 16p11.2 region does not impact upon ATR/ATM-dependent G2/M checkpoint activation. I also investigated the impact of 16p11.2 CNV on the ATR-dependent phosphorylation of Chk1 in response to HU-induced replication stress. WT and 16p11.2 CNV (LBL 12-32, LBL 12-33 and LBL 12-14) patient-derived cell lines were treated with 500μM hydroxyurea (HU) for 2 hours. 50μg of urea-based whole cell extracts were then subjected to SDS-PAGE and immunoblotted for phospho-Chk1 protein expression levels. Chk1 phosphorylation was observed in all treated cell lines suggesting that 16p11.2 CNV (deletion and duplication) were not impaired in ATR-dependent Chk1 phosphorylation (Fig 5.12b). Interestingly, Chk1 phosphorylation did appear to be subtly reduced in the 16p11.2 duplicated cell line (LBL 12-32) compared with control cells and two other 16p11.2 CNV lines, however the physiological significance of this is not clear (Fig 5.12b lanes 3 and 4).

5.2.6: Summary

Here, I have shown that the expression of two proteins (TAOK2 and MAPK3) encoded by genes residing in the 16p11.2 region are increased/decreased consistent with deletion or duplication in patient-derived LBLs. Interestingly, the protein expression of KCTD13, also encoded by a gene within the 16p11.2 region, is reduced in patient-derived LBLs harbouring a hemizygous 16p11.2 deletion but its expression remains unaltered in those harbouring 16p11.2 duplications. All 16p11.2 CNV patient-derived cell lines are efficient in progressing through S-phase, however one 16p11.2 duplicated cell line (LBL 12-32) exhibits sensitivity to HU-induced replication stress in S-phase, the relevance of which remains unclear. I also present evidence to indicate that activation of the DDR appears to be normal in 16p11.2 patient derived-cell lines (deletion and duplication).

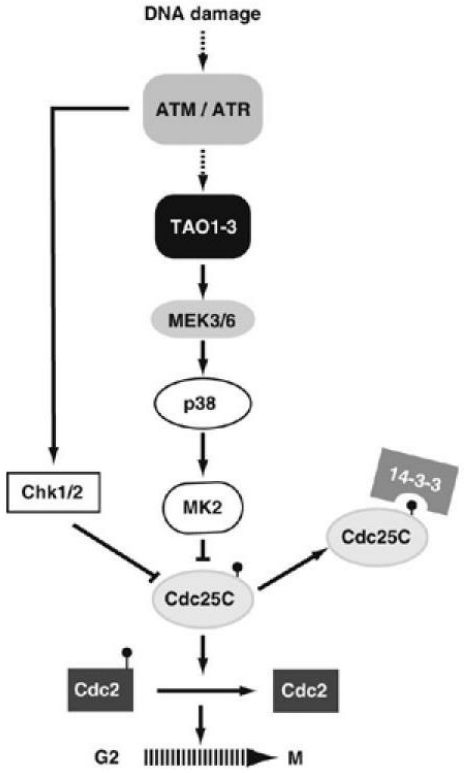

Figure 5.11 – TAO kinases are required for activation of p38 and the G_2M checkpoint in response to DNA damage, as proposed by Raman *et al*, 2007. In the canonical ATR/ATM-dependent model of G_2M checkpoint activation (left hand pathway), DNA damage is sensed by mutiprotein sensor complexes which lead to activation of ATM/ATR. ATM functions primarily in response to DSBs whereas ATR is activated in response to single stranded DNA. Once activated, ATM/ATR relay two parallel cascades that ultimately serve to inactivate Cyclin B-cdc2 complexes. The first cascade shown on the left involves the phosphorylation and inactivation of Cdc25 by Chk1/2 which prevents the activation of cdc2 (also termed cdk1). The slower second parallel pathway shown on the right involves the binding of 14-3-3 to the phosphorylated Cyclin B-cdc2 complex resulting in its export from the nucleus. This occurs through activation of a p53-dependent pathway (not shown). In the TAO kinase-dependent pathway of G_2M checkpoint activation postulated by Raman *et al,* ATM/ATR activate TAO kinases 1-3 which lead to the phosphorylation and activation of MEK3/6 (shown in the middle). Through a downstream cascade involving p38 and MK2, Cdc25C is inactivated leading to persistent phosphorylation of the Cyclin B-cdc2 complex and thus prevents cell cycle progression. ATM, Ataxia-Telangectasia Mutated; ATR, Ataxia Telangectasia and Rad 3-related; Chk1/2, Checkpoint kinase 1/2; TAO1-3, Thousand and one amino acid kinase 1-3; MEK3/6, Mitogen-activated protein kinase kinase 3/6; p38, p38 mitogen-activated protein kinases; MK2, MAPK-activated protein kinase 2; Cdc25, M-phase inducer phosphatase 3; Cdc2, cyclin-dependent kinase-1.

(a)

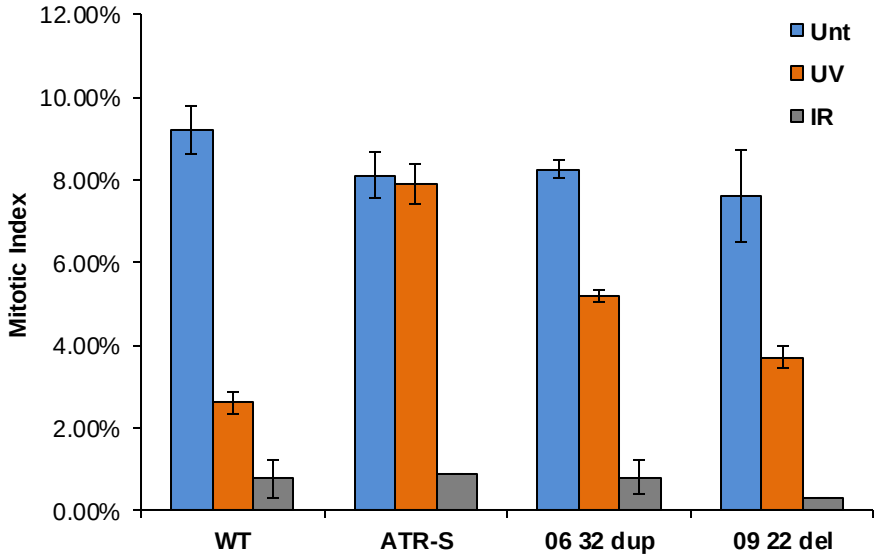

(b)

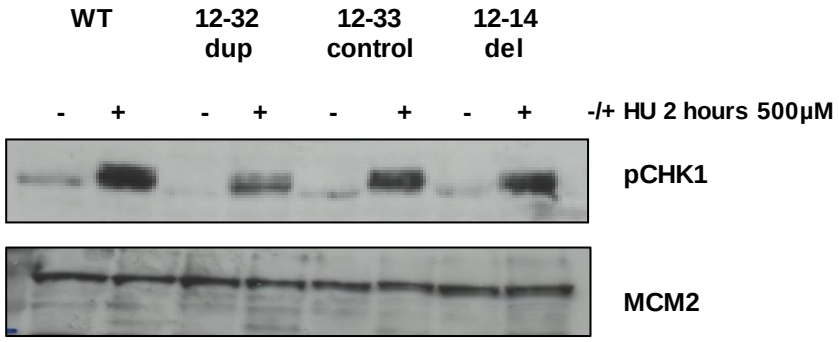

Figure 5.12 – G2M checkpoint arrest is activated in response to UV and IR-induced damage in 16p11.2 CNV LBLs (del; 16p11.2 deletion, dup; 16p11.2 duplication). **(a)** Wild type (WT), 16p11.2 CNV and ATR-Seckel (ATR-S) cells were untreated, irradiated with 7 J m^{-2} UV (UV) or treated with 3 gray IR (IR), incubated for 4 hours in the presence of 0.2µg/ml colcemid and the percentage of mitotic cells counted using the E400 microscope, 100X lens. The results shown represent the mean ±SD of three independent experiments. LBL 06-32; 16p11.2 duplication, LBL 09-22; 16p11.2 deletion, ATR-S; ATR-Seckel LBLs. Work was carried out in associated with Gillian Carpenter. **(b)** Chk1 phosphorylation in response to HU-induced DNA damage is normal in 16p11.2 CNV patient-derived LBLs. WT and 16p11.2 CNV LBLs were treated with 500µM HU for 2 hours. 50µg urea-based whole cell extracts were then subjected to SDS-PAGE and immunoblotted for pChk1 protein expression. The blot was reprobed for MCM2 protein expression as a loading control. LBL 12-32 dup; 16p11.2 duplication, LBL 12-33 control; unaffected father of 12-32, LBL 12-14 del; 16p11.2 deletion.

5.3: Discussion

16p11.2 CNV genomic disorder is associated with a range of neurocognitive deficits including autism, epilepsy and schizophrenia. Intensive phenotypic analyses of patients with 16p11.2 deletions or duplications has revealed incomplete penetrance and variable expressivity of clinical features in patients (Shinawi et al, 2010). However, these analyses have also uncovered strong mirroring phenotypes; the 16p11.2 deletion is associated with macrocephaly whereas the reciprocal duplication is associated with microcephaly.

One gene residing within the 16p11.2 region is *KCTD13*, which has been reported to interact with PCNA and Pol δ (He et al, 2001). This interaction suggests that KCTD13 may play a role in the regulation of DNA replication, defects within which has been shown to impact upon neurogenesis (Kerzendorfer et al, 2013). Consistent with this, Golzio and colleagues recently provided evidence to suggest that *KCTD13* copy number change is causative of the mirroring head size phenotypes of 16p11.2 CNV patients through the regulation of early neurogenesis (Golzio et al, 2012). I examined the impact of 16p11.2 CNV on the protein expression of three genes; *TAO2K*, *MAPK3* and *KCTD13* and revealed unexpected results. The protein expression levels of two genes, *TAOK2* and *MAPK3*, corresponded with the copy number change; protein expression was increased in cell lines from duplication patients and decreased in cells from those patients harbouring a 16p11.2 deletions. However, expression of KCTD13 did not change according to copy number of the *KCTD13* gene whereby expression remained unchanged in cell lines from patients with a 16p11.2 duplication. It is possible that this inconsistency may have arisen due to non-specificity of the KCTD13 antibodies or alternatively, it may reflect the limitations of using patient-derived lymphoblastoid cell lines.

Impaired DNA replication is a fundamental mechanism frequently reported to underlie microcephaly (Kerzendorfer et al, 2013). Many of the genes within the 16p11.2 region encode proteins whose products contribute to both DNA replication and repair. These include; *BOLA2*, *KIF22*, *PPP4C* and *KCTD13*.

Therefore, it is conceivable to suggest that copy number change of these genes may impact on replication/repair and potentially contribute to the macro/microcephalic phenotypes of 16p11.2 deletion/duplication patients respectively. However, I have observed generally normal rates of S-phase transit in 16p11.2 CNV LBLs compared to WT controls. Furthermore, four of the five 16p11.2 CNV cell lines do not exhibit increased sensitivity to HU-induced replication arrest. This is similar to what has been observed in ORC1-mutated Meier-Gorlin Syndrome (Kerzendorfer et al, 2013). These findings indicate that copy number variation of the 16p11.2 region is not associated with a generalized aberrant DNA replication, at least as detectable using patient-derived LBLs. Moreover, the microcephaly seen in 16p duplication patients is therefore not a consequence of impaired DNA replication. It is interesting to note that one of the 16p11.2 duplicated cell lines (12-32) did show increased sensitivity to HU-induced replication stress; however this was in contrast to two other 16p11.2 duplicated lines suggesting that it is not a consistent feature associated with 16p11.2 duplication. The basis of this observation is unclear but may suggest that this patient in particular may harbour additional genomic alterations including mutations which may underlie this specific cellular phenotype and highlights the need for further molecular analysis to clarify this. High density whole genome aCGH combined with whole exome sequencing is actively being pursued in this instance. For example, the CNV could have additional consequences of recessive variant expression (Chapter 1 section 1.3.1 and Fig 1.3).

Defects in the DDR pathway have also frequently been reported as a mechanism underlying microcephaly in certain genomic disorders such as LIG4 and XLF-mutated SCID. Here, the genomic defect manifests as a functional defect in the DDR. Interestingly, microcephaly is observed in patients with a 16p11.2 *duplication* which is suggestive of a potential dominant negative effect. The 16p11.2 region harbours genes whose products contribute to DNA repair including the *TAO2K* gene. TAO2K has been shown to be involved in the DDR through the p38 MAPK pathway and thus a change in copy number of this gene may be predicted to impact upon the DDR. I observed normal G2/M checkpoint arrest in 16p11.2 CNV LBLs compared to WT controls indicating that activation of both the

ATM- and ATR-dependent DDR is normal. Furthermore, ATR-dependent DNA damage signalling appeared normal in 16p11.2 CNV LBLs compared to WT controls; as shown by an increase in Chk1 phosphorylation in response to HU treatment. Collectively, this data indicates that neither impaired replication nor defective DDR signalling are overtly consistent features associated with 16p11.2 CNV.

In summary, the data I have presented here is in contrast to the report by Golzio et al derived from zebrafish models suggesting that *KCTD13* copy number is the major determinant of head size in 16p11.2 CNV patients. Here, I have found that KCTD13 protein expression does not segregate with the micro/macrocephaly phenotype of 16p11.2 CNVs indicating that increased or decreased dosage of this gene is not the sole cause of the opposing head size phenotypes, as had been previously suggested. Additionally, cells from patients with a 16p11.2 deletion or reciprocal duplication do not exhibit a functional cell cycle or DNA repair defect that I can attribute to genes within the CNV region. This indicates that defective DNA replication and/or repair does not underlie the opposing head size phenotypes observed in these patients. It is conceivable to speculate that the consequences of 16p11.2 CNV are fixed during embryogenesis and thus are not observed postnatally; a process termed 'intrauterine programming' (Murga et al, 2009). If this is the case, it poses the question as to whether LBLs are an appropriate model for studying the functional consequences of 16p11.2 CNV, specifically *KCTD13* copy number change. To address this issue, future work should be centred upon investigating the functional consequences of *KCTD13* overexpression alone upon cell replication via ectopic/regulated over-expression systems, particularly in a mammalian neuronal cell model such as N2A or SH-5Y5Y cells. Mutations in genes encoding chromatin remodelling proteins have been also implicated in the pathogenesis of microcephaly (Kerzendorfer et al, 2013). Interestingly, the 16p11.2 region harbours the *INO80E* gene which encodes a subunit of the INO80 chromatin modelling complex. It would be very interesting to investigate the functional consequences of *INO80E* copy number change in the context of micro/macrocephaly. Crucially, this data indicates that much more

intensive investigation is essential to fully understand the functional consequences of 16p11.2 CNV and their relevance to micro/macrocephaly.

Chapter Six

Genotype to Phenotype relationships in Wolf Hirchhorn Syndrome (WHS): a novel impact of CNV of *LETM1*

6.1: Introduction

Wolf Hirschhorn Syndrome (WHS) (OMIM 194190) was first identified independently by Wolf *et al* and by Hirschhorn *et al* in 1965. (Hirschhorn et al, 1965; Wolf et al, 1965). WHS is caused by a small hemizygous sub-telomeric deletion of the short arm of chromosome 4 typically involving two critical regions (Figures 6.1 – 6.3). The first described WHS patients had large 4p deletions all associated with a severe phenotype, however an increasing number of smaller 4p16.3 deletions have been identified in recent years due to advances in techniques for molecular karyotyping.

WHS occurs in approximately one in 50,000 births and WHS patients can be categorized as 'typical' or 'atypical' according to the clinical features and deletion size they present with (Battaglia et al, 2008). Typical (also termed "classical) WHS patients exhibit growth delay, craniofacial dysmorphism, microcephaly, developmental delay, epilepsy and heart defects. The craniofacial features of typical WHS were originally referred to as 'Greek helmet face'; a combination of microcephaly, prominent glabella, broad forehead, hypertelorism, broad nasal bridge, short philtrum, micrognathia and down-turned corners of the mouth. Cleft lip/palate is occasionally present, as is coloboma of the eye (Battaglia et al, 2008). Typical WHS patients have deletions encompassing many genes within the two defined critical regions and deletions measure on average 5-18Mb. In contrast, atypical WHS patients usually harbor smaller deletions not exceeding 3.5Mb, some of which lie outside of the critical regions. Atypical WHS patients present with milder clinical features, however major malformations are uncommon and patients do not usually present with seizures (Fig 6.1d).

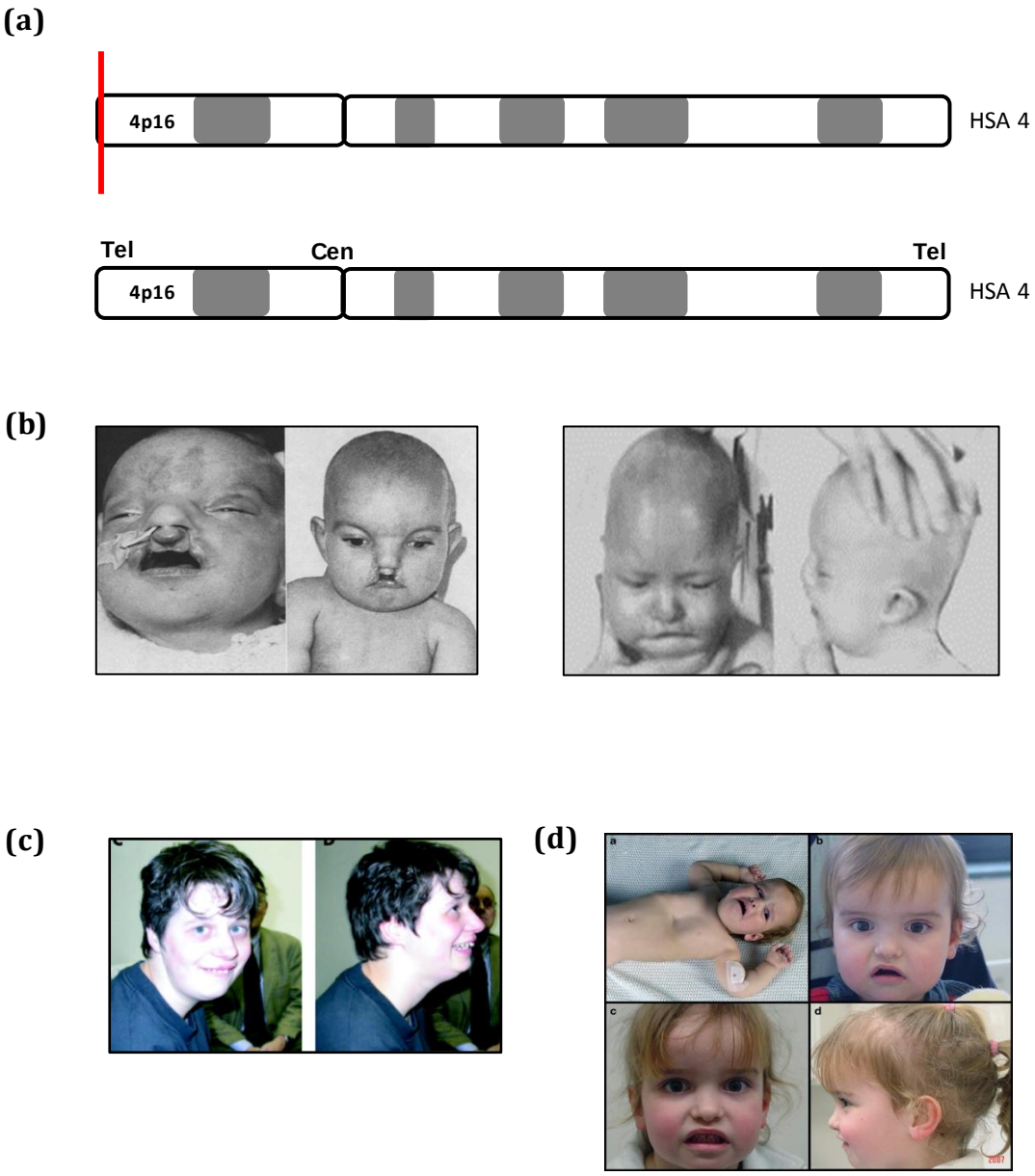

Figure 6.1: Wolf Hirschhorn Syndrome. **(a)** Chromosome 4 pair indicating location (red line) of the subtelomeric deletions causative of WHS. **(b)** Pictures of the first WHS patients identified by Wolf (1965) (left two panels) and Hirschhorn (1965) (right two panels). **(c)** Typical WHS patient with a 3.85Mb deletion identified by Maas et al (2008). **(d)** Atypical WHS patient identified by Engbers et al (2007) whose 1.6Mb deletion lies outside the demarcated critical regions. The patient presents with mild-WHS like facial features such as down-turned corners of the mouth. tel; telomere, cen; centromere.

6.1.1: The WHS critical regions

WHS is a contiguous gene deletion disorder as it arises from the deletion of multiple genes located adjacent to one another on the same chromosome (See table 6.1 and Fig 5.2). A minimal region of overlap between WHS-like patients led to the demarcation of the 'Wolf-Hirschhorn Critical Region 1' (WHSCR-1). This region is limited to a 165kb interval ~2 Mb from the telomere defined by the loci D4S166 and D4S3327 (Wright et al, 1997). The WHSCR-1 encompasses the *WHSC2* gene and the 3' portion of the *WHSC1* gene (Figure 6.3 green section). However, reports of patients harboring deletions distal to the WHSCR1 presenting with a 'typical' WHS facial appearance led to the demarcation of a second critical region termed 'WHSCR-2' (Zollino et al, 2003). This re-defined critical region lies within an interval of 300-600kb between loci DS43327 and D4S98-D4S168 (Zollino et al, 2003). This region includes *LETM1,* the 5' portion of the *WHSC1* gene but does not involve *WHSC2* (Fig 6.3 pink section). The identification of these two critical regions in WHS has strongly implicated the haploinsufficiency of *WHSC1* as a key contributor to core WHS-phenotypes.

6.1.1.1: WHSC1

The *WHSC1* gene, also known as *NSD2* (Nuclear receptor SET domain containing) or *MMSET* (multiple myeloma SET domain containing) encodes a 136kDa protein that is ubiquitously expressed in early development and contains four domains; a PWWP domain, a HMG box, a SET domain and a PHD-type zinc finger (Stec et al, 1998). Recently, WHSC1 was identified as a putative histone methyltransferase involved in the trimethylation of histone 3 lysine 36 (H3K36) (Kim et al, 2008a; Marango et al, 2008). WHSC1 is also reported to be involved in the response to DNA damage through its activity on the H4K20 residue (Hajdu et al, 2011; Pei et al, 2011). In addition to WHS, *WHSC1* has been identified as a gene involved in the t (4:14) (p16:q32) translocation present in approximately 15-50% of multiple myelomas (Chesi et al, 1998; Keats et al, 2005; Kim et al, 2008a; Marango et al, 2008). WHSC1 has also been implicated in gliobastoma, neuroblastoma and urinary bladder and prostate cancers (Ezponda et al, 2012; Hudlebusch et al, 2011;

Li et al, 2008). Many WHS patients harbour deletions encompassing the *WHSC1* gene and its expression pattern, especially in the tissues affected in WHS, suggests that it is a prime candidate causing WHS phenotypes. However, other genes aside from *WHSC1* have been suggested as causative of specific features such as growth retardation and microcephaly (Maas et al, 2008; South et al, 2008).

6.1.1.2: WHSC2

The *WHSC2* gene, also known as *NELF-A,* encodes a component of the Negative ELongation Factor complex (Narita et al, 2007; Yung et al, 2009). The NELF is a four subunit protein complex which plays an important role in suppressing transcription elongation through promoter-proximal pausing of RNA Polymerase II during early stages of transcription. It has also been reported to play a role in the 3'-end processing of histone mRNAs and furthermore, siRNA knockdown of subunits of the NELF result in decreased overall transcription of histone genes (Sun & Li, 2010; Yung et al, 2009). *SLBP*, located telomeric to *WHSC2* is required for optimal histone biogenesis. Replication-dependent histone mRNAs terminate in a conserved stem-loop structure. SLBP is essential for the correct processing of these stem-loop-containing pre-mRNAs and therefore regulates the amount of histone synthesis during S-phase. Recently WHSC2 was found to be required for optimal recruitment of SLBP to the 3' end of histone pre-mRNA. Furthermore, recent work in the O'Driscoll lab reports novel cellular defects associated with WHS, including delayed S-phase progression, reduced DNA synthesis and impaired histone deposition (Kerzendorfer et al, 2012). They provide evidence that the most likely underlying defect is haploinsufficiency of *SLBP* and/or *NELF-A* thus providing insight into the functional consequences of haploinsufficiency of specific genes on 4p16.3 associated with WHS (Kerzendorfer et al, 2012).

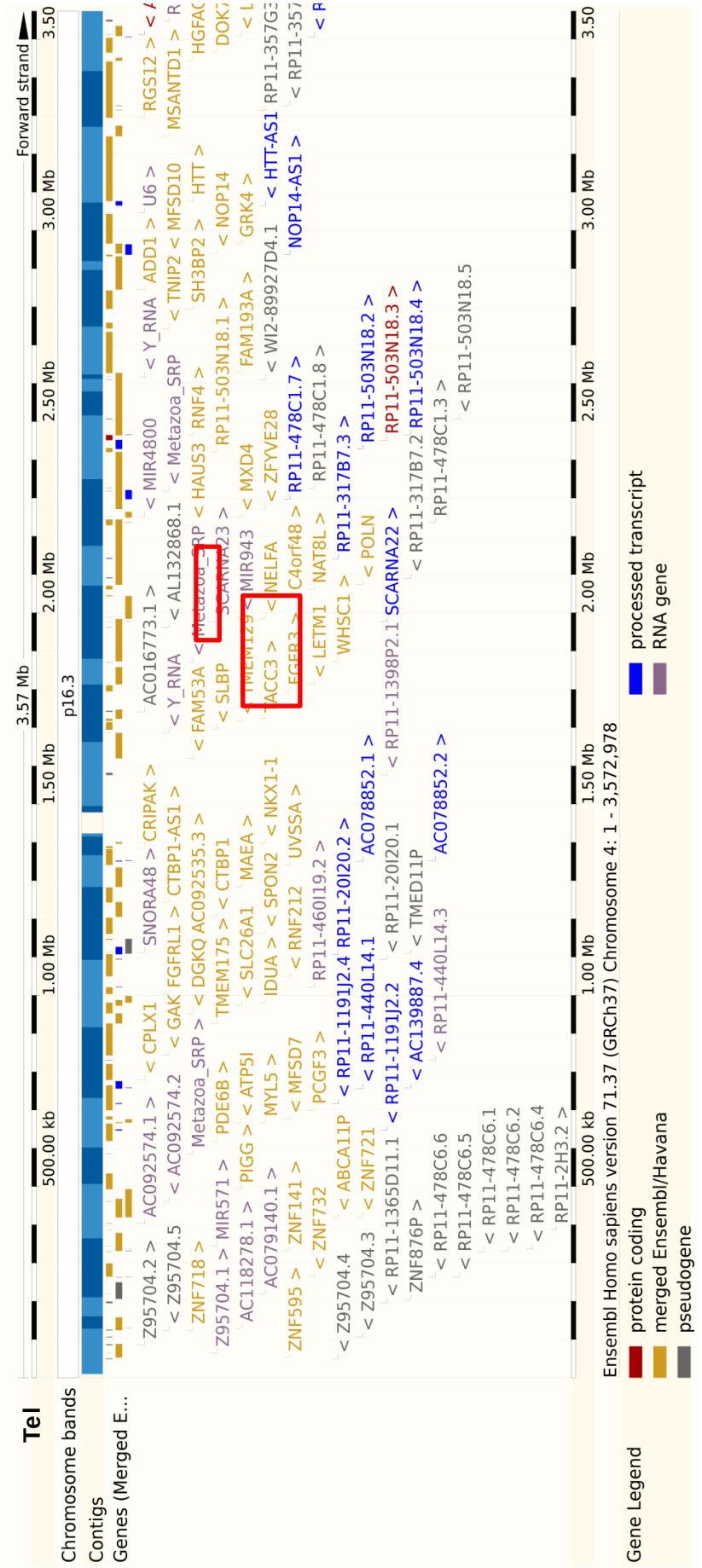

Figure 6.2 - A detailed representation of the 4p16.3 region implicated in WHS (Location 4:1-3,572,978; Ensembl; http://www.ensembl.org/index.html). This figure highlights the vast number of genes residing in this region. Those genes either specifically referred to in the text or of particular interest are highlighted in red; *WHSC1, WHSC2/NELFA* and *LETM1. Tel; telomere.*

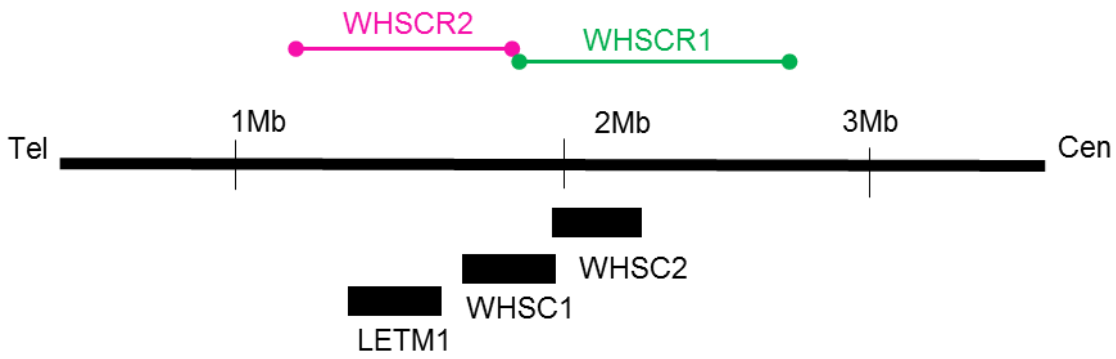

Figure 6.3 – A highly simplified representation of the two WHS critical regions and the genes encompassed by each (relative positioning is shown for simplification). The 165kb WHSCR1 lies ~2Mb from the telomere encompassing all of *WHSC2* and the 3' portion of *WHSC1* (green). The 300-600kb WHSCR2 encompasses the 5' portion of *WHSC1* and all of *LETM1* but specifically not *WHSC2* (pink). Tel: telomere, Cen: centromere.

6.1.1.3: Other genes within 4p16.3 contribute to key WHS features

Although the identification of the two critical regions strongly suggested that haploinsufficiency of the *WHSC1* gene is crucial for key WHS phenotypes, accumulating evidence indicates that haploinsufficiency of genes aside from *WHSC1* contribute to some of the core features such as microcephaly, characteristic facial appearance and growth retardation. Rauch et al reported one unique patient with a micro deletion of the entire WHSCR but minimal adjoining sequences, who presented with a mild WHS-like phenotype (Rauch et al, 2001). The male patient had mild MR and his facial characteristics were subtle suggesting that genes outside of this critical region contribute to some of the key WHS clinical features (Figure 6.5b). Furthermore, reports of a number of atypical patients whose deletions lie outside of both critical regions presenting with mild WHS-like features, again indicate that full-blown WHS is unlikely due to haploinsufficiency of the WHSCR alone (Engbers et al, 2008; South et al, 2007).

6.1.2: Animal models of WHS

Various mouse models carrying deletions of genes within the WHSCRs have been established which display phenotypes that are consistent with those of WHS patients. However, each model fails to recapitulate all aspects of the human phentoype and therefore the specific genes contributing to each phenotype still remain somewhat ill-defined. The region of the mouse genome that is orthologous to the human 4p16.3 is 5B1. Mouse models have been generated for 6 of the genes within the WHSCRs; *Fgfr3, Tacc3, Fam53A, Sax2*, *Maea* and *Ctbp*, four of which are discussed in further detail below (also shown in Table 6.1).

6.1.2.1: Fgfr3

Fibroblast growth factor receptor 3 is a tyrosine kinase receptor expressed in the developing bone, cochlea and spinal cord. Mice homozygous for conditional null mutations in *Fgfr3* exhibit severe kyphosis and long curved femurs. Subsequently

it was found that these phenotypes were secondary to bone dysplasia and prolonged endochondral bone growth (Colvin et al, 1996; Deng et al, 1996). *Fgfr3*-/- mice also display inner ear changes leading to profound deafness (Puligilla et al, 2007). In addition, fgfr3 has been shown to play important roles in neurological development and thus these studies indicate the hemizygosity of the human *FGFR3* gene may contirubute to skeletal and neurological aspects of WHS (Saarimaki-Vire et al, 2007). Furthermore, a small proportion of WHS patients exhibit sensorineural hearing loss and therefore mouse studies suggest that FGFR3 may contribute to this characteristic (Battaglia and Carey, 1999).

6.1.2.2: Tacc3 and Hspx153

Mouse models for the human *TACC3* and *HSPX153* genes both exhibit growth retardation. The Tacc3 protein has established roles in mitosis and transcriptional regulation and mice homozygous for null mutations of *Tacc3* are embryonically lethal (Piekorz et al, 2002). Furthermore, mice homozygous for a hypermorphic allele die immediately after birth showing signs of intrauterine growth retardation and skeletal abnormalities (Yao et al, 2007). In the case of *HSPX153*, which encodes a homeobox transcription factor of the Nxk1 family, mouse models (*Sax2* null) exhibit growth retardation post birth and subsequently die within 3 weeks (Simon & Lufkin, 2003). This is in contrast to the GR exhibited by WHS as the GR in mouse models is only evident post birth. Studies have further suggested that Sax2 is required for the maintenance of energy homeostasis and that the GR exhibited in these null mice is a consequence of energy homeostasis imbalance, something which has not been reported for the GR of WHS patients (Simon & Lufkin, 2003; Simon et al, 2007).

6.1.2.3: Ctbp1

CTBP1 is a well characterized transcriptional co-repressor. *Ctbp* null mice exhibit growth retardation at birth and also show evidence of abnormal skeletogenesis (Hildebrand & Soriano, 2002). WHS frequently experience profound epileptic seizures and it is known that certain forms of epilepsy can be managed by a

ketogenic diet (Cross, 2013). Recent work has suggested that this management is achieved through stimulating Ctbp activity and subsequently repressing the expression of BDNF (Garriga-Canut et al, 2006). BDNF is suspected to be an epileptogenic signaling molecule; therefore *CTBP1* hemizygosity in WHS patients should be considered and investigated as a potential contributor to the seizure phenotype of WHS.

6.1.2.4: Whsc1 and Letm1

WHSC1 has frequently been linked to the characteristic facial features associated with WHS. In 2009, Nimura et al generated a *Whsc1* mouse model and reported that *Whsc1*-/- mice exhibited growth retardation and died within 10 days. Heterozygous (*Whsc1*-/+) mice exhibited growth retardation and some WHS-like midline defects similar to those seen in WHS patients indicating that haploinsufficiency of the *WHSC1* gene contributes to some of the key features of WHS (Nimura et al, 2009).

Haploinsufficiency of *LETM1* has been postulated as potentially causative of the seizure phenotype of many WHS patients (discussed further in section 6.1.5). A Drosophila model of *LETM1* knockdown (*dmLETM1*) has been reported which recapitulates several hallmark features of WHS; small body size and delayed development, reduced locomotor activity and reduced neurotransmitter release at synapses (McQuibban et al, 2010). Until recently, no *LETM1* mouse models had been reported. However this year, Jiang and colleagues reported that *Letm1* deletion in mice is embryonically lethal before gastrulation (E6.5). They also reported that 50% of heterozygous mice, which mimic the situation in WHS patients, died before the day 13.5 of embryogenesis. However, those that survived exhibited altered glucose metabolism, impaired control of brain ATP levels and increased seizure activity. This data is consistent with another report published this year (2013) by Zhang et al, who also demonstrated an association between *Letm1* and epileptic seizures in rats (Zhang et al, 2013). Collectively, these reports support a role for *LETM1* haploinsufficiency in the seizure phenotype of many WHS patients.

Table 6.1 - The predicted and confirmed genes in the region 1.2-2.3Mb from the telomere of Chromosome 4. Also listed are mouse orthologues and predominant features of null mouse models.

Human gene	Mouse orthologue	Function	Null mouse phenotype
MXD4	*Mxd4*	Transcription	NR
POLN	*Poln*	DNA repair	NR
LOC401115	-	-	NR
C4orf15/ HAUS3	NR	Subunit of the human augmin complex; a microtubule-binding complex	NR
FLJ37478/NAT8L	NR	Neuron specific member of the N-acyltransferase family; NAA synthesis	NR
WHSC2/NELF-A	*Whsc2/Nelfa*	Transcription and translation	NR
SCARNA23	NR	RNA modification	NR
WHSC1	*Whsc1*	transcription	Growth retardation and postnatal death
LETM1	*Letm1*	Mitochondrial homeostasis	Seizures and altered glucose oxidation
FGFR3	*Fgfr3*	Growth factor receptor	Skeletal abnormalities
TACC3	*Tacc3*	Mitosis	Embryonically lethal
TMEM129	*Tmem129*	Transmembrane protein	NR
SLBP	*Slbp*	Translation and RNA stability	NR
FAM53A	*Fam53a*	Transcription	Embryonically lethal
HSPX153	*Sax2*	transcription	Post natal growth defects
CRIPAK	NR	Protein kinase inhibitor	NR
NKX1-1	NR	Transcription factor activity	NR
UVSSA	*Uvssa*	Transcription-coupled nucleotide excision repair	NR
MAEA	*maea*	Enucleation, mitosis	Haemopoietic dysgenesis
MGC21675/CTBP-AS1	NR	unknown	NR
CTBP1	*ctbp*	Transcriptional repressor	Growth defects,

6.1.3: Atypical patients highlight correlations between *LETM1* haploinsufficiency and a seizure phenotype

The clinical spectrum and severity of WHS typically depends on deletion size, but clear genotype-phenotype relationships are assumed here and often not experimentally validated. Aside from a few examples (*WHSC1/WHSC2/LETM1*), there is a distinct lack of functional data linking the haploinsufficiency of genes with dysfunctional pathways that may underlie specific features associated with WHS. One such feature is that of the profound, intractable seizures experienced by WHS patients, often obvious before the age of 2 years. During infancy, these seizures can result in permanent disability and even death. The origin of the seizures is unclear yet the literature frequently links haploinsufficiency of the *LETM1* gene (leucine zipper-EF-hand containing transmembrane protein 1) with the seizure phenotype of WHS. However, this is purely assumed based upon deletion size in patients (see examples below) and the proposed functions of LETM1 within the cell (Endele et al, 1999a). To date no functional evidence exists to substantiate the proposed relationship.

Rauch et al described a WHS patient with one of the smallest interstitial deletions of 191.5kb encompassing the WHSCR1, therefore <u>not</u> involving *LETM1* (Rauch et al, 2001). The male patient presented with a mild WHS-like phenotype exhibiting growth retardation, minor facial dysmorphism and some learning deficits. Interestingly, the patient experienced no seizures (Figure 6.4a-c). Furthermore, Engbers et al reported a female patient with a 1.69Mb deletion which did not encompass the *LETM1* gene nor either of the WHSCR's. This atypical female patient also presented with a mild-phenotype but again, specifically no seizures (Figure 6.4b-c). Further correlations between *LETM1* haploinsufficiency and seizures are documented by South et al. They report two unique patients, one presenting with profound seizures whose deletion encompasses *LETM1* and one with no seizure phenotype whose deletion excludes the *LETM1* gene (South et al, 2007). Collectively, these reports provide a strong correlation between *LETM1* haploinsufficiency and the seizure phenotype of WHS.

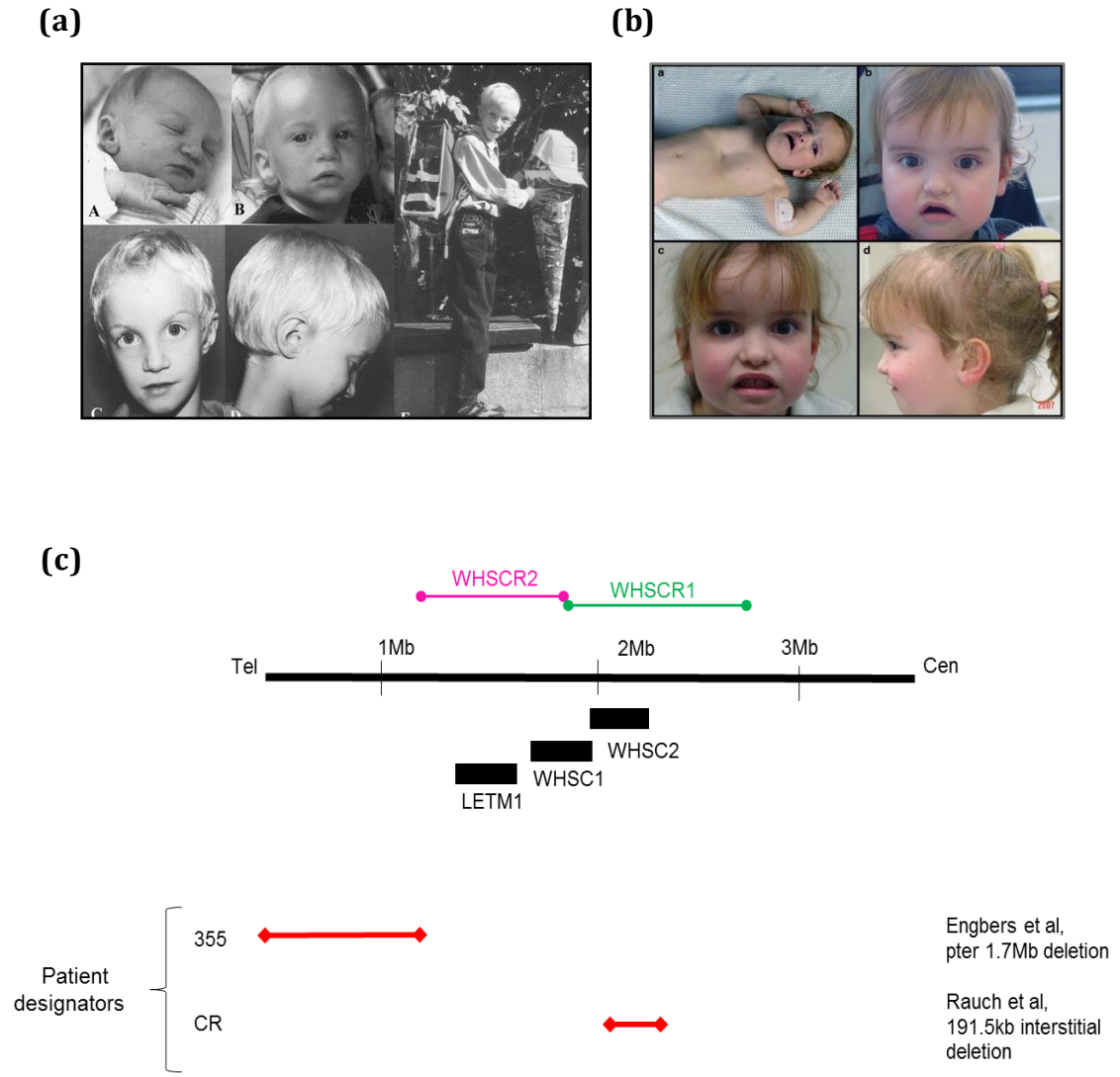

Figure 6.4: Atypical WHS patients refine genotype-phenotype correlations. **(a)** Patient reported by Rauch et al, 2001 with the first known microdeletion (191.5kb) within the WHS critical region. Patient presents with low body weight for height, speech delay, ADHD and minor facial anomalies. **(b)** 1.9 year old female patient reported by Engbers et al, 2008 with a 1.6Mb deletion of 4p16.3. Down-turned corners of the mouth, big eyes and short philtrum are well seen in the top two panels. Bottom two panels are the patient at 4.4 years from frontal and aside; big eyes and short philtrum can be seen. **(c)** Schematic and simplified representation of deletion size in the two patients shown in (a) and (b). Note that neither deletion encompasses the *LETM1* gene. Tel; telomere, Cen; centromere.

6.1.4: *LETM1*; a candidate gene for seizure phenotype of WHS?

LETM1 is located <80kb distal to the WHSCR1 and is encompassed by the WHSCR2 (Fig 6.2). It encodes an 83.5kDa putative inner mitochondrial membrane protein with a single transmembrane domain (Endele et al, 1999a; Nowikovsky et al, 2004; Schlickum et al, 2004) and Fig 6.5. All members of the LETM1 family contain a hydrophobic N-terminal spanning the IMM and a large hydrophilic portion within the matrix. The C-terminal amino acid sequence predicts at least two coiled coil domains and two Ca^{2+} binding EF hand like motifs, the latter of which is not present in the yeast protein. The N-terminal region contains a mitochondria targeting sequence conserved in all orthologues (Nowikovsky et al, 2004; Schlickum et al, 2004). There are two yeast (*S.cerevisiae)* orthologues of *LETM1*; *mdm38 and Mrs7/ylh47. Mdm38* was originally identified in a screen for mutants affecting mitochondrial morphology and therefore was given its named based on its roles in mitochondrial distribution and morphology (Dimmer et al, 2002).

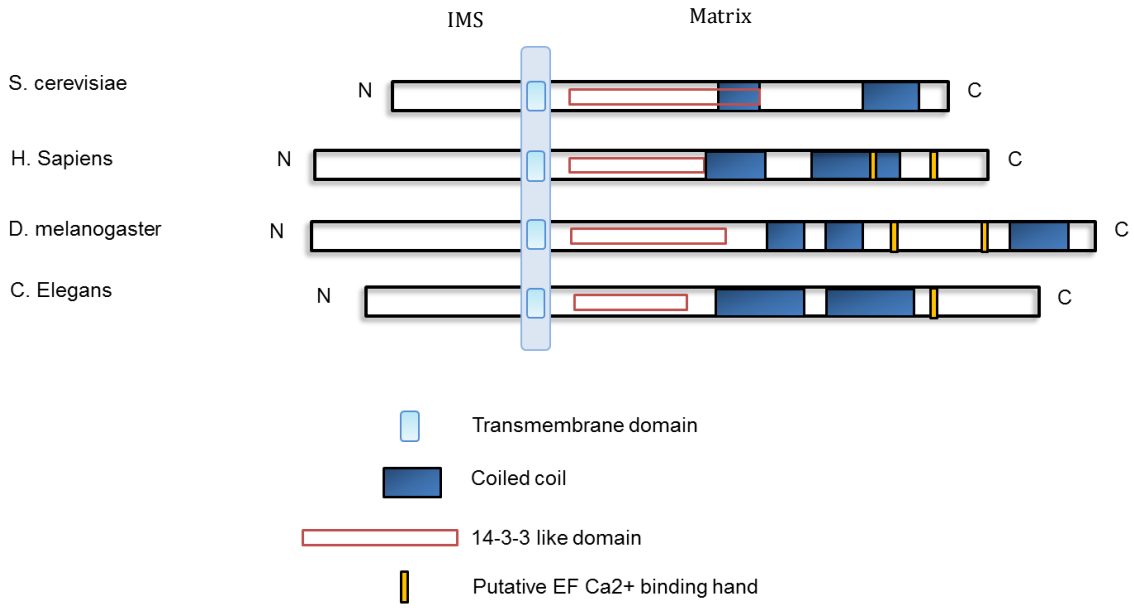

Figure 6.5: A schematic representation of selected members of the LETM1 family with the highly conserved transmembrane domain highlighted in light blue. ims; intermembranal space.

6.1.4.1: LETM1 and potassium-hydrogen exchange activity

LETM1 was identified in a genome-wide unbiased RNAi screen as a Ca^{2+}/H^{+} antiporter catalysing the 1:1 electrogenic exchange of Ca^{2+} for H+ (Jiang et al, 2009a).This report was received with great interest, however subsequent studies have challenged it and propose that LETM1 rather functions in K^{+}/H^{+} exchange (KHE) (Dimmer et al, 2008b; Froschauer et al, 2005a; Nowikovsky et al, 2004; Nowikovsky et al, 2007). Studies have suggested a role for mdm38 in potassium homeostasis by acting either as a K^{+}/H^{+} antiporter or a regulator of its activity. Potassium acetate induced swelling in isolated mitochondria demonstrated that mdm38 is essential for KHE in yeast. Consistent with this data, mitochondria isolated from an *mdm38* mutant lacked this activity confirming that mdm38 is an essential element of the mitochondrial KHE (Froschauer et al, 2005b; Nowikovsky et al, 2004). In addition, *mdm38* depletion resulted in mitochondrial matrix swelling and cristae loss suggesting a role for K^{+} in regulating mitochondrial volume and morphology. This hypothesis was further supported by the finding that the effects of *mdm38* downregulation could be restored by treatment with nigericin, an ionophore which catalyses electroneutral KHE (Hasegawa & van der Bliek, 2007; Nowikovsky et al, 2007) (Figure 6.6).

Dimmer et al provided evidence of a role for LETM1 in the regulation of mitochondrial morphology in human HeLa cells. Downregulation of *LETM1* (~60%) led to altered mitochondrial morphology where mitochondria appeared fragmented and clustered in the perinuclear region (Dimmer et al, 2008b). Interestingly, nigericin was able to fully reverse these phenotypes suggesting a causal link between altered KHE activity and disrupted mitochondrial morphology. They further report that these changes did not require activation of the DRP1-dependent fission pathway and suggest that the fragmentation caused by silencing of LETM1 could therefore represent a mitochondrial morphological response to the inhibition of ion homeostasis. In fact, disruption of K^{+} homeostasis would result in increased levels of mitochondrial K^{+} leading to the influx of water which may underlie the mitochondrial swelling induced by loss of LETM1 (Dimmer et al, 2008b). More recent work has confirmed that siRNA-mediated *LETM1* downregulation (~90%) is associated with loss of mitochondrial tubular networks,

mitochondrial swelling and cristae disorganization in HeLa cells (Tamai et al, 2008a). Mitochondrial membrane potential was found to be reduced in *LETM1* siRNA-transfected cells, consistent with previous reports in yeast *mdm38* mutants (Frazier et al, 2006; Nowikovsky et al, 2004; Tamai et al, 2008a). Furthermore, studies in yeast, Drosophila and mammalian cells have also observed that downregulation of *LETM1/mdm38/dmLETM1* leads to on-going mitophagy as a consequence of mitochondrial dysfunction and osmotic swelling caused by KHE activity shutoff (McQuibban et al, 2010; Nowikovsky et al, 2007).

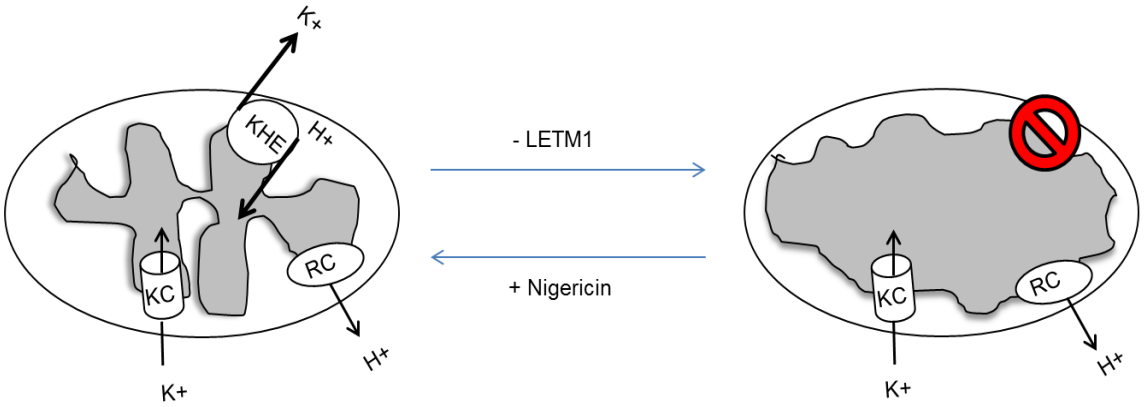

Figure 6.6 – LETM1, mitochondrial K^+ and volume homeostasis as described by Nowikovsky et al (Nowikovsky et al, 2012a). *LETM1* depletion leads to KHE activity shutoff and mitochondrial swelling and cristae loss. These phenotypes can be reversed by the addition of a K^+ ionophore such as nigericin. RC, respiratory chain; KHE, potassium hydrogen exchange; Kc, potassium channels.

6.1.4.2: A putative role for LETM1 in Ca^{2+} transport

As mentioned, LETM1 was identified in a genome-wide unbiased RNAi screen in Drosophila as a Ca^{2+}/H+ antiporter (Jiang et al, 2009a). The findings of this study led the authors to conclude that LETM1 is a H^{+}-Ca^{2+} exchanger mediating RR (ruthenium red)-sensitive Ca^{2+} uptake in energized mitochondria. However, this has been disputed by other authors whereby they suggest that the findings are compatible with an antiporter mechanism but do not prove it (Nowikovsky et al, 2012b) . Interestingly, in a more recent study investigating the roles of LETM1 and UCP2/3 in mitochondrial Ca^{2+} transport, knockdown of *LETM1* strongly diminished the transfer of Ca^{2+} into mitochondria resulting in the reduction of store-operated Ca^{2+} entry (SOCE). This evidence suggests that LETM1 contributes to mitochondrial Ca^{2+} uptake pathways in endothelial cells however much more work is needed to determine whether LETM1 does in fact play an essential role in calcium homeostasis in other cell types (Waldeck-Weiermair et al, 2011).

6.1.4.3: LETM1, mitochondrial biogenesis and the formation of the respiratory chain complexes

Frazier and colleagues reported that mutations in *mdm38* severely affected the transport and insertion of two mtDNA encoded proteins; ATP6 and cytochrome b into respiratory chain complexes (Frazier et al, 2006). They attributed the defective assembly of respiratory complexes III and IV to destabilised interactions of mdm38 with mitochondrial ribosomes however, subsequent investigation revealed that these defects were rescued by the addition of low concentrations of nigericin (Nowikovsky et al, 2007). This suggested that the K^{+} overload induced by *mdm38* downregulation led to the destabilisation of respiratory chain complexes. Tamai et al also reported evidence indicating that *LETM1* downregulation induced disassembly of respiratory chains. In particular, complexes I, III and IV failed to form supercomplexes. Further evidence of a role for LETM1 in mitochondrial biogenesis came from the finding that a double deletion of *mdm38* and *mba1* (a ribosome receptor) led to defective translation and the complete loss of cox1 and cytochrome b (Bauerschmitt et al, 2010). In fact, in a previous study by Piao and

co-workers they demonstrated that LETM1 binds the ribosomal protein, L36 causing an L36-dependent reduction in ATP production (Piao et al, 2009b). These findings suggest that LETM1 plays key roles in mitochondrial biogenesis independent of its essential roles in KHE activity. Indeed, cells with inactivated components of the respiratory complexes do not show signs of mitochondrial swelling as seen in cells lacking LETM1 (Hasegawa & van der Bliek, 2007; Tamai et al, 2008b).

It would be expected that impaired K^+ extrusion, altered morphology and disrupted assembly of respiratory complexes would impart detrimental effects on mitochondrial functioning. Indeed, this is certainly the case in some yeast and human cell models of *LETM1* downregulation where depolarisation of the membrane potential, impaired assembly of respiratory complexes and decreased ATP production have been observed (Frazier et al, 2006; McQuibban et al, 2010; Nowikovsky et al, 2007; Tamai et al, 2008b). However, Dimmer et al were unable to provide evidence of mitochondrial dysfunction in *LETM1*-silenced HeLa cells further complicating the picture (Dimmer et al, 2008b). Furthermore, studies employing WHS patient derived cell lines have failed to identify any mitochondrial dysfunction similar to those observed in yeast, *C.elegens* and cultured mammalian cell models of *LETM1* downregulation such as disruption to the mitochondrial membrane potential and altered assembly of respiratory complexes. Dimmer at al investigated mitochondrial morphology and the levels of LETM1 in two WHS-patient derived cell line models; lymphoblastoid cells and fibroblasts. Unexpectedly, although genetic analysis revealed that one allele of *LETM1* was lacking, the levels of LETM1 protein in the lymphoblastoid cell line were unchanged, also consistent with the findings of van der Bleik and colleagues (Hasegawa & van der Bliek, 2007). They suggested that this could be a cell-specific effect and proceeded to deepen their analysis by generating primary fibroblasts from a different WHS patient where they demonstrated a 50% reduction of the LETM1 gene, messenger and protein. Interestingly, these patient-derived fibroblasts did not exhibit any mitochondrial morphology-related changes (Dimmer et al, 2008a).

One important consideration here is that many of the studies employing yeast and mammalian cell models utilize a full knockdown of *LETM1*. In contrast, WHS patient-derived cell lines display haploinsufficiency of *LETM1* (50%) suggesting that the residual protein here is sufficient to maintain some protein function. In fact, Tamai et al reported that disassembly of the respiratory chain proceeded slowly with increasing *LETM1* inactivation. Cells that were transfected only once with *LETM1* siRNA exhibited swollen mitochondria but the respiratory chain complexes were assembled normally compared to those that were transfected 2-3 times (Tamai et al, 2008). Furthermore, Dimmer et al reported mitochondrial morphological changes following a 60% siRNA-mediated reduction of *LETM1* in HeLa cells, but observed no alterations to respiratory chain activity (Dimmer et al, 2008).

6.1.4.4: Additional roles for LETM1

Mutations in *BCS1L*, an AAA-ATPase, are causative of three different human disorders; Complex III deficiency, GRACILE (*G*rowth *R*etardation, *A*mino aciduria, *C*holestasis, *I*ron overload, Lactic acidosis and *E*arly death) syndrome and Bjornstad syndrome. Bjornstad syndrome is a congenital condition involving deafness and hair abnormalities. Interestingly, certain patients with GRACILE syndrome present with neurological symptoms such as seizures which is also a common feature of WHS patients. Recently, Tamai et al provided the first evidence for a functional relationship between BCS1L and LETM1 in mitochondrial biogenesis (Tamai et al, 2008a). Figure 6.7 depicts the working model that they have proposed whereby LETM1 and BCS1L function in the assembly of the respiratory chain complexes. This evidence may begin to provide some insight that altered *LETM1* copy number could disrupt some aspect of mitochondrial function.

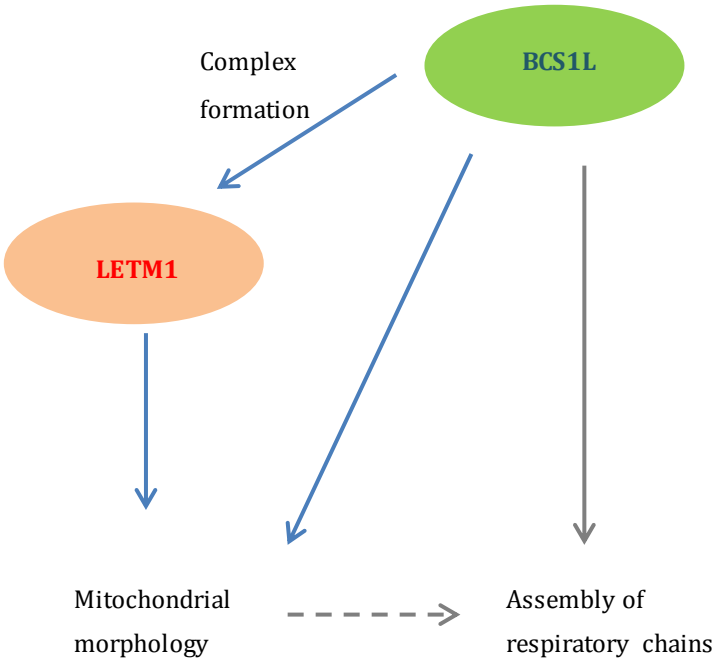

Figure 6.7 - Model of the functions of BCS1L and LETM1 in mitochondrial biogenesis. BCS1L is required for respiratory chain assembly, mitochondrial morphology maintenance and LETM1 major complex formation. LETM1 has a distinct role in the maintenance of mitochondrial volume and shape which helps to achieve efficient assembly of respiratory chains. Blue arrows indicate functions reported by Tamai et al, 2008, grey arrows indicate the BCS1L functions reported previously (Cruciat et al, 1999; de Lonlay et al, 2001).

6.1.5: Mitochondrial dysfunction is frequently associated with epilepsy

Epilepsy is a frequent neurological disorder affecting approximately 0.5-0.7% of the population (Folbergrová and Kunz 2012). The mitochondria have gained significant interest over recent years as playing important roles in epileptogenesis (Cock & Schapira, 1999; Folbergrová & Kunz, 2012; Fukuhara et al, 1980; Kudin et al, 2009; Kunz & S, 2002; Patel, 2002; Torbergsen et al, 1991; Waldbaum & Patel, 2010). Neurons are highly differentiated cells requiring large amounts of ATP for the maintenance of ionic gradients and for neurotransmission. Since the majority of neuronal ATP is generated by oxidative phosphorylation, neurons heavily rely on optimal mitochondrial function. Furthermore, the morphology of neurons is highly complex and thus different segments of neurons i.e. dendrites, soma and axon have different energy demands. Mitochondrial dysfunction resulting in reduced production of ATP may increase neuronal excitability by impairing Na^+-K^+ ATPase activity and decreasing the neuronal plasma membrane potential. Furthermore, energy depletion enhances both synaptosomal and astrocytic glutamate release by interfering with the mitochondrial glutamate-aspartate transporter (McKenna, 2007). In addition to ATP production, neuronal mitochondria also play important roles in Ca^{2+} sequestration and thus mitochondria are able to modulate neuronal excitability and synaptic transmission (Kann & Kovacs, 2007).

The importance of the mitochondria for neuronal function is evident from the neurological phenotypes observed in patients with mutations in genes affecting mitochondrial functions such as oxidative phosphorylation and ATP production (Discussed in detail in Chapter 3 section 3.1.6). Seizures are observed in numerous mitochondrial disorders but are most frequently reported in MERRF, Leigh Syndrome, MELAS and KSS (See Table 3.4 for the key clinical features of these conditions) (Zeviani et al, 1993; Zsurka et al, 2008; Zsurka et al, 2010). Furthermore, consistent with a role for disrupted Ca^{2+} homeostasis as a contributor to seizure predisposition, impaired mitochondrial Ca^{2+} handling is a predominant feature of cybrid cells harbouring the mitochondrial T8356C

mutation associated with MERRF syndrome (Brini et al, 1999). It is proposed that this cellular alteration may potentially underlie the increased excitability seen in this form of myoclonic epilepsy (Brini et al, 1999). Accumulating evidence also suggests that free radicals and oxidative stress are important in the pathogenesis of epilepsy (Jarrett et al, 2008; Waldbaum & Patel, 2010). For example, astroglial and glutamate receptors are extremely sensitive to oxidative damage and thus excessive ROS generation can have direct effects on neuronal excitability (Trotti et al, 1998). Conversely, ROS are thought to be not only a key player in the pathogenesis of seizures but also a key factor resulting from seizures. However, in addition to the well-established role of the mitochondria in energy metabolism, it has recently emerged that mitochondrial dysfunction can trigger neuronal cell death, a prominent feature of therapy-resistant epilepsy (Ott et al, 2007). This may provide insight into the role of the mitochondria in more sporadic forms of epilepsy and also highlights the mitochondria as promising targets for neuroprotective strategies in epilepsy (Kunz, 2002).

The distinct correlation between *LETM1* haploinsufficiency and the presence of seizures in many WHS patients has led many researchers to suggest that haploinsufficiency of the *LETM1* gene may be causative of the seizure phenotype here. However, it is noteworthy that other reports have also recently suggested roles for *CTBP1* in the generation of seizures here. The idea that haploinsufficiency of *LETM1* could play an important pathomechanistic role in the generation of seizures in WHS is substantiated by the findings of altered mitochondrial function and morphology in numerous cell models of *LETM1* downregulation (Dimmer et al, 2008a; Hasegawa & van der Bliek, 2007; McQuibban et al, 2010; Nowikovsky et al, 2004; Tamai et al, 2008a). This degree of mitochondrial dysfunction may have important implications for neuronal development and function in WHS patients. Furthermore, LETM1 was previously identified as a Ca^{2+}-H^{+} antiporter which suggests that it may play critical roles in Ca^{2+} regulation and thus may indirectly modulate neuronal excitability and synaptic transmission. In fact, very recently Zhang et al have provided data to indicate that downregulation of *Letm1* increases seizure susceptibility in a rat pilocarpine-induced epilepsy model. This provides

further supportive evidence of a potential role for LETM1 in the seizure phenotype of WHS (Zhang et al, 2013).

6.1.6: Summary

No single gene is fully responsible for the complete spectrum of the WHS phenotype and thus it is widely accepted that WHS has a multigenic aetiology. Furthermore, emerging evidence identifying patients with deletions outside of the WHSCRs adds to the complexity of this disorder and suggests that other genes, aside from those residing in the critical regions (WHSCR1 and WHSCR2), can contribute to the severity of the disease. Many genotype-phenotype correlation studies have implicated LETM1 in the pathogenesis of seizures here, however to date no functional evidence derived from patient material exists to support this; it is purely assumed based on deletion size in WHS patients and its proposed roles in the cell. *LETM1,* encompassed by the WHSCR2, encodes a mitochondrial protein with several proposed roles including KHE activity and the regulation of mitochondrial morphology. It is well documented that epilepsy/seizures are frequently associated with mitochondrial dysfunction. Therefore, it is plausible to suggest that haploinsufficiency of *LETM1* may impart detrimental effects on mitochondrial functioning which may underlie the seizure phenotype of WHS.

Using a unique panel of WHS-patient derived lymphoblastoid cell lines (LBLs) from patients carrying variously sized sub-microscopic deletions within 4p16.3, including the patients described by Rauch *et al* and Engberts *et al*, I aimed to ascribe a functional deficit to *LETM1* haploinsufficiency which may be relevant in the underlying aetiology of seizures in WHS, particularly those relating to mitochondrial function and dynamics (Figure 6.8). Furthermore, understanding the cellular consequences of *LETM1* haploinsufficiency may enable future advances towards more effective management therapies in WHS. The mitochondria are the biological powerhouse of all cells. In particular, neurons critically rely on mitochondria not only for development and maturation but also for processes such as synaptic transmission and excitability which rely heavily on ATP production and ion signalling. Nevertheless, no studies have been performed in a neuronal model

of *LETM1* haploinsufficiency and this is an area worthy of intensive investigation due to the numerous neurological deficits associated with WHS. Employing a neuronal model of mouse N2A neuroblastoma cells, I investigated the impacts of partial *LETM1* knockdown on mitochondrial function to address this issue.

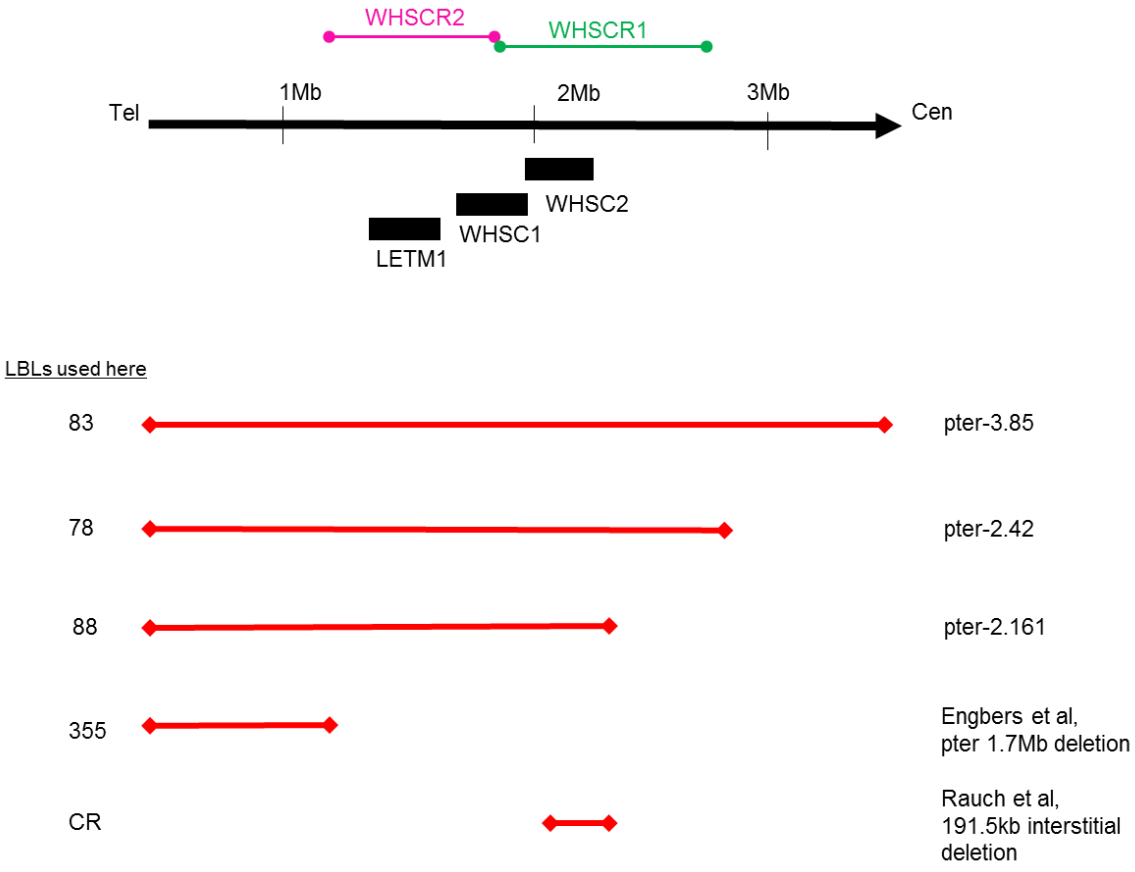

Figure 6.8: A schematic representation of the five WHS patient cell lines employed in this thesis. The commonly deleted critical regions are indicated in green and pink (WHSCR1 and WHSCR2) and the locations of several genes implicated in this condition are shown underneath. The red bars indicate the deleted regions in 5 WHS patients, from whom we derived LBLs for use in this project. The two atypical patients identified by Rauch *et al* and Engbers *et al* are illustrated. Tel; telomere, Cent; Centromere.

6.2: Results

6.2.1: LETM1 expression levels; whole cell and mitochondrial-specific

Haploinsufficiency of *LETM1* has been strongly associated with the seizure phenotype of WHS. However, this association is made with very limited biochemical evidence. In addition, it is yet to be shown that patients with 4p deletions encompassing the *LETM1* gene exhibit reduced expression at the protein level consistent with haploinsufficiency of the gene. In collaboration with Prof. Joris Vermeesch, UZ Leuven, Belgium, I assembled a unique panel of EBV-transformed patient-derived lymphoblastoid cell lines (LBLs) from patients harbouring variously sized submicroscopic deletions within 4p16.3, as illustrated previously in figure 6.8. I characterised these five patient-derived cell lines for LETM1 protein expression levels. As shown in Figure 6.8, LBL: 83, LBL: 78 and LBL: 88 are from patients with hemizygous deletions encompassing both WHS critical regions and clinically manifesting as typical WHS. Their deletions include the *LETM1* gene. These patients are therefore haploinsufficient for *LETM1.* In contrast, LBL: 355 and LBL: CR are from atypical WHS individuals whose deletions do not incorporate the *LETM1* gene and thus remains bi-allelic for *LETM1*.

LETM1 protein levels were found to be reduced consistent with haploinsufficiency in LBL: 83, LBL: 78 and LBL: 88 (Fig 6.9). LETM1 protein levels in LBL: 355 and LBL: CR show similar expression to that of wild-type (WT) LBLs consistent with the normal copy number of the *LETM1* gene in these two lines (Fig 6.9). As LETM1 is a putative mitochondrial protein I investigated the expression levels of LETM1 in isolated mitochondrial extracts. Employing the same magnetic bead technology as described in Chapter 3 section 3.2.4, I isolated mitochondria from four of the WHS patient-derived LBLs; LBL: 83, LBL: 78, LBL: 88 and LBL: 355. Consistent with the findings in whole cell extracts, expression of LETM1 in mitochondrial extracts was reduced in cell lines that are haploinsufficient for *LETM1*; LBL: 83, LBL: 78 and LBL: 88 (Fig 6.10). The mitochondrial protein expression levels of LETM1 were

comparable to those of wild-type LBLs in LBL: 355, consistent with the deletion size in this patient-derived cell line (Fig 6.10). This is the first report demonstrating reduced expression at the protein level of the product of the *LETM1* gene within mitochondrial preparations in addition to whole cell extracts, in cell material derived from WHS patients.

(a)

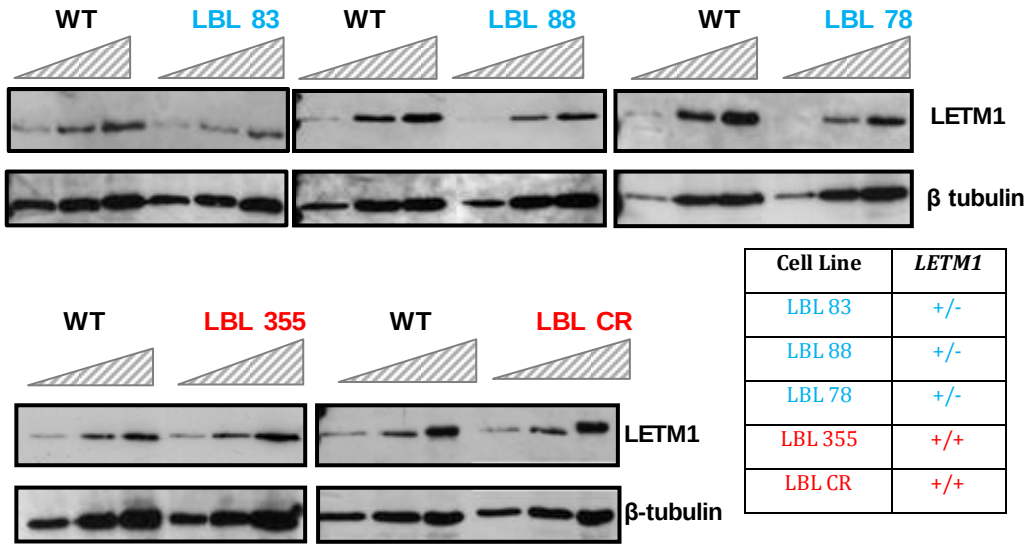

Cell Line	*LETM1*
LBL 83	+/-
LBL 88	+/-
LBL 78	+/-
LBL 355	+/+
LBL CR	+/+

(b)

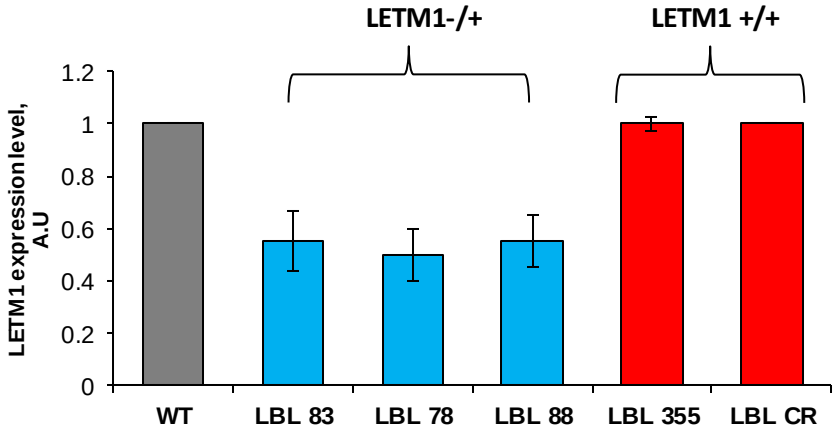

Figure 6.9 - WHS patient-derived LBLs exhibit reduced LETM1 protein expression consistent with deletion size. **(a)** 1-10µg of urea-based whole cell extracts for LBL: 83, LBL: 88, LBL: 78, LBL: 355 and LBL: CR were subjected to SDS-PAGE and immunoblotted for LETM1 protein expression levels. Each blot was then reprobed for β-tubulin as a loading control. **(b)** Histogram showing LETM1 protein expression levels measured by Image J. Data represents the mean of 3 independent measurements ±SD. A.U; arbitrary units.

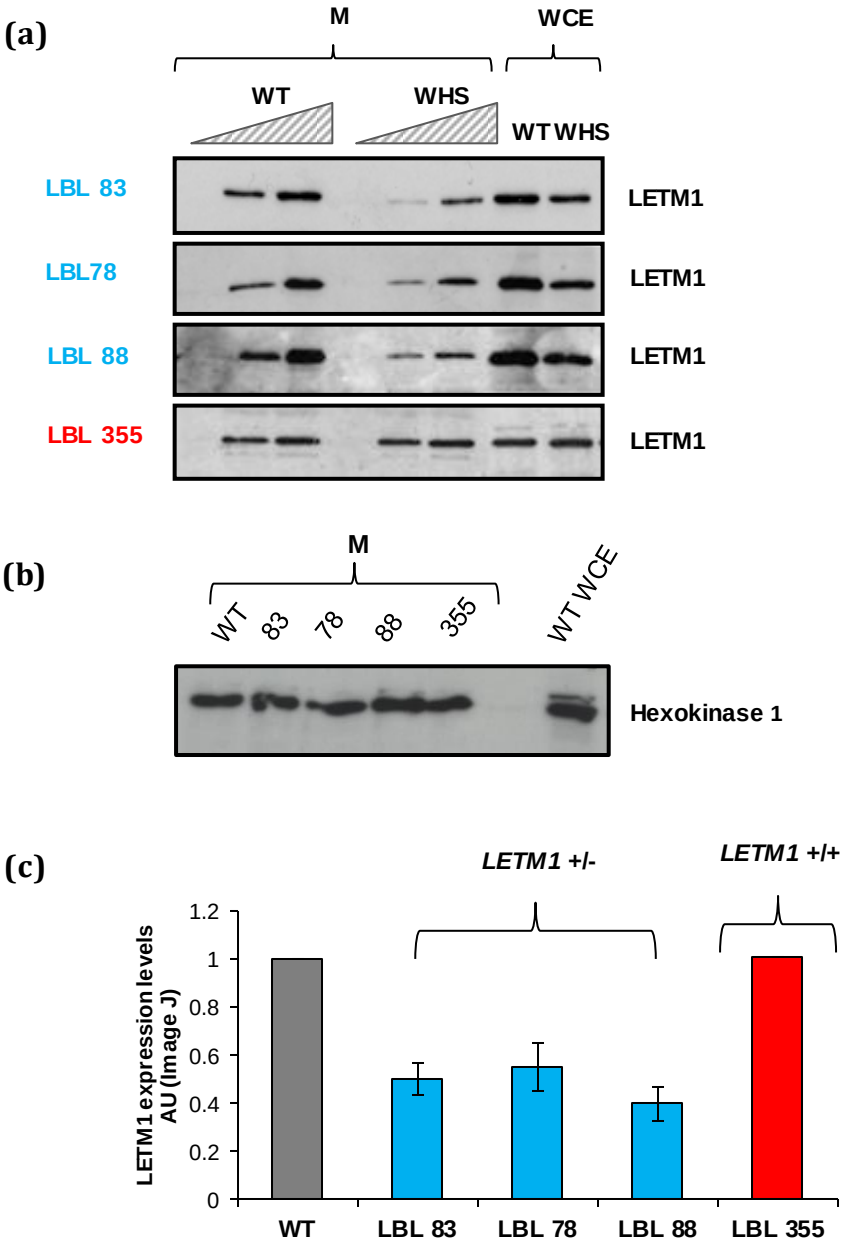

Figure 6.10 - WHS patient-derived mitochondria show reduced LETM1 protein expression consistent with deletion size. **(a)** Mitochondria were isolated from 1 x 10^7 cells using the Miltenyi Biotec mitochondrial isolation kit and lysed in 60uL urea buffer. 0.1-2µL of urea-based mitochondrial extract (M) from each WHS cell line (WHS) were loaded respectively and compared to WT expression levels (WT). 10µg of whole cell extract (WCE) was loaded in the last two columns to serve as a control. Each blot represents extract from wild-type LBLs in wells 1-3 and extracts from WHS patient-derived cell lines, as labelled on the left of each blot, in wells 4-7. **(b)** Loading control inputs; mitochondria were isolated from 1 x 10^7 cells from WT and four WHS-patient derived cell lines. 8µL of each mitochondrial extract was loaded and immunoblotted for Hexokinase 1 protein expression. M; mitochondrial extract, WCE; Whole cell extract. **(c)** Histogram showing LETM1 protein expression levels in mitochondrial extracts measured by Image J. Data represents the mean of 3 independent measurements ±SD. Arb units; arbitrary units.

6.2.2: Mitochondrial dysfunction segregates with *LETM1* haploinsufficiency

The role of the mitochondria was initially thought only to be to generate energy in the form of ATP, and hence they are commonly referred to as the "biological powerhouse" of the cell. However, over the past few decades' research has uncovered irrefutable evidence to suggest that the mitochondria play key roles in a variety of cellular processes ranging from calcium homeostasis to cell death, as discussed previously in Chapter 3. The mitochondria are vital components of all eukaryotic cells however their size, shape and distribution can very between cell types according to cellular need. Neurons in particular rely heavily on the mitochondria where they are actively transported along axons and accumulate in sites with high-energy demands such as the presynaptic terminal and Nodes of Ranvier (Hollenbeck & Saxton, 2005). Mitochondrial disorders arising from mutations in both the mtDNA (mitochondrial DNA) and in the nDNA (nuclear DNA) encoding a mitochondrial protein highlight the importance of correct mitochondrial function in maintaining cellular homeostasis (McKenzie et al, 2004). Moreover, given the multitude of roles for mitochondria within the cell it is not surprising that mitochondrial dysfunction has been implicated in the pathogenesis of many disorders including Parkinson's Disease, Alzheimer's Disease and Ataxia-Telangiectasia (Ambrose et al, 2007; Winklhofer & Haass, 2010).

LETM1 is an inner mitochondrial membrane protein proposed to be involved in ion exchange within the mitochondria (Nowikovsky et al, 2012a). However, there is debate within the literature as to whether it functions as a Ca^{2+}/H^{+} antiporter or plays essential roles in K^{+}/H^{+} activity.(Dimmer et al, 2008b; Endele et al, 1999b; Froschauer et al, 2005a; Jiang et al, 2009a). Nevertheless, the mitochondria rely heavily on the correct functioning of ion exchange pathways and any perturbations here can have detrimental effects on mitochondrial dynamics and physiology (O'Rourke, 2007). With regards to calcium, the primary role of mitochondrial calcium is the stimulation of oxidative phosphorylation. This occurs at many levels including allosteric activation of pyruvate dehydrogenase, isocitrate dehydrogenase and α-ketoglutarate and stimulation of ATP synthase and ANT

(Brookes et al, 2004; McCormack & Denton, 1993). Overall, calcium is a positive regulator of mitochondrial function and thus any disruption to calcium homeostasis will have profound implications for mitochondrial function (Duchen, 2000; Rizzuto et al, 2000). It is well documented that excessive increases in calcium appear to have negative effects on mitochondrial function such as; opening of the mPTP, mitochondrial fragmentation and the generation of reactive oxygen species (Cárdenas & Foskett, 2012; Gordeeva et al, 2003; Wong et al, 2012).

Given the recently identified roles for LETM1 in ion exchange, possibly calcium, it is likely that its loss, in the context of WHS, could negatively impact on mitochondrial function. Furthermore, correct mitochondrial functioning is fundamental for neurons and many neuronal processes such as synaptic plasticity and transmission rely heavily on mitochondria for ATP production and Ca^{2+} sequestration (Kann & Kovacs, 2007). Moreover, mitochondrial dysfunction has long been associated as a pathomechanistic contributor to epilepsy (Folbergrová & Kunz, 2012; Kang et al, 2013). Therefore, due to its key roles in mitochondrial homeostasis, it is likely that haploinsufficiency of *LETM1* may impart detrimental effects on mitochondrial function which could potentially contribute to the pathogenesis of seizures in WHS.

Although multiple studies employing *LETM1* knockdown models have reported mitochondrial dysfunction and altered morphology as a consequence of LETM1 loss, data from WHS patient-derived material has failed to support this (Dimmer et al, 2008b; Nowikovsky et al, 2007). To date, no mitochondrial dysfunction has been identified in WHS patient-derived cells. Therefore, using the unique panel of WHS patient-derived LBLs described in section 6.2.1, I investigated mitochondrial function in the context of *LETM1* haploinsufficiency. I employed the same set of Mitotracker probes described in Chapter 3 to investigate various aspects of mitochondrial function and physiology in the context of WHS.

6.2.2.1: Mitotracker Red: WHS LBLs exhibit hyperpolarisation of the mitochondrial membrane potential, Ψ^m

The mitochondrial membrane potential, as described in Chapter 3, is generated and maintained by the concerted actions of electron donors and acceptors of the electron transport chain, ultimately resulting in the production of ATP. The membrane potential is highly sensitive to changes in ion flux and mitochondrial morphology. Previous studies investigating the cellular consequences of *LETM1* downregulation have reported that its loss is associated with altered KHE activity and mitochondrial swelling. Therefore, this suggests that haploinsufficiency of *LETM1* in the context of WHS may impart effects on the generation of the mitochondrial membrane potential and thus contribute to mitochondrial dysfunction. In fact, previous reports have indicated that *LETM1*-siRNA transfected HeLa cells and mitochondria isolated from yeast *mdm38* mutants exhibit low membrane potential. Furthermore, some studies have suggested a role for LETM1 in respiratory chain biogenesis whereby loss of LETM1 is associated with disrupted assembly of respiratory chain complexes (Frazier et al, 2006; Nowikovsky et al, 2004; Tamai et al, 2008b).

Mitotracker Red CMXRos (MTR) accumulation within the mitochondria is dependent upon an intact and active mitochondrial membrane potential. Decreased or increased MTR fluorescence is therefore indicative of membrane potential disruption and thus mitochondrial dysfunction. Inconsistent with previous reports, the results presented in Figure 6.11a indicates that Mitotracker Red fluorescence was increased in WHS cell lines exhibiting haploinsufficiency of *LETM1* (LBL: 83, LBL: 78 and LBL: 88) compared to WT controls. In contrast, the two WHS patient-derived cell lines that are bi-allelic for *LETM1* (LBL: 355 and LBL: CR) show Mitotracker Red fluorescence of a similar intensity to WT levels (see figure 6.12 for example FACS profiles). This data is inconsistent with previous reports in yeast and mammalian cell models and suggests that haploinsufficiency of *LETM1* is associated with a subtle hyperpolarisation of the membrane potential. However, it is worthy to note that previous reports observed mitochondrial membrane depolarisation upon complete knockdown of *LETM1* which is in contrast to the haploinsufficiency of *LETM1* found in WHS patient-derived LBLs.

Knockdown of *LETM1* in yeast, *Drosophila* and mammalian models has provided evidence to suggest that loss of *LETM1*/*mdm38* results in on-going mitophagy as a result of altered KHE activity (McQuibban et al, 2010; Nowikovsky et al, 2004; Nowikovsky et al, 2007). Mitophagy is a selective form of autophagy which functions to rid the cell of defective mitochondria (Ding & Yin, 2012). If on-going mitophagy were in fact a phenotype of WHS patient derived cells, one may expect to observe a decrease in total mitochondrial mass or content. Furthermore, to ensure that the increase in Mitotracker Red fluorescence was not simply a reflection of increased mitochondrial content, I employed the Mitotracker Green probe (MTG) to analyse mitochondrial mass. MTG accumulates within the mitochondria regardless of the membrane potential giving an indication of mitochondrial mass or content of a cell population. I found that the mitochondrial mass in all 5 WHS patient-derived LBLs was similar to that of WT controls (Fig 6.11b). This suggests that mitochondrial mass is not affected by *LETM1* haploinsufficiency and thus if on-going mitophagy is a phenotype of these cells, as suggested in the literature, it is possible mitochondrial biogenesis may be up regulated as a compensatory mechanism.

Collectively, these data suggests that *LETM1* haploinsufficiency is associated with an increased mitochondrial membrane potential without a concomitant increase in mitochondrial mass. It is frequently stated in the literature that a hyperpolarised (more negative) membrane potential is associated with a higher generation of mitochondrial-derived ROS and this is thought to be due to slowed electron transport (Brookes et al, 2004; Echtay et al, 2002; Hancock et al, 2001). As *LETM1* haploinsufficient mitochondria exhibit hyperpolarisation this suggests that the generation of mitochondrial ROS may also be increased. Furthermore, calcium transport within the mitochondria is highly dependent on an intact membrane potential suggesting that calcium-mediated signalling may be also disrupted by the membrane potential alteration, in this context.

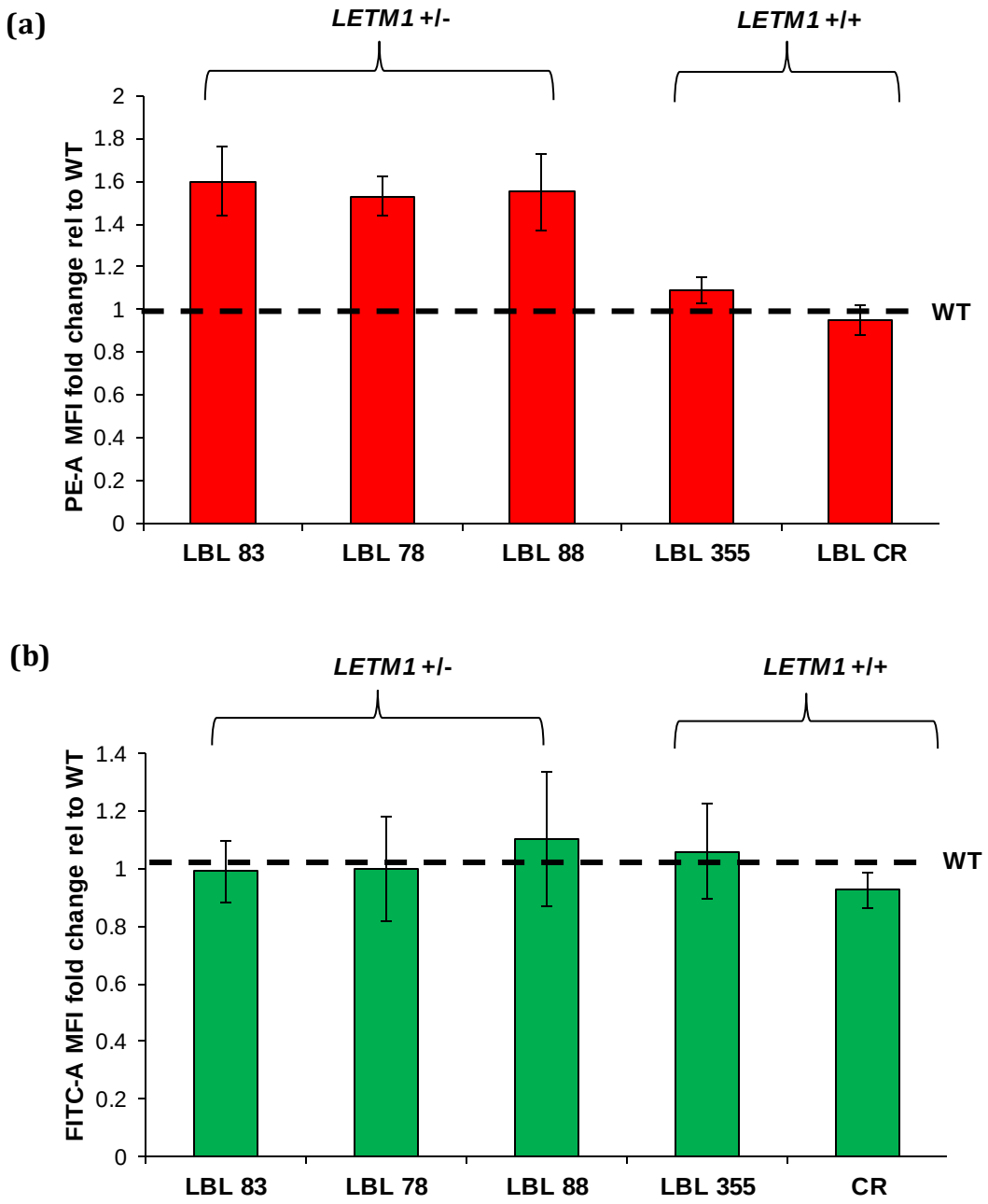

Figure 6.11 - WHS LBLs exhibit hyperpolarisation of the mitochondrial membrane potential with no increase in mitochondrial mass. **(a)** LBLs were incubated with 250nM Mitotracker Red for 15 minutes and then analysed for PE fluorescence using the FACS canto. WHS LBLs exhibiting haploinsufficiency of *LETM1* show hyperpolarisation of the membrane potential (*p<0.05 Student t-test*), whereas those bi-allelic for *LETM1* show similar mean fluorescence relative to wild-type controls (black dashed line). **(b)** WHS LBLs show similar mitochondrial mass compared to wild-type controls (black dashed line) LBLs. LBLs were incubated with 250nM Mitotracker green for 15 mins and analysed for FITC fluorescence using the FACS Canto flow cytometer. The data represents the mean of 3 independent determinations ± SD.

Cell Line	*LETM1*
LBL 83	+/-
LBL 88	+/-
LBL 78	+/-
LBL 355	+/+
LBL CR	+/+

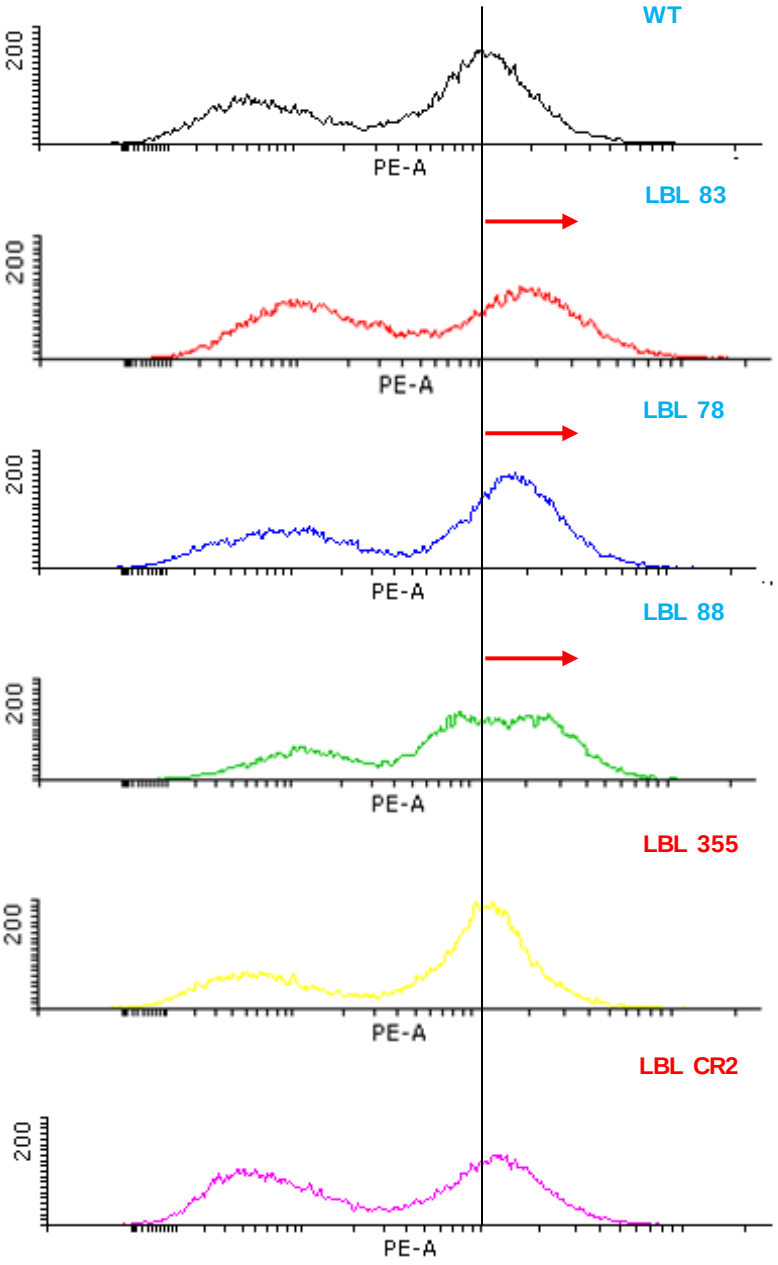

Figure 6.12: *LETM1* -/+ WHS LBLs exhibit hyperpolarisation of the mitochondrial membrane potential compared to *LETM1* +/+ WHS LBLs and WT controls. LBLs were incubated with 250nM Mitotracker Red for 15 minutes and washed once in 1X PBS. Cells were then resuspended into 500µL PBS, filtered in BD FACS Falcon tubes and analysed for PE-A fluorescence using the FACS Canto Flow Cytometer. PE-A MItotracker Red flow cytometry profiles for WT and WHS patient-derived LBLs are shown above. Those cells lines haploinsufficient for *LETM1* (83/78/88) exhibit hyperpolarisation of the mitochondrial membrane potential indicated by a rightward shift in the peak (right side of the black vertical line).

6.2.2.2: Haploinsufficiency of LETM1 is associated with an increase in mitochondria-specific ROS generation

The primary function of the mitochondria is the production of ATP through the process of oxidative phosphorylation. However, in response to various different stimuli, the mitochondria can quickly change into death-promoting organelles producing excessive reactive oxygen species (ROS) and the release of pro-apoptotic proteins which ultimately result in disrupted ATP synthesis and the activation of cell-death pathways. As discussed in detail in Chapter 3, mitochondrial-derived ROS, in the form of superoxide, is generated mainly from complexes I and III of the ETC as a normal by-product of oxidative phosphorylation. Antioxidant systems within the mitochondria such as SODs, glutathione and peroxidases exist to scavenge and remove ROS to prevent deleterious damage to proteins, lipids and DNA (Rabilloud et al, 2001). However, when the generation of ROS surpasses these systems, oxidative stress can ensue. Due to its close proximity to the mtDNA, excessive ROS can damage the mtDNA leading to further mitochondrial dysfunction and thus a cycle is established.

As previously discussed, mitochondrial dysfunction and the excessive generation of ROS is strongly associated with epileptic seizures (Folbergrova & Kunz, 2012). Interestingly, WHS patient-derived LBLs exhibit disruption of the mitochondrial membrane potential resulting in its hyperpolarization. Disruption of this membrane potential has major implications for mitochondrial homeostasis, not only through altered electron transport chain functioning and the subsequent production of ATP but also for the generation of reactive oxygen species. In fact, ETC dysfunction is causally associated with the elevated production of ROS. This suggests that in addition to disruption of the mitochondrial membrane potential, *LETM1* copy number change may be also associated with elevated levels of ROS.

To determine the levels of mitochondria-specific ROS production (O_2^-), I employed the MitoSOX probe previously described in Chapter 3 (section 3.2.2.5). LBLs were incubated with 250nM MitoSOX for 15 minutes and analysed for PE-fluorescence by flow cytometry. WHS patient-derived LBLs haploinsufficient for *LETM1* exhibited dramatically increased levels of superoxide. LBL: 83, LBL: 78 and LBL: 88

exhibited a 1.7-1.8 fold increase in MitoSOX fluorescence relative to wild type controls (Fig 6.13 and Fig 6.14). In contrast, those WHS cell lines with normal *LETM1* copy number (LBL: 355 and LBL: CR) displayed similar levels of ROS to wild type controls (Fig 6.13 and Fig 6.14). Using an additional probe; Cell Rox Red, that detects cellular-wide levels of ROS, it was confirmed that the elevation in ROS levels was specifically mitochondrially-derived (Fig 6.15). Flow cytometry analysis of Cell ROX Red fluorescence revealed similar mean fluorescence intensity between WT and WHS patient-derived LBLs indicating that total ROS was not affected by *LETM1* CNV. Further investigation revealed that this increase in ROS generation was not associated with altered Complex I activity (Fig 6.16). This suggests that the increased generation of ROS in this setting is being produced from an additional complex such as Complex II and III.

Here, using sophisticated mitochondrial probes I have uncovered novel mitochondrial phenotypes which segregate with *LETM1* haploinsufficiency in WHS patient-derived cells. Mitochondrial dysfunction is frequently associated with mitochondrial disorders that present with a seizure phenotype and thus the data presented here may provide novel insight into the underlying aetiology of the seizure phenotype of typical WHS. Furthermore as briefly mentioned, the mitochondrial membrane potential and consequent mitochondrial ROS are intimately linked to calcium homeostasis. Therefore, it is possible that misregulation of calcium also exists in this setting, which I subsequently set out to investigate.

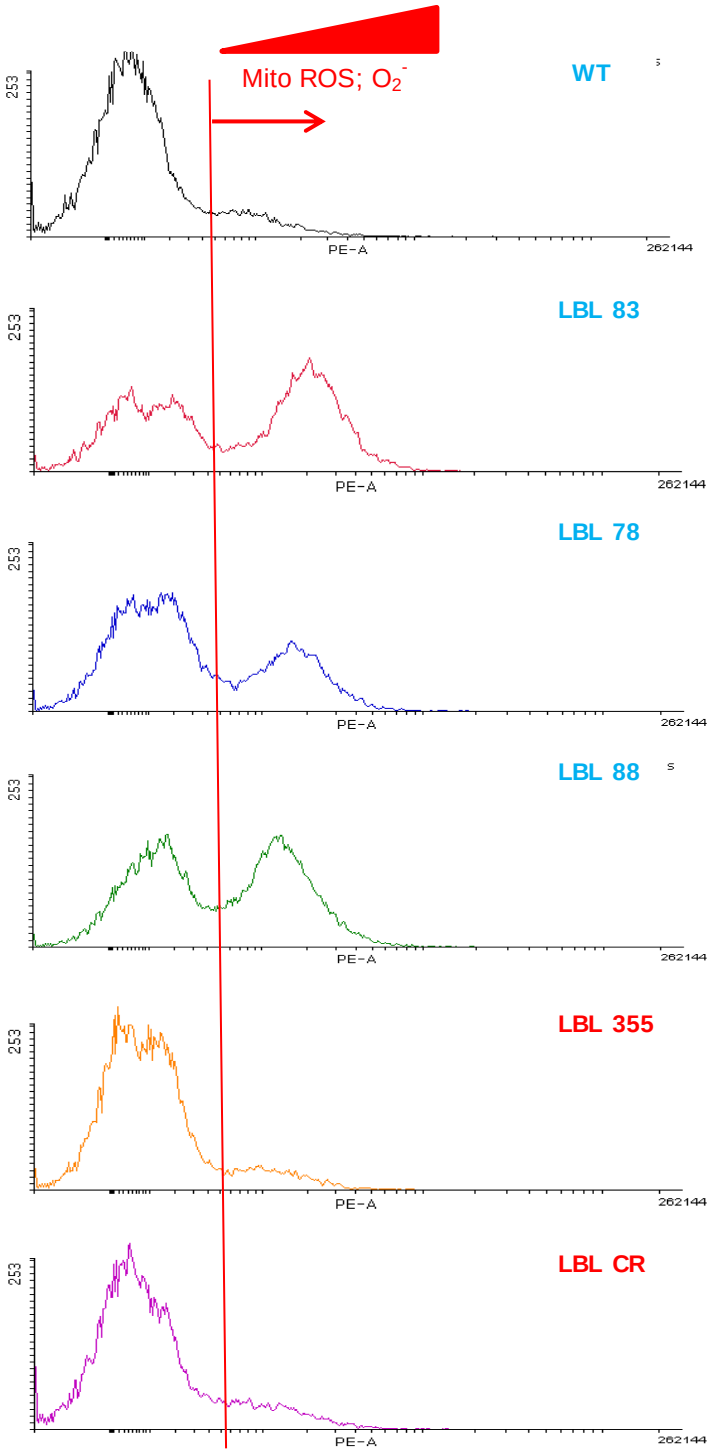

Cell Line	*LETM1*
LBL 83	+/-
LBL 88	+/-
LBL 78	+/-
LBL 355	+/+
LBL CR	+/+

Figure 6.13 - Haploinsufficiency of *LETM1* correlates with elevated levels of mitochondria-specific ROS; FACS profiles. LBLs were incubated with 250nM MitoSOX for 15 minutes and analysed for PE-A flourescence using the FACS Canto flow cytometer. PE-A MitoSOX flow cytometry profiles for WT and WHS patient-derived LBLs are shown above. Those cell lines haploinsufficient for *LETM1* (83/78/88) exhibit elevated ROS levels indicated by a rightward shift in the peak (right side of the red vertical line).

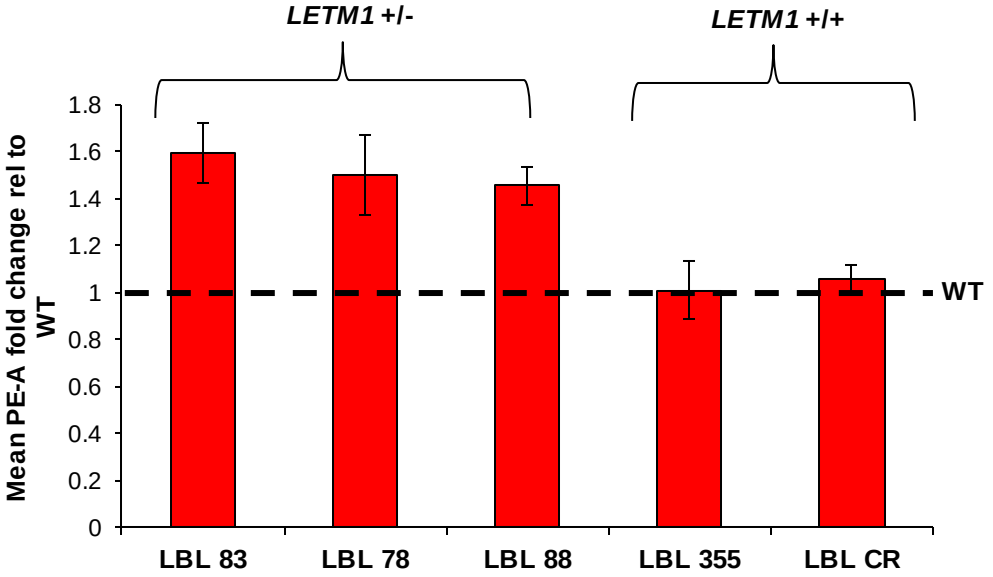

Figure 6.14 - Haploinsufficiency of *LETM1* correlates with elevated levels of mitochondria-specific ROS. A representative histogram showing the mean PE-A fold change in MitoSOX flourescence intensity relative to wildtype (black dashed line). LBLs were incubated with 250nM MitoSOX and analysed for PE-A flourescence using the FACS Canto platform. WHS LBL 83, LBL 78 and LBL 88 exhibit elevated Mitotracker SOX indicative of elevated O_2^- production compared to WT LBLs and LBL 355 and CR (*p<0.05 Student t-test*). This data represents the mean ± SD of 5 independent experiments.

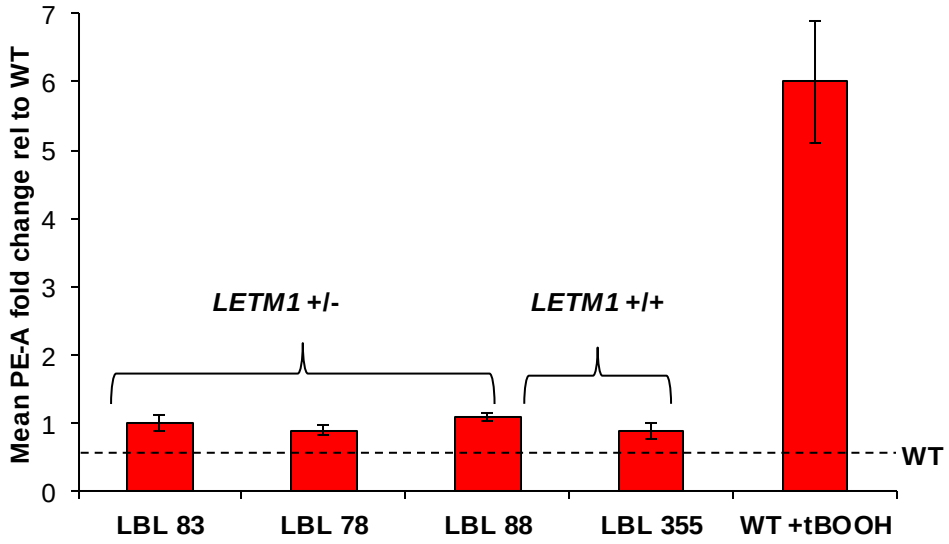

Figure 6.15 – Total cellular ROS is normal in WHS patient-derived LBLs compared to WT control LBLs. A representative histogram showing the mean PE-A fold change relative to wild-type (black dashed line). LBLs were incubated with Cell ROX Red as per manufacturers protocol and analysed for PE-A fluorescence on the FACS Canto flow cytometer. Control WT LBLs were also treated with 100μM tBOOH for 1 hour prior to Cell Rox Red incubation, to induce ROS. All of the WHS LBLs, irrespective of *LETM1* copy number , exhibit a comparable level of Cell Rox Red fluorescence to WT. This data represents the mean ± SD of three independent determinations. WT; wild-type.

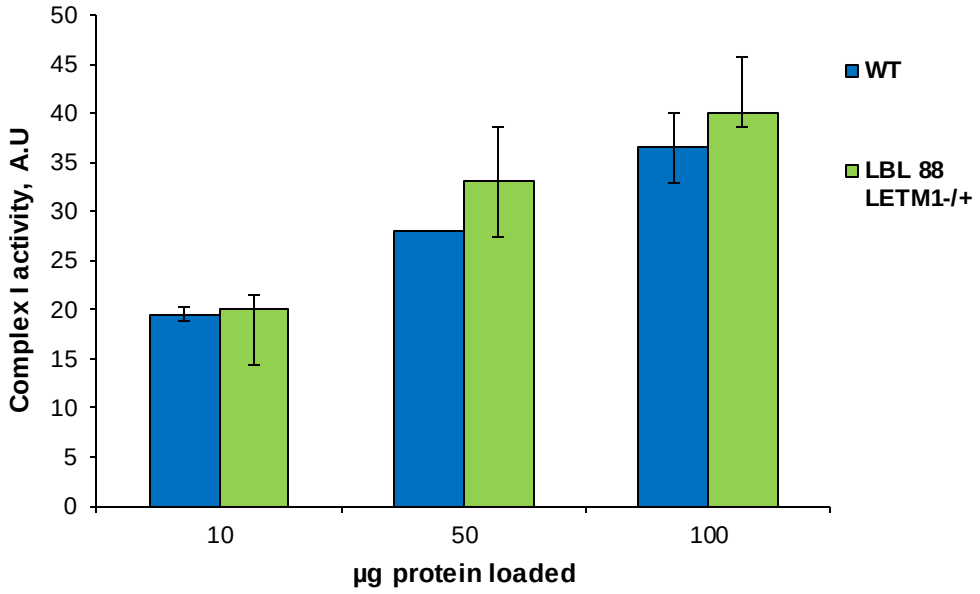

Figure 6.16 - Complex I activity is unchanged in *LETM1* -/+ WHS patient-derived LBLs (LBL 88). Extracts were prepared as per the manufacturers protocol. Increasing amounts of protein extract were loaded onto the complex I assay dipstick and the resultant antibody line was scanned and intensity measured in Image J. A.U; Arbituary units. The data represents the mean of 3 independent determinations ± SD.

6.2.2.3: WHS patient LBLs exhibit elevated levels of intracellular calcium

The report that the putative IMM protein LETM1, previously described as a K^+/H^+ exchanger, could be a Ca^{2+}/H^+ antiporter was received with great interest (Jiang et al, 2009b; Waldeck-Weiermair et al, 2011). However, some suggest that the effects of downregulation or overexpression of *LETM1* on mitochondrial calcium transport could be a secondary effect of altered K^+/H^+ exchange activity (Nowikovsky et al, 2012b). In addition to producing ATP, the mitochondria serve as central players in cellular Ca^{2+} signalling by acting as very efficient mobilisable intracellular Ca^{2+} buffering systems. Ca^{2+} uptake is achieved primarily by the mitochondrial Ca^{2+} uniporter (MCU) and this is highly dependent on the gradient established by the electron transport chain across the inner mitochondrial membrane, the Ψ^m (Gunter et al, 2000; O'Rourke, 2007). Other pathways of Ca^{2+} entry into the mitochondria include the "rapid mode" mechanism (RaM) and the mitochondrial Ryanodine Receptor (mRyR). Conversely, Ca^{2+} efflux is achieved by exchange for Na^+ which, in turn, is exchanged for H^+ (reviewed in Gunter, 2000). Both influx and efflux of Ca^{2+} consumes the mitochondrial membrane potential and are thus highly reliant on optimal mitochondrial functioning.

Ca^{2+} itself is a key regulator of mitochondrial function, acting at several levels to stimulate oxidative phosphorylation and ATP production (reviewed in Tarasov, 2012). Physiological increases in mitochondrial calcium ($[Ca^{2+}_m]$) lead to activation of various TCA cycle enzymes such as pyruvate dehydrogenase and isocitrate dehydrogenase (McCormack & Denton, 1993). Ca^{2+} also stimulates ANT (Complex V) and ATP synthase which upregulates ATP production and thus Ca^{2+} is an overall positive regulator of mitochondrial function (Tarasov, 2012 and Feissner, 2009). However, when overloaded, Ca^{2+} becomes a pathological signal leading to opening of the mPTP and the initiation of apoptosis (Crompton, 1999). ROS generated as a consequence of ATP production in the mitochondria regulate the function of redox sensitive enzymes and ion channels within the cell, including Ca^{2+}. ROS can modulate Ca^{2+} homeostasis at several levels and thus stimulate and inhibit Ca^{2+} channels, pumps and exchangers. Some examples include the oxidation of ryanodine receptors (RyR) resulting in their activation, stimulation of IP3R mediated Ca^{2+} release from the ER, oxidation and subsequent inhibition of SERCA

and PMCA, and modulation of NCX activity (plasma membrane Na+/Ca^{2+} exchange) (Scherer & Deamer, 1986; Xu et al, 1997; Xu et al, 1998; Zaidi & Michaelis, 1999). It is also important to mention that just as redox state can significantly modulate Ca^{2+} signalling, a reciprocal relationship exists where Ca^{2+} also plays a role in the generation of ROS through a number of mechanisms. These include but are not limited to; 1) stimulation of TCA cycle enzymes (isocitrate dehydrogenase and pyruvate dehydrogenase) which enhances oxidative phosphorylation and thus ROS production, 2) stimulation of NOS generates NO which inhibits complex IV enhancing ROS generation, 3) enhancing cytochrome c dislocation from the IMM resulting in respiratory chain blockage at complex III and 4) induction of the mPTP and the loss of antioxidants from the mitochondria which diminishes the antioxidant capacity of the mitochondria (Reviewed in Feissner et al, 2009). Furthermore, evidence also indicates that Ca^{2+} can minimize oxidative stress by stimulating catalase and GSH reductase (Brookes et al, 2004). The underlying mechanisms for Ca^{2+}-induced mitochondrial ROS generation are not fully understood. Nevertheless, it appears that calcium is both a positive and negative regulator of redox state.

The data presented so far indicates the haploinsufficiency of *LETM1* is associated with disruption of the mitochondrial membrane potential and an increased generation of ROS from the mitochondria. Therefore, the mitochondrial phenotypes uncovered so far suggest that altered Ca^{2+} homeostasis may also potentially exist in this setting, consistent with previous reports of a role for LETM1 in Ca^{2+} exchange (Jiang et al, 2009a; Waldeck-Weiermair et al, 2011). I investigated the impact of *LETM1* haploinsufficiency on intracellular Ca^{2+} levels in WHS patient-derived LBLs using the long-wave calcium indicator; Calcium 1-AM. The mechanism of action of Calcium 1-AM has previously been described in detail in Chapter 3, section 3.2.2.7. Flow cytometry analysis of calcium 1-AM fluorescence (FITC/green) revealed that WHS patient-derived LBLs exhibited increased levels of intracellular calcium which segregated with *LETM1* haploinsufficiency (Fig 6.17a and 6.17b). This data is consistent with the phenotypes of excessive ROS generation and disrupted mitochondrial membrane potential presented in the previous sections.

An intricate crosstalk between Ca^{2+}, ROS and membrane potential exists whereby perturbations to one factor can significantly impact on the others. It appears that in the context of *LETM1* copy number change, all three factors are significantly affected, however whether any of these are merely a secondary consequence of altered KHE activity, as suggested in the literature, is unclear. Whilst physiological increases in Ca^{2+} are overall positive regulators of mitochondrial function, Ca^{2+} overloads are detrimental and can quickly become pathological. One important consequence of increased intracellular Ca^{2+} or Ca^{2+} overload is the opening of the mitochondrial permeability transition pore, especially when coupled with increased levels of ROS (Baumgartner et al, 2009; Wong et al, 2012). Therefore, in light of the phenotypes identified so far, I investigated whether opening of the mPTP may be mis-regulated in WHS patient-derived cells.

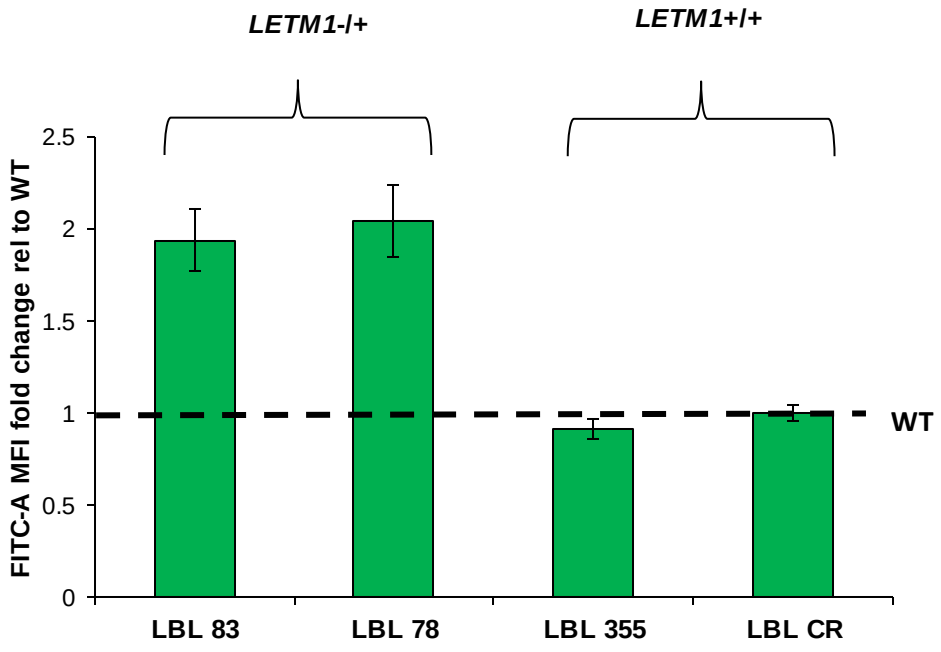

Figure 6.17a – Histogram**;** *LETM1* haploinsufficiency is associated with elevated intracellular calcium levels (*WT versus LBL 83 or LBL 78; p<0.05 Student t-test*). Cells were incubated with 10µM Calcium-1 AM for 20 minutes at 37°C. Cells were then washed in PBS, resuspended in 500µL PBS and analysed by flow cytometry for FITC fluorescence, excitation/emission filters; 506/531. The Y axis represents that fold change in mean fluorescence intensity (MFI) relative to wild type controls (WT). The data represents the mean ±SD of 3 independent experiments relative to wild type controls (black dashed line).

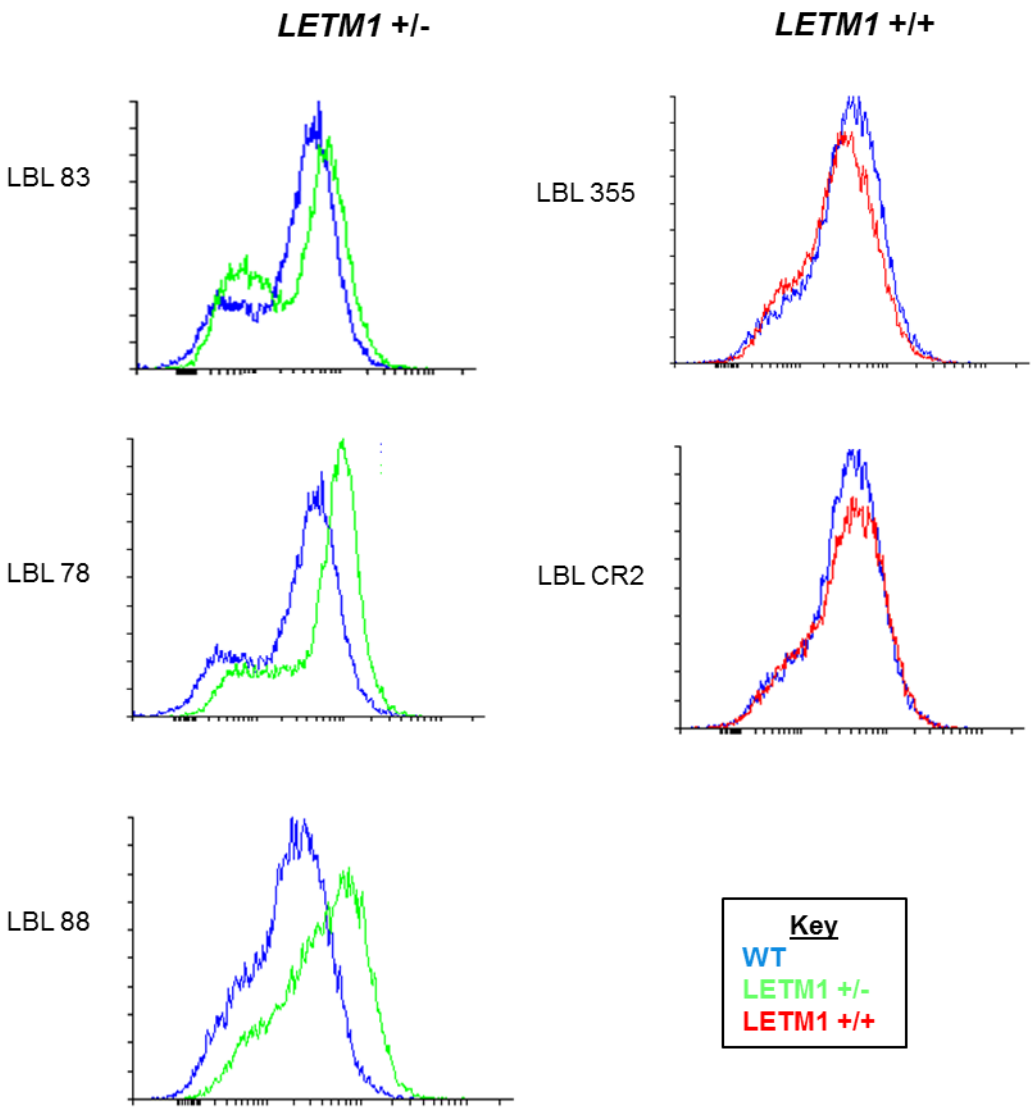

Figure 6.17b – Flow cytometry profiles**;** *LETM1* haploinsufficiency is associated with elevated levels of intracellular calcium. These FACS profiles represent one single experiment of the mean data shown in Figure 6.17a. The FACS profiles for WT control LBLs are shown in blue, *LETM1*+/- LBLs are shown in green and exhibit a rightward shift in FITC fluorescence intensity (x-axis) and *LETM1* +/+ LBLs are shown in red and exhibit a similar profile to WT controls.

6.2.2.4: Decreased opening of the mPTP in LETM1-/+ WHS patient-derived LBLs

As previously described in Chapter 3 section 3.2.2.8, the mitochondrial permeability transition pore (mPTP) is a non-selective, voltage-dependent mitochondrial channel proposed to reside in the IMM. Opening of the mPTP increases the permeability of the IMM to solutes >1.5kDa. Under normal physiological conditions the pore can flicker between an open and closed state, however various stimuli such as ROS and increased levels of Ca^{2+} promote the sustained opening of this pore. Chronic opening of this pore has many consequences; damage to mitochondrial ultrastructure such as mitochondrial swelling, depolarisation of the mitochondrial membrane potential leading to impaired OXPHOS, reduced ATP production and stimulation of ROS generation. Unless pore closure occurs, irreversible damage can ensue leading to cell death via necrotic or apoptotic pathways. The primary trigger stimulating mPTP opening is a rise in mitochondrial Ca^{2+}, especially when accompanied by increased ROS, ATP depletion, increased phosphate concentrations and mitochondrial membrane depolarisation. In contrast, increased ATP production, low pH and increased mitochondrial membrane potential can stabilise the pore in its closed state. In addition Mg^{2+} levels are also reported to inhibit pore opening however the mechanisms behind their inhibitory action are not fully understood (Brenner & Moulin, 2012).

In this chapter I have so far shown that WHS patient-derived LBLs haploinsufficient for *LETM1* display hyperpolarisation of the mitochondrial membrane potential, increased generation of ROS and elevated levels of intracellular Ca^{2+}. Both oxidative stress and rising mitochondrial Ca^{2+} levels can stimulate the sustained opening of the mPTP, whereas the increased membrane potential favours a closed pore state (Baumgartner et al, 2009; Brenner & Moulin, 2012; Wong et al, 2012). It is possible that mitochondrial dysfunction here could lead to hypersensitivity of the mPTP, a phenotype observed in the *CUL4B*-deleted LBLs described in Chapter 3. However, *CUL4B*-deleted LBLs exhibited a striking depolarisation of the mitochondrial membrane potential which is in contrast to the hyperpolarisation seen in this setting. Therefore, it is possible that the altered

mitochondrial physiology here may inhibit pore opening and render the mPTP insensitive to Ca^{2+} overloads, even in the presence of excessive ROS.

I employed the MitoProbe Transition Pore Assay Kit, previously described in Chapter 3, to investigate ionomycin-induced opening of the mPTP in WHS patient-derived LBLs. Briefly, cells are loaded with the acetoxylmethyl ester form of calcein which emits bright green fluorescence once cleaved by esterases inside the cell. The addition of $CoCl_2$ quenches the cytosolic calcein fluorescence but maintains mitochondrial-specific fluorescence resulting in a slight shift in FITC fluorescence intensity. Cells can be treated with $CoCl_2$ and ionomycin at the same time which allows the entry of excess calcium into the mitochondria, triggering opening of the mPTP. Once open, the fluorescing calcein within the mitochondria can exit into the cytosol and be quenched by the $CoCl_2$ resulting in a dramatic shift in fluorescence intensity. It is this shift in fluorescence intensity that indicates the continuous activation of the mPTP (See Chapter 3, Figure 3.26 for schematic).

I evaluated opening of the mPTP under basal conditions; that is with the addition of CaAM and $CoCl_2$ only. This gives indications of the basal level of mPTP flickering between open and closed states without the addition of an activating stimulus. Analysis of calcein fluorescence in the absence of $CoCl_2$ was comparable in all cells lines examined, indicating similar calcein loading. In the presence of $CoCl_2$, calcein fluorescence was higher in *LETM1*-/+ LBLs (LBL: 83) compared to WT controls and WHS LBLs carrying normal copy number for *LETM1* (LBL: 355) (Fig 6.18a). This suggests that flickering of the mPTP between open and closed states was more favoured towards the closed state under basal conditions in *LETM1* haploinsufficient cells. I further investigated whether treatment with ionomycin, a Ca^{2+} ionophore, would induce a decrease in calcein fluorescence, indicative of mPTP opening. As expected, following ionomycin treatment the calcein signal was considerably reduced (~ -60%) in WT and WHS LBLs with normal *LETM1* copy number (LBL: 355), consistent with opening of the mPTP (Fig 6.18b). However, treatment of WHS patient-derived LBLs haploinsufficient for *LETM1* (LBL: 83) with ionomycin had little effect on the calcein signal. WHS83 LBLs exhibited a 20% reduction in calcein signal in comparison to the 60% reduction observed in cells with normal *LETM1* copy number (Fig 6.18b). These observations indicated that

the mPTP was insensitive to Ca^{2+} overloads and thus potentially inhibited. This data also provided support that the higher mitochondrial-specific calcein signal in *LETM1* -/+ LBLs was due to decreased opening of the mPTP under basal conditions.

Although *LETM1*-/+ LBLs exhibit phenotypes reported to stimulate opening of the mPTP, they also display characteristics which favour mPTP inhibition. These inhibitory signals may be sufficient to surpass the activatory signals of excessive ROS and increased Ca^{2+} levels associated with *LETM1* haploinsufficiency and thus inhibition dominates. Furthermore, *LETM1* downregulation has been shown to induce mitochondrial swelling due to altered KHE activity (Nowikovsky et al, 2004). Although this has not been investigated here, it is possible that mitochondrial swelling may *physically* inhibit the pore's capacity to open. It would be interesting to investigate whether treatment with an ionophore, functioning to restore KHE activity, could restore mPTP opening. Alternatively, due to the chronic exposure to ROS and Ca^{2+} overloads, the mPTP may, over time, may be rendered insensitive and thus does not respond to further perturbations.

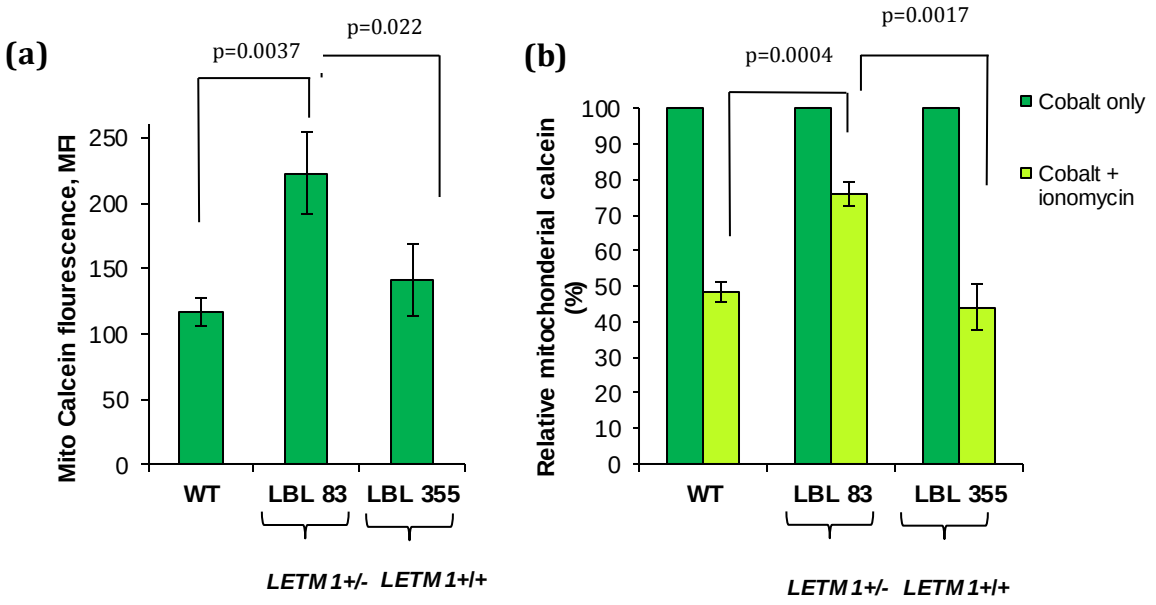

Figure 6.18 - Opening of the mPTP is disrupted in the context of *LETM1* haploinsufficiency. **(a)** Bar graph of the mitochondrial-specific calcein signal in the presence of $CoCl_2$ measured by FACS analysis shows increased mitochondrial calcein signals in *LETM1*-/+ WHS cell line 83 (LBL 83). **(b)** Bar graph of % calcein signal in the presence of $CoCl_2$ ± 500nM ionomycin treatment. *LETM1*-/+ WHS patient cell line 83 (LBL 83) shows increased calcein signal following ionomycin treatment indicative of mPTP inhibition. The *student t-test* was used for statistical analysis, as indicated.

6.2.3: siRNA mediated knockdown of *Letm1*

I have uncovered novel mitochondrial phenotypes associated with *LETM1* haploinsufficiency using a unique panel of WHS patient-derived LBLs with different sized deletions. To confirm that the under-expression of *LETM1* specifically could underlie these phenotypes I investigated mitochondrial function in mouse Neuroblastoma 2A (N2A) cells following siRNA-mediated depletion of *LETM1*. As WHS patients exhibit many features consistent with a neurological deficit, such as seizures and MR, this N2A cell line provides an excellent model for investigating *LETM1* haploinsufficiency in a neuronal setting.

It is important to note that WHS patient-derived LBLs exhibit *haploinsufficiency* of *LETM1* which leads to a 50% reduction in the protein expression levels. Therefore, I aimed to mimic this setting with a 50% siRNA-mediated knockdown of *Letm1*. Western blot analysis confirmed a 50% reduction in Letm1 protein expression levels following a single transfection, thus mimicking the patient genotype (Figure 6.19a). I then sought to investigate the impacts of a 50% *Letm1* knockdown on membrane potential maintenance and ROS generation and found that depletion of Letm1 imparted striking effects on both, consistent with the phenotypes observed in patient-derived LBLs. Partial knockdown of *Letm1* led to a ~1.6 fold increase in the mitochondrial membrane potential with no increase in mitochondrial mass (Fig 6.19b-c). In addition, *Letm1* downregulation led to a dramatic increase in mitochondrial ROS generation whereby siRNA transfected cells exhibited a ~1.7 fold increase in superoxide levels compared to untransfected controls (Fig 6.19b-c). Collectively, these data are identical to the mitochondrial phenotypes observed in WHS patient-derived LBLs and provide further support of a vital role for LETM1 in mitochondrial function and homeostasis.

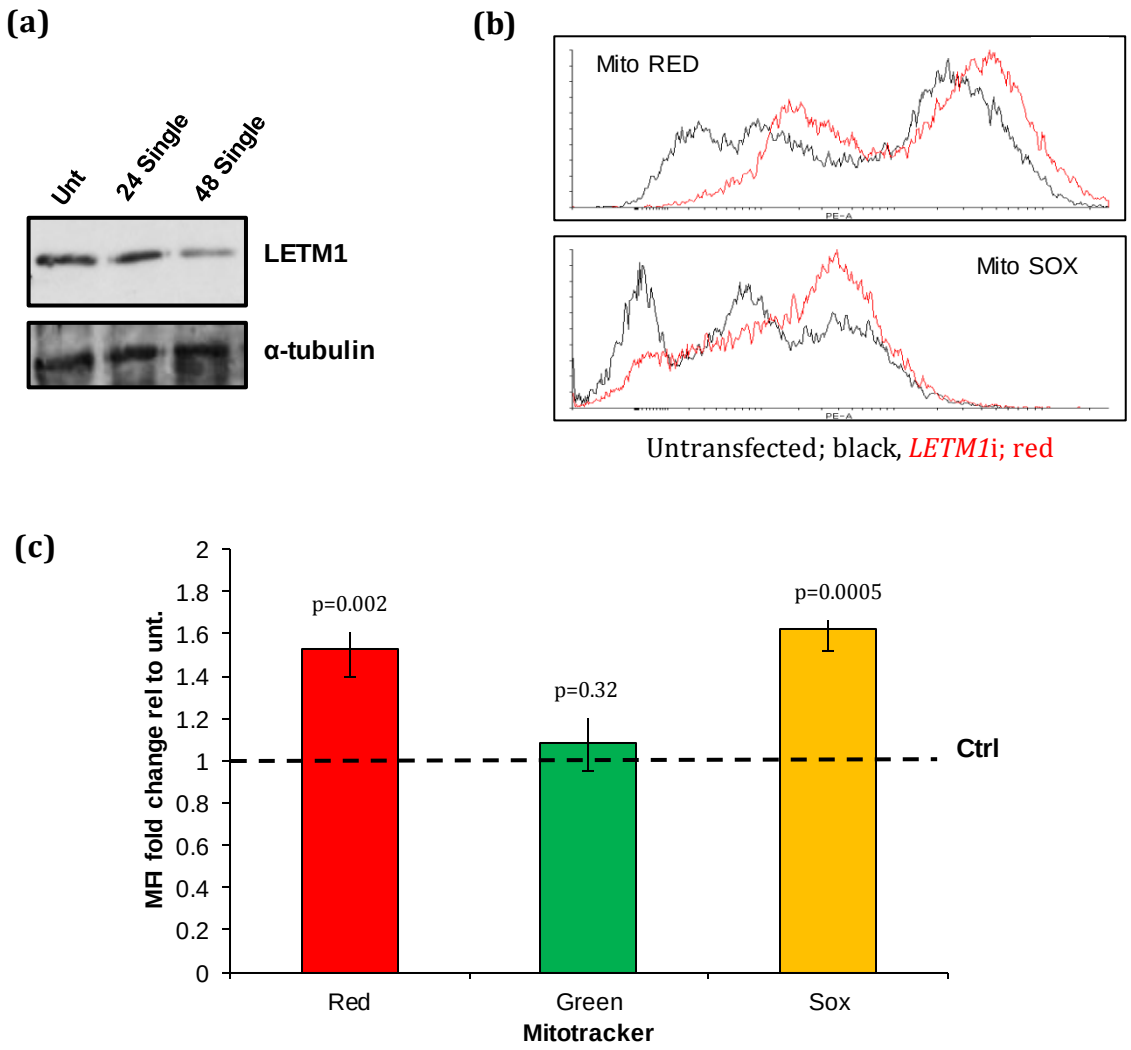

Figure 6.19 – Reduced expression of LETM1 is associated with mitochondrial dysfunction **(a)** N2A cells were transfected with siRNA oligo against *Letm1* and harvested 24-48 hours post-transfection. Whole cell extracts were immunoblotted for Letm1 protein expression levels and confirmed a 50% knockdown of *Letm1*. α-tubulin expression was used a loading control. **(b)** FACS profiles for Mitotracker Red (Mito RED) and MitoSOX (Mito SOX) 48 hours post transfection with siRNA oligo against *Letm1*. Upper panel shows the Mitotracker Red PE-A profiles for untransfected (black) and *Letm1* siRNA-transfected cells (red) N2A cells. Lower panel shows MitoSOX PE-A FACS profile for untransfected (black) and *Letm1* siRNA-transfected (red) N2A cells 48 hours post-transfection. Untransfected cells were treated with Metafectene Pro only. **(c)** Histogram shows the mean fold change in mean fluorescence intensity (MFI) for each Mitotracker probe, as analysed on the FACS Canto flow cytometer, 48 hours post transfection relative to untransfected N2A cells (black dashed 'Ctrl' line). siRNA of *Letm1* is associated with increased hyperpolarisation (elevated ΔΨmito) and elevated O_2^- production, without impacting on mitochondrial mass. Data represents the mean ± SD of 3 independent determinations. p values were obtained by *student t-test* statistical analyses, as indicated.

6.2.4: Ectopic antioxidant treatment fails to rescue the mitochondrial phenotypes associated with *LETM1* haploinsufficiency

ROS are a by-product of mitochondrial respiration and the levels of ROS are kept at a low level by various antioxidant systems within the cell. The definition of an antioxidant as proposed by Halliwell is; *any substance that, when present at low concentrations compared with those of an oxidisable substrate, significantly delays or prevents oxidation of that substrate* (Halliwell, 1995). An important part of the endogenous antioxidant systems are the antioxidant enzymes such as superoxide dismutases and peroxidases. In addition to these enzymes, cells possess small-molecule antioxidants such as α-tocopherol (the active form of Vitamin E) which play equally important roles in the antioxidant defence mechanisms. When the generation of ROS is so excessive that it surpasses these systems, oxidative stress and cellular damage can occur. The data reported here reveals that *LETM1* haploinsufficiency, in the context of WHS, is associated with considerable increases in the generation of mitochondria-specific ROS, specifically superoxide (O_2^-). I investigated whether antioxidant treatment in WHS patient-derived LBLs could rescue the mitochondrial phenotypes observed here.

N-acetyl-Cysteine and Lipoic Acid

I employed the antioxidants N-acetyl-Cysteine (NAC) and Lipoic Acid (LA) in an attempt to rescue the ROS phenotype associated with haploinsufficiency of *LETM1*. WHS patient LBLs were treated with NAC or LA at varying concentrations (500μM – 50mM NAC or 0.1μM-50μM LA) for 1 hour and then analysed for MitoSOX fluorescence by flow cytometry. Neither NAC nor LA treatment resulted in a decrease in the levels of superoxide, under these conditions (Fig 6.20). Furthermore, at some concentrations treatment was found to increase ROS production. This was particularly evident at concentrations of NAC above 20mM however this was later attributed to a change in pH of the media (observed as a colour change from pink to yellow) caused by the very high concentration of NAC. With regards to LA treatment, no considerable difference in ROS levels was

observed following treatment of varying concentrations. Neither NAC nor LA are mitochondrial-specific antioxidants and this could explain why their use here was unable to rescue the mitochondrial-specific phenotypes observed in WHS patient LBLs.

α-tocopherol

Addition of NAC and LA failed to rescue the ROS phenotype of *LETM1*-/+ LBLs possibly due to their non-specific nature. α-tocopherol, also known as Vitamin E, is enriched in the mitochondrial membrane, the site of Complex I and ubiquinone; two complexes that produce ROS. Therefore, I investigated whether treatment with this mitochondria-specific antioxidant could rescue to ROS phenotype of *LETM1 -/+* cells. Following treatment with 1-100μM of α-tocopherol for 24 hours, *LETM1*-/+ LBLs displayed similar levels of ROS to their untreated counterparts indicating that this treatment was not sufficient to decrease the levels of ROS (Fig 6.21a). It is possible that this acute treatment did not allow sufficient time to rescue the phenotype and I therefore investigated the effects of a chronic α-tocopherol treatment. However, chronic treatment of *LETM1*-/+ LBLs (LBL: 83) with 10μM α-tocopherol for 7 days was not sufficient to induce a considerable change in ROS levels either (Fig 6.21b).

Nigericin

Nigericin, a potassium ionophore, has previously been reported to rescue the mitochondrial swelling associated with *LETM1* downregulation (Nowikovsky et al, 2004). Whether the phenotypes I have observed are a cause or consequence of the mitochondrial swelling and loss of KHE associated with *LETM1* haploinsufficiency is unknown, however it is possible that this altered mitochondrial morphology could impart negative effects on mitochondrial function particularly OXPHOS. Therefore, I speculated that treatment with nigericin may rescue the mitochondrial phenotypes identified here by restoring KHE activity and reducing the mitochondrial swelling. Cells were treated with 2μM nigericin for up to 24 hours

and then analysed by flow cytometry for Mitotracker Red and MitoSOX fluorescence. The data presented in Figure 6.22 indicated that the addition of nigericin was not able to restore the mitochondrial membrane potential to a WT level nor was it sufficient to decrease the production of mitochondrial ROS. This suggested that the mitochondrial dysfunction observed here could not be rescued by attempting to restore KHE activity and suggests that LETM1 possesses crucial roles within the mitochondria aside from the regulation of KHE activity and mitochondrial morphology.

Collectively, these data indicate that the addition of exogenous antioxidants fails to restore the ROS phenotype of *LETM1-/+* mitochondria. This could indicate that the ROS phenotype observed here is a consequence, rather than the underlying cause, of the mitochondrial dysfunction. It is also possible that there is a maximum antioxidant capacity for the cell and modifying the levels of one antioxidant causes compensatory changes in the levels of others. Treating cells with exogenous antioxidants may decrease the rate of synthesis or uptake of endogenous antioxidants, so that the antioxidant capacity of the cell remains unaltered. Furthermore, low levels of ROS are beneficial for many signalling processes and antioxidants cannot distinguish between harmful and beneficial reactive species. Therefore, increased intake of antioxidants may disrupt the redox balance and negatively impact on cellular processes which use ROS as signalling molecules thus leading to cellular dysfunction.

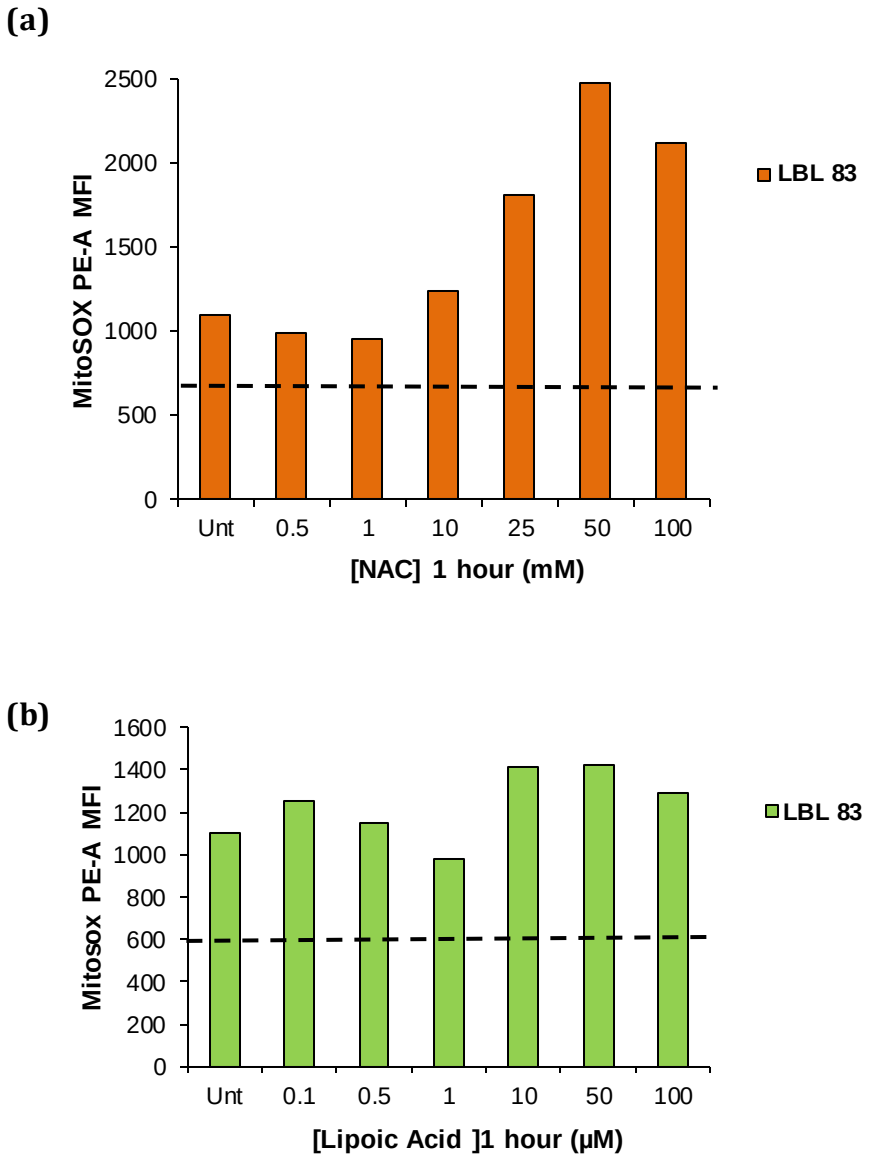

Figure 6.20 – Antioxidant treatment fails to reduce ROS levels in WHS *LETM*1 -/+ LBLs. **(a)** *LETM*1 -/+ patient-derived LBLs (LBL 83) were treated with varying concentrations of N-acetyl-cysteine one hour. LBLs were then incubated with 250nM MitoSOX for 15 minutes and analysed for PE fluorescence using the FACS Canto Flow cytometer. Y axis represents the MitoSOX MFI of 20,000 events. **(b)** *LETM1* -/+ patient-derived LBLs (LBL 83) were treated with varying concentrations of Lipoic Acid for one hour. LBLs were then incubated with 250nM MitoSOX for 15 minutes and analysed for PE fluorescence using the FACS Canto Flow cytometer. The black dashed line represents the mean MitoSOX fluorescence intensity of untreated WT control LBLs for each experiment. MFI; mean fluorescence intensity, Unt; untreated cells.

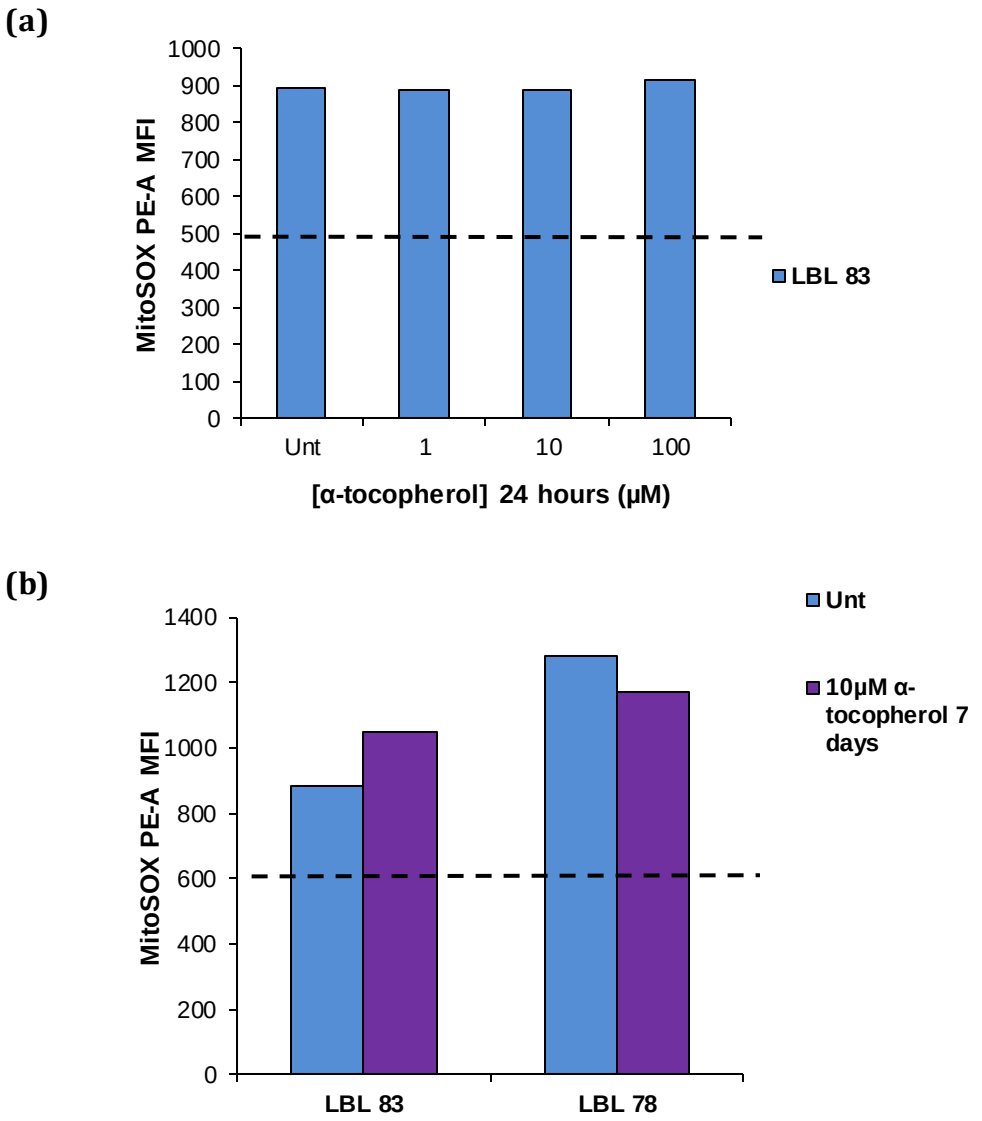

Figure 6.21 – Treatment with the mitochondria-specific antioxidant, α-tocopherol fails to restore ROS levels. **(a)** *LETM1* -/+ patient-derived LBLs (LBL 83) were treated with 1-100μM α-tocopherol for 24 hours and the incubated with 250nM MitoSOX. MitoSOX PE fluorescence was analysed using the FACS Canto flow cytometer. **(b)** Two *LETM1* -/+ WHS patient-derived cell lines were used here; LBL 83 and LBL 78. LBLs were treated with 10μM α-tocopherol for 7 days followed by 15 minute incubation with 250nM MitoSOX. MitoSOX mean PE-A fluorescence of 20,000 events was then analysed on the FACS Canto flow cytometer relative to untreated WT control LBLs (black dashed line).

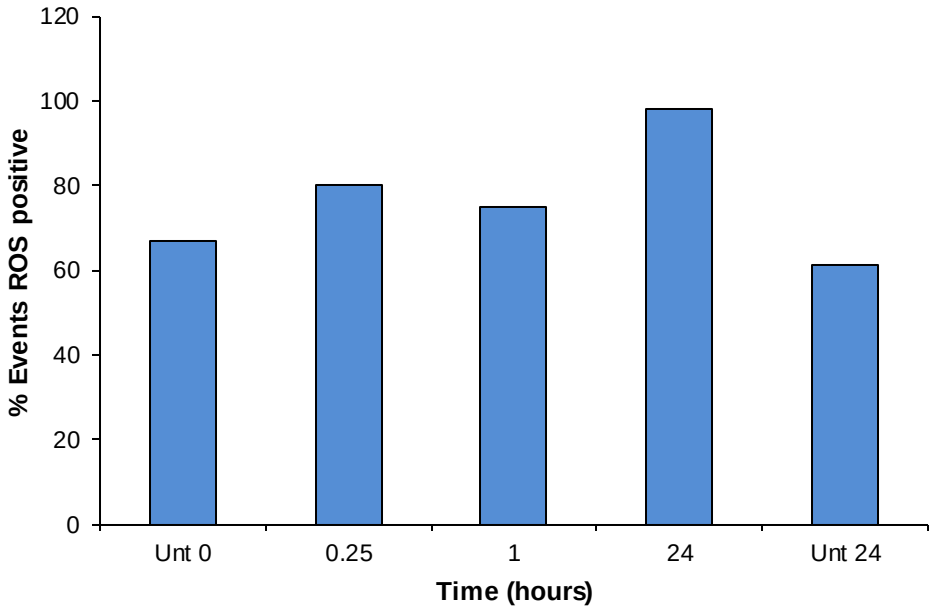

Figure 6.22 – Nigericin treatment fails to reduce ROS generation. *LETM1*-/+ WHS patient-derived LBLs (LBL 83) were incubated with 2μM nigericin for the indicated time points. Cells were incubated with 250nM MitoSOX for 15 minutes following nigericin treatment and analysed for PE-A fluorescence using the FACS Canto flow cytometer. Untreated controls were also analysed for MitoSOX fluorescence at 0 hours and 24 hours post seeding. The histogram represents the % of events with a high fluorescence/ROS positive. 20,000 events were analysed per sample. Unt; untreated.

6.2.5: Treatment with Valproic Acid fails to restore mitochondrial homeostasis in WHS LBLs

Seizures occur in many children with WHS and are frequent cause of death (Battaglia A, 2000; Battaglia et al, 2009; Kagitani-Shimono et al, 2005). The age of onset varies from 3 - 23 months with a peak incidence of 6-12 months. The seizures observed in WHS are frequently triggered by fever and are either unilateral clonic or tonic seizures or generalised tonic-clonic seizures from the onset (Battaglia et al, 2009). Other seizure types observed in WHS patients include alternative hemiconvulsions, myoclonus, focal clonic seizures and epileptic spasms (Kagitani-Shimono et al, 2005). In addition, status epilepticus occurs in approximately 50% of WHS individuals. However, it is worthy to note that 90% of WHS patients display distinctive EEG abnormalities which are not always associated with seizures (Battaglia et al, 2009).

Valproic acid, a simple branched-chain fatty acid, is routinely used as an anticonvulsant and mood-stabilising drug. In particular, it is primarily used in the treatment of epilepsy, bipolar disorder, schizophrenia and major depression (Chronicle & Mulleners, 2004; Fountoulakis et al, 2005; Loscher, 2002). As an anticonvulsant, valproic acid (VPA) is commonly used to control absence seizures, tonic-clonic seizures, myoclonus and complex partial seizures (Loscher, 2002). The mechanisms behind its antiepileptic effects are not fully understood but are thought to involve the enhancement of GABA-mediated neurotransmission, inhibitory effects on voltage-gated Na^+ channels and activation of the ERK signalling pathway (Monti et al, 2009). However, the mechanisms of action of valproate not only involve biochemical effects but also induce changes at the genomic level. HDACs are key enzymes controlling histone acetylation sites and hence epigenetic regulation of gene expression. Recent research suggests that valproate can affect the expression of multiple genes by inhibiting many HDACs (Bosetti et al, 2003; Eyal et al, 2004; Gottlicher et al, 2001; Newton & Duman, 2006; Phiel et al, 2001; Tang et al, 2004). However the contributions of HDAC inhibition to the antiepileptic effects of valproate are unknown. It is likely that

valproate-mediated changes in the expression of multiple genes play an important role in the long-term effects of this drug (Eyal et al, 2004).

It is well documented that the seizures associated with WHS can be well-controlled with VPA treatment (Battaglia A, 2000; Battaglia et al, 2009). Aside from VPA, other drugs such as sodium bromide and benzodiazepines can also be used to control seizures in the form of status epilepticus, clonic and tonic-clonic seizures (Kagitani-Shimono et al, 2005; Valente et al, 2003). Many WHS individuals later develop valproic acid-responsive atypical absences and thus it is important that valproic acid treatment is started soon after the first seizure. In the early years, treatment of seizures can prove difficult however, when properly controlled, seizures tend to disappear with age (Battaglia et al, 2009). In fact, Battaglia et al (2009) recently reported that epilepsy was well-controlled with valproate and phenobarbital in 81% of WHS patients, 55% of which are now seizure-free.

Mitochondrial dysfunction and the excessive generation of ROS are key players in the pathogenesis of seizures. In fact, seizures are a frequently reported clinical feature of many known mitochondrial disorders such as MERRF and MELAS. Therefore, in light of the mitochondrial phenotypes uncovered here I investigated whether treatment with VPA could restore mitochondrial homeostasis in WHS patient-derived LBLs (Folbergrova & Kunz, 2012). More specifically, I sought to identify whether VPA treatment was sufficient to reduce ROS levels in WHS patient-derived LBLs exhibiting *LETM1* haploinsufficiency. If so, this may provide support for a causative role for elevated ROS in the seizure phenotype of WHS.

LETM1 -/+ WHS patient-derived LBLs were incubated with 500μM-1mM VPA for 0-60 minutes followed by incubation with 250nM MitoSOX for 15 minutes. The MitoSOX PE fluorescence of treated cells in comparison to untreated controls was analysed by flow cytometry. The results in Figure 6.23a show that 0-60 minute treatments with VPA were not able to reduce ROS levels in *LETM1*-/+ LBLs (LBL: 83). In fact, 15 minute treatments led to a substantial rise in ROS levels. The data in Figure 6.23a indicated that acute VPA treatments were not sufficient to reduce ROS levels in this setting and suggested that a chronic treatment may be more effective. However, cells treated with VPA for 7 days displayed no reduction in ROS levels

(Fig 6.23b). In fact, on day 7 ROS levels were dramatically increased suggestive of apoptosis and cell death. The data reported here suggests that VPA-mediated control of seizures in WHS is not simply a result of restoring mitochondrial homeostasis. However, WHS patients require long-term treatment with VPA and it is likely that a 7 day treatment here is not sufficient to induce long lasting positive effects on mitochondrial function.

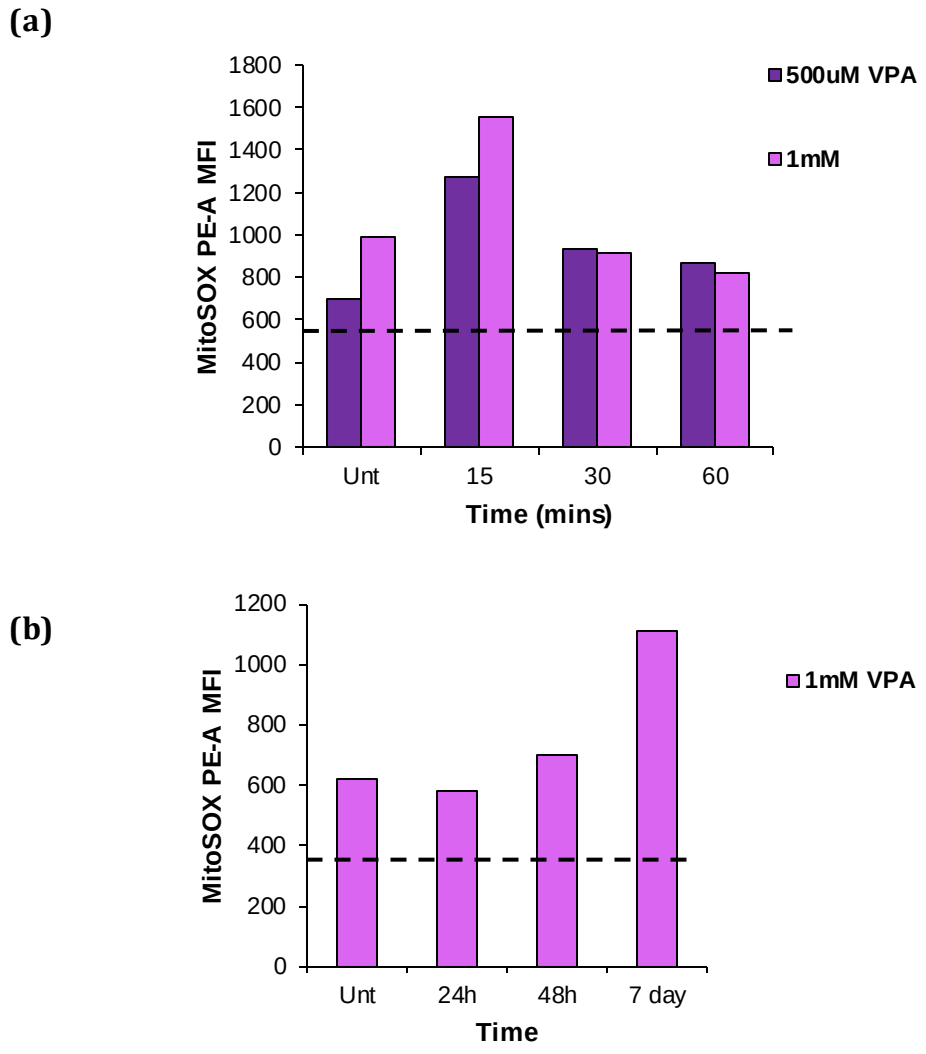

Figure 6.23 – Treatment with an anticonvulsant drug does not rescue the MitoSOX phenotype of *LETM1* -/+ WHS LBLs. **(a)** *LETM1-/+* LBLs (LBL 83) were treated with 500µM-1mM valproic acid for 0-60 minutes followed by a 15 minute incubation with 250nM MitoSOX. MitoSOX PE fluorescence of untreated vs. treated WHS patient-derived LBLs was analysed by flow cytometry. **(b)** WHS patient-derived LBLs (LBL 83) were treated with 1mM valproic acid for 7 days and analysed for MitoSOX fluorescence by flow cytometry at the indicated time points. The black dashed line indicated the MitoSOX MFI of WT controls for each separate experiment. MFI; mean fluorescence intensity of 20,000 events, VPA; valproic acid, Unt; untreated WHS LBL control.

6.2.6: Increased LETM1 copy number is associated with overlapping mitochondrial phenotypes

As discussed in Chapter 1, for many deletion syndromes there is a corresponding reciprocal duplication-associated syndrome. Until recently, no submicroscopic duplications covering the WHSCR had been reported. However in 2010, Hannes et al reported a 15 month old male child with a submicroscopic *de novo* 560 kb interstitial duplication including the WHSCR (Hannes et al, 2010). In particular, this duplication encompassed the *LETM1* gene. The patient presented with features that partially overlapped with the WHS deletion phenotype such as; speech delay, developmental delay and a facial dysmorphism with low set ears. Interestingly, this patient also suffered from seizures suggesting that *overexpression* of *LETM1* may also result in epilepsy. Subsequently, in 2011 Cyr and co-workers reported a second patient with novel 4p16.3 microduplication (Cyr et al, 2011b). The male patient presented with seizures, delayed psychomotor development and dysmorphic features. However in this case, the duplication was distal to *WHSC1* and *WHSC2*. Using a high-density oligonucleotide microarray they identified that this submicroscopic duplication involved the dosage sensitive genes *TACC3*, *FGFR3* and *LETM1*. The presence of seizures in this second reported duplication case further suggested a role for increased *LETM1* copy number in the underlying aetiology of seizures. In addition, as this duplication resides outside of the WHSCR it further supports the notion that additional genes outside of the WHSCR cause some of the key features of this disorder.

The data presented so far suggests that *LETM1* haploinsufficiency is detrimental to mitochondrial function. I aimed to investigate whether *LETM1* overexpression imparted similarly negative effects on mitochondrial function. Unfortunately, patient-derived material from either of the patients described above was unavailable. Therefore, I employed the human glioblastoma cell line T98G to investigate the impacts of modest *LETM1* overexpression on mitochondrial function. Cells were transfected with 2µg of a plasmid encoding *LETM1* (pCMV6-XL4) in the presence of 5µL Metafectene-Pro and harvested 24 hours post-transfection. Western blot analysis of urea-based whole cell extracts revealed a 1.7

fold increase in LETM1 protein expression levels and therefore this provided an excellent model for investigating the mitochondrial consequences of *LETM1* overexpression (Fig 6.24a).

Overexpression of *LETM1* resulted in the elevated generation of superoxide as indicated by a ~1.7 fold increase in MitoSOX fluorescence 24 hours post transfection in comparison to untransfected controls (Fig 6.24b and Fig 6.24c). These results are consistent with a previous report of mitochondrial dysfunction associated with *LETM1* overexpression in HeLa cells (Piao et al, 2009a). This data suggests that a change in copy number of *LETM1*, whether an increase or decrease, is detrimental to mitochondrial function and may potentially underlie the overlapping seizure phenotype associated with 4p16.3 deletions and duplications encompassing the *LETM1* gene.

6.2.7: *LETM1* complementation in a human glioblastoma cell line

Transfection of a plasmid encoding *LETM1* (pCMV6-XL4, OriGene) with Metafectene-Pro failed to complement *LETM1* expression in *LETM1*-/+ WHS patient-derived LBLs, even when used in conjunction with the Neon electroporation system (Invitrogen). This is likely a consequence of the poor transfection efficiency of LBLs. Therefore, I aimed to complement *LETM1*-/+ WHS patient-derived LBLs using a lentiviral-based transduction method (pReciever-Lv105 expressing *LETM1* cDNA from GeneCopoeia). Frustratingly, transduction with commercially produced lentiviral particles was unable to complement *LETM1.* In fact transduction was associated with a very high degree of toxicity. Therefore, I developed a model in a human gliobastoma cell line (T98G) that coupled siRNA knockdown of endogenous *LETM1* and add-back of a *LETM1* cDNA construct (pCMV6-XL4, OriGene). The *LETM1* siRNA construct was designed to the 3'-UTR of the endogenous gene, hence the cDNA construct is siRNA-resistant. Therefore, in this setting any phenotypes observed following *LETM1* siRNA should be rescued by the addition of the siRNA-resistant *LETM1* cDNA construct.

Western blot analysis confirmed that *LETM1* siRNA transfection in human T98G cells was effective in knocking down *LETM1*. The protein expression levels of LETM1 following siRNA were reduced by 60% (Fig 6.25a lane 3). Transfection with the siRNA-resistant *LETM1* cDNA construct alone revealed a 1.7 fold increase in LETM1 protein expression levels (Fig 6.25a lane 2). In section 6.2.6 I reported that marked overexpression of *LETM1* imparts detrimental effects on mitochondrial function similar to those of reduced *LETM1* expression. Therefore, it was important to ensure that add back of the *LETM1* cDNA construct did not result in overexpression of *LETM1*. Cells transfected with both *LETM1* siRNA and the *LETM1* cDNA construct exhibited LETM1 protein expression levels comparable to untreated controls confirming complementation (Fig 6.25a lanes 1 and 4). As expected, siRNA-mediated knockdown of *LETM1* in the T98G cell line led to a striking increase in MitoSOX fluorescence indicative of elevated ROS production (Fig 6.25c). Cells that were co-transfected with both *LETM1* siRNA and the siRNA-resistant *LETM1* cDNA construct exhibited MitoSOX fluorescence that was comparable to that of untransfected controls (Fig 6.24c). Collectively, this data confirms that the mitochondrial dysfunction observed here is *LETM1* expression specific. Furthermore, this data provides novel insight into the potential mitochondria-based mechanisms by which loss of *LETM1* may contribute to the pathogenesis of seizures in WHS.

6.2.8: Summary

In this chapter, I have provided the first evidence of a mitochondrial dysfunction in WHS patient-derived LBLs which segregates with haploinsufficiency of *LETM1* specifically. WHS patient-derived LBLs whose deletions encompass the *LETM1* gene exhibit reduced LETM1 expression, not only in urea-based whole cell extracts but similarly in pure mitochondrial extracts. Flow cytometry-based analyses have revealed that *LETM1*-/+ mitochondria display elevated levels of ROS (O_2^-). LETM1 was previously identified as a Ca^{2+}/H^+ antiporter, yet many have questioned this. However, I have uncovered novel evidence indicating that *LETM1*-/+ is associated with elevated levels of intracellular Ca^{2+} which appear to be localised in the mitochondria. Furthermore, treatment of *LETM1*-/+ mitochondria with the Ca^{2+}

ionophore, ionomycin, does not induce opening of the mPTP suggesting that the pore is inhibited or insensitive indicative of altered Ca^{2+} signalling in the context of *LETM1* haploinsufficiency. Using a siRNA knockdown cDNA add back method, I have further shown that complementation of *LETM1* reduced ROS production to a level similar to that of wild type cells. This indicates that the mitochondrial dysfunction identified here is a consequence of *LETM1* haploinsufficiency specifically. I have also provided evidence to suggest that increased *LETM1* copy number is detrimental to mitochondrial function. More specifically, overexpression of *LETM1* led to disruption of the mitochondrial transmembrane potential and the increased generation of ROS. This is consistent with overexpression of *LETM1* contributing to the seizure phenotype of individuals with the rare duplication of 4p16.

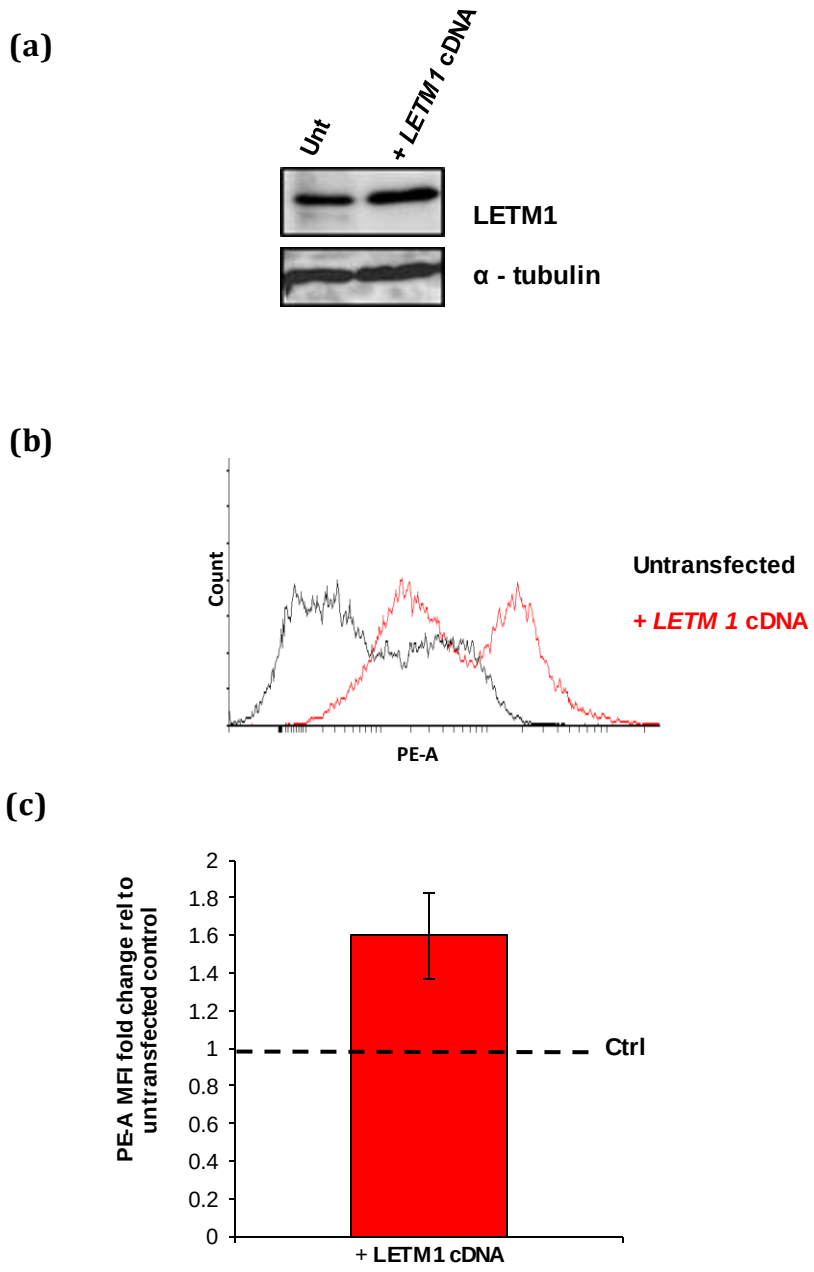

Figure 6.24 – Overexpression of *LETM1* is associated with depolarisation of the membrane and increased generation of ROS. **(a)** T98G cells were transfected with 2µg *LETM1* cDNA and 5µL metafectene and harvested 24 hours post transfection. Whole cell extracts were immunoblotted for LETM1 protein expression levels. Blots were reprobed for β-tubulin as a loading control. **(b)** MitoSOX PE-A FACS profile of untransfected (black line) and 24 hour post-transfection (red line) T98G cells. **(c)** A histogram showing the fold change in MitoSOX mean PE-A fluorescence intensity (MFI) of transfected cells relative to untransfected cells (black dashed line). Cells were incubated with 250nM MitoSOX for 15 mins 24 hours post transfection and analysed on the FACS Canto flow cytometer. Untransfected cells were treated with 5µL metafectene only (black dashed 'Ctrl' line). Cells transfected with the *LETM1* encoding plasmid exhibit a ~1.4-.16 fold increase in Mitotracker SOX fluorescence (*p<0.05 Student t-test*). Data represents the mean of 3 independent experiments ± SD.

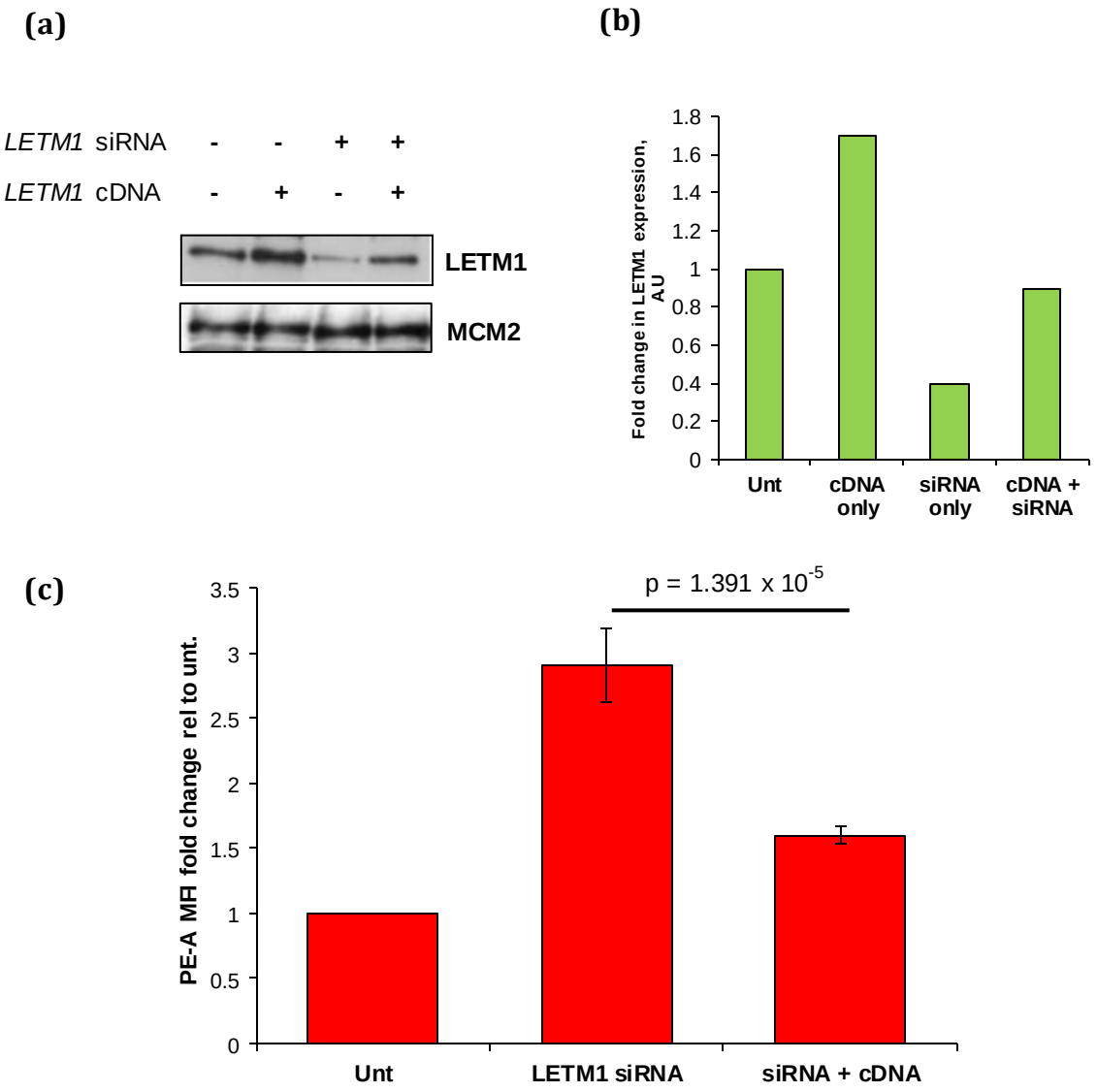

Figure 6.25 – siRNA-mediated knockdown of *LETM1* coupled with addback of a *LETM1*-cDNA construct restores mitochondrial function. **(a)** Human T98G glioblastoma cells were transfected with a cDNA construct alone (2μg), *LETM1* siRNA alone (5μL) or both cDNA and siRNA in the presence of metafectene. Whole cell extracts were prepared in urea-based lysis buffer and 10μg of protein was subjected to SDS-PAGE and immunoblotted for LETM1 protein expression. Western blot analysis confirmed knockdown of LETM1 following siRNA (lane 3) and subsequent LETM1 complementation with the addition of the cDNA construct (lane 4). **(b)** Representative histogram of relative LETM1 protein expression compared to untransfected controls, measured by Image J software (arbitrary units). **(c)** MitoSOX fluorescence intensity is increased 3 fold following *LETM1* knockdown using a 3'-UTR directed oligonucleotide directed against the endogenous gene, compared to untransfected controls (*Unt versus siRNA p<0.05 Student t-test*). Co-transfection with *LETM1* siRNA and an siRNA-resistant *LETM1* cDNA construct reduces the level of Mitotracker SOX fluorescence to that of control cells (*siRNA only versus siRNA+cDNA p<0.05 Student t-test, as indicated*). Unt; untransfected, A.U; arbitrary units. The data represents the mean of 3 independent determinations ± SD.

6.3: Discussion

The clinical spectrum and severity of WHS depends on deletion size and genotype to phenotype relationships are often assumed but not experimentally validated. In particular, WHS patients frequently experience seizures as an invariant clinical feature and much of the literature to date has suggested a role for LETM1 in the seizure phenotype. However, this linkage has been made with no associated explanatory, underlying biochemical deficits and is purely assumed based upon deletion size in patients. Many authors investigating the impacts of *LETM1* downregulation in yeast and mammalian cell models have reported altered mitochondrial morphology as a consequence of *LETM1* deficiency (Dimmer et al, 2008b; Froschauer et al, 2005a; Hasegawa & van der Bliek, 2007; Nowikovsky et al, 2004; Tamai et al, 2008a). Some have also reported disrupted mitochondrial functioning such as mitochondrial membrane depolarization (Nowikovsky et al, 2004). Furthermore, whilst this thesis was being prepared, Jiang et al reported a *Letm1* -/+ mouse and provided compelling evidence to support a role for *LETM1* haploinsufficiency in the seizure phenotype of WHS likely by affecting mitochondrial pathways (Jiang et al, 2013). However, to date, no mitochondrial dysfunction has been identified specifically in WHS-patient derived cells. I employed a unique panel of WHS patient-derived LBLs with differing sized deletions to investigate the cellular consequences of *LETM1* haploinsufficiency. I have provided the first evidence that LETM1 protein levels are reduced consistent with haploinsufficiency in LBLs from WHS patients' haploinsufficient for *LETM1*. Furthermore, consistent with a role for LETM1 in the mitochondria, I found that WHS patient-derived LBLs whose deletions encompass the *LETM1* gene exhibit a considerable degree of mitochondrial dysfunction. More specifically, *LETM1* haploinsufficiency segregates with the distinct mitochondrial phenotypes of increased intracellular free Ca^{2+} concentrations, excessive ROS levels and insensitivity of the mitochondrial transition pore.

The mitochondria are essential components of all cells where they function not only as ATP producers but also act as highly effective Ca^{2+} buffering systems. The

central nervous system (CNS) has an enormous metabolic demand due to the fact that neurons are highly differentiated cells which need large amounts of ATP to maintain ionic gradients necessary for neurotransmission. Since most neuronal ATP is generated by oxidative phosphorylation in the mitochondria, neurons heavily rely on correct mitochondrial function (Kann & Kovacs, 2007). Mitochondrial dysfunction and oxidative stress are frequently regarded as both contributing factors to seizure generation and key factors resulting from epileptic seizures (Chang & Yu, 2010; Frantseva et al, 2000). Mitochondrial dysfunction can disrupt ATP levels, alter Ca^{2+} homeostasis and disrupt neurotransmitter biosynthesis, all of which can impact on neuronal excitability. Furthermore, mitochondria are a primary source of ROS, a feature which renders the mitochondria particularly susceptible to oxidative damage which may play a critical role in controlling neuronal excitability (Folbergrová & Kunz, 2012; Kang et al, 2013; Patel, 2004). However, the mechanisms by which mitochondrial dysfunction contributes to epileptogenesis remain ill-defined. Nevertheless, precedent for a role for mitochondrial dysfunction in seizure generation comes from the observation that the most prominent neurological symptom of many mitochondrial disorders is that of profound seizures (Folbergrova & Kunz, 2012). Specifically, patients with well-characterised mitochondrial disorders such as MELAS, MERRF and Leigh Syndrome experience seizures more frequently (Wu et al, 2010). Furthermore, the use of animal models of epilepsy has greatly aided our understanding of the mechanisms underlying seizure generation (Liang et al, 2000; Waldbaum et al, 2010).

It is well established that mitochondria are important for intracellular Ca^{2+} sequestration in neurons (Duchen, 2000). Therefore, this provides an important pathway by which the mitochondria are able to modulate neuronal excitability and synaptic transmission, both of which are altered in epilepsy. Many authors have concluded that LETM1 functions in ion exchange and that loss of LETM1 impairs KHE activity (K^+-H^+ exchange) (Froschauer et al, 2005b; McQuibban et al, 2010; Nowikovsky et al, 2012a). However, this is currently under debate within the literature with others claiming that LETM1 functions as a Ca^{2+}-H^+ antiporter (Jiang et al, 2009a). Some have further suggested that disrupted Ca^{2+} homeostasis may be

secondary to altered KHE activity (Nowikovsky et al, 2012a). Here, I have shown that intracellular Ca^{2+} levels are increased in *LETM1*-/+ WHS patient-derived LBLs and there is evidence to suggest that the elevated Ca^{2+} levels are specifically localized in the mitochondria. In fact, consistent with the data reported here, Jiang et al recently reported that Letm1 is crucial for mitochondrial Ca^{2+} and H^{+} homeostasis. They speculate that the primary impact of *Letm1* haploinsufficiency in mice manifests as a defect in glucose oxidation, consistent with Ca^{2+} regulation of TCA enzymes such as pyruvate dehydrogenase (Jiang et al, 2013).

In addition to impaired Ca^{2+} homeostasis, I have found that opening of the mPTP in response to a Ca^{2+} ionophore is inhibited or insensitive. However, the precise mechanism/s underlying this inhibition are unclear and are worthy of much deeper investigation. Although not investigated here, it is possible that *LETM1*-/+ mitochondria may display altered morphologies similar to those seen in *LETM1* knockdown models, such as matrical swelling. If so, swelling may physically block the pore rendering it unresponsive, even under conditions that should result in its activation such as calcium overloads. Conversely, as *LETM1*-/+ mitochondria exhibit elevated levels of intracellular Ca^{2+}, indicative of disrupted Ca^{2+} homeostasis, chronic exposure to high levels of intracellular Ca^{2+} could render this pore insensitive.

The importance of oxidative stress in lowering seizure threshold is highlighted by studies in *Sod2*-deficient mice. Sod2 is an important antioxidant and *Sod2*-deficient mice exhibit age-dependent spontaneous seizures thus highlighting the importance of redox balance for maintaining correct neuronal function (Liang & Patel, 2004; Liang et al, 2012). *LETM1*-/+ WHS patient-derived cells exhibit remarkable increases in superoxide levels. One mechanism by which excessive ROS may contribute to increased neuronal excitability is via ROS-induced alterations to ion channels and neurotransmitter transporters. For example, the high-affinity astroglial and neuronal glutamate receptors are required for maintaining low synaptic glutamate levels but are extremely sensitive to oxidative damage (Trotti et al, 1998). Furthermore, a number of ligand- gated ion channels have been shown to be regulated by ROS such as nicotinic acetylcholine receptors, glycine receptors and $GABA_A$ receptors (Campanucci et al, 2008). In particular,

hippocampal large-conductance Ca^{2+}- activated K^+ channels (BK_{Ca}) are proposed to play crucial roles in regulating neuronal excitability (Hou et al, 2009). The role of ROS-induced alterations to these channels has been investigated in many cell types including neurons (Faber & Sah, 2003). It is likely that excessive ROS generation, as a consequence of *LETM1* haploinsufficiency, may increase neuronal excitability above the threshold for seizure generation. On the other hand, prolonged seizure activities are known to result in the production of ROS leading to oxidative stress and thus creating a vicious damaging cycle (Folbergrova & Kunz, 2012). Therefore, it is reasonable to suggest that the excessive ROS generation identified here may in fact be both a cause and consequence of increased neuronal excitability and seizures in WHS.

Interestingly, I found that several antioxidants failed to reduce mitochondrial ROS levels. This may be due to a number of factors; 1). the antioxidant capacity of the mitochondria has already reached a maximum threshold; the addition of exogenous antioxidants will have no beneficial effect, 3). the ROS may be a consequence of mitochondrial dysfunction and simply scavenging the ROS does not stop its excessive production, 4). at low levels, ROS are important signalling molecules and the increased uptake of antioxidants may disrupt the redox balance and negatively impact on pathways which rely on low levels of ROS for signalling. Although cause and effect are somewhat unclear, the marked mitochondrial dysfunction identified here could begin to explain the increased neuronal excitability and subsequent seizure generation associated with WHS.

Previous work has identified that the mitochondrial swelling induced by *LETM1* downregulation could be reduced by the addition of a K+ ionophore, nigericin (Nowikovsky et al, 2004). Therefore, I speculated that the increase in mitochondrial ROS generation may also be a consequence of altered KHE activity and morphology. However, it is noteworthy that KHE activity was not investigated here, it was purely assumed based on previous reports in the literature. I found that ROS levels could not be restored by treatment with nigericin which suggests its excessive generation either occurs upstream of the altered KHE activity or is a phenotype which manifests independently of altered KHE activity. Consistent with these findings, earlier this year (2013) Zhang *et al* generated a *Letm1* knockout rat

model via stereotaxic intra-hippocampus injection of shRNA against *Letm1* and showed that loss of LETM1 is associated with increased seizure susceptibility. They subsequently showed the nigericin was unable to reduce the seizures and suggest that seizure generation here is not simply a consequence of altered KHE activity (Zhang et al, 2013).

Many mitochondrial processes such as Ca^{2+} handling and ROS generation are highly interconnected and perturbations in one process can impact on numerous other processes. One highly relevant example here is that ROS can positively stimulate mitochondrial Ca^{2+} signals and mitochondrial Ca^{2+} can increase ROS generation (Camello-Almaraz et al, 2006). This creates a positive feedback loop which may exacerbate mitochondrial dysfunction. It is likely that such a feedback loop exists in *LETM1-/+* cells which makes it difficult to identify the primary cause of the observed mitochondrial dysfunction. However, it is reasonable to speculate that if LETM1 does in fact function as a Ca^{2+}-H^{+} antiporter, loss or impairment of this efflux mechanism will lead to increased mitochondrial Ca^{2+} concentrations. Furthermore, the addition of mPTP insensitivity will further attenuate Ca^{2+} efflux from the mitochondria leading to mitochondrial Ca^{2+} overloads. Through the feedback loop described above, increased Ca^{2+} will stimulate excessive ROS generation and a damaging cycle may be established. Therefore, it is tempting to speculate that impaired Ca^{2+} handling observed here is the primary cause of mitochondrial dysfunction in *LETM1* haploinsufficient LBLs, consistent with a role for LETM1 in Ca^{2+} transport.

Recently, duplication of *LETM1* within a 560Kb interstitial duplication overlapping the WHS critical region, has been associated with neurodevelopmental delay and seizures (Cyr et al, 2011a; Hannes et al, 2010). This suggests that increased *LETM1* copy number may impart similar detrimental effects on mitochondrial homeostasis. Employing a human T98G cell line *LETM1* overexpression model, I have shown that overexpression of *LETM1* is associated with a strikingly similar level of mitochondrial dysfunction to that described here for *LETM1* haploinsufficiency. Cells overexpressing *LETM1* display elevated production of

ROS. This datum provides further support of a role for LETM1 in regulating mitochondrial function and homeostasis.

In conclusion, my data represents the first evidence of a mitochondrial dysfunction associated with *LETM1* haploinsufficiency in WHS patient-derived cells. Furthermore, I have presented data to indicate that increased *LETM1* copy number is also associated with a substantial degree of mitochondrial dysfunction. It is plausible to suggest that the striking mitochondrial phenotypes identified here may render the brain more susceptible to epileptic seizures. Importantly, these findings provide fundamental insight into the potential underlying aetiology of seizures in both WHS and *LETM1* duplication syndromes, and could serve as a platform for the development of targeted clinical therapies.

Chapter Seven

Discussion

In this thesis I have presented novel insight into the functional consequences of specific CNVs associated with three Genomic Disorders; *CUL4B*-deleted XLMR, 16p11.2 CNV Disorder and Wolf Hirschhorn Syndrome. Many of the clinical features of CUL4B-XLMR patients overlap with those of mitochondrial disorders including ataxia, neuropathy, seizures and muscle wasting, suggesting that mitochondrial dysfunction may play a role here. In Chapter three I provided the first evidence indicating that CUL4B is present in/on the mitochondria. Furthermore, I have identified a distinct set of mitochondrial phenotypes in *CUL4B*-deleted patient-derived cells including disruption to the mitochondrial membrane potential, increased ROS generation and impaired Ca^{2+} homeostasis. It is likely that the mitochondrial dysfunction observed here may contribute to many of the clinical features exhibited by these patients such as ataxia and neuropathy. With regards to the MR exhibited by these patients, it is not clear whether the mitochondrial dysfunction identified here may underlie this phenotype. As mentioned, CUL4B has been implicated in regulating aspects of the mTOR pathway; perturbations in which have been associated with MR. Nevertheless, it is conceivable that mitochondrial dysfunction may be a contributing factor to MR in this instance. This data is the first evidence identifying *CUL4B*-mutated and/or deleted XLMR as a disorder associated with mitochondrial dysfunction and suggests that CUL4B has, as yet, unappreciated roles within the mitochondria.

The data in presented in Chapter Four is suggestive of a reciprocal relationship between CUL4B and Cereblon (CRBN). CRBN has been identified as a novel substrate receptor of a CUL4A-containing E3 ligase complex; however a role for CUL4B here was not excluded (Ito et al, 2010). Interestingly, *si*RNA-mediated knockdown of *Crbn* mimicked that of CUL4B loss in patient-derived cells suggesting that CRBN may also interact with CUL4B. This could be consistent with the existence of a putative CUL4B-CRBN E3 ligase complex that plays a pivotal role in the maintenance of mitochondrial homeostasis, particularly regulating redox status. Due to the MR associated with CUL4B loss, some have suggested that CUL4B may have unidentified neuronal-specific substrates, however the data reported here has been carried out in patient-derived LBLs which suggests that the impacts upon mitochondrial homeostasis in this context are not limited to neuronal cells.

Crucially, these findings open up new avenues for further investigations to identify potential mitochondrial-related CUL4B-specific substrates and provide novel insight into the underlying aetiology of CUL4B-XLMR.

I also investigated the functional impacts of 16p11.2 CNV and revealed unexpected results. Copy number change of *KCTD13*, which encodes a protein with interacts with both pol δ and PCNA, was recently postulated as a causative of the strikingly opposing head size phenotypes in 16p11.2 deletion and duplication patients (Golzio et al, 2012). However, despite harbouring a 16p11.2 duplication incorporating the *KCTD13* gene, duplication of this gene was not translated at the protein level in patient-derived LBLs. This data indicates that *KCTD13* copy number change does not segregate with head size as previously thought and suggests that other genes within the 16p11.2 region may contribute to this phenotype. One provocative candidate worthy of further investigation is *INO80E*, a component of the INO80 chromatin-remodelling complex.

Some of the genes within the 16p11.2 region encode proteins which contribute to DNA replication and/or the DDR. Aberrant DNA replication and/or DDR pathways are frequently postulated as mechanisms underlying microcephaly, possibly through reduced neurogenesis and thus I sought to investigate, based on the genes involved, whether impaired replication or repair may be a feature of 16p11.2 CNV LBLs. Unexpectedly, I failed to identify any consistent deficit in either of these pathways in 16p11.2 CNV patient-derived LBLs. However, it is noteworthy that although Golzio and co-workers identified that *Kctd13* downregulation led to increased proliferative status of cortical progenitors in mice consistent with macrocephaly associated with 16p11.2 deletion in humans, they did not report a *Kctd13* overexpression model (Golzio et al, 2012). One 16p11.2 duplicated cell line did show increased sensitivity to HU-induced replication stress yet this was in contrast to two other 16p11.2 duplicated cell lines suggesting that an additional genomic alteration or mutation may be contributing to this cellular phenotype. Importantly, these data highlight the importance of employing patient-derived material as opposed to knockout and/or overexpression cell models to study the functional impacts of copy number variation. However, in this instance this data also raises the question as to whether LBLs are an appropriate model to

investigate the cellular impacts of 16p11.2 CNV. Furthermore, this data strongly emphasizes the need for more intensive investigation in mammalian model systems into the functional consequences of 16p11.2 CNV, particularly with regards to *KCTD13* copy number change.

Finally, I have uncovered novel mitochondrial phenotypes associated with copy number variation of *LETM1*, supporting a role for LETM1 in mitochondrial maintenance and function. These findings potentially have relevance to the profound seizure phenotype of Wolf-Hirschhorn Syndrome. I have shown that haploinsufficiency of *LETM1* specifically is associated with elevated ROS generation and impaired Ca^{2+} handling; alterations which are strongly associated with seizure generation and epilepsy. I propose that mitochondrial dysfunction, as a consequence of *LETM1* copy number change, is likely to underlie or largely contribute to seizure predisposition in both WHS patients with deletions encompassing *LETM1* and those with the rarer reciprocal duplication of 4p16. Furthermore the CUL4B-XLMR patients described in Chapter 3 also exhibit profound seizures as a clinical phenotype. Therefore, the identification of overlapping mitochondrial deficits in both WHS and *CUL4B*-deleted patient-derived LBLs emphasises the importance of optimal mitochondrial function for development.

In conclusion, in this thesis I have uncovered novel cellular phenotypes and provided crucial insight into genotype-phenotype relationships of three Genomic Disorders. It is hoped that the data presented here may not only improve our understanding of the underlying aetiology of these three complex disorders, but in addition may aid the development of more effective management therapies for these patients. Moreover, it stresses the importance of further molecular analysis to address some of the unanswered questions with regards to 16p11.2 CNV Disorder.

References

The SMART's nrdb database.

Abbas T, Sivaprasad U, Terai K, Amador V, Pagano M, Dutta A (2008) PCNA-dependent regulation of p21 ubiquitylation and degradation via the CRL4Cdt2 ubiquitin ligase complex. *Genes & development* **22:** 2496-2506

Abou-Sleiman PM, Muqit MM, Wood NW (2006) Expanding insights of mitochondrial dysfunction in Parkinson's disease. *Nature reviews Neuroscience* **7:** 207-219

Afroze B, Chaudhry B (2013) Genetics of non-syndromic autosomal recessive mental retardation. *Journal Pakistan Medical Association* **63:** 106-110

Aizawa M, Abe Y, Ito T, Handa H, Nawa H (2011) mRNA distribution of the thalidomide binding protein cereblon in adult mouse brain. *Neuroscience Research* **69:** 343-347

Ambrose M, Goldstine JV, Gatti RA (2007) Intrinsic mitochondrial dysfunction in ATM-deficient lymphoblastoid cells. *Human Molecular Genetics* **16:** 2154-2164

Amrhein JA, Klingensmith GJ, Walsh PC, McKusick VA, Migeon CJ (1977) Partial Androgen Insensitivity. *New England Journal of Medicine* **297:** 350-356

Anderson S, Bankier AT, Barrell BG, de Bruijn MH, Coulson AR, Drouin J, Eperon IC, Nierlich DP, Roe BA, Sanger F, Schreier PH, Smith AJ, Staden R, Young IG (1981) Sequence and organization of the human mitochondrial genome. *Nature* **290:** 457-465

Ando Y, Kitayama H, Kawaguchi Y, Koyanagi Y (2008) Primary target cells of herpes simplex virus type 1 in the hippocampus. *Microbes and Infection* **10:** 1514-1523

Andreazza Ac SLWJYL (2010) MItochondrial complex i activity and oxidative damage to mitochondrial proteins in the prefrontal cortex of patients with bipolar disorder. *Archives of General Psychiatry* **67:** 360-368

Angers S, Li T, Yi X, MacCoss M, Moon R, Zheng N (2006) Molecular architecture and assembly of the DDB1-CUL4A ubiquitin ligase machinery. *Nature* **443:** 590 - 593

Aon MA, Cortassa S, O'Rourke B (2010) Redox-optimized ROS balance: a unifying hypothesis. *Biochimica et biophysica acta* **1797:** 865-877

Arundine M, Tymianski M (2003) Molecular mechanisms of calcium-dependent neurodegeneration in excitotoxicity. *Cell Calcium* **34:** 325-337

Bailey JA, Yavor AM, Massa HF, Trask BJ, Eichler EE (2001) Segmental duplications: organization and impact within the current human genome project assembly. *Genome Research* **11:** 1005-1017

Ballif BC, Hornor SA, Jenkins E, Madan-Khetarpal S, Surti U, Jackson KE, Asamoah A, Brock PL, Gowans GC, Conway RL, Graham JM, Jr., Medne L, Zackai EH, Shaikh TH, Geoghegan J, Selzer RR, Eis PS, Bejjani BA, Shaffer LG (2007) Discovery of a previously unrecognized microdeletion syndrome of 16p11.2-p12.2. *Nature Genetics* **39:** 1071-1073

Barsoum MJ, Yuan H, Gerencser AA, Liot G, Kushnareva Y, Graber S, Kovacs I, Lee WD, Waggoner J, Cui J, White AD, Bossy B, Martinou JC, Youle RJ, Lipton SA, Ellisman MH, Perkins GA, Bossy-Wetzel E (2006) Nitric oxide-induced mitochondrial fission is regulated by dynamin-related GTPases in neurons. *EMBO Journal* **25:** 3900-3911

Bartley JA, Hall BD (1978) Mental retardation and multiple congenital anomalies of unknown etiology: frequency of occurrence in similarly affected sibs of the proband. *Birth Defects Original Artical Series* **14:** 127-137

Basel-Vanagaite L (2007) Genetics of autosomal recessive non-syndromic mental retardation: recent advances. *Clinical Genetics* **72:** 167-174

Basel-Vanagaite L, Attia R, Yahav M, Ferland RJ, Anteki L, Walsh CA, Olender T, Straussberg R, Magal N, Taub E, Drasinover V, Alkelai A, Bercovich D, Rechavi G, Simon AJ, Shohat M (2006) The CC2D1A, a member of a new gene family with C2 domains, is involved in autosomal recessive non-syndromic mental retardation. *Journal of Medical Genetics* **43:** 203-210

Battaglia A CJ (2000) Update on the clinical features and natural history of Wilf Hirschhorn Syndrome (WHS): experience with 48 cases. *American Journal of Human Genetics* **67**

Battaglia A, Filippi T, Carey JC (2008) Update on the clinical features and natural history of Wolf–Hirschhorn (4p-) syndrome: Experience with 87 patients and recommendations for routine health supervision. *American Journal of Medical Genetics Part C: Seminars in Medical Genetics* **148C:** 246-251

Battaglia A, Filippi T, South ST, Carey JC (2009) Spectrum of epilepsy and electroencephalogram patterns in Wolf-Hirschhorn syndrome: experience with 87 patients. *Developmental Medicine and Child Neurology* **51:** 373-380

Bauer MF, Rothbauer U, Mühlenbein N, Smith RJH, Gerbitz K-D, Neupert W, Brunner M, Hofmann S (1999) The mitochondrial TIM22 preprotein translocase is highly conserved throughout the eukaryotic kingdom. *FEBS letters* **464:** 41-47

Bauerschmitt H, Mick DU, Deckers M, Vollmer C, Funes S, Kehrein K, Ott M, Rehling P, Herrmann JM (2010) Ribosome-binding proteins Mdm38 and Mba1 display overlapping functions for regulation of mitochondrial translation. *Molecular Biology of the Cell* **21:** 1937-1944

Baumgartner HK, Gerasimenko JV, Thorne C, Ferdek P, Pozzan T, Tepikin AV, Petersen OH, Sutton R, Watson AJ, Gerasimenko OV (2009) Calcium elevation in mitochondria is the main Ca2+ requirement for mitochondrial permeability transition pore (mPTP) opening. *The Journal of Biological Chemistry* **284:** 20796-20803

Bedard K, Krause KH (2007) The NOX family of ROS-generating NADPH oxidases: physiology and pathophysiology. *Physiological Reviews* **87:** 245-313

Bekker-Jensen S, Rendtlew Danielsen J, Fugger K, Gromova I, Nerstedt A, Lukas C, Bartek J, Lukas J, Mailand N (2010) HERC2 coordinates ubiquitin-dependent assembly of DNA repair factors on damaged chromosomes. *Nature Cell Biology* **12:** 80-86; sup pp 81-12

Belichenko PV, Oldfors A, Hagberg B, Dahlstrom A (1994) Rett syndrome: 3-D confocal microscopy of cortical pyramidal dendrites and afferents. *Neuroreport* **5:** 1509-1513

Berg JS, Brunetti-Pierri N, Peters SU, Kang SH, Fong CT, Salamone J, Freedenberg D, Hannig VL, Prock LA, Miller DT, Raffalli P, Harris DJ, Erickson RP, Cunniff C, Clark GD, Blazo MA, Peiffer DA, Gunderson KL, Sahoo T, Patel A, Lupski JR, Beaudet AL, Cheung SW (2007) Speech delay and autism spectrum behaviors are frequently associated with duplication of the 7q11.23 Williams-Beuren syndrome region. *Genetics in Medicine* **9:** 427-441

Berman SB, Pineda FJ, Hardwick JM (2008) Mitochondrial fission and fusion dynamics: the long and short of it. *Cell Death and Differentiation* **15:** 1147-1152

Bi W, Sapir T, Shchelochkov OA, Zhang F, Withers MA, Hunter JV, Levy T, Shinder V, Peiffer DA, Gunderson KL, Nezarati MM, Shotts VA, Amato SS, Savage SK, Harris DJ, Day-Salvatore DL, Horner M, Lu XY, Sahoo T, Yanagawa Y, Beaudet AL, Cheung SW, Martinez S, Lupski JR, Reiner O (2009) Increased LIS1 expression affects human and mouse brain development. *Nature Genetics* **41:** 168-177

Bijlsma EK, Gijsbers AC, Schuurs-Hoeijmakers JH, van Haeringen A, Fransen van de Putte DE, Anderlid BM, Lundin J, Lapunzina P, Perez Jurado LA, Delle Chiaie B, Loeys B, Menten B, Oostra A, Verhelst H, Amor DJ, Bruno DL, van Essen AJ, Hordijk R, Sikkema-Raddatz B, Verbruggen KT, Jongmans MC, Pfundt R, Reeser HM, Breuning MH, Ruivenkamp CA (2009) Extending the phenotype of recurrent rearrangements of 16p11.2: deletions in mentally retarded patients without autism and in normal individuals. *European Journal of Medical Genetics* **52:** 77-87

Blaker-Lee A, Gupta S, McCammon JM, De Rienzo G, Sive H (2012) Zebrafish homologs of genes within 16p11.2, a genomic region associated with brain disorders, are active during brain development, and include two deletion dosage sensor genes. *Disease Models and Mechanisms* **5:** 834-851

Bleier L, Drose S (2013) Superoxide generation by complex III: From mechanistic rationales to functional consequences. *Biochimica et Biophysica Acta* **1827** (11-12): 1320-1331

Bohgaki T, Bohgaki M, Cardoso R, Panier S, Zeegers D, Li L, Stewart GS, Sanchez O, Hande MP, Durocher D, Hakem A, Hakem R (2011) Genomic instability, defective spermatogenesis, immunodeficiency, and cancer in a mouse model of the RIDDLE syndrome. *PLoS genetics* **7:** e1001381

Bosetti F, Weerasinghe GR, Rosenberger TA, Rapoport SI (2003) Valproic acid down-regulates the conversion of arachidonic acid to eicosanoids via cyclooxygenase-1 and -2 in rat brain. *Journal of Neurochemistry* **85:** 690-696

Brady NR, Hamacher-Brady A, Yuan H, Gottlieb RA (2007) The autophagic response to nutrient deprivation in the hl-1 cardiac myocyte is modulated by Bcl-2 and sarco/endoplasmic reticulum calcium stores. *FEBS Journal* **274:** 3184-3197

Brennan JP, Southworth R, Medina RA, Davidson SM, Duchen MR, Shattock MJ (2006) Mitochondrial uncoupling, with low concentration FCCP, induces ROS-dependent cardioprotection independent of KATP channel activation. *Cardiovascular Research* **72:** 313-321

Brenner C, Moulin M (2012) Physiological roles of the permeability transition pore. *Circulation research* **111:** 1237-1247

Brini M, Pinton P, King MP, Davidson M, Schon EA, Rizzuto R (1999) A calcium signaling defect in the pathogenesis of a mitochondrial DNA inherited oxidative phosphorylation deficiency. *Nature Medicine* **5:** 951-954

Brookes PS, Yoon Y, Robotham JL, Anders MW, Sheu S-S (2004) Calcium, ATP, and ROS: a mitochondrial love-hate triangle. *American Journal of Physiology - Cell Physiology* **287:** C817-C833

Budanov AV, Karin M (2008) p53 Target Genes Sestrin1 and Sestrin2 Connect Genotoxic Stress and mTOR Signaling. *Cell* **134:** 451-460

Bulua AC, Simon A, Maddipati R, Pelletier M, Park H, Kim KY, Sack MN, Kastner DL, Siegel RM (2011) Mitochondrial reactive oxygen species promote production of proinflammatory cytokines and are elevated in TNFR1-associated periodic syndrome (TRAPS). *Journal of Experimental Medicine* **208:** 519-533

Bungard D, Fuerth BJ, Zeng PY, Faubert B, Maas NL, Viollet B, Carling D, Thompson CB, Jones RG, Berger SL (2010) Signaling kinase AMPK activates stress-promoted transcription via histone H2B phosphorylation. *Science* **329:** 1201-1205

Cabelof DC (2012) Haploinsufficiency in mouse models of DNA repair deficiency: modifiers of penetrance. *Cellular and Molecular Life Sciences* **69:** 727-740

Cabezas DA, Slaugh R, Abidi F, Arena JF, Stevenson RE, Schwartz CE, Lubs HA (2000) A new X linked mental retardation (XLMR) syndrome with short stature, small testes, muscle wasting, and tremor localises to Xq24-q25. *Journal of Medical Genetics* **37:** 663-668

Cadenas E, Davies KJ (2000) Mitochondrial free radical generation, oxidative stress, and aging. *Free Radical Biology and Medicine* **29:** 222-230

Cai Q, Sheng Z-H (2009) Mitochondrial transport and docking in axons. *Experimental Neurology* **218:** 257-267

Caliskan M, Chong JX, Uricchio L, Anderson R, Chen P, Sougnez C, Garimella K, Gabriel SB, dePristo MA, Shakir K, Matern D, Das S, Waggoner D, Nicolae DL, Ober C (2011) Exome sequencing reveals a novel mutation for autosomal recessive non-syndromic mental retardation in the TECR gene on chromosome 19p13. *Human Molecular Genetics* **20:** 1285-1289

Camello-Almaraz C, Gomez-Pinilla PJ, Pozo MJ, Camello PJ (2006) Mitochondrial reactive oxygen species and Ca2+ signaling. *American Journal of Physiology - Cell Physiology* **291:** C1082-C1088

Campanucci VA, Krishnaswamy A, Cooper E (2008) Mitochondrial Reactive Oxygen Species Inactivate Neuronal Nicotinic Acetylcholine Receptors and Induce Long-Term Depression of Fast Nicotinic Synaptic Transmission. *The Journal of Neuroscience* **28:** 1733-1744

Cárdenas C, Foskett JK (2012) Mitochondrial Ca2+ signals in autophagy. *Cell Calcium* **52:** 44-51

Cardoso C, Leventer RJ, Ward HL, Toyo-Oka K, Chung J, Gross A, Martin CL, Allanson J, Pilz DT, Olney AH, Mutchinick OM, Hirotsune S, Wynshaw-Boris A, Dobyns WB, Ledbetter DH (2003) Refinement of a 400-kb critical region allows genotypic differentiation between isolated lissencephaly, Miller-Dieker syndrome, and other phenotypes secondary to deletions of 17p13.3. *American Journal of Human Genetics* **72:** 918-930

Cardozo T, Pagano M (2004) The SCF ubiquitin ligase: insights into a molecular machine. *Nature Reviews: Molecular Cell Biology* **5:** 739-751

Carling D, Zammit VA, Hardie DG (1987) A common bicyclic protein kinase cascade inactivates the regulatory enzymes of fatty acid and cholesterol biosynthesis. *FEBS Letters* **223:** 217-222

Carter NP (2007) Methods and strategies for analyzing copy number variation using DNA microarrays. *Nature Genetics* **39:** S16-21

Carvalho CM, Zhang F, Liu P, Patel A, Sahoo T, Bacino CA, Shaw C, Peacock S, Pursley A, Tavyev YJ, Ramocki MB, Nawara M, Obersztyn E, Vianna-Morgante AM, Stankiewicz P, Zoghbi HY, Cheung SW, Lupski JR (2009) Complex rearrangements in patients with duplications of MECP2 can occur by fork stalling and template switching. *Human Molecular Genetics* **18:** 2188-2203

Cesura AM, Pinard E, Schubenel R, Goetschy V, Friedlein A, Langen H, Polcic P, Forte MA, Bernardi P, Kemp JA (2003) The Voltage-dependent Anion Channel Is the Target for a New Class of Inhibitors of the Mitochondrial Permeability Transition Pore. *Journal of Biological Chemistry* **278:** 49812-49818

Chan NC, Salazar AM, Pham AH, Sweredoski MJ, Kolawa NJ, Graham RL, Hess S, Chan DC (2011) Broad activation of the ubiquitin-proteasome system by Parkin is critical for mitophagy. *Human Molecular Genetics* **20:** 1726-1737

Chance PF, Abbas N, Lensch MW, Pentao L, Roa BB, Patel PI, Lupski JR (1994) Two autosomal dominant neuropathies result from reciprocal DNA duplication/deletion of a region on chromosome 17. *Human Molecular Genetics* **3:** 223-228

Chandel NS, Maltepe E, Goldwasser E, Mathieu CE, Simon MC, Schumacker PT (1998) Mitochondrial reactive oxygen species trigger hypoxia-induced transcription. *Proceedings of the National Academy of Sciences* **95:** 11715-11720

Chang SJ, Yu BC (2010) Mitochondrial matters of the brain: mitochondrial dysfunction and oxidative status in epilepsy. *Journal of Bioenergetics and Biomembranes* **42:** 457-459

Charriaut-Marlangue C, Otani S, Creuzet C, Ben-Ari Y, Loeb J (1991) Rapid activation of hippocampal casein kinase II during long-term potentiation. *Proceedings of the National Academy of Sciences of the United States of America* **88:** 10232-10236

Chen C-Y, Tsai M-S, Lin C-Y, Yu I-S, Chen Y-T, Lin S-R, Juan L-W, Chen Y-T, Hsu H-M, Lee L-J, Lin S-W (2012) Rescue of the genetically engineered Cul4b mutant mouse as a potential model for human X-linked mental retardation. *Human Molecular Genetics* **21:** 4270-4285

Chen H, Chomyn A, Chan DC (2005) Disruption of Fusion Results in Mitochondrial Heterogeneity and Dysfunction. *Journal of Biological Chemistry* **280:** 26185-26192

Chen KS, Manian P, Koeuth T, Potocki L, Zhao Q, Chinault AC, Lee CC, Lupski JR (1997) Homologous recombination of a flanking repeat gene cluster is a mechanism for a common contiguous gene deletion syndrome. *Nature Genetics* **17:** 154-163

Chen XJ, Butow RA (2005) The organization and inheritance of the mitochondrial genome. *Nature Reviews Genetics* **6:** 815-825

Chen Y, Azad MB, Gibson SB (2009) Superoxide is the major reactive oxygen species regulating autophagy. *Cell Death and Differentiation* **16:** 1040-1052

Chen Y, McMillan-Ward E, Kong J, Israels SJ, Gibson SB (2007) Mitochondrial electron-transport-chain inhibitors of complexes I and II induce autophagic cell death mediated by reactive oxygen species. *Journal of Cell Science* **120:** 4155-4166

Chen Z, Raman M, Chen L, Lee SF, Gilman AG, Cobb MH (2003) TAO (thousand-and-one amino acid) protein kinases mediate signaling from carbachol to p38 mitogen-activated protein kinase and ternary complex factors. *Journal of Biological Chemistry* **278:** 22278-22283

Chesi M, Nardini E, Lim RS, Smith KD, Kuehl WM, Bergsagel PL (1998) The t(4;14) translocation in myeloma dysregulates both FGFR3 and a novel gene, MMSET, resulting in IgH/MMSET hybrid transcripts. *Blood* **92:** 3025-3034

Cheung SW, Shaw CA, Yu W, Li J, Ou Z, Patel A, Yatsenko SA, Cooper ML, Furman P, Stankiewicz P, Lupski JR, Chinault AC, Beaudet AL (2005) Development and validation of a CGH microarray for clinical cytogenetic diagnosis. *Genetics in Medicine* **7:** 422-432

Chiurazzi P, Schwartz CE, Gecz J, Neri G (2008) XLMR genes: update 2007. *European Journal of Human Genetics* **16:** 422-434

Choi DW (1988) Calcium-mediated neurotoxicity: relationship to specific channel types and role in ischemic damage. *Trends in Neurosciences* **11:** 465-469

Choi P, Ostrerova-Golts N, Sparkman D, Cochran E, Lee JM, Wolozin B (2000) Parkin is metabolized by the ubiquitin/proteosome system. *Neuroreport* **11:** 2635-2638

Chronicle E, Mulleners W (2004) Anticonvulsant drugs for migraine prophylaxis. *Cochrane database of systematic reviews (Online)***:** CD003226

Chu G, Chang E (1988) Xeroderma pigmentosum group E cells lack a nuclear factor that binds to damaged DNA. *Science* **242:** 564-567

Cock H, Schapira AHV (1999) Mitochondrial DNA Mutations and Mitochondrial Dysfunction in Epilepsy. *Epilepsia* **40:** 33-40

Collins FS, Guyer MS, Charkravarti A (1997) Variations on a theme: cataloging human DNA sequence variation. *Science* **278:** 1580-1581

Collins FS, Mansoura MK (2001) The Human Genome Project. Revealing the shared inheritance of all humankind. *Cancer* **91:** 221-225

Colvin JS, Bohne BA, Harding GW, McEwen DG, Ornitz DM (1996) Skeletal overgrowth and deafness in mice lacking fibroblast growth factor receptor 3. *Nature Genetics* **12:** 390-397

Coman DJ, Gardner RM (2007) Deletions Revealing Recessive Genes: Deletions that reveal recessive genes. *European Journal of Human Genetics* **15:** 1103-1104

Cooper GM, Nickerson DA, Eichler EE (2007) Mutational and selective effects on copy-number variants in the human genome. *Nature Genetics* **39:** S22-29

Cox BJ, Vollmer M, Tamplin O, Lu M, Biechele S, Gertsenstein M, van Campenhout C, Floss T, Kuhn R, Wurst W, Lickert H, Rossant J (2010) Phenotypic annotation of the mouse X chromosome. *Genome Research* **20:** 1154-1164

Crepel A, Steyaert J, De la Marche W, De Wolf V, Fryns JP, Noens I, Devriendt K, Peeters H (2011) Narrowing the critical deletion region for autism spectrum disorders on 16p11.2. *American Journal of Medical Genetics Part B, Neuropsychiatric genetics : the official publication of the International Society of Psychiatric Genetics* **156:** 243-245

Crespi B, Summers K, Dorus S (2009) ORIGINAL ARTICLE: Genomic sister-disorders of neurodevelopment: an evolutionary approach. *Evolutionary Applications* **2:** 81-100

Crino PB (2011) mTOR: A pathogenic signaling pathway in developmental brain malformations. *Trends in Molecular Medicine* **17:** 734-742

Crompton M (1999) The mitochondrial permeability transition pore and its role in cell death. *The Biochemical Journal* **341 (Pt 2):** 233-249

Cross JH (2013) New Research With Diets and Epilepsy. *Journal of Child Neurology* **8:** 970-974

Cyr AB, Nimmakayalu M, Longmuir SQ, Patil SR, Keppler-Noreuil KM, Shchelochkov OA (2011a) A novel 4p16.3 microduplication distal to WHSC1 and WHSC2 characterized by oligonucleotide array with new phenotypic features. *American Journal of Medical Genetics Part A* **155:** 2224-2228

Cyr AB, Nimmakayalu M, Longmuir SQ, Patil SR, Keppler-Noreuil KM, Shchelochkov OA (2011b) A novel 4p16.3 microduplication distal to WHSC1 and WHSC2

characterized by oligonucleotide array with new phenotypic features. *American Journal of Medical Genetics Part A* **155A:** 2224-2228

D'Amato RJ, Loughnan MS, Flynn E, Folkman J (1994) Thalidomide is an inhibitor of angiogenesis. *Proceedings of the National Academy of Sciences of the United States of America* **91:** 4082-4085

Dai Q, Wang H (2006) Cullin 4 makes its mark on chromatin. *Cell Division* **1:** 14

Darai-Ramqvist E, Sandlund A, Muller S, Klein G, Imreh S, Kost-Alimova M (2008) Segmental duplications and evolutionary plasticity at tumor chromosome break-prone regions. *Genome Research* **18:** 370-379

Davis AP, Symington LS (2004) RAD51-dependent break-induced replication in yeast. *Molecular and Cellular Biology* **24:** 2344-2351

Davis OS, Butcher LM, Docherty SJ, Meaburn EL, Curtis CJ, Simpson MA, Schalkwyk LC, Plomin R (2010) A three-stage genome-wide association study of general cognitive ability: hunting the small effects. *Behaviour Genetics* **40:** 759-767

de Coo I. F SHJ, Garbreels F. J, Arts N and van Oost B.A (1996) Isolated case of mental retardation and ataxia due to a de novo mitochondrial T8993G mutation. *American Journal of Human Genetics* **58:** 636-638

de Jager M, van Noort J, van Gent DC, Dekker C, Kanaar R, Wyman C (2001) Human Rad50/Mre11 is a flexible complex that can tether DNA ends. *Molecular Cell* **8:** 1129-1135

de Smith AJ, Tsalenko A, Sampas N, Scheffer A, Yamada NA, Tsang P, Ben-Dor A, Yakhini Z, Ellis RJ, Bruhn L, Laderman S, Froguel P, Blakemore AI (2007) Array CGH analysis of copy number variation identifies 1284 new genes variant in healthy white males: implications for association studies of complex diseases. *Human Molecular Genetics* **16:** 2783-2794

Deng C, Wynshaw-Boris A, Zhou F, Kuo A, Leder P (1996) Fibroblast growth factor receptor 3 is a negative regulator of bone growth. *Cell* **84:** 911-921

Deshaies RJ (1999) SCF and Cullin/Ring H2-based ubiquitin ligases. *Annual Review of Cell and Developmental Biology* **15:** 435-467

Devgan SS, Sanal O, Doil C, Nakamura K, Nahas SA, Pettijohn K, Bartek J, Lukas C, Lukas J, Gatti RA (2011) Homozygous deficiency of ubiquitin-ligase ring-finger protein RNF168 mimics the radiosensitivity syndrome of ataxia-telangiectasia. *Cell Death and Differentiation* **18:** 1500-1506

Dias D, Dolios G, Wang R, Pan Z (2002) CUL7: A DOC domain-containing cullin selectively binds Skp1.Fbx29 to form an SCF-like complex. *Proceedings of the National Academy of Sciences* **99:** 16601 - 16606

Dimmer KS, Fritz S, Fuchs F, Messerschmitt M, Weinbach N, Neupert W, Westermann B (2002) Genetic Basis of Mitochondrial Function and Morphology inSaccharomyces cerevisiae. *Molecular Biology of the Cell* **13:** 847-853

Dimmer KS, Navoni F, Casarin A, Trevisson E, Endele S, Winterpacht A, Salviati L, Scorrano L (2008a) LETM1, deleted in Wolf-Hirschhorn syndrome is required for normal mitochondrial morphology and cellular viability. *Human Molecular Genetics* **17:** 201-214

Dimmer KS, Navoni F, Casarin A, Trevisson E, Endele S, Winterpacht A, Salviati L, Scorrano L (2008b) LETM1, deleted in Wolf–Hirschhorn syndrome is required for normal mitochondrial morphology and cellular viability. *Human Molecular Genetics* **17:** 201-214

Ding W-X, Ni H-M, Li M, Liao Y, Chen X, Stolz DB, Dorn GW, Yin X-M (2010) Nix Is Critical to Two Distinct Phases of Mitophagy, Reactive Oxygen Species-mediated Autophagy Induction and Parkin-Ubiquitin-p62-mediated Mitochondrial Priming. *Journal of Biological Chemistry* **285:** 27879-27890

Ding WX, Yin XM (2012) Mitophagy: mechanisms, pathophysiological roles, and analysis. *Biological Chemistry* **393:** 547-564

Ditch S, Paull TT (2012) The ATM protein kinase and cellular redox signaling: beyond the DNA damage response. *Trends in Biochemical Sciences* **37:** 15-22

Doil C, Mailand N, Bekker-Jensen S, Menard P, Larsen DH, Pepperkok R, Ellenberg J, Panier S, Durocher D, Bartek J, Lukas J, Lukas C (2009) RNF168 binds and amplifies ubiquitin conjugates on damaged chromosomes to allow accumulation of repair proteins. *Cell* **136:** 435-446

Douarre C, Sourbier C, Dalla Rosa I, Brata Das B, Redon CE, Zhang H, Neckers L, Pommier Y (2012) Mitochondrial Topoisomerase I is Critical for Mitochondrial Integrity and Cellular Energy Metabolism. *PLoS ONE* **7:** e41094

Dröse S, Brandt U. (2012) Molecular mechanisms of superoxide production by the mitochondrial respiratory chain. Vol. 748, pp. 145-169.

Duchen MR (2000) Mitochondria and calcium: From cell signalling to cell death. *Journal of Physiology* **529:** 57-68

Duchen MR (2004) Roles of Mitochondria in Health and Disease. *Diabetes* **53:** S96-S102

Echtay KS, Roussel D, St-Pierre J, Jekabsons MB, Cadenas S, Stuart JA, Harper JA, Roebuck SJ, Morrison A, Pickering S, Clapham JC, Brand MD (2002) Superoxide activates mitochondrial uncoupling proteins. *Nature* **415:** 96-99

Edelmann L, Pandita RK, Spiteri E, Funke B, Goldberg R, Palanisamy N, Chaganti RS, Magenis E, Shprintzen RJ, Morrow BE (1999) A common molecular basis for rearrangement disorders on chromosome 22q11. *Human Molecular Genetics* **8:** 1157-1167

Egan DF, Shackelford DB, Mihaylova MM, Gelino S, Kohnz RA, Mair W, Vasquez DS, Joshi A, Gwinn DM, Taylor R, Asara JM, Fitzpatrick J, Dillin A, Viollet B, Kundu M, Hansen M, Shaw RJ (2011) Phosphorylation of ULK1 (hATG1) by AMP-Activated Protein Kinase Connects Energy Sensing to Mitophagy. *Science* **331:** 456-461

El-Mahdy MA, Zhu Q, Wang QE, Wani G, Praetorius-Ibba M, Wani AA (2006) Cullin 4A-mediated proteolysis of DDB2 protein at DNA damage sites regulates in vivo lesion recognition by XPC. *The Journal of Biological Chemistry* **281:** 13404-13411

Endele S, Fuhry M, Pak S-J, Zabel BU, Winterpacht A (1999a) LETM1, A Novel Gene Encoding a Putative EF-Hand Ca2+-Binding Protein, Flanks the Wolf–Hirschhorn Syndrome (WHS) Critical Region and Is Deleted in Most WHS Patients. *Genomics* **60:** 218-225

Endele S, Fuhry M, Pak SJ, Zabel BU, Winterpacht A (1999b) LETM1, a novel gene encoding a putative EF-hand Ca(2+)-binding protein, flanks the Wolf-Hirschhorn syndrome (WHS) critical region and is deleted in most WHS patients. *Genomics* **60:** 218-225

Engbers H, van der Smagt JJ, Van 't Slot R, Vermeesch JR, Hochstenbach R, Poot M (2008) Wolf-Hirschhorn syndrome facial dysmorphic features in a patient with a terminal 4p16.3 deletion telomeric to the WHSCR and WHSCR 2 regions. *European Journal of Human Genetics* **17:** 129-132

Ensenauer RE, Adeyinka A, Flynn HC, Michels VV, Lindor NM, Dawson DB, Thorland EC, Lorentz CP, Goldstein JL, McDonald MT, Smith WE, Simon-Fayard E, Alexander AA, Kulharya AS, Ketterling RP, Clark RD, Jalal SM (2003) Microduplication 22q11.2, an emerging syndrome: clinical, cytogenetic, and molecular analysis of thirteen patients. *American Journal of Human Genetics* **73:** 1027-1040

Esteves AR, Lu J, Rodova M, Onyango I, Lezi E, Dubinsky R, Lyons KE, Pahwa R, Burns JM, Cardoso SM, Swerdlow RH (2010) Mitochondrial respiration and respiration-associated proteins in cell lines created through Parkinson's subject mitochondrial transfer. *Journal of Neurochemistry* **113:** 674-682

Esworthy RS, Ho YS, Chu FF (1997) The Gpx1 gene encodes mitochondrial glutathione peroxidase in the mouse liver. *Archives of Biochemistry and Biophysics* **340:** 59-63

Eyal S, Yagen B, Sobol E, Altschuler Y, Shmuel M, Bialer M (2004) The activity of antiepileptic drugs as histone deacetylase inhibitors. *Epilepsia* **45:** 737-744

Ezponda T, Popovic R, Shah MY, Martinez-Garcia E, Zheng Y, Min DJ, Will C, Neri A, Kelleher NL, Yu J, Licht JD (2012) The histone methyltransferase MMSET/WHSC1 activates TWIST1 to promote an epithelial-mesenchymal transition and invasive properties of prostate cancer. *Oncogene* **32** (23): 2882-2890

Faber ESL, Sah P (2003) Calcium-Activated Potassium Channels: Multiple Contributions to Neuronal Function. *The Neuroscientist* **9:** 181-194

Fang C, Bourdette D, Banker G (2012) Oxidative stress inhibits axonal transport: implications for neurodegenerative diseases. *Molecular Neurodegeneration* **7:** 29

Fassone E, Taanman J-W, Hargreaves IP, Sebire NJ, Cleary MA, Burch M, Rahman S (2011) Mutations in the mitochondrial complex I assembly factor NDUFAF1 cause fatal infantile hypertrophic cardiomyopathy. *Journal of Medical Genetics* **48:** 691-697

Feenstra I, Fang J, Koolen DA, Siezen A, Evans C, Winter RM, Lees MM, Riegel M, de Vries BBA, Van Ravenswaaij CMA, Schinzel A (2006) European Cytogeneticists Association Register of Unbalanced Chromosome Aberrations (ECARUCA); an online database for rare chromosome abnormalities. *European Journal of Medical Genetics* **49:** 279-291

Feldblum S, Rougier A, Loiseau H, Loiseau P, Cohadon F, Morselli PL, Lloyd KG (1988) Quinolinic-phosphoribosyl transferase activity is decreased in epileptic human brain tissue. *Epilepsia* **29:** 523-529

Feng X, Liu X, Zhang W, Xiao W (2011) p53 directly suppresses BNIP3 expression to protect against hypoxia-induced cell death. *The EMBO journal* **30:** 3397-3415

Feng Z, Hu W, de Stanchina E, Teresky AK, Jin S, Lowe S, Levine AJ (2007) The Regulation of AMPK β1, TSC2, and PTEN Expression by p53: Stress, Cell and Tissue Specificity, and the Role of These Gene Products in Modulating the IGF-1-AKT-mTOR Pathways. *Cancer Research* **67:** 3043-3053

Fernandez-Capetillo O, Lee A, Nussenzweig M, Nussenzweig A (2004) H2AX: the histone guardian of the genome. *DNA Repair* **3:** 959-967

Fimia GM, Stoykova A, Romagnoli A, Giunta L, Di Bartolomeo S, Nardacci R, Corazzari M, Fuoco C, Ucar A, Schwartz P, Gruss P, Piacentini M, Chowdhury K, Cecconi F (2007) Ambra1 regulates autophagy and development of the nervous system. *Nature* **447:** 1121-1125

Firth HV, Richards SM, Bevan AP, Clayton S, Corpas M, Rajan D, Vooren SV, Moreau Y, Pettett RM, Carter NP (2009) DECIPHER: Database of Chromosomal Imbalance

and Phenotype in Humans Using Ensembl Resources. *The American Journal of Human Genetics* **84:** 524-533

Fleury C, Mignotte B, Vayssiere JL (2002) Mitochondrial reactive oxygen species in cell death signaling. *Biochimie* **84:** 131-141

Folbergrova J, Kunz WS (2012) Mitochondrial dysfunction in epilepsy. *Mitochondrion* **12:** 35-40

Fountoulakis KN, Vieta E, Sanchez-Moreno J, Kaprinis SG, Goikolea JM, Kaprinis GS (2005) Treatment guidelines for bipolar disorder: a critical review. *Journal of Affective Disorders* **86:** 1-10

Franks ME, Macpherson GR, Figg WD (2004) Thalidomide. *The Lancet* **363:** 1802-1811

Frantseva MV, Velazquez JLP, Hwang PA, Carlen PL (2000) Free radical production correlates with cell death in an in vitro model of epilepsy. *European Journal of Neuroscience* **12:** 1431-1439

Fraser FC (1988) Thalidomide retrospective: what did we learn? *Teratology* **38:** 201-202

Frazier AE, Taylor RD, Mick DU, Warscheid B, Stoepel N, Meyer HE, Ryan MT, Guiard B, Rehling P (2006) Mdm38 interacts with ribosomes and is a component of the mitochondrial protein export machinery. *The Journal of Cell Biology* **172:** 553-564

Fridlyand J, Snijders AM, Ylstra B, Li H, Olshen A, Segraves R, Dairkee S, Tokuyasu T, Ljung BM, Jain AN, McLennan J, Ziegler J, Chin K, Devries S, Feiler H, Gray JW, Waldman F, Pinkel D, Albertson DG (2006) Breast tumor copy number aberration phenotypes and genomic instability. *BMC cancer* **6:** 96

Fridovich I (1995) Superoxide radical and superoxide dismutases. *Annual Review of Biochemistry* **64:** 97-112

Froschauer E, Nowikovsky K, Schweyen RJ (2005a) Electroneutral K+/H+ exchange in mitochondrial membrane vesicles involves Yol027/Letm1 proteins. *Biochimica et Biophysica Acta - Biomembranes* **1711:** 41-48

Froschauer E, Nowikovsky K, Schweyen RJ (2005b) Electroneutral K+/H+ exchange in mitochondrial membrane vesicles involves Yol027/Letm1 proteins. *Biochimica et biophysica acta* **1711:** 41-48

Fu C, Cawthon B, Clinkscales W, Bruce A, Winzenburger P, Ess KC (2012) GABAergic Interneuron Development and Function Is Modulated by the Tsc1 Gene. *Cerebral Cortex* **22:** 2111-2119

Fukuhara N, Tokiguchi S, Shirakawa K, Tsubaki T (1980) Myoclonus epilepsy associated with ragged-red fibres (mitochondrial abnormalities): disease entity or a syndrome? Light-and electron-microscopic studies of two cases and review of literature. *Journal of the Neurological Sciences* **47:** 117-133

Fukunaga K, Muller D, Miyamoto E (1996) CaM KINASE II in long-term potentiation. *Neurochemistry International* **28:** 343-358

Ganesh J, Wong L-JC, Gorman EB (2013) Mitochondrial Respiratory Chain Complex II. In *Mitochondrial Disorders Caused by Nuclear Genes*, Wong L-JC (ed), 13, pp 203-218. Springer New York

Garapaty S, Xu C-F, Trojer P, Mahajan MA, Neubert TA, Samuels HH (2009) Identification and Characterization of a Novel Nuclear Protein Complex Involved in Nuclear Hormone Receptor-mediated Gene Regulation. *Journal of Biological Chemistry* **284:** 7542-7552

Garelick MG, Kennedy BK (2011) TOR on the brain. *Experimental Gerontology* **46:** 155-163

Garriga-Canut M, Schoenike B, Qazi R, Bergendahl K, Daley TJ, Pfender RM, Morrison JF, Ockuly J, Stafstrom C, Sutula T, Roopra A (2006) 2-Deoxy-D-glucose reduces epilepsy progression by NRSF-CtBP-dependent metabolic regulation of chromatin structure. *Nature Neuroscience* **9:** 1382-1387

Garshasbi M, Hadavi V, Habibi H, Kahrizi K, Kariminejad R, Behjati F, Tzschach A, Najmabadi H, Ropers HH, Kuss AW (2008) A Defect in the TUSC3 Gene Is Associated with Autosomal Recessive Mental Retardation. *American Journal of Human Genetics* **82:** 1158-1164

Gautier C, Giaime E, Caballero E, Nunez L, Song Z, Chan D, Villalobos C, Shen J (2012) Regulation of mitochondrial permeability transition pore by PINK1. *Molecular Neurodegeneration* **7:** 22

Gegg ME, Cooper JM, Chau K-Y, Rojo M, Schapira AHV, Taanman J-W (2010) Mitofusin 1 and mitofusin 2 are ubiquitinated in a PINK1/parkin-dependent manner upon induction of mitophagy. *Human Molecular Genetics* **19:** 4861-4870

Geisler S, Holmstrom KM, Skujat D, Fiesel FC, Rothfuss OC, Kahle PJ, Springer W (2010) PINK1/Parkin-mediated mitophagy is dependent on VDAC1 and p62/SQSTM1. *Nature cell biology* **12:** 119-131

Gellert M (2002) V(D)J Recombination: RAG protein, repair factors, and regulation. *Annual Review of Biochemistry* **71:** 101-132

Ghosh P, Wu M, Zhang H, Sun H (2008) mTORC1 signaling requires proteasomal function and the involvement of CUL4-DDB1 ubiquitin E3 ligase. *Cell cycle* **7:** 373-381

Giorgio V, von Stockum S, Antoniel M, Fabbro A, Fogolari F, Forte M, Glick GD, Petronilli V, Zoratti M, Szabo I, Lippe G, Bernardi P (2013) Dimers of mitochondrial ATP synthase form the permeability transition pore. **110 (15):** 5887-5892

Golani I, Wolgin DL, Teitelbaum P (1979) A proposed natural geometry of recovery from akinesia in the lateral hypothalamic rat. *Brain Research* **164:** 237-267

Golzio C, Willer J, Talkowski ME, Oh EC, Taniguchi Y, Jacquemont S, Reymond A, Sun M, Sawa A, Gusella JF, Kamiya A, Beckmann JS, Katsanis N (2012) KCTD13 is a major driver of mirrored neuroanatomical phenotypes of the 16p11.2 copy number variant. *Nature* **485:** 363-367

Gomes LC, Scorrano L (2008) High levels of Fis1, a pro-fission mitochondrial protein, trigger autophagy. *Biochimica et Biophysica Acta* **1777:** 860-866

Gordeeva AV, Zvyagilskaya RA, Labas YA (2003) Cross-Talk between Reactive Oxygen Species and Calcium in Living Cells. *Biochemistry* **68:** 1077-1080

Gottlicher M, Minucci S, Zhu P, Kramer OH, Schimpf A, Giavara S, Sleeman JP, Lo Coco F, Nervi C, Pelicci PG, Heinzel T (2001) Valproic acid defines a novel class of HDAC inhibitors inducing differentiation of transformed cells. *The EMBO journal* **20:** 6969-6978

Groisman R, Polanowska J, Kuraoka I, Sawada J, Saijo M, Drapkin R, Kisselev A, Tanaka K, Nakatani Y (2003) The ubiquitin ligase activity in the DDB2 and CSA complexes is differentially regulated by the COP9 signalosome in response to DNA damage. *Cell* **113:** 357 - 367

Grunnet M, Kaufmann WA (2004) Coassembly of big conductance Ca2+-activated K+ channels and L-type voltage-gated Ca2+ channels in rat brain. *The Jouranl of Biological Chemistry* **279:** 36445-36453

Gu W, Zhang F, Lupski JR (2008) Mechanisms for human genomic rearrangements. *PathoGenetics* **1:** 4

Guerrero-Santoro J, Kapetanaki MG, Hsieh CL, Gorbachinsky I, Levine AS, Rapic-Otrin V (2008) The cullin 4B-based UV-damaged DNA-binding protein ligase binds to UV-damaged chromatin and ubiquitinates histone H2A. *Cancer Research* **68:** 5014-5022

Gunter TE, Buntinas L, Sparagna G, Eliseev R, Gunter K (2000) Mitochondrial calcium transport: mechanisms and functions. *Cell Calcium* **28:** 285-296

Gwinn DM, Shackelford DB, Egan DF, Mihaylova MM, Mery A, Vasquez DS, Turk BE, Shaw RJ (2008) AMPK phosphorylation of raptor mediates a metabolic checkpoint. *Molecular Cell* **30:** 214-226

Hajdu I, Ciccia A, Lewis SM, Elledge SJ (2011) Wolf-Hirschhorn syndrome candidate 1 is involved in the cellular response to DNA damage. *Proceedings of the National Academy of Sciences of the United States of America* **108:** 13130-13134

Hajszan T, MacLusky NJ, Leranth C (2008) Role of androgens and the androgen receptor in remodeling of spine synapses in limbic brain areas. *Hormones and Behavior* **53:** 638-646

Han D, Canali R, Rettori D, Kaplowitz N (2003) Effect of Glutathione Depletion on Sites and Topology of Superoxide and Hydrogen Peroxide Production in Mitochondria. *Molecular Pharmacology* **64:** 1136-1144

Hancock JT, Desikan R, Neill SJ (2001) Role of reactive oxygen species in cell signalling pathways. *Biochemical Society Transactions* **29:** 345-350

Hanna RA, Quinsay MN, Orogo AM, Giang K, Rikka S, Gustafsson ÅB (2012) Microtubule-associated Protein 1 Light Chain 3 (LC3) Interacts with Bnip3 Protein to Selectively Remove Endoplasmic Reticulum and Mitochondria via Autophagy. *Journal of Biological Chemistry* **287:** 19094-19104

Hannah J, Zhou P (2009) Regulation of DNA damage response pathways by the cullin-RING ubiquitin ligases. *DNA Repair* **8:** 536-543

Hannes F, Drozniewska M, Vermeesch JR, Haus O (2010) Duplication of the Wolf-Hirschhorn syndrome critical region causes neurodevelopmental delay. *European Journal of Medical Genetics* **53:** 136-140

Hansen JM, Gong S-G, Philbert M, Harris C (2002) Misregulation of gene expression in the redox-sensitive NF-κb-dependent limb outgrowth pathway by thalidomide. *Developmental Dynamics* **225:** 186-194

Hansen JM, Harris C (2004) A novel hypothesis for thalidomide-induced limb teratogenesis: redox misregulation of the NF-kappaB pathway. *Antioxidant and Redox Signalling* **6:** 1-14

Hardie DG (2007) AMP-activated/SNF1 protein kinases: conserved guardians of cellular energy. *Nature reviews Molecular Cell Biology* **8:** 774-785

Hardie DG, Ross FA, Hawley SA (2012) AMPK: a nutrient and energy sensor that maintains energy homeostasis. *Nature reviews Molecular Cell Biology* **13:** 251-262

Hasegawa A, van der Bliek AM (2007) Inverse correlation between expression of the Wolfs Hirschhorn candidate gene Letm1 and mitochondrial volume in C. elegans and in mammalian cells. *Human Molecular Genetics* **16:** 2061-2071

Hashimoto S, Boissel S, Zarhrate M, Rio M, Munnich A, Egly J-M, Colleaux L (2011) MED23 mutation links intellectual disability to dysregulation of immediate early gene expression. *Science* **333:** 1161-1163

Hastings PJ, Ira G, Lupski JR (2009a) A microhomology-mediated break-induced replication model for the origin of human copy number variation. *PLoS genetics* **5:** e1000327

Hastings PJ, Lupski JR, Rosenberg SM, Ira G (2009b) Mechanisms of change in gene copy number. *Nature Reviews Genetics* **10:** 551-564

He F, Lu D, Jiang B, Wang Y, Liu Q, Liu Q, Shao C, Li X, Gong Y (2013) X-linked intellectual disability gene CUL4B targets Jab1/CSN5 for degradation and regulates bone morphogenetic protein signaling. *Biochimica et Biophysica Acta - Molecular Basis of Disease* **1832:** 595-605

He H, Tan C-K, Downey KM, So AG (2001) A tumor necrosis factor α- and interleukin 6-inducible protein that interacts with the small subunit of DNA polymerase δ and proliferating cell nuclear antigen. *Proceedings of the National Academy of Sciences* **98:** 11979-11984

He YJ, McCall CM, Hu J, Zeng Y, Xiong Y (2006) DDB1 functions as a linker to recruit receptor WD40 proteins to CUL4-ROC1 ubiquitin ligases. *Genes & Development* **20:** 2949-2954

Henrichsen CN, Vinckenbosch N, Zollner S, Chaignat E, Pradervand S, Schutz F, Ruedi M, Kaessmann H, Reymond A (2009) Segmental copy number variation shapes tissue transcriptomes. *Nature Genetics* **41:** 424-429

Higa LA, Mihaylov IS, Banks DP, Zheng J, Zhang H (2003) Radiation-mediated proteolysis of CDT1 by CUL4-ROC1 and CSN complexes constitutes a new checkpoint. *Nature Cell Biology* **5:** 1008-1015

Higa LA, Yang X, Zheng J, Banks D, Wu M, Ghosh P, Sun H, Zhang H (2006) Involvement of CUL4 ubiquitin E3 ligases in regulating CDK inhibitors Dacapo/p27Kip1 and cyclin E degradation. *Cell cycle* **5:** 71-77

Higgins J, Hao J, Kosofsky B, Rajadhyaksha A (2008) Dysregulation of large-conductance Ca2+-activated K+ channel expression in nonsyndromal mental retardation due to a cereblon p.R419X mutation. *Neurogenetics* **9:** 219-223

Higgins JJ, Pucilowska J, Lombardi RQ, Rooney JP (2004a) Candidate genes for recessive non-syndromic mental retardation on chromosome 3p (MRT2A). *Clinical Genetics* **65:** 496-500

Higgins JJ, Pucilowska J, Lombardi RQ, Rooney JP (2004b) A mutation in a novel ATP-dependent Lon protease gene in a kindred with mild mental retardation. *Neurology* **63:** 1927-1931

Higgins JJ, Rosen DR, Loveless JM, Clyman JC, Grau MJ (2000) A gene for nonsyndromic mental retardation maps to chromosome 3p25-pter. *Neurology* **55:** 335-340

Higgins JJ, Tal AL, Sun X, Hauck SC, Hao J, Kosofosky BE, Rajadhyaksha AM (2010) Temporal and spatial mouse brain expression of cereblon, an ionic channel regulator involved in human intelligence. *Journal of Neurogenetics* **24:** 18-26

Hildebrand JD, Soriano P (2002) Overlapping and unique roles for C-terminal binding protein 1 (CtBP1) and CtBP2 during mouse development. *Molecular and Cellular Biology* **22:** 5296-5307

Hirano R, Interthal H, Huang C, Nakamura T, Deguchi K, Choi K, Bhattacharjee MB, Arimura K, Umehara F, Izumo S, Northrop JL, Salih MAM, Inoue K, Armstrong DL, Champoux JJ, Takashima H, Boerkoel CF (2007) Spinocerebellar ataxia with axonal neuropathy: consequence of a Tdp1 recessive neomorphic mutation? *EMBO Journal* **26:** 4732-4743

Hirschhorn K, Cooper HL, Firschein IL (1965) Deletion of short arms of chromosome 4-5 in a child with defects of midline fusion. *Humangenetik* **1:** 479-482

Hoeffer CA, Klann E (2010) mTOR signaling: at the crossroads of plasticity, memory and disease. *Trends in Neurosciences* **33:** 67-75

Hohberger B, Enz R (2009) Cereblon is expressed in the retina and binds to voltage-gated chloride channels. *FEBS Letters* **583:** 633-637

Hollenbeck PJ, Saxton WM (2005) The axonal transport of mitochondria. *Journal of Cell Science* **118:** 5411-5419

Holt, Harding, Morgan-Hughes (1988) Deletions of muscle mitochondrial DNA in patients with mitochondrial myopathies. *Nature* **331:** 717-719

Horev G, Ellegood J, Lerch JP, Son Y-EE, Muthuswamy L, Vogel H, Krieger AM, Buja A, Henkelman RM, Wigler M, Mills AA (2011) Dosage-dependent phenotypes in models of 16p11.2 lesions found in autism. *Proceedings of the National Academy of Sciences* **108:** 17076-17081

Hou S, Heinemann SH, Hoshi T (2009) Modulation of BKCa Channel Gating by Endogenous Signaling Molecules. *Physiology* **24:** 26-35

Høyer-Hansen M, Bastholm L, Szyniarowski P, Campanella M, Szabadkai G, Farkas T, Bianchi K, Fehrenbacher N, Elling F, Rizzuto R, Mathiasen IS, Jäättelä M (2007) Control of Macroautophagy by Calcium, Calmodulin-Dependent Kinase Kinase-^{2}, and Bcl-2. *Molecular Cell* **25:** 193-205

Hu H, Eggers K, Chen W, Garshasbi M, Motazacker MM, Wrogemann K, Kahrizi K, Tzschach A, Hosseini M, Bahman I, Hucho T, Muhlenhoff M, Gerardy-Schahn R, Najmabadi H, Ropers HH, Kuss AW (2011) ST3GAL3 mutations impair the development of higher cognitive functions. *American Journal of Human Genetics* **89:** 407-414

Hu J, Zacharek S, He YJ, Lee H, Shumway S, Duronio RJ, Xiong Y (2008a) WD40 protein FBW5 promotes ubiquitination of tumor suppressor TSC2 by DDB1-CUL4-ROC1 ligase. *Genes and Development* **22:** 866-871

Hu J, Zacharek S, He YJ, Lee H, Shumway S, Duronio RJ, Xiong Y (2008b) WD40 protein FBW5 promotes ubiquitination of tumor suppressor TSC2 by DDB1-CUL4-ROC1 ligase. *Genes & Development* **22:** 866-871

Huang J, Chen J (2008) VprBP targets Merlin to the Roc1-Cul4A-DDB1 E3 ligase complex for degradation. *Oncogene* **27:** 4056-4064

Huang Q, Wu YT, Tan HL, Ong CN, Shen HM (2009) A novel function of poly(ADP-ribose) polymerase-1 in modulation of autophagy and necrosis under oxidative stress. *Cell Death and Diifferentiation* **16:** 264-277

Huber C, Dias-Santagata D, Glaser A, O'Sullivan J, Brauner R, Wu K, Xu X, Pearce K, Wang R, Uzielli ML, Dagoneau N, Chemaitilly W, Superti-Furga A, Dos Santos H, Megarbane A, Morin G, Gillessen-Kaesbach G, Hennekam R, Van der Burgt I, Black GC, Clayton PE, Read A, Le Merrer M, Scambler PJ, Munnich A, Pan ZQ, Winter R, Cormier-Daire V (2005) Identification of mutations in CUL7 in 3-M syndrome. *Nature Genetics* **37:** 1119-1124

Hudlebusch HR, Santoni-Rugiu E, Simon R, Ralfkiaer E, Rossing HH, Johansen JV, Jorgensen M, Sauter G, Helin K (2011) The histone methyltransferase and putative oncoprotein MMSET is overexpressed in a large variety of human tumors. *Clinical Cancer Research* **17:** 2919-2933

Hurley RL, Anderson KA, Franzone JM, Kemp BE, Means AR, Witters LA (2005) The Ca2+/Calmodulin-dependent Protein Kinase Kinases Are AMP-activated Protein Kinase Kinases. *Journal of Biological Chemistry* **280:** 29060-29066

Iafrate AJ, Feuk L, Rivera MN, Listewnik ML, Donahoe PK, Qi Y, Scherer SW, Lee C (2004) Detection of large-scale variation in the human genome. *Nature Genetics* **36:** 949-951

Inoki K, Corradetti MN, Guan KL (2005) Dysregulation of the TSC-mTOR pathway in human disease. *Nature Genetics* **37:** 19-24

Isidor B, Pichon O, Baron S, David A, Le Caignec C (2010) Deletion of the CUL4B gene in a boy with mental retardation, minor facial anomalies, short stature, hypogonadism, and ataxia. *American Journal of Medical Genetics Part A* **152A:** 175-180

Ito T, Ando H, Handa H (2011) Teratogenic effects of thalidomide: molecular mechanisms. *Cellular and Molecular Life Sciences* **68:** 1569-1579

Ito T, Ando H, Suzuki T, Ogura T, Hotta K, Imamura Y, Yamaguchi Y, Handa H (2010) Identification of a Primary Target of Thalidomide Teratogenicity. *Science* **327:** 1345-1350

Jackson SP, Bartek J (2009) The DNA-damage response in human biology and disease. *Nature* **461:** 1071-1078

Jackson SP, Durocher D (2013) Regulation of DNA Damage Responses by Ubiquitin and SUMO. *Molecular Cell* **49:** 795-807

Jager S, Handschin C, St-Pierre J, Spiegelman BM (2007) AMP-activated protein kinase (AMPK) action in skeletal muscle via direct phosphorylation of PGC-1alpha. *Proceedings of the National Academy of Sciences of the United States of America* **104:** 12017-12022

Jarrett SG, Liang L-P, Hellier JL, Staley KJ, Patel M (2008) Mitochondrial DNA damage and impaired base excision repair during epileptogenesis. *Neurobiology of Disease* **30:** 130-138

Jensen PK (1966) Antimycin-insensitive oxidation of succinate and reduced nicotinamide-adenine dinucleotide in electron-transport particles. I. pH dependency and hydrogen peroxide formation. *Biochimica et Biophysica Acta* **122:** 157-166

Jiang D, Zhao L, Clapham DE (2009a) Genome-wide RNAi screen identifies Letm1 as a mitochondrial Ca2+/H+ antiporter. *Science* **326:** 144-147

Jiang D, Zhao L, Clapham DE (2009b) Genome-Wide RNAi Screen Identifies Letm1 as a Mitochondrial Ca2+/H+ Antiporter. *Science* **326:** 144-147

Jiang D, Zhao L, Clish CB, Clapham DE (2013) Letm1, the mitochondrial Ca2+/H+ antiporter, is essential for normal glucose metabolism and alters brain function in Wolf-Hirschhorn syndrome. *Proceedings of the National Academy of Sciences of the United States of America* **110:** 28

Jin SM, Lazarou M, Wang C, Kane LA, Narendra DP, Youle RJ (2010) Mitochondrial membrane potential regulates PINK1 import and proteolytic destabilization by PARL. *The Journal of Cell Biology* **191:** 933-942

Jo S, Lee KH, Song S, Jung YK, Park CS (2005) Identification and functional characterization of cereblon as a binding protein for large-conductance calcium-activated potassium channel in rat brain. *Journal of Neurochemistry* **94:** 1212-1224

Joo JH, Dorsey FC, Joshi A, Hennessy-Walters KM, Rose KL, McCastlain K, Zhang J, Iyengar R, Jung CH, Suen DF, Steeves MA, Yang CY, Prater SM, Kim DH, Thompson CB, Youle RJ, Ney PA, Cleveland JL, Kundu M (2011) Hsp90-Cdc37 chaperone complex regulates Ulk1- and Atg13-mediated mitophagy. *Molecular Cell* **43:** 572-585

Kabeya Y, Mizushima N, Yamamoto A, Oshitani-Okamoto S, Ohsumi Y, Yoshimori T (2004) LC3, GABARAP and GATE16 localize to autophagosomal membrane depending on form-II formation. *Journal of Cell Science* **117:** 2805-2812

Kadowaki T, Bevins CL, Cama A, Ojamaa K, Marcus-Samuels B, Kadowaki H, Beitz L, McKeon C, Taylor SI (1988) Two mutant alleles of the insulin receptor gene in a patient with extreme insulin resistance. *Science* **240:** 787-790

Kagitani-Shimono K, Imai K, Otani K, Kamio N, Okinaga T, Toribe Y, Suzuki Y, Ozono K (2005) Epilepsy in Wolf-Hirschhorn syndrome (4p-). *Epilepsia* **46:** 150-155

Kamura T, Maenaka K, Kotoshiba S, Matsumoto M, Kohda D, Conaway R, Conaway J, Nakayama K (2004) VHL-box and SOCS-box domains determine binding specificity for Cul2-Rbx1 and Cul5-Rbx2 modules of ubiquitin ligases. *Genes and Development* **18:** 3055 - 3065

Kang H-C, Lee Y-M, Kim HD (2013) Mitochondrial disease and epilepsy. *Brain and Development* **35(8):** 757-761

Kang KW, Lee SJ, Kim SG (2005) Molecular mechanism of Nrf2 activation by oxidative stress. *Antioxidants and Redox Signaling* **7:** 1664-1673

Kann O, Kovacs R (2007) Mitochondria and neuronal activity. *American Journal of Physiology - Cell Physiology* **292:** 641-657

Kapetanaki MG, Guerrero-Santoro J, Bisi DC, Hsieh CL, Rapic-Otrin V, Levine AS (2006) The DDB1-CUL4ADDB2 ubiquitin ligase is deficient in xeroderma pigmentosum group E and targets histone H2A at UV-damaged DNA sites. *Proceedings of the National Academy of Sciences U S A* **103:** 2588-2593

Kapur N, Barker S, Burrows EH, Ellison D, Brice J, Illis LS, Scholey K, Colbourn C, Wilson B, Loates M (1994) Herpes simplex encephalitis: Long term magnetic resonance imaging and neuropsychological profile. *Journal of Neurology Neurosurgery and Psychiatry* **57:** 1334-1342

Katiyar S, Liu E, Knutzen CA, Lang ES, Lombardo CR, Sankar S, Toth JI, Petroski MD, Ronai Ze, Chiang GG (2009) REDD1, an inhibitor of mTOR signalling, is regulated by the CUL4A-DDB1 ubiquitin ligase. *EMBO Reports* **10:** 866-872

Keats JJ, Maxwell CA, Taylor BJ, Hendzel MJ, Chesi M, Bergsagel PL, Larratt LM, Mant MJ, Reiman T, Belch AR, Pilarski LM (2005) Overexpression of transcripts originating from the MMSET locus characterizes all t(4;14)(p16;q32)-positive multiple myeloma patients. *Blood* **105:** 4060-4069

Kelman Z (1997) PCNA: structure, functions and interactions. *Oncogene* **14:** 629-640

Kerzendorfer C, Colnaghi R, Abramowicz I, Carpenter G, O'Driscoll M (2013) Meier-Gorlin syndrome and Wolf-Hirschhorn syndrome: Two developmental disorders highlighting the importance of efficient DNA replication for normal development and neurogenesis. *DNA Repair* **22:** 97-99

Kerzendorfer C, Hannes F, Colnaghi R, Abramowicz I, Carpenter G, Vermeesch JR, O'Driscoll M (2012) Characterizing the functional consequences of haploinsufficiency of NELF-A (WHSC2) and SLBP identifies novel cellular phenotypes in Wolf-Hirschhorn syndrome. *Human Molecular Genetics* **21:** 2181-2193

Kerzendorfer C, Hart L, Colnaghi R, Carpenter G, Alcantara D, Outwin E, Carr AM, O'Driscoll M (2011) CUL4B-deficiency in humans: Understanding the clinical consequences of impaired Cullin 4-RING E3 ubiquitin ligase function. *Mechanisms of Ageing and Development* **132**: 366-373

Kerzendorfer C, Whibley A, Carpenter G, Outwin E, Chiang S-C, Turner G, Schwartz C, El-Khamisy S, Raymond FL, O'Driscoll M (2010) Mutations in Cullin 4B result in a human syndrome associated with increased camptothecin-induced topoisomerase I-dependent DNA breaks. *Human Molecular Genetics* **19:** 1324-1334

Khan M, Rafiq M, Noor A, Ali N, Ali G, Vincent J, Ansar M (2011) A novel deletion mutation in the TUSC3 gene in a consanguineous Pakistani family with autosomal recessive nonsyndromic intellectual disability. *BMC Medical Genetics* **12:** 56

Kim J-Y, Kee HJ, Choe N-W, Kim S-M, Eom G-H, Baek HJ, Kook H, Kook H, Seo S-B (2008a) Multiple Myeloma-Related WHSC1/MMSET Isoform RE-IIBP Is a Histone Methyltransferase with Transcriptional Repression Activity. *Molecular and Cellular Biology* **28:** 2023-2034

Kim JH, Choi SY, Kang BH, Lee SM, Park HS, Kang GY, Bang JY, Cho EJ, Youn HD (2013) AMP-activated protein kinase phosphorylates CtBP1 and down-regulates its activity. *Biochemical and Biophysical Research Communications* **431:** 8-13

Kim Y, Starostina NG, Kipreos ET (2008b) The CRL4Cdt2 ubiquitin ligase targets the degradation of p21Cip1 to control replication licensing. *Genes & Development* **22:** 2507-2519

Kleinjan DA, van Heyningen V (2005) Long-range control of gene expression: emerging mechanisms and disruption in disease. *The American Journal of Human Genetics* **76:** 8-32

Knobloch J, Ruther U (2008) Shedding light on an old mystery: thalidomide suppresses survival pathways to induce limb defects. *Cell Cycle* **7:** 1121-1127

Knott AB, Bossy-Wetzel E (2008) Impairing the Mitochondrial Fission and Fusion Balance: A New Mechanism of Neurodegeneration. *Annals of the New York Academy of Sciences* **1147:** 283-292

Kolas NK, Chapman JR, Nakada S, Ylanko J, Chahwan R, Sweeney FD, Panier S, Mendez M, Wildenhain J, Thomson TM, Pelletier L, Jackson SP, Durocher D (2007) Orchestration of the DNA-damage response by the RNF8 ubiquitin ligase. *Science* **318:** 1637-1640

Koolen DA, Vissers LE, Pfundt R, de Leeuw N, Knight SJ, Regan R, Kooy RF, Reyniers E, Romano C, Fichera M, Schinzel A, Baumer A, Anderlid BM, Schoumans J, Knoers NV, van Kessel AG, Sistermans EA, Veltman JA, Brunner HG, de Vries BB (2006) A new chromosome 17q21.31 microdeletion syndrome associated with a common inversion polymorphism. *Nature Genetics* **38:** 999-1001

Kopanja D, Roy N, Stoyanova T, Hess RA, Bagchi S, Raychaudhuri P (2011) Cul4A is essential for spermatogenesis and male fertility. *Developmental Biology* **352:** 278-287

Kopanja D, Stoyanova T, Okur MN, Huang E, Bagchi S, Raychaudhuri P (2009) Proliferation defects and genome instability in cells lacking Cul4A. *Oncogene* **28:** 2456-2465

Kraft C, Deplazes A, Sohrmann M, Peter M (2008) Mature ribosomes are selectively degraded upon starvation by an autophagy pathway requiring the Ubp3p/Bre5p ubiquitin protease. *Nature Cell Biology* **10:** 602-610

Kudin AP, Zsurka G, Elger CE, Kunz WS (2009) Mitochondrial involvement in temporal lobe epilepsy. *Experimental Neurology* **218:** 326-332

Kumar RA, KaraMohamed S, Sudi J, Conrad DF, Brune C, Badner JA, Gilliam TC, Nowak NJ, Cook EH, Jr., Dobyns WB, Christian SL (2008) Recurrent 16p11.2 microdeletions in autism. *Human Molecular Genetics* **17:** 628-638

Kumar RA, Marshall CR, Badner JA, Babatz TD, Mukamel Z, Aldinger KA, Sudi J, Brune CW, Goh G, Karamohamed S, Sutcliffe JS, Cook EH, Geschwind DH, Dobyns

WB, Scherer SW, Christian SL (2009) Association and mutation analyses of 16p11.2 autism candidate genes. *PLoS ONE* **4:** 26

Kundu M, Lindsten T, Yang CY, Wu J, Zhao F, Zhang J, Selak MA, Ney PA, Thompson CB (2008) Ulk1 plays a critical role in the autophagic clearance of mitochondria and ribosomes during reticulocyte maturation. *Blood* **112:** 1493-1502

Kunz, S W (2002) The role of mitochondria in epileptogenesis. *Current Opinion in Neurology* **15:** 179-184

Kurotaki N, Shen JJ, Touyama M, Kondoh T, Visser R, Ozaki T, Nishimoto J, Shiihara T, Uetake K, Makita Y, Harada N, Raskin S, Brown CW, Hoglund P, Okamoto N, Lupski JR (2005) Phenotypic consequences of genetic variation at hemizygous alleles: Sotos syndrome is a contiguous gene syndrome incorporating coagulation factor twelve (FXII) deficiency. *Genetics in medicine : official journal of the American College of Medical Genetics* **7:** 479-483

Kwiatkowski DJ (2003) Tuberous sclerosis: from tubers to mTOR. *Annals of Human Genetics* **67:** 87-96

Kwok PY, Deng Q, Zakeri H, Taylor SL, Nickerson DA (1996) Increasing the information content of STS-based genome maps: identifying polymorphisms in mapped STSs. *Genomics* **31:** 123-126

Laumonnier F, Roger S, Guerin P, Molinari F, M'Rad R, Cahard D, Belhadj A, Halayem M, Persico AM, Elia M, Romano V, Holbert S, Andres C, Chaabouni H, Colleaux L, Constant J, Le Guennec JY, Briault S (2006) Association of a functional deficit of the BKCa channel, a synaptic regulator of neuronal excitability, with autism and mental retardation. *American Journal of Psychiatry* **163:** 1622-1629

Le Belle JE, Orozco NM, Paucar AA, Saxe JP, Mottahedeh J, Pyle AD, Wu H, Kornblum HI (2011) Proliferative neural stem cells have high endogenous ROS levels that regulate self-renewal and neurogenesis in a PI3K/Akt-dependant manner. *Cell Stem Cell* **8:** 59-71

Lebiedzinska M, Karkucinska-Wieckowska A, Giorgi C, Karczmarewicz E, Pronicka E, Pinton P, Duszynski J, Pronicki M, Wieckowski MR (2010) Oxidative stress-dependent p66Shc phosphorylation in skin fibroblasts of children with mitochondrial disorders. *Biochimica et Biophysica Acta* **1797:** 952-960

Lebovitz RM, Zhang H, Vogel H, Cartwright J, Dionne L, Lu N, Huang S, Matzuk MM (1996) Neurodegeneration, myocardial injury, and perinatal death in mitochondrial superoxide dismutase-deficient mice. *Proceedings of the National Academy of Sciences* **93:** 9782-9787

Lee AY, Hsu CH, Wu SH (2004) Functional domains of Brevibacillus thermoruber lon protease for oligomerization and DNA binding: role of N-terminal and sensor

and substrate discrimination domains. *Journal of Biological Chemistry* **279:** 34903-34912

Lee C, Iafrate AJ, Brothman AR (2007a) Copy number variations and clinical cytogenetic diagnosis of constitutional disorders. *Nature Genetics* **39:** S48-54

Lee DK, Chang C (2003) Endocrine mechanisms of disease: Expression and degradation of androgen receptor: mechanism and clinical implication. *Journal of Clinical Endocrinology and Metabolism* **88:** 4043-4054

Lee HC, Wei YH (2000) Mitochondrial role in life and death of the cell. *Journal of Biomedical Science* **7:** 2-15

Lee J-Y, Nagano Y, Taylor JP, Lim KL, Yao T-P (2010a) Disease-causing mutations in Parkin impair mitochondrial ubiquitination, aggregation, and HDAC6-dependent mitophagy. *The Journal of Cell Biology* **189:** 671-679

Lee J, Zhou P (2007) DCAFs, the Missing Link of the CUL4-DDB1 Ubiquitin Ligase. *Molecular Cell* **26:** 775-780

Lee JA, Carvalho CM, Lupski JR (2007b) A DNA replication mechanism for generating nonrecurrent rearrangements associated with genomic disorders. *Cell* **131:** 1235-1247

Lee KJ, Lee KM, Jo S, Kang KW, Park C-S (2010b) Induction of cereblon by NF-E2-related factor 2 in neuroblastoma cells exposed to hypoxia-reoxygenation. *Biochemical and Biophysical Research Communications* **399:** 711-715

Lee KM, Jo S, Kim H, Lee J, Park C-S (2011) Functional modulation of AMP-activated protein kinase by cereblon. *Biochimica et Biophysica Acta (BBA) - Molecular Cell Research* **1813:** 448-455

Lee KM, Yang S-J, Kim YD, Choi YD, Nam JH, Choi CS, Choi H-S, Park C-S (2013) Disruption of the cereblon gene enhances hepatic AMPK activity and prevents high fat diet-induced obesity and insulin resistance in mice. *Diabetes* **62:** 1855-1864

Leonard H, Wen X (2002) The epidemiology of mental retardation: challenges and opportunities in the new millennium. *Mental Retardation and Developmental Disability Research Reviews* **8:** 117-134

Leshinsky-Silver E, Zinger A, Bibi CN, Barash V, Sadeh M, Lev D, Sagie TL (2002) MEHMO (Mental retardation, Epileptic seizures, Hypogenitalism, Microcephaly, Obesity): a new X-linked mitochondrial disorder. *European Journal of Human Genetics : EJHG* **10:** 226-230

Leung-Pineda V, Huh J, Piwnica-Worms H (2009) DDB1 targets Chk1 to the Cul4 E3 ligase complex in normal cycling cells and in cells experiencing replication stress. *Cancer Research* **69:** 2630-2637

Leung AWC, Varanyuwatana P, Halestrap AP (2008) The mitochondrial phosphate carrier interacts with cyclophilin D and may play a key role in the permeability transition. *Journal of Biological Chemistry* **283:** 26312-26323

Li B, Jia N, Kapur R, Chun KT (2006) Cul4A targets p27 for degradation and regulates proliferation, cell cycle exit, and differentiation during erythropoiesis. *Blood* **107:** 4291-4299

Li B, Ruiz JC, Chun KT (2002) CUL-4A is critical for early embryonic development. *Molecular and Cellular Biology* **22:** 4997-5005

Li J, Al-Azzawi F (2009) Mechanism of androgen receptor action. *Maturitas* **63:** 142-148

Li J, Yin C, Okamoto H, Mushlin H, Balgley BM, Lee CS, Yuan K, Ikejiri B, Glasker S, Vortmeyer AO, Oldfield EH, Weil RJ, Zhuang Z (2008) Identification of a novel proliferation-related protein, WHSC1 4a, in human gliomas. *Neuro-oncology* **10:** 45-51

Li X, Lu D, He F, Zhou H, Liu Q, Wang Y, Shao C, Gong Y (2011) Cullin 4B Protein Ubiquitin Ligase Targets Peroxiredoxin III for Degradation. *Journal of Biological Chemistry* **286:** 32344-32354

Li Y, Huang T-T, Carlson EJ, Melov S, Ursell PC, Olson JL, Noble LJ, Yoshimura MP, Berger C, Chan PH (1995) Dilated cardiomyopathy and neonatal lethality in mutant mice lacking manganese superoxide dismutase. *Nature genetics* **11:** 376-381

Liang L-P, Patel M (2004) Mitochondrial oxidative stress and increased seizure susceptibility in Sod2−/+ mice. *Free Radical Biology and Medicine* **36:** 542-554

Liang LP, Ho YS, Patel M (2000) Mitochondrial superoxide production in kainate-induced hippocampal damage. *Neuroscience* **101:** 563-570

Liang LP, Waldbaum S, Rowley S, Huang TT, Day BJ, Patel M (2012) Mitochondrial oxidative stress and epilepsy in SOD2 deficient mice: attenuation by a lipophilic metalloporphyrin. *Neurobiology of Disease* **45:** 1068-1076

Lifton RP, Dluhy RG, Powers M, Rich GM, Cook S, Ulick S, Lalouel JM (1992) A chimaeric 11 beta-hydroxylase/aldosterone synthase gene causes glucocorticoid-remediable aldosteronism and human hypertension. *Nature* **355:** 262-265

Lin MT, Beal MF (2006) Mitochondrial dysfunction and oxidative stress in neurodegenerative diseases. *Nature* **443:** 787-795

Liolitsa D, Rahman S, Benton S, Carr LJ, Hanna MG (2003) Is the mitochondrial complex I ND5 gene a hot-spot for MELAS causing mutations? *Annals of Neurology* **53:** 128-132

Liu J, Furukawa M, Matsumoto T, Xiong Y (2002) NEDD8 modification of CUL1 dissociates p120(CAND1), an inhibitor of CUL1-SKP1 binding and SCF ligases. *Molecular Cell* **10:** 1511-1518

Liu L, Lee S, Zhang J, Peters S, Hannah J, Zhang Y, Yin Y, Koff A, Ma L, Zhou P (2009) CUL4A abrogation augments DNA damage response and protection against skin carcinogenesis. *Molecular Cell* **34:** 451 - 460

Liu L, Yin Y, Li Y, Prevedel L, Lacy EH, Ma L, Zhou P (2012) Essential role of the CUL4B ubiquitin ligase in extra-embryonic tissue development during mouse embryogenesis. *Cell Research* **22:** 1258-1269

Loschen G, Azzi A, Richter C, Flohe L (1974) Superoxide radicals as precursors of mitochondrial hydrogen peroxide. *FEBS Letters* **42:** 68-72

Loschen G, Flohe L, Chance B (1971) Respiratory chain linked H(2)O(2) production in pigeon heart mitochondria. *FEBS Letters* **18:** 261-264

Loscher W (2002) Basic pharmacology of valproate: a review after 35 years of clinical use for the treatment of epilepsy. *CNS Drugs* **16:** 669-694

Lou Z, Minter-Dykhouse K, Franco S, Gostissa M, Rivera MA, Celeste A, Manis JP, van Deursen J, Nussenzweig A, Paull TT, Alt FW, Chen J (2006) MDC1 maintains genomic stability by participating in the amplification of ATM-dependent DNA damage signals. *Molecular Cell* **21:** 187-200

Lupski JR (1998) Genomic disorders: structural features of the genome can lead to DNA rearrangements and human disease traits. *Trends in Genetics* **14:** 417-422

Lupski JR (2007) Genomic rearrangements and sporadic disease. *Nature genetics* **39:** S43-47

Lupski JR, de Oca-Luna RM, Slaugenhaupt S, Pentao L, Guzzetta V, Trask BJ, Saucedo-Cardenas O, Barker DF, Killian JM, Garcia CA, Chakravarti A, Patel PI (1991) DNA duplication associated with Charcot-Marie-Tooth disease type 1A. *Cell* **66:** 219-232

Lupski JR, Stankiewicz P (2005) Genomic disorders: molecular mechanisms for rearrangements and conveyed phenotypes. *PLoS genetics* **1:** e49

Lupski JR, Wise CA, Kuwano A, Pentao L, Parke JT, Glaze DG, Ledbetter DH, Greenberg F, Patel PI (1992) Gene dosage is a mechanism for Charcot-Marie-Tooth disease type 1A. *Nature Genetics* **1:** 29-33

Ma H, Cai Q, Lu W, Sheng ZH, Mochida S (2009) KIF5B motor adaptor syntabulin maintains synaptic transmission in sympathetic neurons. *The Journal of Neuroscience* **29:** 13019-13029

Maas NMC, Van Buggenhout G, Hannes F, Thienpont B, Sanlaville D, Kok K, Midro A, Andrieux J, Anderlid B-M, Schoumans J, Hordijk R, Devriendt K, Fryns J-P, Vermeesch JR (2008) Genotype–phenotype correlation in 21 patients with Wolf–Hirschhorn syndrome using high resolution array comparative genome hybridisation (CGH). *Journal of Medical Genetics* **45:** 71-80

MacDonald SHF, Ruth P, Knaus HG, Shipston MJ (2006) Increased large conductance calcium-activated potassium (BK) channel expression accompanied by STREX variant downregulation in the developing mouse CNS. *BMC Developmental Biology* **6**

MacIntosh GC, Bassham DC (2011) The connection between ribophagy, autophagy and ribosomal RNA decay. *Autophagy* **7:** 662-663

Madamanchi NR, Runge MS (2007) Mitochondrial Dysfunction in Atherosclerosis. *Circulation Research* **100:** 460-473

Magri C, Sacchetti E, Traversa M, Valsecchi P, Gardella R, Bonvicini C, Minelli A, Gennarelli M, Barlati S (2010) New copy number variations in schizophrenia. *PLoS One* **5:** e13422

Mahrour N, Redwine W, Florens L, Swanson S, Martin-Brown S, Bradford W, Staehling-Hampton K, Washburn M, Conaway R, Conaway J (2008) Characterization of Cullin-box sequences that direct recruitment of Cul2-Rbx1 and Cul5-Rbx2 modules to Elongin BC-based ubiquitin ligases. *Journal of Biological Chemistry* **283:** 8005 - 8013

Mailand N, Bekker-Jensen S, Faustrup H, Melander F, Bartek J, Lukas C, Lukas J (2007) RNF8 ubiquitylates histones at DNA double-strand breaks and promotes assembly of repair proteins. *Cell* **131:** 887-900

Mailand N, Falck J, Lukas C, Syljuasen RG, Welcker M, Bartek J, Lukas J (2000) Rapid destruction of human Cdc25A in response to DNA damage. *Science* **288:** 1425-1429

Manke IA, Nguyen A, Lim D, Stewart MQ, Elia AE, Yaffe MB (2005) MAPKAP kinase-2 is a cell cycle checkpoint kinase that regulates the G2/M transition and S phase progression in response to UV irradiation. *Molecular Cell* **17:** 37-48

Marango J, Shimoyama M, Nishio H, Meyer JA, Min D-J, Sirulnik A, Martinez-Martinez Y, Chesi M, Bergsagel PL, Zhou M-M, Waxman S, Leibovitch BA, Walsh MJ, Licht JD (2008) The MMSET protein is a histone methyltransferase with characteristics of a transcriptional corepressor. *Blood* **111:** 3145-3154

Marin I (2009) Diversification of the cullin family. *BMC Evolutional Biology* **9:** 267

Marshall CR, Noor A, Vincent JB, Lionel AC, Feuk L, Skaug J, Shago M, Moessner R, Pinto D, Ren Y, Thiruvahindrapduram B, Fiebig A, Schreiber S, Friedman J, Ketelaars CE, Vos YJ, Ficicioglu C, Kirkpatrick S, Nicolson R, Sloman L, Summers A, Gibbons CA, Teebi A, Chitayat D, Weksberg R, Thompson A, Vardy C, Crosbie V, Luscombe S, Baatjes R, Zwaigenbaum L, Roberts W, Fernandez B, Szatmari P, Scherer SW (2008) Structural variation of chromosomes in autism spectrum disorder. *American Journal of Human Genetics* **82:** 477-488

Martin KC (2004) Local protein synthesis during axon guidance and synaptic plasticity. *Current Opinion in Neurobiology* **14:** 305-310

Mathias N, Johnson S, Winey M, Adams A, Goetsch L, Pringle J, Byers B, Goebl M (1996) Cdc53p acts in concert with Cdc4p and Cdc34p to control the G1-to-S-phase transition and identifies a conserved family of proteins. *Molecular and Cellular Biology* **16:** 6634 - 6643

Mazzucchelli C, Vantaggiato C, Ciamei A, Fasano S, Pakhotin P, Krezel W, Welzl H, Wolfer DP, Pages G, Valverde O, Marowsky A, Porrazzo A, Orban PC, Maldonado R, Ehrengruber MU, Cestari V, Lipp HP, Chapman PF, Pouyssegur J, Brambilla R (2002) Knockout of ERK1 MAP kinase enhances synaptic plasticity in the striatum and facilitates striatal-mediated learning and memory. *Neuron* **34:** 807-820

McCall CM, Hu J, Xiong Y (2005) Recruiting substrates to cullin 4-dependent ubiquitin ligases by DDB1. *Cell cycle* **4:** 27-29

McClintock B (1951) Chromosome organization and gene expression. *Cold Spring Harbor Symposia on Quantitative Biology* **16:** 13-47

McCormack JG, Denton RM (1993) Mitochondrial Ca2+ transport and the role of intramitochondrial Ca2+ in the regulation of energy metabolism. *Developmental Neuroscience* **15:** 165-173

McDermid HE, Morrow BE (2002) Genomic disorders on 22q11. *The American Journal of Human Genetics* **70:** 1077-1088

McKenna MC (2007) The glutamate-glutamine cycle is not stoichiometric: Fates of glutamate in brain. *Journal of Neuroscience Research* **85:** 3347-3358

McKenzie M, Liolitsa D, Hanna MG (2004) Mitochondrial disease: mutations and mechanisms. *Neurochemical Research* **29:** 589-600

McKinnon PJ (2012) ATM and the molecular pathogenesis of ataxia telangiectasia. *Annual Review of Pathology* **7:** 303-321

McQuibban AG, Joza N, Megighian A, Scorzeto M, Zanini D, Reipert S, Richter C, Schweyen RJ, Nowikovsky K (2010) A Drosophila mutant of LETM1, a candidate gene for seizures in Wolf-Hirschhorn syndrome. *Human Molecular Genetics* **19:** 987-1000

Melov S, Schneider JA, Day BJ, Hinerfeld D, Coskun P, Mirra SS, Crapo JD, Wallace DC (1998) A novel neurological phenotype in mice lacking mitochondrial manganese superoxide dismutase. *Nature genetics* **18:** 159-163

Merla G, Howald C, Henrichsen CN, Lyle R, Wyss C, Zabot MT, Antonarakis SE, Reymond A (2006) Submicroscopic deletion in patients with Williams-Beuren syndrome influences expression levels of the nonhemizygous flanking genes. *American Journal of Human Genetics* **79:** 332-341

Mir A, Kaufman L, Noor A, Motazacker MM, Jamil T, Azam M, Kahrizi K, Rafiq MA, Weksberg R, Nasr T, Naeem F, Tzschach A, Kuss AW, Ishak GE, Doherty D, Ropers HH, Barkovich AJ, Najmabadi H, Ayub M, Vincent JB (2009) Identification of mutations in TRAPPC9, which encodes the NIK- and IKK-beta-binding protein, in nonsyndromic autosomal-recessive mental retardation. *American Journal of Human Genetics* **85:** 909-915

Misonou H, Menegola M, Buchwalder L, Park EW, Meredith A, Rhodes KJ, Aldrich RW, Trimmer JS (2006) Immunolocalization of the Ca2+-activated K+ channel Slo1 in axons and nerve terminals of mammalian brain and cultured neurons. *The Journal of Comparative Neurology* **496:** 289-302

Mizushima N, Levine B, Cuervo AM, Klionsky DJ (2008) Autophagy fights disease through cellular self-digestion. *Nature* **451:** 1069-1075

Mizushima N, Noda T, Ohsumi Y (1999) Apg16p is required for the function of the Apg12p-Apg5p conjugate in the yeast autophagy pathway. *The EMBO Journal* **18:** 3888-3896

Mizushima N, Yoshimori T (2007) How to interpret LC3 immunoblotting. *Autophagy* **3:** 542-545

Mochida GH, Mahajnah M, Hill AD, Basel-Vanagaite L, Gleason D, Hill RS, Bodell A, Crosier M, Straussberg R, Walsh CA (2009) A Truncating Mutation of TRAPPC9 Is Associated with Autosomal-Recessive Intellectual Disability and Postnatal Microcephaly. *American Journal of Human Genetics* **85:** 897-902

Molinari F, Foulquier F, Tarpey PS, Morelle W, Boissel S, Teague J, Edkins S, Futreal PA, Stratton MR, Turner G, Matthijs G, Gecz J, Munnich A, Colleaux L (2008)

Oligosaccharyltransferase-subunit mutations in nonsyndromic mental retardation. *American Journal of Human Genetics* **82:** 1150-1157

Molinari F, Rio M, Meskenaite V, Encha-Razavi F, Auge J, Bacq D, Briault S, Vekemans M, Munnich A, Attie-Bitach T, Sonderegger P, Colleaux L (2002) Truncating neurotrypsin mutation in autosomal recessive nonsyndromic mental retardation. *Science* **298:** 1779-1781

Monks DA, Johansen JA, Mo K, Rao P, Eagleson B, Yu Z, Lieberman AP, Breedlove SM, Jordan CL (2007) Overexpression of wild-type androgen receptor in muscle recapitulates polyglutamine disease. *Proceedings of the National Academy of Sciences of the United States of America* **104:** 18259-18264

Monti B, Polazzi E, Contestabile A (2009) Biochemical, molecular and epigenetic mechanisms of valproic acid neuroprotection. *Current Molecular Pharmacology* **2:** 95-109

Morris JR, Solomon E (2004) BRCA1 : BARD1 induces the formation of conjugated ubiquitin structures, dependent on K6 of ubiquitin, in cells during DNA replication and repair. *Human Molecular Genetics* **13:** 807-817

Motazacker MM, Rost BR, Hucho T, Garshasbi M, Kahrizi K, Ullmann R, Abedini SS, Nieh SE, Amini SH, Goswami C, Tzschach A, Jensen LR, Schmitz D, Ropers HH, Najmabadi H, Kuss AW (2007) A defect in the ionotropic glutamate receptor 6 gene (GRIK2) is associated with autosomal recessive mental retardation. *American Journal of Human Genetics* **81:** 792-798

Muller FL, Liu Y, Van Remmen H (2004) Complex III releases superoxide to both sides of the inner mitochondrial membrane. *The Journal of Biological Chemistry* **279:** 49064-49073

Murga M, Bunting S, Montana MF, Soria R, Mulero F, Canamero M, Lee Y, McKinnon PJ, Nussenzweig A, Fernandez-Capetillo O (2009) A mouse model of ATR-Seckel shows embryonic replicative stress and accelerated aging. *Nature Genetics* **41:** 891-898

Murphy MP, Holmgren A, Larsson NG, Halliwell B, Chang CJ, Kalyanaraman B, Rhee SG, Thornalley PJ, Partridge L, Gems D, Nyström T, Belousov V, Schumacker PT, Winterbourn CC (2011) Unraveling the biological roles of reactive oxygen species. *Cell Metabolism* **13:** 361-366

Nagamani SC, Zhang F, Shchelochkov OA, Bi W, Ou Z, Scaglia F, Probst FJ, Shinawi M, Eng C, Hunter JV, Sparagana S, Lagoe E, Fong CT, Pearson M, Doco-Fenzy M, Landais E, Mozelle M, Chinault AC, Patel A, Bacino CA, Sahoo T, Kang SH, Cheung SW, Lupski JR, Stankiewicz P (2009) Microdeletions including YWHAE in the Miller-Dieker syndrome region on chromosome 17p13.3 result in facial dysmorphisms, growth restriction, and cognitive impairment. *Journal of Medical Genetics* **46:** 825-833

Najmabadi H, Motazacker MM, Garshasbi M, Kahrizi K, Tzschach A, Chen W, Behjati F, Hadavi V, Nieh SE, Abedini SS, Vazifehmand R, Firouzabadi SG, Jamali P, Falah M, Seifati SM, Gruters A, Lenzner S, Jensen LR, Ruschendorf F, Kuss AW, Ropers HH (2007) Homozygosity mapping in consanguineous families reveals extreme heterogeneity of non-syndromic autosomal recessive mental retardation and identifies 8 novel gene loci. *Human Genetics* **121:** 43-48

Nakagawa T, Xiong Y (2011) X-Linked Mental Retardation Gene CUL4B Targets Ubiquitylation of H3K4 Methyltransferase Component WDR5 and Regulates Neuronal Gene Expression. *Molecular Cell* **43:** 381-391

Narendra D, Kane LA, Hauser DN, Fearnley IM, Youle RJ (2010a) p62/SQSTM1 is required for Parkin-induced mitochondrial clustering but not mitophagy; VDAC1 is dispensable for both. *Autophagy* **6:** 1090-1106

Narendra D, Tanaka A, Suen D-F, Youle RJ (2008) Parkin is recruited selectively to impaired mitochondria and promotes their autophagy. *The Journal of Cell Biology* **183:** 795-803

Narendra DP, Jin SM, Tanaka A, Suen D-F, Gautier CA, Shen J, Cookson MR, Youle RJ (2010b) PINK1 Is Selectively Stabilized on Impaired Mitochondria to Activate Parkin. *PLoS Biol* **8:** e1000298

Narita T, Yung TMC, Yamamoto J, Tsuboi Y, Tanabe H, Tanaka K, Yamaguchi Y, Handa H (2007) NELF Interacts with CBC and Participates in 3′ End Processing of Replication-Dependent Histone mRNAs. *Molecular Cell* **26:** 349-365

Nathans J, Piantanida TP, Eddy RL, Shows TB, Hogness DS (1986) Molecular genetics of inherited variation in human color vision. *Science* **232:** 203-210

Navarro A, Boveris A (2007) The mitochondrial energy transduction system and the aging process. *American Journal of Physiology - Cell Physiology* **292:** C670-C686

Newton SS, Duman RS (2006) Chromatin remodeling: a novel mechanism of psychotropic drug action. *Molecular Pharmacology* **70:** 440-443

Nguyen DQ, Webber C, Ponting CP (2006) Bias of selection on human copy-number variants. *PLoS Genetics* **2:** e20

Nimura K, Ura K, Shiratori H, Ikawa M, Okabe M, Schwartz RJ, Kaneda Y (2009) A histone H3 lysine 36 trimethyltransferase links Nkx2-5 to Wolf-Hirschhorn syndrome. *Nature* **460:** 287-291

Nishitani H, Shiomi Y, Iida H, Michishita M, Takami T, Tsurimoto T (2008) CDK Inhibitor p21 Is Degraded by a Proliferating Cell Nuclear Antigen-coupled Cul4-DDB1Cdt2 Pathway during S Phase and after UV Irradiation. *Journal of Biological Chemistry* **283:** 29045-29052

Nishitani H, Sugimoto N, Roukos V, Nakanishi Y, Saijo M, Obuse C, Tsurimoto T, Nakayama KI, Nakayama K, Fujita M, Lygerou Z, Nishimoto T (2006) Two E3 ubiquitin ligases, SCF-Skp2 and DDB1-Cul4, target human Cdt1 for proteolysis. *The EMBO journal* **25:** 1126-1136

Nolan DK, Chen P, Das S, Ober C, Waggoner D (2008) Fine mapping of a locus for nonsyndromic mental retardation on chromosome 19p13. *American Journal of Medical Genetics Part A* **146A:** 1414-1422

Nowikovsky K, Froschauer EM, Zsurka G, Samaj J, Reipert S, Kolisek M, Wiesenberger G, Schweyen RJ (2004) The LETM1/YOL027 Gene Family Encodes a Factor of the Mitochondrial K+ Homeostasis with a Potential Role in the Wolf-Hirschhorn Syndrome. *Journal of Biological Chemistry* **279:** 30307-30315

Nowikovsky K, Pozzan T, Rizzuto R, Scorrano L, Bernardi P (2012a) The Pathophysiology of LETM1. *The Journal of General Physiology* **139:** 445-454

Nowikovsky K, Pozzan T, Rizzuto R, Scorrano L, Bernardi P (2012b) Perspectives on: SGP symposium on mitochondrial physiology and medicine: the pathophysiology of LETM1. *Journal of General Physiology* **139:** 445-454

Nowikovsky K, Reipert S, Devenish RJ, Schweyen RJ (2007) Mdm38 protein depletion causes loss of mitochondrial K+/H+ exchange activity, osmotic swelling and mitophagy. *Cell Death and Differentiation* **14:** 1647-1656

O'Driscoll M, Gennery AR, Seidel J, Concannon P, Jeggo PA (2004) An overview of three new disorders associated with genetic instability: LIG4 syndrome, RS-SCID and ATR-Seckel syndrome. *DNA Repair* **3:** 1227-1235

O'Rourke B (2007) Mitochondrial ion channels. *Annual Review of Physiology* **69:** 19-49

O'Driscoll M, Jeggo PA (2008) The role of the DNA damage response pathways in brain development and microcephaly: Insight from human disorders. *DNA Repair* **7:** 1039-1050

Ohashi M, Runge MS, Faraci FM, Heistad DD (2006) MnSOD deficiency increases endothelial dysfunction in ApoE-deficient mice. *Arteriosclerosis, Thrombosis, and Vascular Biology* **26:** 2331-2336

Ohtake F, Baba A, Takada I, Okada M, Iwasaki K, Miki H, Takahashi S, Kouzmenko A, Nohara K, Chiba T, Fujii-Kuriyama Y, Kato S (2007) Dioxin receptor is a ligand-dependent E3 ubiquitin ligase. *Nature* **446:** 562-566

Okamoto S, Sherman K, Bai G, Lipton SA (2002) Effect of the ubiquitous transcription factors, SP1 and MAZ, on NMDA receptor subunit type 1 (NR1)

expression during neuronal differentiation. *Brain Research: Molecular Brain Research* **107:** 89-96

Okatsu K, Saisho K, Shimanuki M, Nakada K, Shitara H, Sou YS, Kimura M, Sato S, Hattori N, Komatsu M, Tanaka K, Matsuda N (2010) p62/SQSTM1 cooperates with Parkin for perinuclear clustering of depolarized mitochondria. *Genes to Cells : Devoted to Molecular and Cellular Mechanisms* **15:** 887-900

Ott M, Gogvadze V, Orrenius S, Zhivotovsky B (2007) Mitochondria, oxidative stress and cell death. *Apoptosis* **12:** 913-922

Pallardó F, Lloret A, Lebel M, d'Ischia M, Cogger V, Le Couteur D, Gadaleta M, Castello G, Pagano G (2010) Mitochondrial dysfunction in some oxidative stress-related genetic diseases: Ataxia-Telangiectasia, Down Syndrome, Fanconi Anaemia and Werner Syndrome. *Biogerontology* **11:** 401-419

Pan ZQ, Kentsis A, Dias DC, Yamoah K, Wu K (2004) Nedd8 on cullin: building an expressway to protein destruction. *Oncogene* **23:** 1985-1997

Panier S, Durocher D (2009) Regulatory ubiquitylation in response to DNA double-strand breaks. *DNA Repair* **8:** 436-443

Pankiv S, Clausen TH, Lamark T, Brech A, Bruun J-A, Outzen H, Øvervatn A, Bjørkøy G, Johansen T (2007) p62/SQSTM1 Binds Directly to Atg8/LC3 to Facilitate Degradation of Ubiquitinated Protein Aggregates by Autophagy. *Journal of Biological Chemistry* **282:** 24131-24145

Papia Ghosh MW, Hui Zhang and Hong Sun (2008) mTORC1 signaling requires proteasomal function and the involvement of CUL4-DDB1 ubiquitin E3 ligase. *Cell cycle* **7:** 373 - 381

Parman T, Wiley MJ, Wells PG (1999) Free radical-mediated oxidative DNA damage in the mechanism of thalidomide teratogenicity. *Nature Medicine* **5:** 582-585

Parone PA, Da Cruz S, Tondera D, Mattenberger Y, James DI, Maechler P, Barja F, Martinou J-C (2008) Preventing Mitochondrial Fission Impairs Mitochondrial Function and Leads to Loss of Mitochondrial DNA. *PLoS ONE* **3:** e3257

Patel M (2004) Mitochondrial dysfunction and oxidative stress: cause and consequence of epileptic seizures. *Free Radical Biology and Medicine* **37:** 1951-1962

Patel MN (2002) Oxidative Stress, Mitochondrial Dysfunction, and Epilepsy. *Free Radical Research* **36:** 1139-1146

Patron M, Raffaello A, Granatiero V, Tosatto A, Merli G, De Stefani D, Wright L, Pallafacchina G, Terrin A, Mammucari C, Rizzuto R (2013) The Mitochondrial

Calcium Uniporter (MCU): molecular identity and physiological roles. *The Journal of Biological Chemistry*

Pattingre S, Tassa A, Qu X, Garuti R, Liang XH, Mizushima N, Packer M, Schneider MD, Levine B (2005) Bcl-2 Antiapoptotic Proteins Inhibit Beclin 1-Dependent Autophagy. *Cell* **122:** 927-939

Pei H, Zhang L, Luo K, Qin Y, Chesi M, Fei F, Bergsagel PL, Wang L, You Z, Lou Z (2011) MMSET regulates histone H4K20 methylation and 53BP1 accumulation at DNA damage sites. *Nature* **470:** 124-128

Peng TI, Jou MJ (2010) Oxidative stress caused by mitochondrial calcium overload. *Annals of the New York Academy of Sciences* **1201:** 183-188

Peoples R, Franke Y, Wang YK, Perez-Jurado L, Paperna T, Cisco M, Francke U (2000) A physical map, including a BAC/PAC clone contig, of the Williams-Beuren syndrome--deletion region at 7q11.23. *American Journal of Human Genetics* **66:** 47-68

Perry GH, Ben-Dor A, Tsalenko A, Sampas N, Rodriguez-Revenga L, Tran CW, Scheffer A, Steinfeld I, Tsang P, Yamada NA, Park HS, Kim JI, Seo JS, Yakhini Z, Laderman S, Bruhn L, Lee C (2008) The fine-scale and complex architecture of human copy-number variation. *American Journal of Human Genetics* **82:** 685-695

Petroski M, Deshaies R (2005a) Function and regulation of cullin-RING ubiquitin ligases. *Nature Reviews Molecular Cell Biology* **6:** 9 - 20

Petroski MD, Deshaies RJ (2005b) Function and regulation of cullin-RING ubiquitin ligases. *Nature reviews Molecular cell biology* **6:** 9-20

Phiel CJ, Zhang F, Huang EY, Guenther MG, Lazar MA, Klein PS (2001) Histone deacetylase is a direct target of valproic acid, a potent anticonvulsant, mood stabilizer, and teratogen. *The Journal of Biological Chemistry* **276:** 36734-36741

Piao L, Li Y, Kim SJ, Byun HS, Huang SM, Hwang S-K, Yang K-J, Park KA, Won M, Hong J, Hur GM, Seok JH, Shong M, Cho M-H, Brazil DP, Hemmings BA, Park J (2009a) Association of LETM1 and MRPL36 Contributes to the Regulation of Mitochondrial ATP Production and Necrotic Cell Death. *Cancer Research* **69:** 3397-3404

Piao L, Li Y, Kim SJ, Byun HS, Huang SM, Hwang SK, Yang KJ, Park KA, Won M, Hong J, Hur GM, Seok JH, Shong M, Cho MH, Brazil DP, Hemmings BA, Park J (2009b) Association of LETM1 and MRPL36 contributes to the regulation of mitochondrial ATP production and necrotic cell death. *Cancer Research* **69:** 3397-3404

Pick E, Lau O, Tsuge T, Menon S, Tong Y, Dohmae N, Plafker S, Deng X, Wei N (2007) Mammalian DET1 regulates Cul4A activity and forms stable complexes

with E2 ubiquitin-conjugating enzymes. *Molecular and Cellular Biology* **27:** 4708 - 4719

Piekorz RP, Hoffmeyer A, Duntsch CD, McKay C, Nakajima H, Sexl V, Snyder L, Rehg J, Ihle JN (2002) The centrosomal protein TACC3 is essential for hematopoietic stem cell function and genetically interfaces with p53-regulated apoptosis. *The EMBO Journal* **21:** 653-664

Pinkel D, Segraves R, Sudar D, Clark S, Poole I, Kowbel D, Collins C, Kuo WL, Chen C, Zhai Y, Dairkee SH, Ljung BM, Gray JW, Albertson DG (1998) High resolution analysis of DNA copy number variation using comparative genomic hybridization to microarrays. *Nature Genetics* **20:** 207-211

Pipiras E, Coquelle A, Bieth A, Debatisse M (1998) Interstitial deletions and intrachromosomal amplification initiated from a double-strand break targeted to a mammalian chromosome. *EMBO Journal* **17:** 325-333

Potocki L, Bi W, Treadwell-Deering D, Carvalho CM, Eifert A, Friedman EM, Glaze D, Krull K, Lee JA, Lewis RA, Mendoza-Londono R, Robbins-Furman P, Shaw C, Shi X, Weissenberger G, Withers M, Yatsenko SA, Zackai EH, Stankiewicz P, Lupski JR (2007) Characterization of Potocki-Lupski syndrome (dup(17)(p11.2p11.2)) and delineation of a dosage-sensitive critical interval that can convey an autism phenotype. *American Journal of Human Genetics* **80:** 633-649

Potocki L, Chen K-S, Koeuth T, Killian J, Iannaccone ST, Shapira SK, Kashork CD, Spikes AS, Shaffer LG, Lupski JR (1999) DNA rearrangements on both homologues of chromosome 17 in a mildly delayed individual with a family history of autosomal dominant carpal tunnel syndrome. *American Journal of Human Genetics* **64:** 471-478

Priest JH, Thuline HC, Laveck GD, Jarvis DB (1961) An approach to genetic factors in mental retardation. Studies of families containing at least two siblings admitted to a state institution for the retarded. *American Journal of Mental Deficiency* **66:** 42-50

Pryor WA (1986) Oxy-Radicals and Related Species: Their Formation, Lifetimes, and Reactions. *Annual Review of Physiology* **48:** 657-667

Puddu P, Barboni P, Mantovani V, Montagna P, Cerullo A, Bragliani M, Molinotti C, Caramazza R (1993) Retinitis pigmentosa, ataxia, and mental retardation associated with mitochondrial DNA mutation in an Italian family. *British Journal of Ophthalmology* **77:** 84-88

Puligilla C, Feng F, Ishikawa K, Bertuzzi S, Dabdoub A, Griffith AJ, Fritzsch B, Kelley MW (2007) Disruption of fibroblast growth factor receptor 3 signaling results in defects in cellular differentiation, neuronal patterning, and hearing impairment. *Developmental Dynamics* **236:** 1905-1917

Quinsay MN, Thomas RL, Lee Y, Gustafsson ÅB (2010) Bnip3-mediated mitochondrial autophagy is independent of the mitochondrial permeability transition pore. *Autophagy* **6:** 855-862

Rabilloud T, Heller M, Rigobello M-P, Bindoli A, Aebersold R, Lunardi J (2001) The mitochondrial antioxidant defence system and its response to oxidative stress. *Proteomics* **1:** 1105-1110

Racioppi L, Means AR (2012) Calcium/Calmodulin-dependent Protein Kinase Kinase 2: Roles in Signaling and Pathophysiology. *Journal of Biological Chemistry* **287:** 31658-31665

Raeymaekers P, Timmerman V, Nelis E, De Jonghe P, Hoogenduk J, Baas F, Barker D, Martin J-J, De Visser M, Bolhuis P (1991) Duplication in chromosome 17p11. 2 in Charcot-Marie-Tooth neuropathy type 1a (CMT 1a). *Neuromuscular disorders* **1:** 93-97

Rafiq MA, Kuss AW, Puettmann L, Noor A, Ramiah A, Ali G, Hu H, Kerio NA, Xiang Y, Garshasbi M, Khan MA, Ishak GE, Weksberg R, Ullmann R, Tzschach A, Kahrizi K, Mahmood K, Naeem F, Ayub M, Moremen KW, Vincent JB, Ropers HH, Ansar M, Najmabadi H (2011) Mutations in the alpha 1,2-mannosidase gene, MAN1B1, cause autosomal-recessive intellectual disability. *American Journal of Human Genetics* **89:** 176-182

Rahman S, Blok RB, Dahl HHM, Danks DM, Kirby DM, Chow CW, Christodoulou J, Thorburn DR (1996) Leigh syndrome: Clinical features and biochemical and DNA abnormalities. *Annals of Neurology* **39:** 343-351

Rajadhyaksha AM, Ra S, Kishinevsky S, Lee AS, Romanienko P, DuBoff M, Yang C, Zupan B, Byrne M, Daruwalla ZR, Mark W, Kosofsky BE, Toth M, Higgins JJ (2012) Behavioral characterization of cereblon forebrain-specific conditional null mice: a model for human non-syndromic intellectual disability. *Behavioural Brain Research* **226:** 428-434

Raman M, Earnest S, Zhang K, Zhao Y, Cobb MH (2007) TAO kinases mediate activation of p38 in response to DNA damage. *EMBO Journal* **26:** 2005-2014

Rauch A, Schellmoser S, Kraus C, Dörr HG, Trautmann U, Altherr MR, Pfeiffer RA, Reis A (2001) First known microdeletion within the Wolf-Hirschhorn syndrome critical region refines genotype–phenotype correlation. *American Journal of Medical Genetics* **99:** 338-342

Ravikumar B, Vacher C, Berger Z, Davies JE, Luo S, Oroz LG, Scaravilli F, Easton DF, Duden R, O'Kane CJ, Rubinsztein DC (2004) Inhibition of mTOR induces autophagy and reduces toxicity of polyglutamine expansions in fly and mouse models of Huntington disease. *Nature Genetics* **36:** 585-595

Ravn K, Lindquist SG, Nielsen K, Dahm TL, Tümer Z Deletion of CUL4B leads to concordant phenotype in a monozygotic twin pair. *Clinical Genetics* **82:** 292-294

Ravn K, Lindquist SG, Nielsen K, Dahm TL, Tümer Z (2012) Deletion of CUL4B leads to concordant phenotype in a monozygotic twin pair. *Clinical Genetics* **82:** 292-294

Redon R, Ishikawa S, Fitch KR, Feuk L, Perry GH, Andrews TD, Fiegler H, Shapero MH, Carson AR, Chen W, Cho EK, Dallaire S, Freeman JL, Gonzalez JR, Gratacos M, Huang J, Kalaitzopoulos D, Komura D, MacDonald JR, Marshall CR, Mei R, Montgomery L, Nishimura K, Okamura K, Shen F, Somerville MJ, Tchinda J, Valsesia A, Woodwark C, Yang F, Zhang J, Zerjal T, Zhang J, Armengol L, Conrad DF, Estivill X, Tyler-Smith C, Carter NP, Aburatani H, Lee C, Jones KW, Scherer SW, Hurles ME (2006) Global variation in copy number in the human genome. *Nature* **444:** 444-454

Reiter LT, Murakami T, Koeuth T, Pentao L, Muzny DM, Gibbs RA, Lupski JR (1996) A recombination hotspot responsible for two inherited peripheral neuropathies is located near a mariner transposon-like element. *Nature Genetics* **12:** 288-297

Revy P, Malivert L, Villartay JPD (2006) Cernunnos-XLF, a recently identified non-homologous end-joining factor required for the development of the immune system. *Current Opinion in Allergy and Clinical Immunology* **6:** 416-420

Rhee SG (1999) Redox signaling: hydrogen peroxide as intracellular messenger. *Experimental & Molecular Medicine* **31:** 53-59

Ricard G, Molina J, Chrast J, Gu W, Gheldof N, Pradervand S, Schütz F, Young JI, Lupski JR, Reymond A (2010) Phenotypic consequences of copy number variation: insights from Smith-Magenis and Potocki-Lupski syndrome mouse models. *PLoS Biology* **8:** e1000543

Rizzuto R, Bernardi P, Pozzan T (2000) Mitochondria as all-round players of the calcium game. *The Journal of Physiology* **529:** 37-47

Roa BB, Garcia CA, Lupski JR (1991) Charcot-Marie-Tooth disease type 1A: molecular mechanisms of gene dosage and point mutation underlying a common inherited peripheral neuropathy. *International Journal of Neurology* **25-26:** 97-107

Ropers HH (2006) X-linked mental retardation: many genes for a complex disorder. *Current Opinions in Genetics and Development* **16:** 260-269

Rottenberg H, Covian R, Trumpower BL (2009) Membrane potential greatly enhances superoxide generation by the cytochrome bc 1 complex reconstituted into phospholipid vesicles. *Journal of Biological Chemistry* **284:** 19203-19210

Rovelet-Lecrux A, Hannequin D, Raux G, Le Meur N, Laquerriere A, Vital A, Dumanchin C, Feuillette S, Brice A, Vercelletto M, Dubas F, Frebourg T, Campion D

(2006) APP locus duplication causes autosomal dominant early-onset Alzheimer disease with cerebral amyloid angiopathy. *Nature Genetics* **38:** 24-26

Rustin P, Rotig A (2002) Inborn errors of complex II--unusual human mitochondrial diseases. *Biochimica et Biophysica Acta* **17:** 1-2

Saarimaki-Vire J, Peltopuro P, Lahti L, Naserke T, Blak AA, Vogt Weisenhorn DM, Yu K, Ornitz DM, Wurst W, Partanen J (2007) Fibroblast growth factor receptors cooperate to regulate neural progenitor properties in the developing midbrain and hindbrain. *The Journal of Neuroscience* **27:** 8581-8592

Sakamoto S, Kabe Y, Hatakeyama M, Yamaguchi Y, Handa H (2009) Development and application of high-performance affinity beads: Toward chemical biology and drug discovery. *The Chemical Record* **9:** 66-85

Sánchez C, Sánchez I, Demmers JAA, Rodriguez P, Strouboulis J, Vidal M (2007) Proteomics Analysis of Ring1B/Rnf2 Interactors Identifies a Novel Complex with the Fbxl10/Jhdm1B Histone Demethylase and the Bcl6 Interacting Corepressor. *Molecular & Cellular Proteomics* **6:** 820-834

Sandoval H, Thiagarajan P, Dasgupta SK, Schumacher A, Prchal JT, Chen M, Wang J (2008) Essential role for Nix in autophagic maturation of erythroid cells. *Nature* **454:** 232-235

Sarikas A, Hartmann T, Pan Z-Q (2011) The cullin protein family. *Genome Biology* **12:** 220

Sarikas A, Xu X, Field LJ, Pan Z-Q (2008) The Cullin7 E3 ubiquitin ligase: A novel player in growth control. *Cell cycle* **7:** 3154-3161

Satoh M, Fujimoto S, Haruna Y, Arakawa S, Horike H, Komai N, Sasaki T, Tsujioka K, Makino H, Kashihara N (2005) NAD(P)H oxidase and uncoupled nitric oxide synthase are major sources of glomerular superoxide in rats with experimental diabetic nephropathy. *American Journal of Physiology - Renal Physiology* **288:** F1144-F1152

Schallert T, Whishaw I, Ramirez V, Teitelbaum P (1978) Compulsive, abnormal walking caused by anticholinergics in akinetic, 6-hydroxydopamine-treated rats. *Science* **199:** 1461-1463

Schalock RL, Luckasson RA, Shogren KA, Borthwick-Duffy S, Bradley V, Buntinx WH, Coulter DL, Craig EM, Gomez SC, Lachapelle Y, Reeve A, Snell ME, Spreat S, Tasse MJ, Thompson JR, Verdugo MA, Wehmeyer ML, Yeager MH (2007) The renaming of mental retardation: understanding the change to the term intellectual disability. *Intellectual and Developmental Disabilities* **45:** 116-124

Scherer NM, Deamer DW (1986) Oxidative stress impairs the function of sarcoplasmic reticulum by oxidation of sulfhydryl groups in the Ca2+-ATPase. *Archives of Biochemistry and Biophysics* **246:** 589-601

Scherz-Shouval R, Shvets E, Fass E, Shorer H, Gil L, Elazar Z (2007) Reactive oxygen species are essential for autophagy and specifically regulate the activity of Atg4. *The EMBO Journal* **26:** 1749-1760

Schlickum S, Moghekar A, Simpson JC, Steglich C, O'Brien RJ, Winterpacht A, Endele SU (2004) LETM1, a gene deleted in Wolf–Hirschhorn syndrome, encodes an evolutionarily conserved mitochondrial protein. *Genomics* **83:** 254-261

Schon EA, Santra S, Pallotti F, Girvin ME (2001) Pathogenesis of primary defects in mitochondrial ATP synthesis. *Seminars in Cell and Developmental Biology* **12:** 441-448

Schrofelbauer B, Yu Q, Zeitlin SG, Landau NR (2005) Human immunodeficiency virus type 1 Vpr induces the degradation of the UNG and SMUG uracil-DNA glycosylases. *Journal of Virology* **79:** 10978-10987

Schweers RL, Zhang J, Randall MS, Loyd MR, Li W, Dorsey FC, Kundu M, Opferman JT, Cleveland JL, Miller JL, Ney PA (2007) NIX is required for programmed mitochondrial clearance during reticulocyte maturation. *Proceedings of the National Academy of Sciences* **104:** 19500-19505

Sebat J, Lakshmi B, Troge J, Alexander J, Young J, Lundin P, Maner S, Massa H, Walker M, Chi M, Navin N, Lucito R, Healy J, Hicks J, Ye K, Reiner A, Gilliam TC, Trask B, Patterson N, Zetterberg A, Wigler M (2004) Large-scale copy number polymorphism in the human genome. *Science* **305:** 525-528

Seo AY, Joseph A-M, Dutta D, Hwang JCY, Aris JP, Leeuwenburgh C (2010) New insights into the role of mitochondria in aging: mitochondrial dynamics and more. *Journal of Cell Science* **123:** 2533-2542

Shaffer LG, Kashork CD, Saleki R, Rorem E, Sundin K, Ballif BC, Bejjani BA (2006) Targeted genomic microarray analysis for identification of chromosome abnormalities in 1500 consecutive clinical cases. *The Journal of Pediatrics* **149:** 98-102

Sharp AJ, Hansen S, Selzer RR, Cheng Z, Regan R, Hurst JA, Stewart H, Price SM, Blair E, Hennekam RC, Fitzpatrick CA, Segraves R, Richmond TA, Guiver C, Albertson DG, Pinkel D, Eis PS, Schwartz S, Knight SJL, Eichler EE (2006) Discovery of previously unidentified genomic disorders from the duplication architecture of the human genome. *Nature Genetics* **38:** 1038-1042

Sharp AJ, Mefford HC, Li K, Baker C, Skinner C, Stevenson RE, Schroer RJ, Novara F, De Gregori M, Ciccone R, Broomer A, Casuga I, Wang Y, Xiao C, Barbacioru C, Gimelli G, Bernardina BD, Torniero C, Giorda R, Regan R, Murday V, Mansour S,

Fichera M, Castiglia L, Failla P, Ventura M, Jiang Z, Cooper GM, Knight SJ, Romano C, Zuffardi O, Chen C, Schwartz CE, Eichler EE (2008) A recurrent 15q13.3 microdeletion syndrome associated with mental retardation and seizures. *Nature Genetics* **40:** 322-328

Shaw CJ, Lupski JR (2004) Implications of human genome architecture for rearrangement-based disorders: the genomic basis of disease. *Human Molecular Genetics* **13 Spec No 1:** R57-64

Shih AY, Imbeault S, Barakauskas V, Erb H, Jiang L, Li P, Murphy TH (2005) Induction of the Nrf2-driven antioxidant response confers neuroprotection during mitochondrial stress in vivo. *Journal of Biological Chemistry* **280:** 22925-22936

Shimizu S, Matsuoka Y, Shinohara Y, Yoneda Y, Tsujimoto Y (2001) Essential Role of Voltage-Dependent Anion Channel in Various Forms of Apoptosis in Mammalian Cells. *The Journal of Cell Biology* **152:** 237-250

Shinawi M, Liu P, Kang SH, Shen J, Belmont JW, Scott DA, Probst FJ, Craigen WJ, Graham BH, Pursley A, Clark G, Lee J, Proud M, Stocco A, Rodriguez DL, Kozel BA, Sparagana S, Roeder ER, McGrew SG, Kurczynski TW, Allison LJ, Amato S, Savage S, Patel A, Stankiewicz P, Beaudet AL, Cheung SW, Lupski JR (2010) Recurrent reciprocal 16p11.2 rearrangements associated with global developmental delay, behavioural problems, dysmorphism, epilepsy, and abnormal head size. *Journal of Medical Genetics* **47:** 332-341

Shiotani B, Zou L (2009) ATR signaling at a glance. *Journal of Cell Science* **122:** 301-304

Shlien A, Tabori U, Marshall CR, Pienkowska M, Feuk L, Novokmet A, Nanda S, Druker H, Scherer SW, Malkin D (2008) Excessive genomic DNA copy number variation in the Li-Fraumeni cancer predisposition syndrome. *Proceedings of the National Academy of Sciences of the United States of America* **105:** 11264-11269

Siemen D, Ziemer M (2013) What is the nature of the mitochondrial permeability transition pore and What is it Not? *IUBMB Life* **65:** 255-262

Simon R, Lufkin T (2003) Postnatal lethality in mice lacking the Sax2 homeobox gene homologous to Drosophila S59/slouch: evidence for positive and negative autoregulation. *Molecular and Cellular Biology* **23:** 9046-9060

Simon R, Lufkin T, Bergemann AD (2007) Homeobox gene Sax2 deficiency causes an imbalance in energy homeostasis. *Developmental Dynamics* **236:** 2792-2799

Singhal S, Mehta J, Desikan R, Ayers D, Roberson P, Eddlemon P, Munshi N, Anaissie E, Wilson C, Dhodapkar M, Zeddis J, Barlogie B (1999) Antitumor activity of thalidomide in refractory multiple myeloma. *The New England Journal of Medicine* **341:** 1565-1571

Skre H (1974) Genetic and clinical aspects of Charcot-Marie-Tooth's disease. *Clinical Genetics* **6:** 98-118

Slack A, Thornton PC, Magner DB, Rosenberg SM, Hastings PJ (2006) On the mechanism of gene amplification induced under stress in Escherichia coli. *PLoS Genetics* **2:** e48

Slager RE, Newton TL, Vlangos CN, Finucane B, Elsea SH (2003) Mutations in RAI1 associated with Smith-Magenis syndrome. *Nature Genetics* **33:** 466-468

Smith J, Tho LM, Xu N, Gillespie DA (2010) The ATM-Chk2 and ATR-Chk1 Pathways in DNA Damage Signaling and Cancer. *Advances in Cancer Research* **108:** 40-40

Solinas-Toldo S, Lampel S, Stilgenbauer S, Nickolenko J, Benner A, Döhner H, Cremer T, Lichter P (1997) Matrix-based comparative genomic hybridization: Biochips to screen for genomic imbalances. *Genes, Chromosomes and Cancer* **20:** 399-407

South ST, Bleyl SB, Carey JC (2007) Two unique patients with novel microdeletions in 4p16.3 that exclude the WHS critical regions: Implications for critical region designation. *American Journal of Medical Genetics Part A* **143A:** 2137-2142

South ST, Hannes F, Fisch GS, Vermeesch JR, Zollino M (2008) Pathogenic significance of deletions distal to the currently described Wolf–Hirschhorn syndrome critical regions on 4p16.3. *American Journal of Medical Genetics Part C: Seminars in Medical Genetics* **148C:** 270-274

Stankiewicz P, Lupski JR (2002) Genome architecture, rearrangements and genomic disorders. *Trends in Genetics* **18:** 74-82

Stankiewicz P, Lupski JR (2010) Structural Variation in the Human Genome and its Role in Disease. *Annual Review of Medicine* **61:** 437-455

Stec I, Wright TJ, van Ommen G-JB, de Boer PAJ, van Haeringen A, Moorman AFM, Altherr MR, den Dunnen JT (1998) WHSC1, a 90 kb SET Domain-Containing Gene, Expressed in Early Development and Homologous to a Drosophila Dysmorphy Gene Maps in the Wolf-Hirschhorn Syndrome Critical Region and is Fused to IgH in t(1;14) Multiple Myeloma. *Human Molecular Genetics* **7:** 1071-1082

Stefansson H, Rujescu D, Cichon S, Pietilainen OP, Ingason A, Steinberg S, Fossdal R, Sigurdsson E, Sigmundsson T, Buizer-Voskamp JE, Hansen T, Jakobsen KD, Muglia P, Francks C, Matthews PM, Gylfason A, Halldorsson BV, Gudbjartsson D, Thorgeirsson TE, Sigurdsson A, Jonasdottir A, Jonasdottir A, Bjornsson A, Mattiasdottir S, Blondal T, Haraldsson M, Magnusdottir BB, Giegling I, Moller HJ, Hartmann A, Shianna KV, Ge D, Need AC, Crombie C, Fraser G, Walker N, Lonnqvist J, Suvisaari J, Tuulio-Henriksson A, Paunio T, Toulopoulou T, Bramon E, Di Forti M, Murray R, Ruggeri M, Vassos E, Tosato S, Walshe M, Li T, Vasilescu C, Muhleisen TW, Wang AG, Ullum H, Djurovic S, Melle I, Olesen J, Kiemeney LA, Franke B, Sabatti

C, Freimer NB, Gulcher JR, Thorsteinsdottir U, Kong A, Andreassen OA, Ophoff RA, Georgi A, Rietschel M, Werge T, Petursson H, Goldstein DB, Nothen MM, Peltonen L, Collier DA, St Clair D, Stefansson K (2008) Large recurrent microdeletions associated with schizophrenia. *Nature* **455:** 232-236

Steinmann K, Cooper DN, Kluwe L, Chuzhanova NA, Senger C, Serra E, Lazaro C, Gilaberte M, Wimmer K, Mautner VF, Kehrer-Sawatzki H (2007) Type 2 NF1 deletions are highly unusual by virtue of the absence of nonallelic homologous recombination hotspots and an apparent preference for female mitotic recombination. *American Journal of Human Genetics* **81:** 1201-1220

Stephens PJ, Greenman CD, Fu B, Yang F, Bignell GR, Mudie LJ, Pleasance ED, Lau KW, Beare D, Stebbings LA, McLaren S, Lin ML, McBride DJ, Varela I, Nik-Zainal S, Leroy C, Jia M, Menzies A, Butler AP, Teague JW, Quail MA, Burton J, Swerdlow H, Carter NP, Morsberger LA, Iacobuzio-Donahue C, Follows GA, Green AR, Flanagan AM, Stratton MR, Futreal PA, Campbell PJ (2011) Massive genomic rearrangement acquired in a single catastrophic event during cancer development. *Cell* **144:** 27-40

Stewart GS (2009) Solving the RIDDLE of 53BP1 recruitment to sites of damage. *Cell cycle* **8:** 1532-1538

Stewart GS, Panier S, Townsend K, Al-Hakim AK, Kolas NK, Miller ES, Nakada S, Ylanko J, Olivarius S, Mendez M, Oldreive C, Wildenhain J, Tagliaferro A, Pelletier L, Taubenheim N, Durandy A, Byrd PJ, Stankovic T, Taylor AM, Durocher D (2009) The RIDDLE syndrome protein mediates a ubiquitin-dependent signaling cascade at sites of DNA damage. *Cell* **136:** 420-434

Stewart GS, Stankovic T, Byrd PJ, Wechsler T, Miller ES, Huissoon A, Drayson MT, West SC, Elledge SJ, Taylor AMR (2007) RIDDLE immunodeficiency syndrome is linked to defects in 53BP1-mediated DNA damage signaling. *Proceedings of the National Academy of Sciences* **104:** 16910-16915

Stewart GS, Wang B, Bignell CR, Taylor AM, Elledge SJ (2003) MDC1 is a mediator of the mammalian DNA damage checkpoint. *Nature* **421:** 961-966

Stokin GB, Goldstein LS (2006) Axonal transport and Alzheimer's disease. *Annual Review of Biochemistry* **75:** 607-627

Stone HR, Morris JR (2013) DNA damage emergency: cellular garbage disposal to the rescue? *Oncogene*: **Advanced online publication, doi: 10.1036/onc.2013.60**

Stucki M, Clapperton JA, Mohammad D, Yaffe MB, Smerdon SJ, Jackson SP (2005) MDC1 directly binds phosphorylated histone H2AX to regulate cellular responses to DNA double-strand breaks. *Cell* **123:** 1213-1226

Sullivan M, Morgan DO (2007) Finishing mitosis, one step at a time. *Nature Reviews Molecular Cell Biology* **8:** 894-903

Sun J, Li R (2010) Human Negative Elongation Factor Activates Transcription and Regulates Alternative Transcription Initiation. *Journal of Biological Chemistry* **285:** 6443-6452

Swaminathan GJ, Bragin E, Chatzimichali EA, Corpas M, Bevan AP, Wright CF, Carter NP, Hurles ME, Firth HV (2012) DECIPHER: web-based, community resource for clinical interpretation of rare variants in developmental disorders. *Human Molecular Genetics* **21:** R37-44

Swiech L, Perycz M, Malik A, Jaworski J (2008) Role of mTOR in physiology and pathology of the nervous system. *Biochimica et Biophysica Acta* **1784:** 116-132

Takashima H, Boerkoel CF, John J, Saifi GM, Salih MAM, Armstrong D, Mao Y, Quiocho FA, Roa BB, Nakagawa M, Stockton DW, Lupski JR (2002) Mutation of TDP1, encoding a topoisomerase I-dependent DNA damage repair enzyme, in spinocerebellar ataxia with axonal neuropathy. *Nature Genetics* **32:** 267-272

Takemoto-Kimura S, Suzuki K, Kamijo S, Ageta-Ishihara N, Fujii H, Okuno H, Bito H (2010) Differential roles for CaM kinases in mediating excitation–morphogenesis coupling during formation and maturation of neuronal circuits. *European Journal of Neuroscience* **32:** 224-230

Tal MC, Iwasaki A (2009) Autophagic control of RLR signaling. *Autophagy* **5:** 749-750

Talbot DA, Lambert AJ, Brand MD (2004) Production of endogenous matrix superoxide from mitochondrial complex I leads to activation of uncoupling protein 3. *FEBS Letters* **556:** 111-115

Tamai S, Iida H, Yokota S, Sayano T, Kiguchiya S, Ishihara N, Hayashi J, Mihara K, Oka T (2008b) Characterization of the mitochondrial protein LETM1, which maintains the mitochondrial tubular shapes and interacts with the AAA-ATPase BCS1L. *The Journal of Cell Science* **121:** 2588-2600

Tanaka A, Cleland MM, Xu S, Narendra DP, Suen DF, Karbowski M, Youle RJ (2010) Proteasome and p97 mediate mitophagy and degradation of mitofusins induced by Parkin. *Journal of Cell Biology* **191:** 1367-1380

Tang SJ, Reis G, Kang H, Gingras AC, Sonenberg N, Schuman EM (2002) A rapamycin-sensitive signaling pathway contributes to long-term synaptic plasticity in the hippocampus. *Proceedings of the National Academy of Sciences of the United States of America* **99:** 467-472

Tang Y, Glauser TA, Gilbert DL, Hershey AD, Privitera MD, Ficker DM, Szaflarski JP, Sharp FR (2004) Valproic acid blood genomic expression patterns in children with epilepsy - a pilot study. *Acta Neurologica Scandinavica* **109:** 159-168

Tarpey P, Raymond F, O'Meara S, Edkins S, Teague J, Butler A, Dicks E, Stevens C, Tofts C, Avis T, Barthorpe S, Buck G, Cole J, Gray K, Halliday K, Harrison R, Hills K, Jenkinson A, Jones D, Menzies A, Mironenko T, Perry J, Raine K, Richardson D, Shepherd R, Small A, Varian J, West S, Widaa S, Mallya U (2007a) Mutations in CUL4B, which encodes a ubiquitin E3 ligase subunit, cause an X-linked mental retardation syndrome associated with aggressive outbursts, seizures, relative macrocephaly, central obesity, hypogonadism, pes cavus, and tremor. *American Journal of Human Genetics* **80:** 345 - 352

Tarpey PS, Raymond FL, O'Meara S, Edkins S, Teague J, Butler A, Dicks E, Stevens C, Tofts C, Avis T, Barthorpe S, Buck G, Cole J, Gray K, Halliday K, Harrison R, Hills K, Jenkinson A, Jones D, Menzies A, Mironenko T, Perry J, Raine K, Richardson D, Shepherd R, Small A, Varian J, West S, Widaa S, Mallya U, Moon J, Luo Y, Holder S, Smithson SF, Hurst JA, Clayton-Smith J, Kerr B, Boyle J, Shaw M, Vandeleur L, Rodriguez J, Slaugh R, Easton DF, Wooster R, Bobrow M, Srivastava AK, Stevenson RE, Schwartz CE, Turner G, Gecz J, Futreal PA, Stratton MR, Partington M (2007b) Mutations in CUL4B, Which Encodes a Ubiquitin E3 Ligase Subunit, Cause an X-linked Mental Retardation Syndrome Associated with Aggressive Outbursts, Seizures, Relative Macrocephaly, Central Obesity, Hypogonadism, Pes Cavus, and Tremor. *The American Journal of Human Genetics* **80:** 345-352

Taussig HB (1962) Thalidomide and phocomelia. *Pediatrics* **30:** 654-659

Taylor BJ, Nik-Zainal S, Wu YL, Stebbings LA, Raine K, Campbell PJ, Rada C, Stratton MR, Neuberger MS (2013) DNA deaminases induce break-associated mutation showers with implication of APOBEC3B and 3A in breast cancer kataegis. *Elife* **16**

Therapontos C, Erskine L, Gardner ER, Figg WD, Vargesson N (2009) Thalidomide induces limb defects by preventing angiogenic outgrowth during early limb formation. *Proceedings of the National Academy of Sciences of the United States of America* **106:** 8573-8578

Toime LJ, Brand MD (2010) Uncoupling protein-3 lowers reactive oxygen species production in isolated mitochondria. *Free Radical Biology and Medicine* **49:** 606-611

Torbergsen T, Mathiesen E, Aasly J (1991) Epilepsy in a mitochondrial disorder. *Journal of Neurology, Neurosurgery & Psychiatry* **54:** 1073-1076

Tripathi R, Kota SK, Srinivas UK (2007) Cullin4B/E3-ubiquitin ligase negatively regulates beta-catenin. *Journal of Biosciences* **32:** 1133-1138

Trojanowski JQ (2003) Rotenone neurotoxicity: a new window on environmental causes of Parkinson's disease and related brain amyloidoses. *Experimental Neurology* **179:** 6-8

Trotti D, Danbolt NC, Volterra A (1998) Glutamate transporters are oxidant-vulnerable: a molecular link between oxidative and excitotoxic neurodegeneration? *Trends in Pharmacological Sciences* **19:** 328-334

Turner DJ, Miretti M, Rajan D, Fiegler H, Carter NP, Blayney ML, Beck S, Hurles ME (2008) Germline rates of de novo meiotic deletions and duplications causing several genomic disorders. *Nature Genetics* **40:** 90-95

Turrens JF (2003) Mitochondrial formation of reactive oxygen species. *The Journal of Physiology* **552:** 335-344

Tuzun E, Sharp AJ, Bailey JA, Kaul R, Morrison VA, Pertz LM, Haugen E, Hayden H, Albertson D, Pinkel D, Olson MV, Eichler EE (2005) Fine-scale structural variation of the human genome. *Nature genetics* **37:** 727-732

Ulane CM, Horvath CM (2002) Paramyxoviruses SV5 and HPIV2 assemble STAT protein ubiquitin ligase complexes from cellular components. *Virology* **304:** 160-166

Valente KD, Freitas A, Fiore LA, Kim CA (2003) A study of EEG and epilepsy profile in Wolf–Hirschhorn syndrome and considerations regarding its correlation with other chromosomal disorders. *Brain and Development* **25:** 283-287

Van Humbeeck C, Cornelissen T, Hofkens H, Mandemakers W, Gevaert K, De Strooper B, Vandenberghe W (2011) Parkin interacts with Ambra1 to induce mitophagy. *Journal of Neuroscience* **31:** 10249-10261

van Muiswinkel FL, Kuiperij HB (2005) The Nrf2-ARE Signalling pathway: promising drug target to combat oxidative stress in neurodegenerative disorders. *Current Drug Targets-CNS & Neurological Disorders* **4:** 267-281

van Rhee F, Dhodapkar M, Shaughnessy JD, Jr., Anaissie E, Siegel D, Hoering A, Zeldis J, Jenkins B, Singhal S, Mehta J, Crowley J, Jagannath S, Barlogie B (2008) First thalidomide clinical trial in multiple myeloma: a decade. *Blood* **112:** 1035-1038

Veitia RA, Birchler JA (2010) Dominance and gene dosage balance in health and disease: why levels matter! *The Journal of Pathology* **220:** 174-185

Velagaleti GV, Bien-Willner GA, Northup JK, Lockhart LH, Hawkins JC, Jalal SM, Withers M, Lupski JR, Stankiewicz P (2005) Position effects due to chromosome breakpoints that map approximately 900 Kb upstream and approximately 1.3 Mb downstream of SOX9 in two patients with campomelic dysplasia. *American Journal of Human Genetics* **76:** 652-662

Verstreken P, Ly CV, Venken KJ, Koh TW, Zhou Y, Bellen HJ (2005) Synaptic mitochondria are critical for mobilization of reserve pool vesicles at Drosophila neuromuscular junctions. *Neuron* **47:** 365-378

Vieira HL, Belzacq AS, Haouzi D, Bernassola F, Cohen I, Jacotot E, Ferri KF, El Hamel C, Bartle LM, Melino G, Brenner C, Goldmacher V, Kroemer G (2001) The adenine nucleotide translocator: a target of nitric oxide, peroxynitrite, and 4-hydroxynonenal. *Oncogene* **20:** 4305-4316

Vital A, Vital C (2012) Mitochondria and Peripheral Neuropathies. *Journal of Neuropathology & Experimental Neurology* **71:** 1036-1046

Waldbaum S, Liang LP, Patel M (2010) Persistent impairment of mitochondrial and tissue redox status during lithium-pilocarpine-induced epileptogenesis. *Journal of Neurochemistry* **115:** 1172-1182

Waldbaum S, Patel M (2010) Mitochondrial dysfunction and oxidative stress: a contributing link to acquired epilepsy? *Journal of Bioenergetics and Biomembranes* **42:** 449-455

Waldeck-Weiermair M, Jean-Quartier C, Rost R, Khan MJ, Vishnu N, Bondarenko AI, Imamura H, Malli R, Graier WF (2011) Leucine zipper EF hand-containing transmembrane protein 1 (Letm1) and uncoupling proteins 2 and 3 (UCP2/3) contribute to two distinct mitochondrial Ca2+ uptake pathways. *Journal of Biological Chemistry* **286:** 28444-28455

Wang B, Elledge SJ (2007) Ubc13/Rnf8 ubiquitin ligases control foci formation of the Rap80/Abraxas/Brca1/Brcc36 complex in response to DNA damage. *Proceedings of the National Academy of Sciences of the United States of America* **104:** 20759-20763

Wang B, Matsuoka S, Ballif BA, Zhang D, Smogorzewska A, Gygi SP, Elledge SJ (2007) Abraxas and RAP80 form a BRCA1 protein complex required for the DNA damage response. *Science* **316:** 1194-1198

Wang DO, Martin KC, Zukin RS (2010) Spatially restricting gene expression by local translation at synapses. *Trends in Neurosciences* **33:** 173-182

Wang HL, Chang NC, Weng YH, Yeh TH (2013) XLID CUL4B mutants are defective in promoting TSC2 degradation and positively regulating mTOR signaling in neocortical neurons. *Biochimica et Biophysica Acta* **1832:** 585-593

Wang X, Winter D, Ashrafi G, Schlehe J, Wong Yao L, Selkoe D, Rice S, Steen J, LaVoie Matthew J, Schwarz Thomas L (2011) PINK1 and Parkin Target Miro for Phosphorylation and Degradation to Arrest Mitochondrial Motility. *Cell* **147:** 893-906

Wang Y-L, Faiola F, Xu M, Pan S, Martinez E (2008) Human ATAC Is a GCN5/PCAF-containing Acetylase Complex with a Novel NC2-like Histone Fold Module That Interacts with the TATA-binding Protein. *Journal of Biological Chemistry* **283:** 33808-33815

Wannenes F, Caprio M, Gatta L, Fabbri A, Bonini S, Moretti C (2008) Androgen receptor expression during C2C12 skeletal muscle cell line differentiation. *Molecular and Cellular Endocrinology* **292:** 11-19

Watt MJ, Holmes AG, Pinnamaneni SK, Garnham AP, Steinberg GR, Kemp BE, Febbraio MA (2006) Regulation of HSL serine phosphorylation in skeletal muscle and adipose tissue. *American Journal of Physiology, Endocrinology and Metabolism* **290:** E500-508

Wayman GA, Lee Y-S, Tokumitsu H, Silva A, Soderling TR (2008) Calmodulin-Kinases: Modulators of Neuronal Development and Plasticity. *Neuron* **59:** 914-931

Weiss LA, Shen Y, Korn JM, Arking DE, Miller DT, Fossdal R, Saemundsen E, Stefansson H, Ferreira MA, Green T, Platt OS, Ruderfer DM, Walsh CA, Altshuler D, Chakravarti A, Tanzi RE, Stefansson K, Santangelo SL, Gusella JF, Sklar P, Wu BL, Daly MJ (2008) Association between microdeletion and microduplication at 16p11.2 and autism. *New England Journal of Medicine* **358:** 667-675

Wertz IE, O'Rourke KM, Zhang Z, Dornan D, Arnott D, Deshaies RJ, Dixit VM (2004) Human De-etiolated-1 regulates c-Jun by assembling a CUL4A ubiquitin ligase. *Science* **303:** 1371-1374

Winklhofer KF, Haass C (2010) Mitochondrial dysfunction in Parkinson's disease. *Biochimica et Biophysica Acta (BBA) - Molecular Basis of Disease* **1802:** 29-44

Wisniewski AB, Migeon CJ, Meyer-Bahlburg HFL, Gearhart JP, Berkovitz GD, Brown TR, Money J (2000) Complete Androgen Insensitivity Syndrome: Long-Term Medical, Surgical, and Psychosexual Outcome. *Journal of Clinical Endocrinology & Metabolism* **85:** 2664-2669

Wolf U, Reinwein H, Porsch R, Schroter R, Baitsch H (1965) [Deficiency on the short arms of a chromosome No. 4]. *Humangenetik* **1:** 397-413

Wong KK, deLeeuw RJ, Dosanjh NS, Kimm LR, Cheng Z, Horsman DE, MacAulay C, Ng RT, Brown CJ, Eichler EE, Lam WL (2007) A comprehensive analysis of common copy-number variations in the human genome. *American Journal of Human Genetics* **80:** 91-104

Wong R, Steenbergen C, Murphy E (2012) Mitochondrial permeability transition pore and calcium handling. *Methods in Molecular Biology* **810:** 235-242

Woods A, Johnstone SR, Dickerson K, Leiper FC, Fryer LGD, Neumann D, Schlattner U, Wallimann T, Carlson M, Carling D (2003) LKB1 Is the Upstream Kinase in the AMP-Activated Protein Kinase Cascade. *Current Biology* **13:** 2004-2008

Wright SW, Tarjan G, Eyer L (1959) Investigation of families with two or more mentally defective siblings; clinical observations. *AMA Journal of Diseases of Children* **97:** 445-463

Wright TJ, Ricke DO, Denison K, Abmayr S, Cotter PD, Hirschhorn K, Keinänen M, McDonald-McGinn D, Somer M, Spinner N, Yang-Feng T, Zackai E, Altherr MR (1997) A Transcript Map of the Newly Defined 165 kb Wolf-Hirschhorn Syndrome Critical Region. *Human Molecular Genetics* **6:** 317-324

Wu F, Xing J, Wang S, Li M, Zheng C (2011) Screening and identification of host factors interacting with UL14 of herpes simplex virus 1. *Medical Microbiology and Immunology* **200:** 203-208

Wu J, Huen MS, Lu LY, Ye L, Dou Y, Ljungman M, Chen J, Yu X (2009) Histone ubiquitination associates with BRCA1-dependent DNA damage response. *Molecular and Cellular Biology* **29:** 849-860

Wu SB, Ma YS, Wu YT, Chen YC, Wei YH (2010) Mitochondrial DNA mutation-elicited oxidative stress, oxidative damage, and altered gene expression in cultured cells of patients with MERRF syndrome. *Molecular Neurobiology* **41:** 256-266

Wu Z, Chen Y, Yang T, Gao Q, Yuan M, Ma L (2012) Targeted Ubiquitination and Degradation of G-Protein-Coupled Receptor Kinase 5 by the DDB1-CUL4 Ubiquitin Ligase Complex. *PLoS ONE* **7:** e43997

Xin W, Xiaohua N, Peilin C, Xin C, Yaqiong S, Qihan W (2008) Primary function analysis of human mental retardation related gene CRBN. *Molecular Biology Reports* **35:** 251-256

Xu KY, Zweier JL, Becker LC (1997) Hydroxyl radical inhibits sarcoplasmic reticulum Ca(2+)-ATPase function by direct attack on the ATP binding site. *Circulation Research* **80:** 76-81

Xu L, Eu JP, Meissner G, Stamler JS (1998) Activation of the cardiac calcium release channel (ryanodine receptor) by poly-S-nitrosylation. *Science* **279:** 234-237

Xu X, Sarikas A, Dias-Santagata DC, Dolios G, Lafontant PJ, Tsai S-C, Zhu W, Nakajima H, Nakajima HO, Field LJ, Wang R, Pan Z-Q (2008) The CUL7 E3 Ubiquitin Ligase Targets Insulin Receptor Substrate 1 for Ubiquitin-Dependent Degradation. *Molecular Cell* **30:** 403-414

Yao R, Natsume Y, Noda T (2007) TACC3 is required for the proper mitosis of sclerotome mesenchymal cells during formation of the axial skeleton. *Cancer Science* **98:** 555-562

Yoshii SR, Kishi C, Ishihara N, Mizushima N (2011) Parkin mediates proteasome-dependent protein degradation and rupture of the outer mitochondrial membrane. *Journal of Biological Chemistry* **286:** 19630-19640

Yung TM, Narita T, Komori T, Yamaguchi Y, Handa H (2009) Cellular dynamics of the negative transcription elongation factor NELF. *Experimental Cell Research* **315:** 1693-1705

Zaidi A, Michaelis ML (1999) Effects of reactive oxygen species on brain synaptic plasma membrane Ca(2+)-ATPase. *Free Radical Biology and Medicine* **27:** 810-821

Zeviani M, Muntoni F, Savarese N, Serra G, Tiranti V, Carrara F, Mariotti C, DiDonato S (1993) A MERRF/MELAS overlap syndrome associated with a new point mutation in the mitochondrial DNA tRNA(Lys) gene. *European Journal of Human Genetics* **1:** 80-87

Zeviani M, Simonati A, Bindoff LA (2012) Chapter 22 - Ataxia in mitochondrial disorders. In *Handbook of Clinical Neurology*, Sankara HS, Alexandra D (eds), Vol. Volume 103, pp 359-372. Elsevier

Zhang D, Lu H, Li J, Shi X, Huang C (2006) Essential roles of ERKs and p38K in up-regulation of GST A1 expression by Maotai content in human hepatoma cell line Hep3B. *Molecular and Cellular Biochemistry* **293:** 161-171

Zhang F, Carvalho CM, Lupski JR (2009a) Complex human chromosomal and genomic rearrangements. *Trends in Genetics* **25:** 298-307

Zhang F, Carvalho CM, Lupski JR (2009b) Complex human chromosomal and genomic rearrangements. *Trends in Genetics* **25:** 298-307

Zhang F, Gu W, Hurles ME, Lupski JR (2009c) Copy number variation in human health, disease, and evolution. *Annual Review of Genomics and Human Genetics* **10:** 451-481

Zhang F, Khajavi M, Connolly AM, Towne CF, Batish SD, Lupski JR (2009d) The DNA replication FoSTeS/MMBIR mechanism can generate genomic, genic and exonic complex rearrangements in humans. *Nature Genetics* **41:** 849-853

Zhang H, Barceló JM, Lee B, Kohlhagen G, Zimonjic DB, Popescu NC, Pommier Y (2001) Human mitochondrial topoisomerase I. *Proceedings of the National Academy of Sciences* **98:** 10608-10613

Zhang X, Chen G, Lu Y, Liu J, Fang M, Luo J, Cao Q, Wang X (2013) Association of Mitochondrial Letm1 with Epileptic Seizures. *Cerebral Cortex;* Epub ahead of print, doi: 10.1093/cercor/bht118

Zhang Y, Gao J, Chung KKK, Huang H, Dawson VL, Dawson TM (2000) Parkin functions as an E2-dependent ubiquitin– protein ligase and promotes the degradation of the synaptic vesicle-associated protein, CDCrel-1. *Proceedings of the National Academy of Sciences* **97:** 13354-13359

Zhang Y, Morrone G, Zhang J, Chen X, Lu X, Ma L, Moore M, Zhou P (2003) CUL-4A stimulates ubiquitylation and degradation of the HOXA9 homeodomain protein. *EMBO Journal* **22:** 6057-6067

Zhang Y, Qiu J, Wang X, Zhang Y, Xia M (2011) AMP-activated protein kinase suppresses endothelial cell inflammation through phosphorylation of transcriptional coactivator p300. *Arteriosclerosis, Thrombosis, and Vascular Biology* **31:** 2897-2908

Zhao Y, Xiong X, Jia L, Sun Y (2012) Targeting Cullin-RING ligases by MLN4924 induces autophagy via modulating the HIF1-REDD1-TSC1-mTORC1-DEPTOR axis. *Cell Death and Disease* **3:** e386

Zheng J, Yang X, Harrell JM, Ryzhikov S, Shim EH, Lykke-Andersen K, Wei N, Sun H, Kobayashi R, Zhang H (2002a) CAND1 binds to unneddylated CUL1 and regulates the formation of SCF ubiquitin E3 ligase complex. *Molecular Cell* **10:** 1519-1526

Zheng N, Schulman B, Song L, Miller J, Jeffrey P, Wang P, Chu C, Koepp D, Elledge S, Pagano M, Conaway R, Conaway J, Harper J, Pavletich N (2002b) Structure of the Cul1-Rbx1-Skp1-F boxSkp2 SCF ubiquitin ligase complex. *Nature* **416:** 703 - 709

Zhivotovsky B, Galluzzi L, Kepp O, Kroemer G (2009) Adenine nucleotide translocase: a component of the phylogenetically conserved cell death machinery. *Cell Death and Differentiation* **16:** 1419-1425

Zhong W, Feng H, Santiago FE, Kipreos ET (2003) CUL-4 ubiquitin ligase maintains genome stability by restraining DNA-replication licensing. *Nature* **423:** 885-889

Zhou P. Pathogenic role of the CRL4 ubiquitin ligase in human disease. *Frontiers in Oncology* **6;** 2:21

Zhu YX, Braggio E, Shi CX, Bruins LA, Schmidt JE, Van Wier S, Chang XB, Bjorklund CC, Fonseca R, Bergsagel PL, Orlowski RZ, Stewart AK (2011) Cereblon expression is required for the antimyeloma activity of lenalidomide and pomalidomide. *Blood* **118:** 4771-4779

Zollino M, Lecce R, Fischetto R, Murdolo M, Faravelli F, Selicorni A, Buttè C, Memo L, Capovilla G, Neri G (2003) Mapping the Wolf-Hirschhorn Syndrome Phenotype Outside the Currently Accepted WHS Critical Region and Defining a New Critical Region, WHSCR-2. *American Journal of Human Genetics* **72:** 590-597

Zou Y, Liu Q, Chen B, Zhang X, Guo C, Zhou H, Li J, Gao G, Guo Y, Yan C, Wei J, Shao C, Gong Y (2007) Mutation in CUL4B, Which Encodes a Member of Cullin-RING Ubiquitin Ligase Complex, Causes X-Linked Mental Retardation. *The American Journal of Human Genetics* **80:** 561-566

Zsurka G, Baron M, Stewart JD, Kornblum C, Bös M, Sassen R, Taylor RW, Elger CE, Chinnery PF, Kunz WS (2008) Clonally expanded mitochondrial DNA mutations in epileptic individuals with mutated DNA polymerase γ. *Journal of Neuropathology and Experimental Neurology* **67:** 857-866

Zsurka G, Hampel KG, Nelson I, Jardel C, Mirandola SR, Sassen R, Kornblum C, Marcorelles P, Lavoué S, Lombès A, Kunz WS (2010) Severe epilepsy as the major symptom of new mutations in the mitochondrial tRNA Phe gene. *Neurology* **74:** 507-512